Université de Montréal

Prevention of Atherosclerosis by Modulating PCSK9 Expression and Function

par

Samaneh Samami

Faculté de Médecine

Département de pharmacologie et physiologie

Thèse présentée à la Faculté de Médecine

en vue de l'obtention du grade de Philosophiae Doctor (Ph.D)

en Pharmacologie

Avril 2019

Université de Montréal

Faculté de Médecine

Cette thèse intitulée:

Prevention of Atherosclerosis by Modulating PCSK9 Expression and Function

Présentée par :

Samaneh Samami

a été évaluée par un jury composé des personnes suivantes :

Dr. Réjean Couture: Président-rapporteur

Dr. Gaétan Mayer: Directeur

Dr. Eric Rhéaume : Codirecteur

Dre. Marie Lordkipanidzé: Membre du jury

Dr. Robert Scott Kiss (Université McGill): Examinateur externe

Résumé

L'hypercholestérolémie familiale autosomique dominante (ADH) est un trouble génétique caractérisé par des taux élevés de lipoprotéine de basse densité (LDL) plasmatique. Un niveau élevé de LDL plasmatique est connu pour contribuer au développement de l'athérosclérose, une cause majeure des crises cardiaques et des accidents vasculaires cérébraux. Le récepteur des LDL (LDLR) est la principale voie d'élimination des particules de LDL. En revanche, la proprotéine convertase subtilisine/kexine de type 9 (PCSK9), une glycoprotéine sécrétée par le foie, se lie au LDLR et augmente sa dégradation dans les lysosomes, ce qui entraîne une augmentation de LDL plasmatique et un risque plus élevé de maladie cardiovasculaire. En outre, des mutations de-perte-de fonction de PCSK9 peuvent considérablement réduire les niveaux de LDL plasmatiques et réduire le risque de maladie coronarienne jusqu'à ~ 88%. Toutes ces découvertes ont fait de PCSK9 une cible importante pour le traitement de l'hypercholestérolémie. Des anomalies génétiques du LDLR, de PCSK9 ou de l'apolipoprotéine B (apoB), le ligand du LDLR, peuvent provoquer l'ADH, mais dans certaines familles ADH il n'a pas été possible d'identifier de mutation de ces gènes, suggérant que d'autres anomalies génétiques pourraient également être impliquées dans la maladie.

Dans la présente thèse, qui repose sur deux études (articles), nous avons étudié les protéines d'interaction de PCSK9 (premier article, chapitre 2) et l'effet de PCSK9 sur l'athérosclérose (deuxième article, chapitre 3). Dans notre première étude, l'analyse par spectrométrie de masse des protéines interagissant avec PCSK9 a révélé que la Golgi glycoprotéine 1 (GLG1) est une nouvelle protéine d'interaction de PCSK9. Leur co-

immunoprécipitation révélée par immunobuvardage et leur co-localisation par microscopie confocale par immunofluorescence ont confirmé que GLG1 est un partenaire de PCSK9. De plus, nos résultats ont montré que GLG1 interagit aussi avec le LDLR et l'apoB. En utilisant un modèle murin, nous avons montré des taux sanguins plus faibles de PCSK9, de cholestérol et de triglycérides chez les souris knockdown GLG1. De plus, le déficit en GLG1 a réduit l'activité de la protéine de transfert des triglycérides microsomales (MTP) et induit l'agrégation périnucléaire de l'apoB, réduisant ainsi la sécrétion d'apoB. Dans notre deuxième étude, nous avons développé un modèle d'athérosclérose chez la souris pour étudier l'effet de l'absence de PCSK9 sur les plaques d'athérosclérose. Nous avons montré que la surexpression d'un mutant gain-de-fonction de PCSK9 dans le foie de souris a accéléré le développement de plaques d'athérosclérose dans la racine aortique et que celles-ci ont ensuite été réduites en induisant la régulation négative de PCSK9 en utilisant le système Tet-on.

En conclusion, nous avons contribué à l'identification d'une nouvelle protéine interagissant avec PCSK9, GLG1, qui régule le taux plasmatique de cholestérol et représente une cible potentielle pour le traitement de l'hypercholestérolémie. Nous avons également démontré que la modulation du gène PCSK9 régule directement le niveau de plaques d'athérosclérose dans la racine de l'aorte. Ces études aideront à développer des thérapies efficaces pour réduire l'hypercholestérolémie et le risque de maladie cardiovasculaire.

Mots-clés: ADH, LDLR, PCSK9, GLG1, cholestérol, athérosclérose

Abstract

Autosomal dominant hypercholesterolemia (ADH) is a genetic disorder characterized by high plasma low-density lipoprotein (LDL) cholesterol levels. Elevated plasma LDL level is known to contribute to the development of atherosclerosis, a leading cause of heart attack and stroke. Liver LDL receptor (LDLR) acts as a primary pathway for endocytosis and clearance of LDL particles. In contrast, PCSK9, a liver-secreted glycoprotein, binds to LDLR and enhances its lysosomal degradation, resulting in increased plasma LDL concentrations and a higher risk of cardiovascular disease. Genetic defects in LDLR, PCSK9, and apolipoprotein B (apoB), the ligand of LDLR, can cause ADH, but in some ADH-families no mutations can be found in these genes, suggesting that other gene defects may also be involved in ADH. Furthermore, loss-of-function mutations in PCSK9 can greatly reduce plasma LDL levels and lower risk of coronary heart disease by up to ~88%. All these findings have made PCSK9 an attractive target for the treatment of hypercholesterolemia.

In the present thesis, which is based on two studies (articles), we investigated protein interactors of PCSK9 (first article, chapter 2) and the effect of PCSK9 on atherosclerosis (Second article, chapter 3). In our first study, mass spectrometry analysis of PCSK9 interacting proteins revealed that Golgi glycoprotein 1 (GLG1) is a novel PCSK9 interactor. Co-immunoprecipitation, Western blotting, and colocalization by confocal immunofluorescence microscopy confirmed that GLG1 is an endogenous PCSK9 binding partner. We also demonstrated that LDLR and apoB interact with GLG1. Using a mouse model, we found lower levels of circulating PCSK9, cholesterol, and triglycerides in Glg1 knockdown mice. Moreover, GLG1 deficiency reduced microsomal

triglyceride transfer protein (MTP) activity and induced perinuclear aggregation of apoB, thereby, reducing apoB secretion. In our second study, we developed a mouse model of atherosclerosis to investigate the effect of PCSK9 modulation on the regression of atherosclerotic plaques. We showed that overexpression of a PCSK9 gain-of-function in mouse liver accelerated the development of atherosclerotic lesions in the aortic root, which were then reduced by inducing PCSK9 downregulation using a Tet-on system.

In conclusion, we have contributed to the identification of a novel PCSK9 interacting protein, GLG1, which regulates plasma level of cholesterol and represents a potential target for hypercholesterolemia treatment. We also demonstrated that PCSK9 gene modulation directly regulates the level of atherosclerotic plaques in the aortic root. We showed in our study that the wild-type mice, overexpressing PCSK9-D377Y in an inducible manner, is a useful mouse model for understanding the molecular role of PCSK9 on atherosclerotic plaques development. These studies will help to develop effective therapies to reduce hypercholesterolemia and the risk of cardiovascular disease.

Keywords: ADH, LDLR, PCSK9, GLG1, cholesterol, atherosclerosis

Table of Contents

List of Tables

List of Figures

Chapter 1: Literature Review

Chapter 2: PCSK9 and GLG1

Chapter 3: PCSK9 and Atherosclerosis

List of Abbreviations

3-MA	3-Methyladenine
AAV	Adeno-associated virus
AD	Alzheimer disease
ADH	Autosomal Dominant Hypercholesterolemia
AHA	American Heart Association
ANGPTl3	Angiopoietin-like3
AnxA2	Annexin A2
APLP2	Amyloid precursor-like protein 2
APN	Adiponectin
apoA-1	apolipoprotein A-I
apoB	apolipoprotein B
apoER2	apolipoprotein E receptor 2
APP	Amyloid precursor protein
ARH	Autosomal recessive hypercholesterolemia
ATase	Acetyltransferases
Aβ	Amyloid β
BACE1	β-site amyloid precursor protein (APP)-cleaving enzyme 1
BFA	Brefeldin A
CAD	Coronary artery disease
CD36	Cluster of differentiation 36
CETP	Cholesteryl ester transfer protein
CFR	Cysteine-rich fibroblast growth factor receptor
CGR-1	Homocysteine-rich fibroblast growth factor receptor
CHD	Coronary heart disease
CHO	Chinese hamster ovary
CHRD	Cys-His-rich Domain
CHX	Cycloheximide
CM	Chylomicrons
CMVm	CMV minimal promoter
CRISPR	Clustered regularly interspaced short palindromic repeats
CVD	Cardiovascular diseases
DLK	Delta-like protein
EGF-A	Epidermal growth factor-like repeat A
EL	Endothelial lipase
ER	Endoplasmic reticulum
ERGIC	ER-Golgi intermediate compartment
ESL-1	E-Selectin Ligand-1
FDB	Familial defective apolipoprotein B
FFA	Free fatty acid

FGF	Fibroblast growth factor
FGFR	FGF receptor
FH	Familial hypercholesterolemia
FITC	Fluorescein isothiocyanate
FPLC	Fast protein liquid chromatography
HNF1	Hepatocyte nuclear factor 1
GAPDH	Glyceraldehyde 3-phosphate dehydrogenase
GLG1	Golgi glycoprotein 1
GOF	Gain-of-function
GPC3	Glypican 3
GRP78	Glucose-regulated protein 78/BiP
HEK293	Human embryonic kidney 293 cell line
HPS	Hematoxylin-phloxine-saffron
HSC	Hepatic stellate cells
HSPG	Heparan sulfate proteoglycans
INSIG	Insulin-induced gene proteins
LAP	Latency-associated peptides
LDL	Low-density lipoprotein
LDL-C	LDL-cholesterol
LDLR	Low-density lipoprotein receptor
LDLRAP1	LDLR adapter protein 1
LNA	Locked nucleic acid
LOF	Loss-of-function
LOX	Lectin-like oxLDL receptor
LP(a)	Lipoprotein(a)
LPL	Lipoprotein lipase
LPS	Lipopolysaccharide
LRP1	Low-density lipoprotein receptor-related protein 1
LRP8	Low-density lipoprotein receptor-related protein 8
LTBP	Latent transforming growth factor- β1 binding protein
LTCP-1	Latent transforming growth factor-β complex protein 1
MG-160	Golgi Sialoglycoprotein/GLG1
MI	Myocardial infarction
MMP-2	Matrix metalloproteinase-2
MTP	Microsomal triglyceride transfer protein
NARC-I	Neural apoptosis regulated convertase
NF-κB	Nuclear factor κB
OA	Oleic acid
ORF	Open reading frame
PC	Proprotein convertase
PCSK9	Proprotein convertase subtilisin/kexin type 9
PEI	Polyethylenimine

PERPP	Post-ER pre-secretory proteolysis
PK	Pharmacokinetic
PolySia	polysialic acid
Pref-1	Preadipocyte factor 1
PTHrP	Parathyroid hormone-related peptide
PUFAs	Polyunsaturated fatty acids
SAR1B	Secretion associated Ras-related GTPase 1B
shRNA	Short hairpin RNA
siRNA	Small interfering RNA
SMC	Smooth muscle cells
SPR	Surface plasmon resonance
TBP	TATA-box binding protein
TG	Triglycerides
TGF-β	Transforming growth factor-β
TGN	Trans-Golgi network
TNF	Tumor necrosis factor
UPR	Unfolded Protein Response
VLDLR	Very low-density lipoprotein receptor
WTD	Western type diet

Acknowledgments

I would first like to thank my supervisor, Dr. Gaétan Mayer, for providing a wonderful research environment with a dedicated team, and for his training, support, and positive energy, which was always encouraging. I am forever grateful for all the time and effort he has given me to accomplish a Ph.D. program. To a similar extent, I wish to thank my co-supervisors, Dr. Eric Rhéaume, and Dr. Jean-Claude Tardif who have provided expertise with the great opportunity to collaborate with their group. I would like to extend my appreciation to Dr. Denis Deblois and Dr. Eric Thorin for serving on my advisory committee, and Dr. René Cardinal for all his support during the last 6 years.

My appreciation goes to my lab mates, especially Dr. Annie Demers and Dr. Steve Poirier, for their valuable scientific input and laboratory technical assistance. Many thanks to Azadeh Kashani, Inna Lapshin, Hocine Aithamouda, Dr. Emilienne Tudor Ngo Sock, and Run Zhou Ye for their companionship and for making my learning experience a pleasant one. I have also been fortunate to work with many great persons at the Montreal Heart Institute. Many thanks to Maya Mamarbachi for her incredible help in molecular biology, to Louis Villeneuve for his insightful comments in confocal microscopy, to Natacha Duquette and Teodora Mihalache-Avram for their indispensable help with the animal work, and to Daniel Rivas for his assistance in cryosectioning of tissue samples.

I am deeply thankful to my parents, Nahid and Reza, for their dedication and the many years of support during my studies. This last word of acknowledgment I have saved for my forever love, Mohsen, who has been with me on this journey from the beginning. Thank you with all my heart.

CHAPTER 1

1 LITERATURE REVIEW

CHAPTER 1: LITERATURE REVIEW

1.1 Cardiovascular disease

Cardiovascular diseases (CVDs), including heart disease and stroke, are a variety of conditions that involve abnormalities in heart function and blood vessels (Mathers et al., 2001). They account for nearly one-third of all deaths throughout the world (Roth et al., 2017). The most common form of CVD is atherosclerosis, which is characterized by the accumulation of fatty materials in artery walls. The progressive development of atherosclerotic plaques in artery walls can lead to thrombus formation, reducing or even blocking blood flow to vital organs (Soutar and Naoumova, 2007). Thrombus formation in artery walls can have devastating results such as heart attacks, strokes, and peripheral vascular disease.

The epidemic of CVD started after the Second World War, affecting mostly businessmen in the fifth decade of their life. At that time, life-stress was thought to be the most critical risk factor for CVD (Keys et al., 1963). At about the same time, Ancel Keys, the father of the low-fat diet, and his colleagues at the University of Minnesota showed a direct relationship between dietary fat intake and CVD in an extensive study on 12,000 individuals (Keys, 1980; Leren, 1970). Another six-year follow-up experience with 5209 persons, aged 30 to 59, in the town of Framingham (MA, USA) showed that reducing fat consumption could lower the risk of CVDs (Kannel et al., 1961). In this study, various serum lipids were evaluated as predictors of coronary heart disease (Kannel et al., 1961). The Framingham Heart Study is a long-term ongoing cardiovascular cohort study launched in 1948 on residents of the city of Framingham, Massachusetts. The original goal of the study was to find

common factors or characteristics that contribute to cardiovascular disease (Mahmood et al. 2014). In parallel with these studies, Fredrickson and his colleagues classified abnormal circulatory lipids based on their clinical features and electrophoretic lipoprotein patterns (Fredrickson et al., 1967). Their study helped to differentiate type III Familial Dysbetalipoproteinemia (FD) from type IIa Familial Hypercholesterolemia (FH) and resulted in having global attention to the lipoproteins and lipid disorders (Fredrickson, 1971). The type IIa FH, characterized by elevated cholesterol transported by low-density lipoproteins (LDL), results from a lack of functional LDL receptors (LDLR) on cell membranes as a result of various mutations. The Type III FD is caused by mutations in APOE that impair the ability of apoE, found on chylomicrons (CM) and very-LDL (VLDL), to bind to its receptor on the liver. This substantially disturbs the metabolism of cholesterol and triglyceride (TG)-rich lipoproteins by reducing the uptake of CM and highly atherogenic VLDL remnants. Thus, premature atherosclerotic CVD is common in patients with FD.

Individuals with an unhealthy lifestyle and genetic predisposition are more susceptible to develop a premature CVD, which occurs in men/women before reaching age 55-65. Patients with a premature CVD have a higher prevalence of dyslipidemia, an abnormal amount of blood lipids, compared to the age-matched control group. Therefore, it is required that they use pharmacological therapies at an early age to avoid premature CVD (Genest et al., 1992; Roncaglioni et al., 1992). The progress of CVD was first slowed down by lowering the circulatory level of cholesterol-rich lipoproteins (Gotto, 2002a; Gotto, 2002b). However, CVD was not completely prevented in dyslipidemic patients with FH (Genest et al., 1992; Roncaglioni et al., 1992). The progress of CVD was first slowed down by lowering

the circulatory level of cholesterol-rich lipoproteins (Gotto, 2002a; Gotto, 2002b). However, CVD was not completely prevented in dyslipidemic patients with FH (Genest et al., 1992). According to the INTER-HEART study (Kannel et al., 1961), a case-control study conducted in > 50 countries aiming to find CVD risk factors in different populations, people with dyslipidemia have a higher chance of developing myocardial infarction (Yusuf et al., 2004). Other risk factors for the development of CVD in this study were identified as smoking, physical inactivity, familial history of CVD, abdominal obesity, diabetes mellitus, hypertension and hypercholesterolemia (Yusuf et al., 2004).

Patients with metabolic syndrome are at higher risk of calcified atherosclerotic plaques formation and coronary artery disease. The metabolic syndrome is associated with clustering of risk factors such as elevated level of plasma triglycerides, hyperglycemia, hypercholesterolemia, hypertension, diabetes, and obesity (Ellison et al., 2005). Also, patients suffering from chronic inflammatory diseases, like rheumatoid arthritis and systemic lupus erythematosus, are more likely to develop cardiovascular diseases (Sarzi-Puttini et al., 2003; Slater et al., 2011). It has been reported that blood pressure-lowering therapies, can significantly reduce the risk of CVD in patients, including those who suffer from diabetes or chronic kidney disease (Ettehad et al., 2016).

All risk factors of CVD are divided into two groups: modifiable and non-modifiable risk factors. Modifiable, behavioral, risk factors are associated with more than 90% of the risk of myocardial infarction and can be prevented merely by lifestyle intervention, including weight loss, smoking cessation, regular physical activity, and healthy eating (Ruff and Braunwald, 2011). Also, a Mendelian randomization

analysis of 260,000 individuals suggested that a reduction in alcohol consumption is beneficial for cardiovascular health (Holmes et al., 2014). Moreover, the firm correlation of psychological stress with acute cardiac events, including vasospastic angina and plaque rupture demonstrated the importance of emotion management, especially in coronary heart disease patients (Fernandez et al., 2010). CVD with non-modifiable risk factors like genetic, gender, and age needs to be cured by drug therapy (Ruff and Braunwald, 2011). However, cholesterol-lowering medications are not effective in all cases to reduce the level of cholesterol to their target levels. They can also cause different side effects, such as myopathy, drug intolerance, and rhabdomyolysis occasionally (Stone et al., 2014).

1.2 Lipoproteins

Lipoproteins, as their name implies, are composed of lipids and specific proteins (apolipoproteins) linked by non-covalent interactions. They have the structure of a hydrophobic core composed of triglycerides (TG) and cholesteryl esters (CE) that are surrounded by an envelope containing phospholipids (PLs), unesterified cholesterol, and one or several specific apolipoproteins (Figure 1.1). Lipoproteins mediate transport of TG and cholesterol between organs in blood.

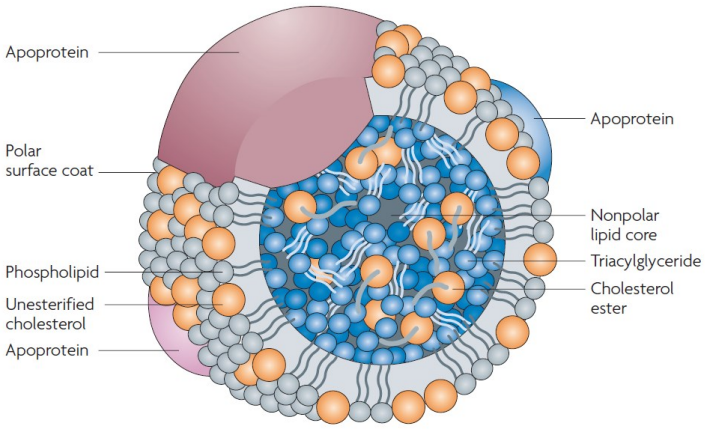

Figure 1.1 Lipoprotein structure

The nonpolar lipoprotein core composed mainly of triglycerides and cholesterol esters. They are surrounded by a single layer of phospholipid and cholesterol molecules. Apolipoproteins span the phospholipid monolayer and give lipoproteins structural and functional identity. Copyright permission has been obtained for the use of the figure in the thesis. License Number: 4652610415444 (adapted from Wasan et al., 2008).

Lipoproteins are divided into different groups based on their size, density, shape, composition, and function. The four distinct lipoprotein classes are chylomicrons (CM), very-low-density lipoproteins (VLDL), low-density lipoproteins (LDL), and high-density lipoproteins (HDL) (Figure 1.2). The main protein component of all lipoproteins, except HDL, is apoB. Chylomicrons contain apoB48, a truncated translation product of the *APOB* gene, but LDL-C particles have a single apoB in human (Tennyson et al., 1989). The main protein component of HDL is apolipoprotein AI (apoA1) and has a different contribution to vascular disease compared to the other lipoproteins.

Chylomicrons are very large TG-rich lipoproteins that are synthesized in the intestine to transport dietary TG (~ 85% of their lipid content) and cholesterol to the peripheral tissues.

1.2.1 Lipoproteins formation, secretion, and degradation

The absorbed free fatty acids and monoacylglycerols are assembled into TGs. Monoacylglycerol acyltransferase and diacylglycerol transferase are two key enzymes required for TGs synthesis. The formed TGs are packaged with cholesterol esters along with apoB48, apoA1, and phospholipids into chylomicrons in the endoplasmic reticulum of the small intestine. The size and composition of chylomicrons are dependent on the amount and type of fat ingested and absorbed by the intestine. ApoB48 and Microsomal triglyceride transfer protein (MTP) are required for synthesis and secretion of chylomicrons. MTP facilitates the transfer of lipid from the endoplasmic reticulum to the apoB48. MTP has been shown to interact with apoB, which is necessary for the secretion of apoB lipoproteins (Bakillah et al., 2000). Poorly lipidated apoB cannot fold properly and therefore is more likely to be delivered to ubiquitination machinery for degradation.

VLDLs are assembled in the liver and composed of cholesterol and TG. VLDL transport endogenous TG synthesized in the liver to cells in the body. Similar to the chylomicrons, the VLDL synthesis is mediated by MTP and availability of triglycerides and their specific apoB100 (Rustaeus et al., 1995). When TGs level is low, the newly synthesized apoB is degraded. Loss of function mutations in either apoB100 or MTP leads to the suppression of VLDL and triglyceride and cholesterol levels in plasma. It has been shown that MTP inhibition reduces both apoB100 and

apoB48 secretion. Apo100 secretion was found to be more sensitive than apoB48 secretion (Kulinski, A., 2002). The synthesized VLDLs in the lumen of the ER are transported to the Golgi via a complex multistep process, mediated by the VLDL transport vesicle. The VLDL particles undergo several modifications in the Golgi and then transported to the plasma membrane and secreted into the systemic circulation. The exact pathway by which the synthesized VLDLs are secreted from the liver into the circulation is not yet fully clear.

VLDLs and chylomicrons are hydrolyzed by lipoprotein lipase (LPL) in plasma to deliver free fatty acids to adipose tissue for energy storage and production, respectively (reviewed by Olivecrona, 2016). LPL is synthesized in muscle, heart, and adipose tissue. Hydrolysis of VLDL by LPL leads to an exchange of apoCII and apoE with HDL (Goldberg, 1996). Thus, remodeled VLDL particles, with less TG and apoCII, become intermediate-density lipoproteins (IDL). IDLs are either subjected to further lipase activity to produce LDL or removed by the liver. LDL Metabolism and clearance will be described in details in section 1.2.3. IDLs might be cleared from the circulation *via* LDLR, VLDL receptor (VLDLR) (Kobayashi et al., 1996) or LDLR-related protein 1 (LRP1) (Herz et al., 1995). The apoE on the chylomicron remnants binds to hepatic receptors such as the LDL receptor and LRP, and the whole package is taken up by the hepatocytes.

LDL-C particles, “bad cholesterol,” have the propensity through apoB to bind to the connective tissue in the intimal sublayer of arteries, which is a primary step in atherosclerotic plaque formation (Mourão and Bracamonte, 1984). Conversely, HDL-C or “good cholesterol,” mostly synthesized by the liver (80%) and the intestine

(20%) (Brunham et al., 2006), helps vascular health by removing the excess of cholesterol from tissues and delivering it back to the liver.

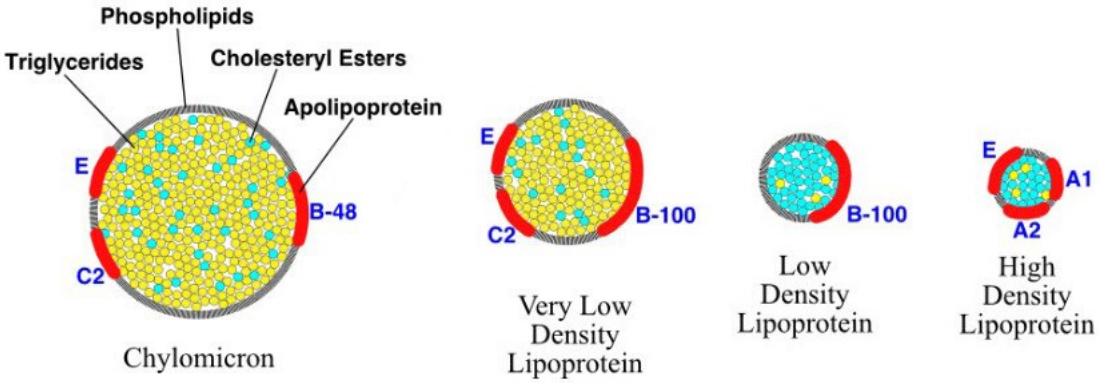

	Chylomicron	VLDL	LDL	HDL
Major Protein	apoB48	apoB100	apoB100	apoA1
Major Lipid	Triglycerides	Triglycerides	Cholesteryl Esters	Cholesteryl Esters

Figure 1.2 Lipoproteins classification and structure

Chylomicrons, VLDL, LDL, and HDL are four types of lipoproteins. The core of chylomicron and VLDL is composed of triglycerides. Chylomicrons serve to transport dietary triglyceride from intestine to peripheral tissues and cholesterol to the liver. VLDL is produced in the liver in response to nutrients and hormones and released into the plasma to supply triglycerides for the body tissues. LDL and HDL with a high content of cholesteryl esters are known as bad and good cholesterol, respectively. LDL is the key player in transporting cholesterol to the cells. In contrast, the most important function of HDL is transporting the excess of cholesterol from cells to the liver, which is called reverse cholesterol transport. Copyright permission has been obtained for the use of the figure in the thesis. License Number: 4652610415444 (adapted from www.apoa1.org).

1.2.2 apoB intracellular trafficking

apoB is a secretory protein, which is synthesized on the surface of the endoplasmic reticulum (ER) (Pariyarath et al., 2001). Various intracellular mechanisms contribute to the synthesis and secretion of apoB-containing

lipoproteins. Translocation of nascent apoB into the ER lumen is required for its lipidation and lipoprotein conformation (Jiang et al., 2007). Also, the availability of lipids (Burnett et al., 1999) and MTP (Benoist and Grand-Perret, 1997), are other important required factors. MTP is a lipid transfer protein, which is required for the assembly and secretion of VLDL by the liver and chylomicrons by the intestine.
In addition, the presence of chaperone proteins in the ER, such as 94 kDa glucose-regulated protein (GRP94), GRP78 and calreticulin facilitate the proper folding of apoB and its assembly into lipoprotein particles (Zhang and Herscovitz, 2003).

Dietary fats are the main factors regulating apoB production and its co-translational and post-translational degradation (Burnett et al., 1998). ApoB levels are primarily regulated via degradation. Presence of inadequate lipid ligands such as CE, TG, and phospholipid inhibits apoB-MTP interaction (Burnett et al., 1999) and thus newly synthesized apoB forms a polypeptide loop into the cytosol, which leads to its cotranslational proteasomal degradation (Liang et al., 1998). Degradation of apoB-loops in the cytosol is through the ER-associated degradation (ERAD) pathway by ubiquitination of the nascent apoB peptide (Liao et al., 2003; Pariyarath et al., 2001). Post-ER pre-secretory proteolysis (PERPP) is another degradation pathway for apoB-lipoprotein particles, which occurs in post-ER compartments (Neurath, 1989) when TG and lipids are available for lipoprotein particle formation (Fisher et al., 2001; Pan et al., 2008). Insulin (Sparks et al., 1996) and dietary intake of polyunsaturated fatty acids (PUFAs) (Pan et al., 2004; Pan et al., 2008) induce PERPP and thereby reduce the secretion of apoB-lipoprotein particles. Pan et al. (2004) demonstrated an increased level of lipid peroxidation and oxidative stress in hepatic cells that were incubated with PUFAs. They later found that oxidative stress

in the Golgi apparatus increased aggregation, sequestration, and autophagy degradation of VLDL lipoprotein particles in hepatic cells (Pan et al., 2008).

The link between autophagy and apoB100 was first discovered by Ohsaki Y. et al. (2006) who showed that proteasomal inhibition increases the level of apoB around lipid droplets to make "apoB-crescents" in human Huh7 cells. The level of apoB-crescents was reduced after 12-24 h of proteasomal inhibition, but the decrease was blocked by an autophagy inhibitor (Ohsaki et al., 2006). In another study by Zhong et al. (2010), a non-synonymous mutation of human apoB100, A31P, associated with familial hypobetalipoproteinemia, increased autophagic degradation of the apoB mutant, leading to reduced apoB and TG secretion. It has also been shown that autophagy may play an important role in the degradation of misfolded apoB under ER stress conditions (Qiu et al., 2011). Several studies now show apoB degradation through autophagy under certain conditions. However, the detailed molecular mechanism for apoB intracellular autophagy is still unknown.

Proteasomal degradation of apoB can be initiated from the ER. Translocated apoB-containing lipoprotein particles to the post-ER compartments or endocytosed lipoproteins can be degraded by lysosomes. Interaction of liver receptors such as LDLR with apoB-lipoprotein particles within the secretory pathway induces lysosomal degradation of the complex (Blasiole et al., 2008; Twisk et al., 2000).

1.2.3 LDLR and LDL clearance

The LDLR, primary element in the endogenous cholesterol pathway, is a transmembrane glycoprotein found in most cells and tissues and highly expressed

in the liver (Brown and Goldstein, 1983). More than 70% of LDL particles are cleared from the plasma by the LDLR localized at the surface of hepatocytes. The extracellular domain of LDLR consists of a ligand-binding domain containing seven cysteine-rich repeats, two epidermal growth factor (EGF)-like repeats, and a β-propeller domain followed by a third EGF-like repeat (Figure 1.3). Mutations in EGF-precursor homology domain of LDLR prevent LDLR recycling to the cell surface, which lead to a decrease in clearance of plasma level of LDL (Hobbs et al., 1992; Van der Westhuyzen et al., 1991). ApoB100 and apoE carried on VLDL remnant, IDL, LDL and some classes of HDL can bind to the extracellular ligand-binding domain of LDLR (Innerarity et al., 1980).

The LDL clearance pathway was first described by Brown and Goldstein in 1975 (Brown and Goldstein, 1975). Binding of LDL to the LDLR, *via* its sole protein component apoB100, leads to the invagination of the plasma membrane to form an endosome (Figure 1.4). The complex internalizes into the endosome *via clathrin*-coated vesicles and recruits adapter proteins autosomal recessive hypercholesterolemia (ARH) (Morris and Cooper, 2001). Low pH of endosome facilitates dissociation of the LDLR-LDL complex, recycling LDLR back to the surface for the clearance of more LDL particles from the plasma. Internalized LDL particles are digested in lysosomes and release cholesterol, fatty acids, and amino-acid components. Released cholesterol and fatty acids are either stored in lipid droplets or re-used by the cells. Released amino acids will be used for overall protein synthesis or metabolism (Goldstein et al., 1985).

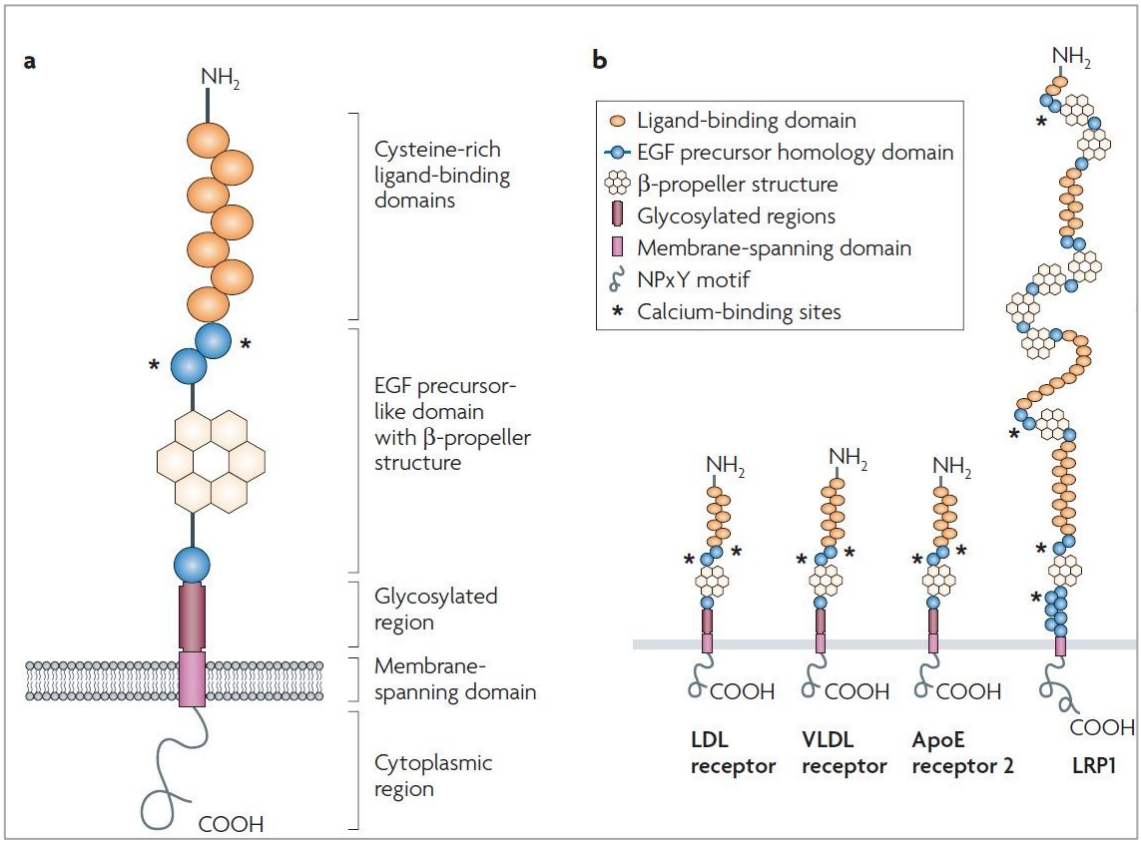

Figure 1.3 The LDLR structure and family members

The left illustration shows the LDLR structure that is common for all LDLR family members. It is composed of cysteine-rich ligand-binding domains, epidermal growth factor (EGF)-like regions, β-propeller domain, glycosylated region, membrane-spanning domain, and a small cytosolic domain. The right illustration shows functional domains of different LDLR family members, which have a similar structural organization with the exception of LRP1. Copyright permission has been obtained for the use of the figure in the thesis. License Number: 4652610415444 (Adapted from Wasan et al., 2008).

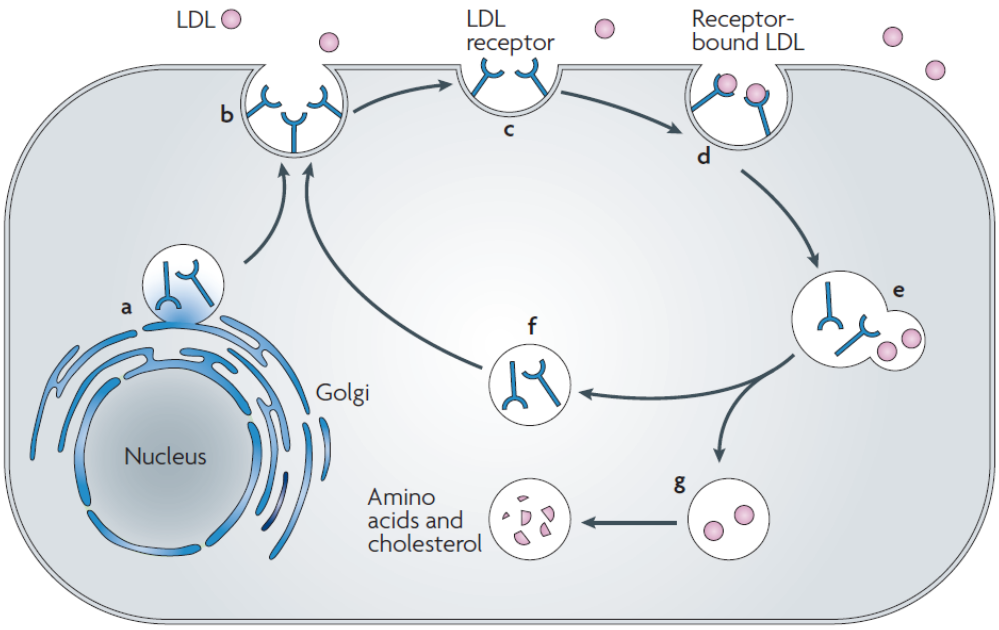

Figure 1.4 The LDLR recycling pathway

Schematic diagram illustrating the LDLR life cycle. LDLR is synthesized in the secretory pathway (ER and Golgi) (a), transported to the cell membrane(b) and clustered within clathrin-coated pits (c). LDL cholesterol particles bind to the LDLR through apoB100 (d) and internalize into the endosomes via clathrin-coated vesicles (e). Low pH of endosomes leads to the dissociation of LDLR-LDL complex, transporting LDLR back to the cell surface (f) whereas LDL particles are digested in lysosomes releasing cholesterol, fatty acids and amino-acid components (g) (adapted from (Wasan et al., 2008).

1.3 Familial hypercholesterolemia and PCSK9

Familial hypercholesterolemia (FH) is a genetic disorder that is characterized by high cholesterol levels, especially very high plasma level of LDL-C. FH is classified as a type 2 familial dyslipidemia based on the genetic abnormality (often due to LDLR defect) and altered lipid profile (high LDL). Elevated levels of LDL is associated with the development of atherosclerosis, which can be seen at an early age in many patients suffering from FH (Goldstein, 2001). FH was first described by

Carl Muller in the 1930s (Müller, 1938), and it was later classified into heterozygous FH (HeFH) and a more severe form of FH, homozygous FH (HoFH), according to the mode of inheritance (Khachadurian, 1964).

Heterozygous FH, inherited in an autosomal dominant pattern, often occurs with the ratio of 1 in 200-300 people in Europe (NordesTgaard et al., 2013), and even more common in some French-Canadian population (1 in 150 people) (Couture et al., 1999). HoFH, caused by the presence of biallelic disruptive mutations in the LDLR gene, is a much rarer disease, which is occurring in about 1 in 160,000-300,000 individuals (Cuchel et al., 2014). Affected HoFH patients are at higher risk of premature CVD, myocardial infarction, or even death in childhood *(Awan et al., 2008)*.

ARH, a phenocopy of HoFH, is characterized by a recessive mode of inheritance. It is caused by disruptive variants in both alleles of the LDLR adaptor protein-1 (LDLRAP1) gene, also known as ARH gene (Garcia et al., 2001). The LDLRAP1 protein contains a phosphotyrosine binding domain that interacts with the cytoplasmic tail of the LDLR. ARH protein is required for receptor-mediated hepatic uptake of LDL. Thus, ARH plays a crucial role in the endocytic internalization of LDLR-LDL complex in hepatocytes and contributes to a high plasma level of LDL (Garcia et al., 2001).

In untreated patients with HeFH, level of LDL-C can be >140 mg/dl (7.0±0.2 mmol/L) and >400 mg/dl (13.4±0.7 mmol/L) in patients with HoFH; while the level of TG remains unchanged (Rader et al., 2003). An optimal range for LDL in healthy individuals is less than 100 mg/dL (2.6 mmol/L (O'Keefe et al., 2004). Homozygotes patients with ARH mutations have an intermediate level of circulating LDL, between

that of HeFH and HoFH patients (Soutar et al., 2003). A lifelong elevated level of LDL in patients with FH can lead to premature cardiovascular disease, narrowing and hardening of the arteries causing atherosclerosis, and manifest as angina (pain in the chest), myocardial infarction (MI), peripheral vascular disease or even death.

The first identified gene mutation leading to elevated plasma level of LDL-C in FH was found in LDLR (Goldstein et al., 1974) located on chromosome 19 (FH1;19p13.1-13.3) (Francke et al., 1984). A large number of different mutations causing FH is now identified in the LDLR gene (Heath et al., 2000; Villéger et al., 2002). They are divided into different groups, such as mutations that lead to defective synthesis of LDLR, defective transport of LDLR from the ER to the trans-Golgi network (TGN), defective binding of LDLR to the apoB100 or defective internalization of LDLR (Goldstein and Brown, 1987; Hobbs et al., 1987). *APOB* is the second identified gene for which a mutation can cause ADH or familial defective apolipoprotein B-100(Innerarity et al., 1990). *APOB* is located at chromosome 2 (FH2, 2p23- 24) (Knott et al., 1985; Law and Heath, 1985) and patients with mutations in this gene, demonstrate the same clinical features as patients with a mutated form of LDLR (Innerarity et al., 1990). The third autosomal dominant locus that is associated with FH is located on chromosome 1p32 (Hunt et al., 2000; Varret et al., 1999) and corresponds to *proprotein convertase subtilisin/kexin type 9* (*PCSK9*) gene, previously identified as neural apoptosis-regulated convertase-I (NARC-I) (Abifadel et al., 2003; Seidah et al., 2003). Although mutations in *APOB, LDLR,* and *PCSK9* are associated with ~85% of cases of FH, several genome-wide association studies (GWAS) attempted to identify new genomic regions that are linked to elevated plasma level of LDL-C (Wang et al., 2005). Studies on ADH-

families without any mutations in *APOB, LDLR* and *PCSK9* reported that a fourth unknown gene possibly involved in ADH is either located at the 16q22.1 locus containing 154 genes (Marques-Pinheiro et al., 2010) or on chromosome 8 (8q24.22) (Cenarro et al., 2011). Identification of new genes associated with FH will bring new insights into the cardiovascular field.

In contrast to common hypercholesterolemia (polygenic and multifactorial), FH is a monogenic disorder with a very high level of plasma LDL-C that can be observed at the time of birth. Mutations in *ARH*, located on chromosome 1p35, can also contribute to a high level of plasma LDL (Garcia et al., 2001). Homozygotes patients with ARH mutations have an intermediate level of circulating LDL-C, between that of HeFH and HoFH patients (Soutar et al., 2003). A lifelong elevated level of LDL-C in patients with FH can lead to premature cardiovascular disease, narrowing and hardening of the arteries causing atherosclerosis, and manifest as angina (pain in the chest), myocardial infarction (MI), peripheral vascular disease or even death.

Therefore, it is important to diagnose and treat FH at the earliest stage to produce a favorable clinical outcome. The recognition of xanthomas in the first decade of life is often the first indication of a diagnosis of FH (especially HoFH) in children (Kolansky et al., 2008; Macchiaiolo et al., 2012; Schrott et al., 1972). Physical signs such as lipid deposition near the eyelid (xanthelasmas), or over the skin of hands, elbows, knees, and ankles (xanthomas) and clinical signs such as a systolic murmur, angina, or the signs of clinical artery disease can help for the early detection of FH. However, diagnoses of FH at an early age is not always easy, since

some of the phenomena occur only in adulthood (e.g., tendon xanthomas) (Kwiterovich et al., 1974).

1.3.1 PCSK9 structure

PCSK9, composed of 692 amino acids (aa), is mainly expressed in the liver and less so in the intestine and the kidney in both human and mice. Figure 1.5 shows the PCSK9 expression level in mouse tissues. PCSK9 is formed of a signal peptide (aa 1-30), a prodomain (aa 31-152), a catalytic domain (aa 153-404), a hinge region (HR; aa 405–454), and a C-terminal cysteine- and histidine-rich domain (CHRD) (aa 455-692) (Seidah et al., 2003; Poirier and Mayer, 2013). Cleavage of the signal peptide in the ER leads to the formation of pro-PCSK9, a ~72-kDa precursor protein, which undergoes autocatalytic cleavage between the prodomain and catalytic domain (Figure 1.6) (Naureckiene et al., 2003). However, unlike other subtilisin-like proteases, the prodomain (~14-kDa) is not released after the cleavage and remains non-covalently attached to its catalytic domain (Cunningham et al., 2007; Piper et al., 2007). The prodomain functions as an intramolecular chaperone, which is essential for proper folding and exit from the ER (Naureckiene et al., 2003). Moreover, PCSK9, unlike other PCSK family members, does not have a P domain, which is required for its protease activity (Naureckiene et al., 2003).

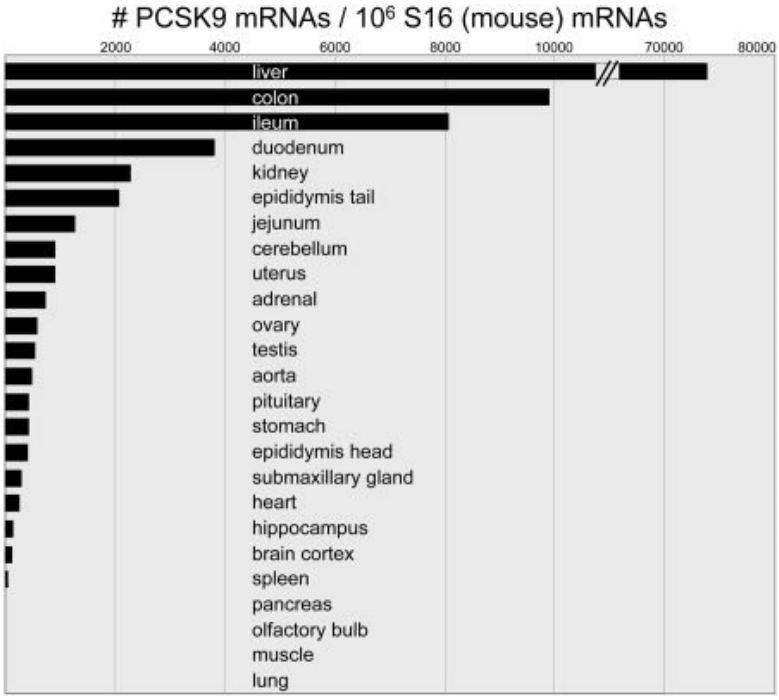

Figure 1.5 PCSK9 expression in mouse tissues

Quantification of PCSK9 mRNA expression in mouse tissues, normalized to S16 mRNA level (Adapted from Zaid et al., 2008).

Different from other PCSKs, cleavage of PCSK9 prodomain at SVFAQ^{152}↓SIP, does not require calcium (Benjannet et al., 2004; Poirier and Mayer, 2013). Mature PCSK9 undergoes several post-translational modifications in the Golgi apparatus, including glycosylation of asparagine residue at position 533 and tyrosine sulfation at position 38 (Benjannet et al., 2006). In addition, PCSK9 is phosphorylated in its prodomain (serine residue at position 47) and C-terminal domain (serine at position 688) by Golgi casein kinase-like kinase which regulates its proteolysis (Dewpura et al., 2008). Interestingly, serine phosphorylation of PCSK9 is correlated with insulin resistance in obese patients (Gauthier et al., 2015). The C-terminal CHRD is

required for LDLR degradation since PCSK9 lacking the C-terminal domain is unable to degrade LDLR (Zhang et al., 2008; Poirier et al., 2016).

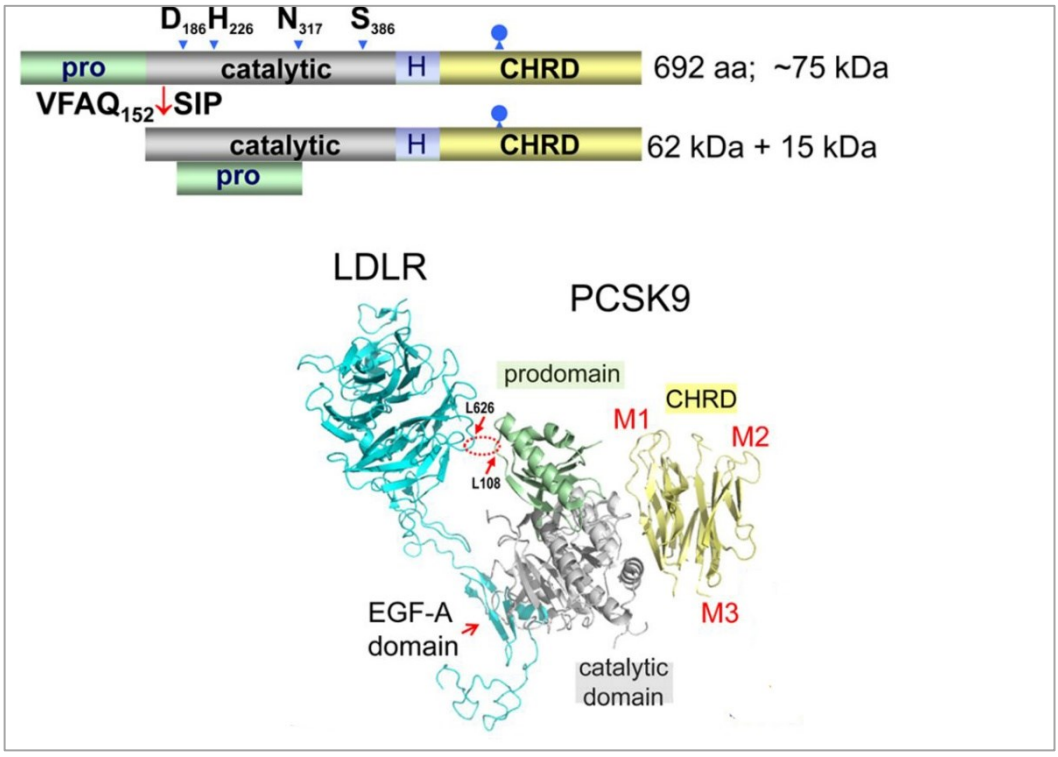

Figure 1.6 PCSK9 domains and crystal structure

ProPCSK9 (75 kDa) is autocatalytically cleaved at VFAQ152↓SIP within the endoplasmic reticulum, resulting in mature PCSK9 containing the prosegment, catalytic domain, hinge region (H), and a C-terminal CHRD. The crystal structure shows the interaction of LDLR-EGF-A domain with PCSK9-catalytic domain, and the three subdomains in the CHRD (M1, M2, and M3). Copyright permission has been obtained for the use of the figure in the thesis. License Number 4652620882527 (Adapted from Seidah et al., 2014).

1.3.2 Regulation of PCSK9 and LDLR expression by SREBP2

Sterol regulatory element-binding proteins (SREBPs) are members of the basic-helix-loop-helix leucine zipper class of transcription factors that regulates many genes involved in cholesterol homeostasis (Horton et al., 2003). SREBPs

consists of three isoforms: SREBP-1a, SREBP-1c, and SREBP-2. Both SREBP-1a and SREBP-1c are products of the same gene, *SREBF*-1, through the use of alternate promoters, resulting in different forms of exon-1 (Yokoyama et al., 1993). SREBP-2 is the product of a separate gene, *SREBF-2*, and is 47% identical to SREBP-1a (Hua et al., 1993). SREBP-1c mainly regulates fatty acids and TG synthesis and insulin-mediated lipogenesis and glucose metabolism (Foretz et al., 1999), whereas SREBP-2 regulates all enzymes responsible of cholesterol synthesis, most notably HMG-CoA reductase (3-hydroxy-3-methyl-glutaryl-coenzyme A reductase; HMGCR) (Horton et al. 1998). SREBP-1a seems to be expressed in most tissues and activates genes in both lipid and cholesterol pathways (Eberlé et al., 2004).

SREBPs are synthesized as inactive precursors bound to the ER membrane. Each SREBP precursors contains about 1150 amino acids including three domains: a cytosolic NH2-terminal domain, a short hydrophilic loop that projects into the ER lumen, and a COOH-terminal domain (Horton et al., 2002). To act as a transcription factor, SREBPs must translocate from the ER to the Golgi for the proteolytic processing that releases the NH2-terminal domain from the membrane. SREBP cleavage-activating protein (SCAP) binds to SREBPs and escorts them from the ER to the Golgi. SCAP can sense the levels of sterols in the cell, and if it is low, escort SREBP for activation. Other important proteins for transport of SREBPs from the ER to the Golgi are insulin-induced gene proteins (INSIGs) including INSIG1 and INSIG2 (Hua et al., 1996). During high sterol level conditions, SCAP/SREBPs complex binds to the INSIGs which prevent the complex from entering the coat protein complex II (COPII)-dependent ER-Golgi trafficking. When intracellular cholesterol levels are

low, SCAP undergoes a conformational change, allowing its dissociation from INSIGs, resulting in the interaction with the COPII trafficking complex and proper transport of SREBPs to the Golgi, where the two proteases, site-1 protease (S1P) and site-2 protease (S2P) reside. S1P, a membrane-bound serine protease, encoded by *MBTPS1* gene, and S2P, a membrane-bound zinc metalloproteinase, encoded by *MBTPS2* gene, cleaves the SREBP and release the active NH_2-terminal domain that translocates to the nucleus. In the nucleus, the NH2-terminal domain binds to a sterol response element (SRE) in the promoter region of lipid metabolism genes, such as HMGCR and the LDLR, increasing their transcription (Horton et al., 2002).

SREBP activity is not only controlled by cholesterol level in the cells. It has been shown that a number of post-translational modifications, such as ubiquitination, phosphorylation, and acetylation are regulating SREBPs activity. The ubiquitin-proteasome system can degrade nuclear SREBPs by ubiquitin-related modifier (SUMO)-1 and controls the expression of SREBP target genes (Hirano et al., 2001). It has also been shown that phosphorylation of Thr-426 and Ser-430 in the C-terminal domain of SREBP1 creates a docking site for the ubiquitin ligase, Fbw7, which enhances SREBP1 degradation (Bengoechea-Alonso and Ericsson, 2009). Also, SIRT1 (sirtuin 1), a member of class III NAD+-dependent family of protein deacetylases can directly deacetylate SREBP, resulting in changes SREBP ubiquitination, protein stability, and target gene expression (Ponugoti et al., 2010)

Expression of *PCSK9* and *LDLR* genes are regulated by the intracellular level of cholesterol *via* SREBPs (Edwards et al., 2000; Maxwell et al., 2003). PCSK9 and LDLR promoters contain an SRE that regulates their expression by sterol at the transcriptional level. Therefore, mRNA expression of PCSK9 would be suppressed by high plasma cholesterol level or increased by SREBPs in low cholesterol conditions (Horton et al., 2003). Jeong et al. (2008) showed that fasting decreases mRNA levels *of* PCSK9 in mouse hepatocytes *via* suppression of SREBP2, suggesting that sterol-dependent regulation of PCSK9 is mediated predominantly by SREBP2. Beside the SRE region, a functional hepatocyte nuclear factor 1 (HNF1) binding site has been identified in PCSK9 promoter that binds to HNF1α for basal expression of PCSK9 (Li et al., 2009). In this study, a mutation of HNF1 decreased PCSK9 promoter binding to sterols and reduced SREBP2 effect on PCSK9 expression, suggesting that the HNF1 site may work cooperatively with the SRE. HNF1 is a transcription factor, highly expressed in the liver, and is known to regulate many genes in liver and intestine (Mendel et al., 1991; Odom et al., 2004). PCSK9 can also be regulated by insulin. Costet et al. (2006) reported that insulin stimulates SREBP1c expression in hepatocytes resulting in increased PCSK9 expression in mice. They also showed that liver X receptor agonist (T0901317), which is involved in cholesterol metabolism could regulate PCSK9 expression *via* this same pathway.

1.3.3 PCSK9 and LDLR degradation

PCSK9 is acting as a sort of molecular chaperone to induce LDLR degradation in human hepatic cell lines and mouse liver (Grefhorst et al., 2008; McNutt et al., 2007). PCSK9 induces LDLR degradation not through proteolytic activity but rather by direct binding and targeting the receptor for lysosomal degradation (Figure 1.7) (Horton et al., 2009; Lagace et al., 2006; Zhang et al., 2007). PCSK9 can induce LDLR degradation by two different pathways (Figure 1.8); 1) interaction of PCSK9 with LDLR in the Golgi directing the complex from the trans-Golgi to the lysosome for degradation by an intracellular pathway, (Poirier et al., 2009) and 2) secreted PCSK9 binds to the EGF-A domain of LDLR at the cell-surface (Lagace et al., 2006; Zhang et al., 2007), induces complex internalization into the endosome by clathrin-mediated endocytosis, and re-routes the LDLR to the lysosome for degradation (Surdo et al., 2011; Zhang et al., 2008).

Crystallographic analysis has revealed that PCSK9 directly binds to the EGF-A domain of LDLR through its catalytic domain (Kwon et al., 2008). Although the catalytic domain of PCSK9 binds with the LDLR, the C-terminal domain of PCSK9 is required for LDLR degradation (Zhang et al., 2008). Zhang et al. (2008) suggested that PCSK9 C-terminal domain may provide a site for interaction with other proteins involved in PCSK9 trafficking. However, Holla et al. (2011) indicated that positive charge and size of PCSK9 C-terminal domain are important for PCSK9 activity toward LDLR, while the sequence of the C-terminal domain is not involved in regulating the PCSK9 activity or protein interaction. The presence of ARH is essential for complex internalization into the endosome (Lagace et al., 2006). At the low pH of endosomes (pH < 6), LDLR changes from an open to a closed

conformation, which leads to dissociation of the LDLR-LDL complex, recycling of LDLR to the cell surface, and release of LDL particles to the lysosomes for degradation. Although the acidic pH of endosomal compartments is not required for PCSK9-induced LDLR degradation, it significantly enhances (>150-fold) the affinity of PCSK9-LDLR binding compared to a neutral pH. (Fisher et al., 2007). Formation of a highly stable PCSK9-LDLR complex at acidic pH prevents of LDLR recycling to the cell surface and ultimately induces LDLR lysosomal degradation (Zhang et al., 2007).

Gain-of-function (GOF) mutations in PCSK9 cause a rare form of ADH, resulting in high plasma level of LDL-C and a higher risk of coronary heart disease (CHD) (Abifadel et al., 2003). Conversely, loss-of-function (LOF) PCSK9 mutations are associated with CHD protection by reducing the plasma level of LDL-C (Cohen et al., 2005; Cohen et al., 2006). Therefore, there is a direct relation between PCSK9 function and circulating level of LDL-C (Abifadel et al., 2009).

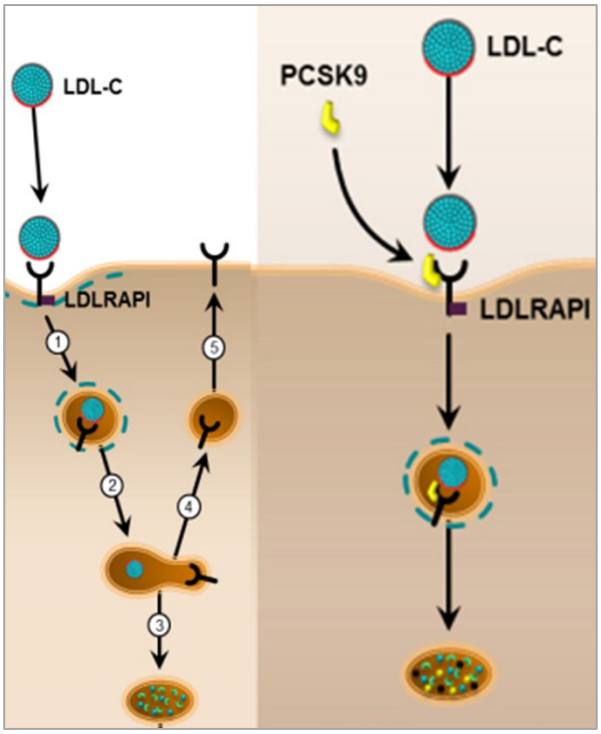

Figure 1.7 Mechanism of PCSK9-induced LDLR degradation

Left: Binding of LDL to the LDLR on the cell surface at neutral pH causes 1) internalization of LDLR-LDL-C complex into the endosome. 2) Dissociation of LDLR and LDL occurs at low pH of endosomes, which leads to 3) lysosomal degradation of LDL and 4) recycling of LDLR to 5) the cell surface. Right: Binding of PCSK9 to the LDLR leads to internalization of the complex into the endosome. Low pH of the endosomes increases PCSK9-LDLR affinity, preventing LDLR recycling, and finally causes lysosomal LDLR degradation. The LDLR adapter protein 1 (LDLRAP1) protein, coded by LDLRAP1 gene (also known as ARH), interacts with LDLR and plays an important role in LDLR-LDL-C complex internalization. The LDLRAP1 protein contains a phosphotyrosine binding domain that interacts with the cytoplasmic tail of the LDLR (Adapted from https://atlasofscience.org/, by Safarova MS and Iftikhar J Kullo. 2016).

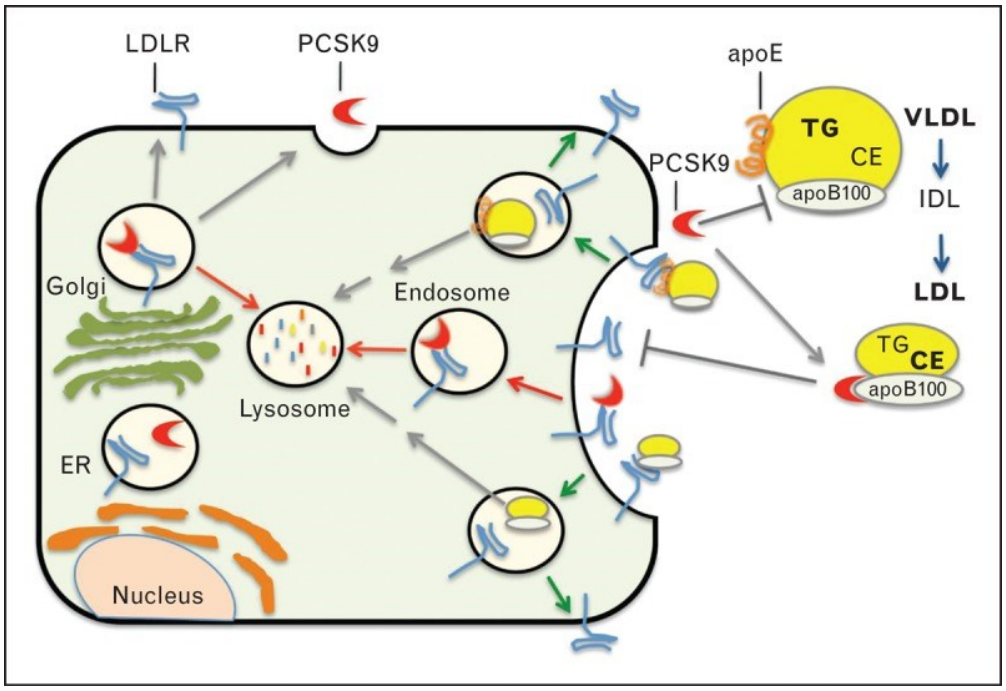

Figure 1.8 Intra- and extra-cellular pathways of PCSK9-induced LDLR degradation

PCSK9 induces LDLR degradation through two different pathways. PCSK9 can bind to LDLR in the Golgi and directs the complex from the trans-Golgi to the lysosome for degradation. Alternatively, secreted PCSK9 binds to the LDLR at the cell surface; the complex internalizes into the endosome and is degraded in lysosomes. Copyright permission has been obtained for the use of the figure in the thesis.License Number 4652630622369 (Adapted from Lagace, 2014).

The significant decrease (~60%) in plasma level of LDL-C upon blocking the interaction of secreted PCSK9 with LDLR at the cell surface using a therapeutic monoclonal antibody against PCSK9 catalytic domain demonstrates that the primary function of PCSK9 on LDLR is through the extracellular pathway in the liver (Stein and Swergold, 2013). Also, the interaction of PCSK9 to the EGF-A domain of LDLR is the key conduit for the clearance of plasma PCSK9 (Grefhorst et al., 2008).

1.3.4 PCSK9 trafficking pathways

ER to Golgi trafficking is a critical step to distinguish mature, well-folded and assembled proteins (cargo) from immature and ER-resident proteins. The transport of cargo proteins from the ER to Golgi (anterograde transport) and from the Golgi to ER (retrograde transport) is mediated by coat protein complex II (COPII) and coat protein complex I (COPI), respectively (Lee et al., 2004). *In vitro* inhibition of COPII vesicle formation has been shown to prevent PCSK9 secretion, suggesting a COPII-mediated mechanism for the export of PCSK9 from the ER to the Golgi (Chen et al., 2013). Specific Sec proteins in vesicles mediate cargo selection and transport direction (McMahon and Mills, 2004). Inner-coat heterodimer Sec23-Sec24 selects and separates cargo proteins into different carriers for ER-to-Golgi transportation in a way that Sec24 interact directly with the sorting signals of either cargo or cargo receptors (Watanabe and Riezman, 2004). SEC24 subunit of the COPII complex has four paralogs, A, B, C and D that mediate ER exit of different proteins. Deletion mutation of each isoform of SEC24 was performed to investigate the specific dependencies of proteins to SEC24 paralogs (Miller and Schekman, 2013). A deletion mutation of Sec24A in mice resulted in a marked decrease in PCSK9 secretion and plasma level of LDL-C without any other effect on physiological functions, growth, fertility rates and survival (Chen et al., 2013). Thus, SEC24A was identified as a crucial and specific cytosolic component of the COPII complex regulating the exit of PCSK9 from the ER. After crossing the Golgi cisternae, PCSK9 reaches the TGN, another major sorting organelle. In the TGN, PCSK9 either binds to LDLR or is sorted into secretory vesicles. The PCSK9-LDLR complex in TGN

directs the LDLR towards late-endosomes/lysosomes for degradation, while PCSK9 that is sorted into vesicles is secreted at the plasma membrane.

A study on normolipidemic subjects demonstrated that more than 30% of PCSK9 in plasma is bound to LDL (Tavori et al., 2013). Also, a direct protein-protein interaction between PCSK9 and apoB100 has been shown (Sun et al., 2012). However, there is no interaction between PCSK9 and apoB100 moiety on VLDL (Kosenko et al., 2013). This may be related to the availability of the binding site on apoB in different lipoproteins (Lagace, 2014). It is also interesting to note that the presence of the N-terminal region of PCSK9 prodomain (residues 31-52) is required for binding the LDL particles in plasma (Kosenko et al., 2013). Importantly, the interaction of PCSK9 and LDL particles decreases the ability of PCSK9 to induce LDLR degradation. It has been reported that overexpression of PCSK9 in hepatocytes leads to an increase in circulating LDL-C independently of LDLR (Benjannet et al., 2004). A comparison between hypercholesterolemic patients with a GOF mutation in PCSK9 (S127R) and patients with a mutation in LDLR (non-functional LDLR) was made to understand the association of LDLR, and the function of PCSK9 on plasma level of apoB100 (Ouguerram et al., 2004). It is possible that the observed effect is only related to the overactive PCSK9 since overexpression of PCSK9 did not cause any change in the secretion/synthesis of apoB100 in LDLR knockout mice (Park et al., 2004). Moreover, FPLC (fast protein liquid chromatography) analysis demonstrated no change in the distribution of cholesterol / lipoproteins in LDLR-deficient mice upon overexpression of PCSK9 (Maxwell and Breslow, 2004). The effect of the absence of PCSK9 on reduction of plasma level of LDL particles (apoB100) is more likely due to the increased uptake of apoB-

containing lipoproteins by LDLR than a decrease in VLDL synthesis (Rashid et al., 2005; Zaid et al., 2008).

Interaction of newly synthesized apoB100 with LDLR in the ER induces apoB degradation and reduces its secretion (Blasiole et al., 2008; Gillian-Daniel et al., 2002). Also, the increase in cell-surface expression of functional LDLR reduces secretion and increases uptake of apoB-containing lipoproteins (Twisk et al., 2000). This suggests that LDLR needs to exit the ER to regulate apoB100 secretion.

Gillian-Daniel et al. (2002) fused the ER-retention sequence, lys-asp-glu-leu (KDEL) at the C-terminus of LDLR to retain the receptor in the secretory pathway. In their study, ER-localized LDLR reduced apoB secretion. However, further analysis is required to better understand the detailed mechanism in the regulation of apoB100 secretion by LDLR and PCSK9 expression.

1.3.5 PCSK9 interacting partners

The C-terminal domain of PCSK9 with about 240-aa, rich in cysteine and histidine, does not bind the LDLR but is essential for its degradation. This suggests that PCSK9 C-terminal domain is a possible interacting site that binds to other proteins involved in PCSK9 trafficking (Zhang et al., 2008). The important role of PCSK9 in the regulation of circulating level of LDL-C underlines the importance of identifying other PCSK9 interacting proteins. It has been reported that unidentified PCSK9-interacting proteins might induce or block PCSK9-LDLR interaction (Surdo et al., 2011). After LDLR, other proteins were found to interact with PCSK9, some of which were new targets routed for degradation, and others were proteins regulating

its function. It is therefore important to understand the different functions of PCSK9 and to identify proteins that can modulate those functions.

LDLR, VLDLR, and apoER2: The first PCSK9 interacting proteins found after LDLR were VLDLR and apoER2, which have the most similar structure to LDLR (Figure 1.3). ApoER2, also known as LDLR-related protein 8 (LRP8), belongs to the LDLR family. ApoER2 is involved in brain development by affecting neuronal apoptosis and mediating reelin signaling pathway (Howell and Herz, 2001). VLDLR is active in several tissues, including heart, skeletal muscles, and adipose tissue. This receptor also interacts with reelin and plays an important role in brain development (Howell and Herz, 2001). PCSK9 interacts with EGF-A–like domains of LDLR, VLDLR, and apoER2 *via* its catalytic domain and induces their lysosomal degradation (Figure 1.9) (Poirier et al., 2008). However, amino acids of EGF-A–like domain of LDLR interacting with PCSK9, Asn^{295}, Glu^{296}, Asp^{310}, Tyr^{315}, and Leu^{318}, are not all the same as those found in VLDLR and apoER2. For example, Leu^{318} is only present in LDLR EGF-A domain and not conserved in VLDLR and apoER2 (Gu et al., 2013). Poirier et al. (2008) demonstrated that the presence of LDLR in cells resulted in less PCSK9 association with VLDLR. They further explained that it might be a competition between LDLR and VLDLR for PCSK9 binding. while this competition was much less or not detectable between LDLR and apoER2.

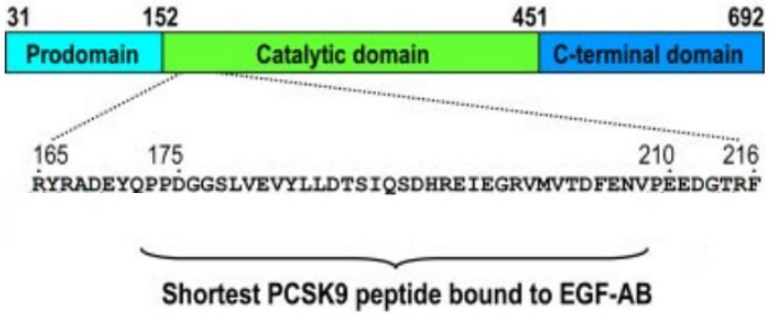

Figure 1.9 Schematic diagram of PCSK9 peptide bound to LDLR-EGFA

The shortest PCSK9 peptide sequence bound to EGF-AB is being shown. Copyright permission has been obtained for the use of the figure in the thesis. License Id: 4652631049028 (adapted from Bottomley et al. (2009).

Annexin A2 (AnxA2): The first identified endogenous partner of PCSK9 that could prevent PCSK9-induced LDLR degradation was Annexin A2 (AnxA2) (Mayer et al., 2008). Annexins are soluble proteins with a protein core containing four calcium-binding sites, which are required to keep their association with membranes (Rescher and Gerke, 2004). Experimental analysis demonstrated the localization of AnxA2 at the extracellular layer of the plasma membrane in different cell lines including tumor cells (Yeatman et al., 1993), endothelial cells (Cesarman et al., 1994), epithelial cells (Patchell et al., 2007) and skin keratinocytes (Ma et al., 1994). Very high level of AnxA2 expression is found at the surface of endothelial cells in a variety of organs including lungs, adrenals, and small intestines, and may explain the reason for PCSK9 inability to cause LDLR degradation in the adrenals (Grefhorst et al., 2008; Seidah et al., 2012). Mayer et al. (2008) demonstrated that AnxA2 interacts with the C-terminal domain of PCSK9 *via* its N-terminal repeat R1. They further suggested a possible competition between AnxA2 and LDLR for interacting

with PCSK9 at the cell-surface (Mayer et al., 2008). Thus, an association of PCSK9 with AnxA2 could reduce its interaction with LDLR, and consequently decrease LDLR degradation. AnxA2 variants were recently found to be associated with LDL-C levels in human, and thus highlights the importance of this protein as a potential therapeutic target for LDL-C lowering (Fairoozy et al., 2017).

APLP2: Amyloid precursor protein (APP) and its close family member, amyloid precursor-like protein 2 (APLP2), interact with the C-terminal domain of PCSK9 *via* their large extracellular domains in a pH-dependent manner (DeVay et al., 2013). Different tissues and cell-types express APP and APLP2, single-pass transmembrane proteins, which are homologous in function (Wasco et al., 1993) and play roles in synaptic plasticity, synaptogenesis, neurite growth and neuronal differentiation (Heber et al., 2000). DeVay et al. (2013) suggested that APP and APLP2 regulate the level of LDLR in a clear manner. They further explained that APP is not involved in direct regulation of the PCSK9 function. However, it could protect PCSK9 from lysosomal degradation by competing with APLP2 for the binding site on PCSK9. APLP2 functions as a new bridge for delivering multiple PCSK9-targets to the lysosome for degradation. It also facilitates the postendocytic transport of PCSK9/APLP2 complex to the lysosomes (DeVay et al., 2013). However, Butkinaree et al. (2015) reported that overexpression or deficiency of APLP2 in human hepatocyte cell lines or mouse liver, respectively, does not affect on PCSK9 function, level of LDLR, and mouse plasma cholesterol level. Interestingly, APLP2 can interact with sortilin, another PCSK9 binding partner, which will be discussed in this chapter.

ApoB: apoB is the ligand of LDLR and the sole protein component of LDL, which is cleared from circulation *via* LDLR. Therefore, an increase in LDLR degradation by PCSK9 results in increased plasma level of apoB-lipoproteins, which is associated with coronary artery disease (Sniderman et al., 2010). Moreover, Sun et al. (2012) demonstrated that PCSK9 directly, in an LDLR-independent fashion, interacts with apoB and regulates its production and secretion in the ER. The physical interaction between PCSK9 and apoB prevents intracellular degradation of apoB through the autophagosome/lysosome pathway and increases its secretion in apoB-lipoprotein particles (Sun et al., 2012). In consequence, increased circulating level of apoB-containing particles leads to an increase in plasma level of cholesterol (Sun et al., 2012). More recently, Sun et al. (2018) showed that PCSK9 deficiency in animals lacking the LDLR reduces the secretion of apoB by modulating the autophagy signaling pathway and increasing hepatic autophagy flux. The potential PCSK9-apoB-autophagy pathway is novel with important implications as it has important effects on lipoprotein metabolism.

Non-acetylated BACE1: PCSK9 can interact with non-acetylated β-site amyloid precursor protein (APP)-cleaving enzyme 1 (BACE1) in the ER and mediates its degradation in the early secretory pathway, most probably in a post-ER compartment, while acetylated BACE1 can exit from the ER and traffic to the Golgi (Jonas et al., 2008). Moreover, Jonas et al. (2008) demonstrated that the addition of purified PCSK9 in cell culture media could induce internalization and degradation of BACE1 with a similar mechanism as LDLR. BACE1 is a transmembrane aspartyl protease that displays the known functional characteristics of APP β-secretase (Vassar et al., 1999). β-Secretase cleavage of APP by BACE1 lead to the formation

of the soluble fragment (sAPP) and a membrane end (-CTF) (Vassar et al., 1999). Cleavage of APP-CTF by λ-secretase releases predominant amyloidogenic fragments, amyloid Aβ-40, and Aβ42 peptides, which are the major cause of Alzheimer disease (AD) pathology (Hardy, 2006). Jonas et al. (2008) reported that deficiency of PCSK9 results in increased steady-state protein level of BACE1 and generation of Aβ in mouse brain. They further proposed two different mechanisms for BACE1 degradation by PCSK9. The first mechanism of BACE1 degradation was dependent on the catalytic activity of PCSK9 and was observed in the intracellular pathway of transfected cells with full-length PCSK9, while the latter is *via* the extracellular pathway. However, it is still not known if the first mechanism of BACE1 degradation is *via* the catalytic activity (very unlikely as several studies demonstrated no or extremely low activity of mature PCSK9) of PCSK9 or other unknown proteases. Ko and Puglielli (2009) identified two-proteins, acetyltransferases 1 (ATase1) and ATase2, which regulate ER-Golgi intermediate compartment (ERGIC) based acetyltransferases. The authors further asserted that these two enzymes are involved in regulating the steady-state levels of BACE1 by protecting it from degradation by PCSK9 (Ko and Puglielli, 2009).

These results suggest that inhibition of PCSK9 to treat hypercholesterolemia could increase the risk of the AD. However, another study was published with controversial results (Liu et al., 2010). The results of Liu et al. (2010) demonstrated that knockout of PCSK9 in mouse brain is not leading to any change in the steady-state protein level of BACE1. In addition, their analysis demonstrated no change in the total level of APP-CTF or Aβ40 upon knockout of PCSK9 (Liu et al., 2010).

PCSK9 regulates neuronal apoptosis by keeping it at a low level in cell lines (Wu et al., 2014). PCSK9 inhibitors may have a protective role for AD, but more detailed role of PCSK9 in brain physiology still needs to be clarified.

LRP1: The low-density lipoprotein receptor-related protein 1 (LRP1) resembles LDLR and is responsible for the clearance of apoE-enriched lipoproteins such as chylomicrons and VLDL remnants from plasma (Kowal et al., 1989). Similar extracellular domain and charge distribution of LDLR and LRP1 (Herz and Bock, 2002) suggested the possibility of PCSK9 interacting with LRP1. Park et al. (2004) reported that the protein level of LRP1 was not changed by overexpression of PCSK9 in mouse liver. Lagace et al. (2006) found a link between LRP1 and PCSK9 in LDLR-deficient mouse embryonic fibroblasts, which might result in the uptake of PCSK9 by LRP1 at high concentrations of PCSK9. Also, Canuel et al. (2013) reported that PCSK9 interacts with LRP1 and induces its degradation in HEK293 and HepG2 cells. They further demonstrated that LRP1 competes with LDLR for interaction with PCSK9. However, no change in LRP1 levels was found in *PCSK9* knockout mice (Canuel et al. 2013). Moreover, reduction in cell-surface expression of LRP1 upon direct interaction with PCSK9 was observed, in mouse peritoneal macrophages (MPM) lacking apoE and expressing hPCSK9 exclusively in macrophages (Giunzioni et al., 2016). Secreted PCSK9 from macrophages and reduced level of LRP1 resulted in an increased level of pro-inflammatory markers and reduced those of the anti-inflammatory monocytes in plaques (Giunzioni et al., 2016). However, the increased level of pro-inflammatory monocytes in lesions did not lead to any change in lesion size of atherosclerotic plaques (Giunzioni et al., 2016). PCSK9 protein was not detected in lesions of *Ldlr* knockout mice and did not

affect macrophage, suggesting that all PCSK9 effects were dependant of LDLR (Giunzioni et al., 2016).

Sortilin: Mature PCSK9 is transported from the ER to the Golgi apparatus through the Sec24A subunit of the coat protein complex II (COPII)-coated vesicles and from the Golgi to the plasma membrane *via* sortilin receptor (Gustafsen et al., 2014). However, it was later reported that plasma total PCSK9 level in sortilin knockout mice is similar to wild type mice, suggesting that sortilin is not critical for PCSK9 secretion (Butkinaree et al., 2015). Therefore, more experiments are needed to clarify the PCSK9 secretion pathway.

Sortilin is a sorting receptor, from the family of vacuolar protein sorting 10 protein (VPS10P) domain receptors, which contains a ten-bladed β-propeller that forms a hollow channel for binding to the soluble ligands (Kjolby et al., 2010). Moreover, it consists of a short cytoplasmic tail for interaction with subcellular sorting adaptor proteins. This receptor has previously been appreciated for its essential role in intracellular sorting of brain-derived neurotrophic factor (Chen et al., 2005) as well as lipoprotein metabolism (Nielsen et al., 1999) and cardiovascular health (Nilsson et al., 2008). Co-localization of sortilin with PCSK9 was observed in the TGN (Gustafsen et al., 2014). Also, the lack of sortilin in mice resulted in a robust decrease in circulating level of PCSK9 and an increase in the hepatic level of LDLR (Gustafsen et al., 2014). However, Butkinaree et al. (2015) reported that deficiency/overexpression of sortilin in cells or mice did not alter the plasma level of PCSK9 and its function on LDLR degradation (Butkinaree et al., 2015). Thus, the detailed mechanism of sortilin and PCSK9 interaction and its functional role in lipoprotein metabolism needs more investigation.

CD36: Cluster of differentiation 36 (CD36), a scavenger receptor, is involved in different cellular functions including the cellular uptake of long-chain fatty acids and storage of TG (Abumrad et al., 1993). Presence of hypertrophic adipocytes and increased cellular uptake of free fatty acids (FFAs) in adipose tissue of *Pcsk9* knockout mice suggested the presence of higher level of CD36 and/or VLDLR (Demers et al., 2015; Roubtsova et al., 2011). Our group found that CD36 is a PCSK9-interacting protein (Demers et al., 2015). Our data indicated that knockdown of endogenous PCSK9 in hepatic cells or knockout of Pcsk9 in mice resulted in a strong increase (>3 fold) of CD36 protein levels in hepatic cells as well as mouse liver and adipose tissue. Increased level of hepatic CD36 protein was correlated with an increased uptake of fatty acid and accumulation of TG and lipid droplets in *Pcsk9*$^{-/-}$ mice (Demers et al., 2015). We further demonstrated that direct interaction of PCSK9 with CD36 results in CD36 degradation *via* both ubiquitin-proteasome and lysosomal systems in the liver and visceral adipose tissue (Demers et al., 2015). Our results highlighted the importance of PCSK9 in TG metabolism beyond its role in regulating plasma LDL-C, which is reviewed by Moore and Goldberg (2016).

GRP94: Glucose-regulated protein 78 (GRP78), GRP94, calnexin, and calreticulin are ER-resident proteins (Lewis et al., 1985) that are involved in maintaining cellular integrity under physiological or stress conditions (Ni and Lee, 2007). ER is the most important organelle for the synthesis and folding of proteins (Lee, 1992). Chaperones are group of proteins that assist in protein folding. Receptor-associated protein (RAP) is a chaperone of LDLR family members. RAP has been shown to bind with LDLR and protect the receptor from being bound by their ligands (Willnow et al., 1996). There is no strong evidence that shows RAP

prevents PCSK9 binding to LDLR. However, it is possible that RAP prevents LDLR-PCSK9 binding in the ER and protects LDLR from degradation before reaching to the Golgi (Shan et al., 2008).

GRP94, also known as HSP90B1, GP96 (Koch et al., 1985), endoplasmin (Smith and Koch, 1987) or ERp99 (Lewis et al., 1986), is a high-capacity calcium- and peptide-binding protein (Lee, 2014), which is involved in protein folding within the secretory pathway. Poirier et al. (2015) reported that interaction of PCSK9 with GRP94 leads to the blockade of PCSK9-induced LDLR degradation and consequently regulate plasma level of cholesterol in mice. The group of Dr. Mayer further explained that GRP94 is an endogenous inhibitor of PCSK9, which protects LDLR from degradation by preventing early binding of PCSK9 to the LDLR within the ER of hepatocytes (Poirier et al., 2015).

Resistin: Resistin is an adipocyte-derived hormone (adipokine), detectable in adipocytes and blood, which is encoded by the *RETN* gene (Steppan et al., 2001). The molecular function of resistin is not yet completely understood, although the association of its gene with metabolic diseases was reported previously (Steppan and Lazar, 2004). The similar structure between the C-terminal domain of PCSK9 and resistin suggested that they might form aggregation complexes to target/compete for a common receptor, likely LDLR (Hampton et al., 2007). Furthermore, the study of Melone et al. (2012) demonstrated that resistin increases RNA and protein level of PCSK9, and thereby increases LDLR degradation in HepG2 cells. The authors explained that circulating resistin regulates PCSK9 expression positively, which in turn, downregulates LDLR in hepatocytes of obese subjects (Melone et al., 2012). Li et al. (2015) demonstrated that there is a direct link

between plasma level of resistin and PCSK9 level in coronary artery disease patients with healthy body weight. Costandi et al. (2011) suggested that resistin might be a proper approach for reducing plasma level of TG-rich lipoproteins due to its direct deleterious role on human hepatic lipid and lipoprotein regulation. They showed that treatment of human hepatocytes with resistin increases VLDL and apoB secretion because of increased microsomal triglyceride transfer protein (MTP) activity and induction of hepatocyte insulin resistance (Costandi et al. 2011). In addition, the association of resistin with the hypertriglyceridemic condition was further confirmed by determining the effect of resistin on VLDL production (Rashid and Kastelein, 2013) and protein level of TNF-α (Ferri and Ruscica, 2016). The similarity in the structure of resistin and PCSK9 and their biological activity suggest the possibility of a resistin-PCSK9 association. However, the direct interaction between them has not yet been observed (Ricci et al., 2017).

Heparan sulfate proteoglycans (HSPGs) and Glypican 3 (GPC3): The liver cell surface is covered with HSPG receptors that mediate the clearance of triglyceride-rich lipoproteins. Heparan sulphate is a repeating linear disaccharide unit of sulphated uronic acid and glucosamine (Foley and Esko, 2010). It is mainly composed of glucuronic acid 1-4 linked to glucosamine but also contains substantial levels of iduronic acid (Hileman et al., 1998). It has recently been shown that the PCSK9 prodomain contains a cluster of amino acid residues that are aligned with consensus sequences for interaction with HSPG (Gustafsen et al., 2017). HSPG captures PCSK9 and facilitates its subsequent PCSK9-LDLR complex formation, thereby directing LDLR to lysosomes for degradation (Gustafsen et al., 2017). Importantly, their results demonstrated that HSPG binding was required for PCSK9-

induced LDLR degradation in HepG2 cells and BALB6/cJRj mouse liver. Gustafsen et al. (2017) found potent inhibitors of PCSK9-HSPG interaction using heparin mimetics molecules, and an antibody directed explicitly at the HSPG-binding site in PCSK9.

GPC3 is one of the six members of the glypican family, a subgroup of HSPG family, and plays an important role in cell division and growth. It is bound to the cell surface of the plasma membrane through a glycosylphosphatidylinositol anchor on its C-terminal domain along with two heparan sulfate side chains (Filmus and Selleck, 2001). GPC3 mRNA is abundant in liver, small intestine, and kidney where PCSK9 is also significantly expressed (Ly et al., 2016). Ly et al. (2016) indicated that GPC3 interacts with pro-PCSK9 and immature LDLR in hepatic cells. They further showed that PCSK9 could degrade GPC3 independent of LDLR, possibly through an LRP1-dependent mechanism. Their results demonstrated that PCSK9-GPC3 interaction competes with PCSK9-LDLR binding on the cell-surface of hepatic cell lines (HepG2 and Huh7 cells), which in turn reduces the PCSK9-induced LDLR degradation and increases the LDL uptake (Ly et al., 2016).

Sec24a, Secretion associated Ras-related GTPase 1B (SAR1B) and Matrix metalloproteinase-2 (MMP-2): SEC24 protein, a component of COPII coat protein complex, plays a crucial role in vesicle trafficking from the ER to Golgi. This has been described with more details in section 1.34 of the thesis. Chen et al. (2013) showed that SEC24A-deficient mice exhibit normal survival and development but have about 40% reduction in HDL-C, and about 60% reduction in LDL-C in their plasma. Interestingly, SEC24A deficiency increased liver LDLR levels *via* reduced

secretion of PCSK9, which led to the accumulation of PCSK9 in the ER (Chen et al., 2013).

The SAR1B protein belongs to the Sar1-ADP-ribosylation factor family of small GTPases, which is involved in the COPII-dependent transport of proteins from the ER to the Golgi apparatus (Gürkan et al., 2006). Mutations in the *SAR1B* gene have been linked to lipid absorption disorders and chylomicron retention disease (Roy et al., 1987; Jones et al., 2003). In an *in vitro* study using intestinal Caco-2/15 cells, Sar1B overexpression reduced the expression of intestinal LDLR and PCSK9 (Sane et al., 2015).

Matrix metalloproteinase-2 (MMP-2) is zinc-requiring endopeptidase that degrades extracellular matrix proteins. This enzyme also has essential roles in many functions, such as cell growth and migration, angiogenesis, inflammation, and metabolism (Parks et al., 2004; Kessenbrock et al., 2010). It has been shown that MMP-2 binds PCSK9 and cleaves PCSK9 pro- and catalytic-domains in mouse Hepa1-c1c7 cells (Wang et al., 2015). As a result, MMP-2 protects the LDLR from PCSK9-induced degradation. In this study, MMP-2 overexpression did not change LDLR protein basal level but reduced PCSK9-induced LDLR degradation in mouse hepatic cells (Wang et al., 2015).

1.4 Atherosclerosis

Atherosclerosis is a chronic inflammatory disease that results from disruption of lipid homeostasis and a maladaptive immune response prompted by the accumulation of cholesterol-laden macrophages in the arterial vessel walls (Moore et al., 2013). It is the underlying cause of heart attacks, strokes, ischemic heart pain,

peripheral vascular disease, which are the principal causes of death worldwide (Mathers and Loncar, 2006; Weber and Noels, 2011). The development of atherosclerosis can begin in early childhood and continue throughout life. Different factors such as high-fat diets, hypertension, smoking, stress, diabetes, obesity, high level of plasma LDL-C, and lack of physical activity can accelerate atherosclerosis. Among these factors, a high plasma level of LDL-C is one of the most critical factors in the development of atherosclerosis and the cause of familial hypercholesterolemia (Nordestgaard et al., 2013).

Elevated plasma level of LDL-C, leads to its accumulation in the sub-endothelial layer of arteries, particularly regions in which blood flow is disturbed by bends or branch points (Williams and Tabas, 1995). Accumulated LDL-C can undergo oxidative modifications, becoming oxidized LDL (oxLDL) and take on properties of damage-associated molecular patterns (Parthasarathy et al., 1988). A large variety of stressful events and diseases such as hypertension, diabetes, drugs, and toxins can accelerate this process. oxLDL activates vascular cells such as endothelial cells, macrophages, and smooth muscle cells (SMC) *via* binding to toll-like receptors (TLRs) and scavenger receptors including lectin-like oxLDL receptor 1 (LOX-1) and CD36 (Tsukamoto et al. 2002). They also activate monocyte chemotactic protein-1 (MCP-1) and adhesion molecules, mainly intercellular adhesion molecule-1 and vascular cell adhesion molecule-1, on the SMCs that may facilitate the accumulation of monocytes within the vascular wall (Vielma et al. 2004). Monocytes differentiate into macrophages that express scavenger receptors and engulf oxLDL, which leads to marked accumulation of cholesterol, converting them to foam cells and initiate atherosclerotic lesion development (Proudlock et al., 1973).

Foam cells secrete different pro-inflammatory mediators and trigger more monocytes and other inflammatory cells including T-cells, B cells, dendritic cells, and mast cells to induce plaque formation (Jonasson et al., 1986). This immune reaction leads to a fibroproliferative response in which the extracellular matrix (ECM) plays an important role. The ECM mainly contains collagen and elastic microfibrils (elastin, fibrillins), glycoproteins and proteoglycans that provide structural support to the atrial wall. During atherosclerotic plaque development, pronounced changes have been observed in the ECM composition. SMCs and accumulated monocytes and macrophages produce matrix metalloproteinases (MMPs), a large family of proteolytic enzymes, which play an important role in atherosclerosis by degrading the ECM and weakening of the vascular wall.

Plaque evolution and proliferation of macrophages can lead to the formation of advanced and unstable plaques (Figure 1.10) (Kolodgie et al., 2001). oxLDL also reduces nitric oxide bioavailability and synthesis that can impair endothelium-dependent arterial relaxation, which is considered as a risk factor for atherosclerosis disease (Kugiyama et al., 1990). Furthermore, oxLDL induces apoptosis of arterial smooth muscle cells (Björkerud et al., 1996). Apoptotic vascular smooth muscle cells may contribute to the pathogenesis of atherosclerosis by generating fatty streaks that develop into plaques (Kockx, 1998), or by reducing synthesis and secretion of extracellular matrix proteins that increase the risk of plaque instability and rupture (Bauriedel et al. 1999).

Atherosclerotic plaques consist of a lipid core containing many constituents like foam cells, leukocytes, macrophages, lipoproteins and TG that are surrounded by fibrous tissue in thickened intima (Ross, 1999). Formation of atherosclerotic

plaques in human is usually in the aorta, coronary, carotid and cerebral arteries (Lusis, 2000). Disease progression leads to the build-up of plaques in a sub-endothelial layer of the tunica intima, vessel thickening and narrowing of the lumen (Wilkinson et al., 2009). Atherosclerotic plaques often remain stable for a long time. Further growth of the plaques in the artery walls leads to plaque calcification and blood flow obstruction. The destruction of extracellular matrix from the fibrous cap, covering the necrotic core of atherosclerotic plaques, can initiate plaque rupture. Rupture of atherosclerotic plaques can trigger thrombus formation (McGill et al., 2000), and consequently leading to vessel obstruction in vital organs, such as the heart (MI), and the brain (strokes) (Chen et al., 2016).

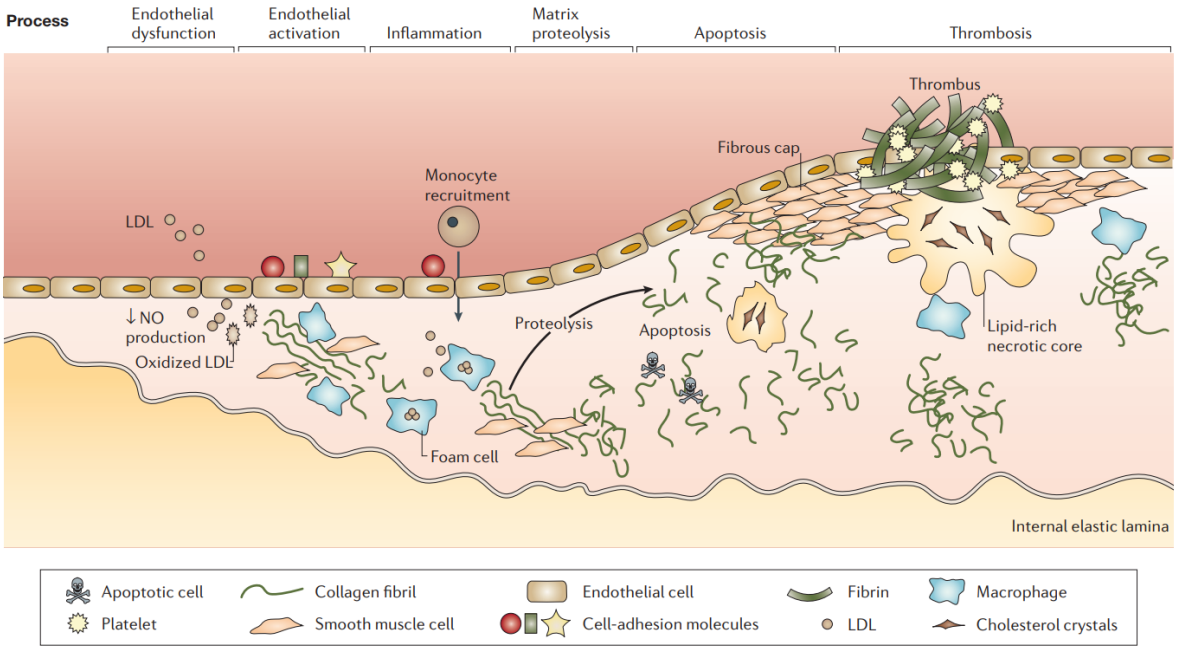

Figure 1.10 Molecular mechanism of plaque formation in the artery

High level of LDL and endothelium barrier dysfunctions increase the entry of LDL particles to the artery wall, initiating an inflammatory response, recruiting monocytes, which then differentiate into macrophages. Macrophages ingest LDL particles and transform into foam cells, which trigger more monocytes and results in the development and growth of plaque formation. Degradation of collagen

fibrils through proteolysis and apoptosis of vascular smooth muscle cells lead to building up of plaques containing a fibrous cap and a lipid-rich core (adapted from Choudhury et al., 2004).

1.4.1 Animal models of atherosclerosis

Several animal species have been used as an experimental model of atherosclerosis, such as rabbits (Konstantinov and Jankovic, 2013), mice, pigs and nonhuman primates (Fuster et al., 2012; Kapourchali et al., 2014). The vast majority of these animal models need to consume high fat and high cholesterol diet for plaque development. A valuable animal model should have different criteria such as being easily accessible, reasonable maintenance cost, easy to handle with well-known genetic characteristics, and resembles human pathophysiology to be used in medical and pharmaceutical research. The ideal atherosclerosis animal model develops lesions in a spontaneous manner by consuming a high-fat/cholesterol diet as it occurs in humans. Moreover, they should share a similarity in the topography of the lesions with humans (Getz and Reardon, 2012).

The mouse is the predominant experimental model of atherosclerosis, because of its fast reproduction, ability to develop atherosclerotic plaques in a reasonable period of time, and ease of genetic manipulation (VanderLaan et al., 2004). However, unlike human, the lipid profile of mice is made of a high level of HDL-C, due to the lack of cholesteryl ester transfer protein (CETP), shallow concentration of atherogenic LDL-C and VLDL-C, making them resistant to the development of atherosclerosis (Vergeer et al., 2010). Therefore, manipulation of the genes that are involved in lipid metabolism is required to overcome this issue (Getz and Reardon, 2012). For example, mice deficient in LDLR (*Ldlr*$^{-/-}$ mice) have

lower LDL-C clearance and therefore, high plasma level of cholesterol. Consumption of high fat/cholesterol diet leads to faster growth of atherosclerotic plaque phenotype in these two mice models. Véniant et al. (2001) showed that the total plasma cholesterol levels in *apoe*$^{-/-}$ mice are higher than in *Ldlr*$^{-/-}$ mice on a regular chow diet. They indicated, however, that the total plasma cholesterol levels in *Ldlr*$^{-/-}$ and *apoe*$^{-/-}$ mice homozygous for the *hapoB-100* transgenic allele fed a regular diet are approximately similar but more atherosclerotic lesions appeared in *Ldlr*$^{-/-}$; *apoB*$^{100/100}$ mice than the *apoe*$^{-/-}$; *apoB*$^{100/100}$ mice. They further explained that the differences in atherosclerosis susceptibility are due to the possible effect of lipoprotein size and number on atherosclerosis, independent of the plasma cholesterol levels (Véniant et al., 2001).

Table 1.1 Overview of animal models of atherosclerosis *

Model	**Lipid profile**	**Advantages & Limitations**
Rabbit	VLDL 4 ug/ml LDL 8 ug/ml HDL 18 ug/ml	+ Similar lipoprotein metabolism with humans - Lack of hepatic lipase - No atherosclerotic lesions in the abdominal aorta
Pig	VLDL 5 ug/ml LDL 39 ug/ml HDL 52 ug/ml	+ Many similarities of the cardiovascular system with humans + Develop spontaneous atherosclerotic lesions - Required long-time consumption of a rich cholesterol diet to develop atherosclerotic lesions - High cost, not easy to handle
Wild Type mice C57BL/6	VLDL 8 ug/ml LDL 21 ug/ml HDL 97 ug/ml	+ No genetic modification needed, fast and cost-effective - Different lipid metabolism compared to human

		- Resistant to atherosclerosis development due to high level of HDL
Apoe knockout mice	↑↑ VLDL** ↑ LDL ↑ HDL	+ Develop atherosclerotic lesions with normal diet - Different lipid metabolism compared to human - ApoE plays a role in plaque development
Ldlr knockout mice	↑ VLDL ↑↑ LDL = HDL	+ Human-like lipid profile - Requires high-fat diet - Varies in atherosclerotic plaques development - No spontaneous atherosclerotic development
Apoe/Ldlr double-knockout mice	↑↑ VLDL ↑↑ LDL ↓ HDL	+ Develop atherosclerotic lesions with normal diet - Not suitable for studying the effect of PCSK9 as both genes are required for PCSK9 function
ApoE3-Leiden mice	↑↑VLDL ↑ LDL ↑ HDL	+ It has functional apoE + Similar lipoprotein profile to human - Limited accessibility and need several time-consuming and costly backcrosses
AAV-PCSK9 mice	↑ VLDL ↑ LDL = HDL	+ No genetic modification needed, fast and cost-effective + Similar lipoprotein profile to human - PCSK9 express consistently at high levels which make this model difficult to study PCSK9 regression (our 2nd study)
Dog, Hamster, Birds, Guinea pigs	These models have not extensively studied or used due to their significant amount of limitations	

* Contents are compiled from Veseli et al. (2017), Kapourchali et al.(2014) and Yin et al. (2012).

** Lipid profile in genetically modified mice models is expressed compared with wild-type mice model.

***ApoE* knockout mice:** apoE, a structural component of all lipoprotein particles except LDL, is a glycoprotein with a molecular weight of ~34 kDa, mainly synthesized in the liver and the brain. ApoE not only serves as a ligand for cell surface receptors to clear chylomicrons and VLDL remnants from plasma but also functions in cholesterol homeostasis, dietary absorption and biliary excretion of cholesterol and local redistribution of cholesterol (Mahley, 1988). In addition, it provides anti-oxidative, anti-proliferative, and anti-inflammatory effects after its synthesis by monocytes and macrophages (Curtiss and Boisvert, 2000). Apo*e* knockout was the first developed mouse model with genetic modification (Piedrahita et al., 1992). They were born with the expected frequency and similar body weight as wild-type mice (Plump et al., 1992). Apo*e* knockout mice demonstrated a 5-fold increase in plasma level of cholesterol (400 mg/dl, 10.34 mmol/l) compared to the wild-type mice despite consuming a low-fat diet (Plump and Breslow, 1995). On a high-fat diet, plasma cholesterol level in apoe deficient mice is about 1821 mg/dl (47mmol/l). This marked hypercholesterolemia is primarily due to elevated levels of VLDL, IDL, and chylomicrons (Zhang et al., 1992). The vast majority of remnant lipoproteins in *apoe* knockout mice contain apoB48. Lipoproteins bind to the ligand-binding domain that consists of seven LDLR type A (LA) repeats. LDL binding requires LA repeats 3–7, which interact with apoB100 on LDL (Brown et al., 1981; Russell et al., 1989). The binding of VLDL and VLDL-remnants involves LA repeats 4 and 5, which associate with apoE. Another clearance pathway for VLDL is through LRP, which requires apoE as a ligand.

In this genetically modified mouse model, atherosclerotic lesions are developed spontaneously in the aortic root, arch, and different branch points along

the aorta (Smith and Breslow, 1997). Moreover, feeding the mice with a high-fat diet for 10–14 weeks profoundly increased plasma level of total cholesterol (1000 mg/dl) and accelerated the formation of plaques in the sinus of the aorta, because apoe deficient mice are highly responsive to dietary fat and cholesterol (Reddick et al., 1994).

There are different factors that limit the usage of this model. First, they have a different lipid metabolism compared to the human. In apoe deficient mice, most of the plasma cholesterol is accumulated in VLDL particles, unlike humans, where the majority of cholesterol is in LDL (Knouff et al., 1999). Secondly, it has been observed that apoE is not only involved in the clearance of plasma lipoproteins but also provides atheroprotective properties (Getz and Reardon, 2009). Thus, plaques appearance in the aorta of apoe deficient mice might not be only related to its plasma lipid levels.

***Ldlr* knockout mice:** To overcome the limitations of the *apoe*$^{-/-}$ mice, *Ldlr* deficient mice were generated (Sanan et al., 1998). LDLR, with a molecular weight of 160 kDa, is a membrane receptor with the primary function of cholesterol-rich LDL clearance. It also mediates the endocytosis of apolipoprotein B48- and E- containing lipoproteins such as chylomicron remnants and small size VLDL particles (Véniant et al., 2001). Therefore, it is easier to ascribe the effect of LDLR deficiency to lipoprotein homeostasis than any other process such as inflammation or cell proliferation (Getz and Reardon, 2012). The first *Ldlr*$^{-/-}$ mice model was developed in 1993 (Ishibashi et al., 1993). Impaired clearance of LDL in *Ldlr*$^{-/-}$ mice fed standard diet, resulted in an elevated plasma level of LDL, which led to a mild increase in plasma level of total cholesterol (250 mg/dl) (Ishibashi et al., 1993). *Ldlr*$^{-/-}$ mice fed

high-fat diet demonstrated a severe increase in plasma level of total cholesterol (900 mg/dl), accumulation of VLDL and LDL in plasma and extended atherosclerotic plaques in the aorta (Merat et al., 1999). Plaque development is a time-dependent process, which starts in the proximal aorta and continues by spreading toward the distal aorta. Advanced lesions in *Ldlr*$^{-/-}$ mice fed with a Western-type diet contains a collagen-rich fibrous cap (Hartvigsen et al., 2007).

LDLR mutations are more common in humans than those of apoe (Hobbs et al., 1990). The absence or deficiency in the function of the *LDLR* gene is responsible for the high prevalence of the FH phenotype (Defesche, 2004). *Ldlr*$^{-/-}$ mice and human subjects that are suffering from FH due to mutations in LDLR share similar lipid profile as well as similar characterization in the development of lesions in aortic valves and the aortic root (VanderLaan et al., 2009). Mice lacking LDLR compared to the apoE-deficient mice are more susceptible to diabetes and obesity. Thus, Ldlr$^{-/-}$ mice are an appropriate model for studying the association between diabetes and atherosclerosis (Merat et al., 1999).

The *Ldlr* knockout mice model has its own drawbacks, making it an imperfect model for studying atherosclerosis. First, *Ldlr* knockout mice, compared to the *apoE* deficient mice, are not an appropriate model for studying the molecular mechanisms in restenosis following angioplasty (Ali et al., 2006), since they are resistant to the injury-induced neointimal formation (Tian et al., 2006). The second problem of LDLR deficient mice is due to its limitation in developing atherosclerotic lesions when fed a standard diet (Herijgers et al., 1997). Also, *Ldlr*$^{-/-}$ mice fed with various concentration of dietary cholesterol respond differently regarding atherosclerotic plaques development (Ma et al., 2012). This caused difficulty in determining the

standard characteristics of the models developed in different laboratories. In most cases, the genetic background of the parental strain is C57BL/6 mouse, but it could be 129 strain. Thus, it is important to analyze the genetic background of the parental strain to ensure that it does not bias the results.

***Apoe/Ldlr* double-knockout mice:** Shortly after the development of single *apoe*$^{-/-}$ and *Ldlr*$^{-/-}$ mice, a new mouse model with a double knockout of *apoE* and *Ldlr* was generated to accelerate the development of plaques in the aorta (Bonthu et al., 1997). A noticeable increase was detected in the spontaneous formation of atherosclerotic plaques and progression of atherosclerosis in double apoe/Ldlr knockout mice compared to the *apoe*$^{-/-}$ mice (Witting et al., 1999).

The liver in mice produces two types of apolipoprotein B, apo B-100, and apo B-48 that are incorporated into VLDL (Scott, 1989). VLDLs that contain apo B-100 can be cleared from plasma by LDLR (Brown and Goldstein, 1983). The clearance of apo B-48 particles from plasma depends on their ability in accepting large amounts of apo E, which is a ligand for the chylomicron remnant receptor and the LDLR (Mahley, 1988). Elevated plasma level of apoB48 and apoB100 has been reported in *apoe/Ldlr* double knockout mice (Ishibashi et al., 1994). Without considering the high level of both types of mouse apoB, no significant difference was observed in the lipoprotein profile of *apoe*$^{-/-}$ and *apoe/Ldlr* double knockout mice (Caligiuri et al., 1999). The advantages of double *Ldlr/apoe* knockout mice over the mice deficient for *apoe or Ldlr* alone is its (Jawien et al., 2004). Therefore, this mouse model is appropriate for evaluating the effect of new treatments on atherosclerosis. However, they are not suitable for studying the effect of PCSK9 regression on atherosclerosis because apoE and LDLR, both are required for

increasing the LDLR expression by inhibition of PCSK9 function (Ason et al., 2014; Denis et al., 2012). Ason et al. (2014) reported a minimal atheroprotective effect of PCSK9 inhibition in *Ldlr*$^{-/-}$ and *apoe*$^{-/-}$ strains. They suggested that the presence of apoE is needed for the uptake and intracellular trafficking of LDLR-bound lipoproteins. In this situation when there is no shuttling of the LDLR into the lysosomal degradation pathway, PCSK9 inhibition cannot be effective for rescuing the LDLR from degradation (Ason et al., 2014).

ApoE3-Leiden mice: apoE3-Leiden mice model is attributed to the genetic form of hyperlipidemia and developed by isolation of a DNA construct from the APOE3-Leiden proband, which contains apoE gene, and all regulatory elements (Lutgens et al., 1999). The apoE3-Leiden mutation causes impaired VLDL-TG secretion (Mensenkamp et al., 2001), and apoE3-Leiden transgenic mice were generated to study the effect of the apoE3-Leiden mutation *in vivo*. ApoE3-Leiden mice fed a Western-type diet, demonstrated a high plasma level of total cholesterol and triglycerides that is due to the elevated level of VLDL and LDL particles. Thus, apoE3-Leiden mice demonstrate a similar lipoprotein profile to human (Van Vlijmen et al., 1994). Since apoE3-Leiden mice are able to synthesize functional apoE, it can overcome the drawbacks of *apoe*$^{-/-}$ mice in the inflammatory process. Therefore, it serves as a suitable model for studying the associated factors in the metabolism of apoE and high level of lipid in plasma (Gijbels et al., 1999). ApoE3-Leiden mice (37±0.6 weeks old) can develop early foam cell lesions after receiving standard mouse chow diet for 9 months. If they are fed high-fat/high-cholesterol diet, they will develop advanced atherosclerotic lesions in the aorta and large vessels after 6 months (Lutgens et al., 1999). ApoE3-Leiden mice and humans demonstrated

similar vascular remodeling upon venous bypass grafting. This resulted in the conclusion that this mouse model is appropriate for evaluating the vascular problems that might occur after a clinical procedure of bypassing the obstruction of an atherosclerotic artery (Lardenoye et al., 2002). However, this model did not show any critical events, like thrombus formation and/or plaque rupture, which are the significant occurrences of human atherosclerosis (Lutgens et al., 1999).

AAV-PCSK9 mice: A new mouse model of atherosclerosis without any germline genetic engineering was developed in 2014 by two independent research groups (Bjoerklund et al., 2014; Roche-Molina et al., 2015). The so-called Adeno-associated virus (AAV)-PCSK9 is a fast and cost-effective mouse model of atherosclerosis, which can be used for different purposes. The function of PCSK9 in inducing the lysosomal degradation of LDLR and increasing the plasma concentration of LDL (Li et al., 2007) has been explained extensively earlier.

AAV is one of the best candidates among viral vectors (Daya and Berns, 2008) to cause long-term transgene expression in mice, non-human primates and humans (Zsebo et al., 2013). Stable mRNA expression of PCSK9 was detected in mouse liver after a single intravenous injection of AAV serotype 8, a liver tropism, expressing a mutant form of human (D374Y)- or mice (D377Y) PCSK9 (Bjoerklund et al., 2014). This resulted in ~10000-fold increase in plasma level of PCSK9 one-month post-injection of low dosage ($2.0X10^{10}$) of virus (Bjoerklund et al., 2014). High plasma level of PCSK9 remained stable even 1 year after viral infection. AAV-$PCSK9^{D374Y}$ mice, fed western-type diet, demonstrated a very high plasma level of cholesterol (1165 mg/dl), which was distributed equally between VLDL and LDL particles (Roche-Molina et al., 2015). Moreover, atherosclerotic lesion formation was

observed in the aorta in a dose-dependent manner (Bjoerklund et al., 2014; Roche-Molina et al., 2015). Remarkably, aortic lesions further developed to the fibro-atheromatous stage (Bjoerklund et al., 2014; Roche-Molina et al., 2015) in a period of 15–20 weeks post-virus injection (Goettsch et al., 2016). In addition, no adverse effect, immunologic response or liver damage was observed in animals following AAV viral infection (Roche-Molina et al., 2015). Notably, the hypercholesterolemic phenotype of AAV-PCSK9^{DY} mice resembled that of *Ldlr*$^{-/-}$ mice. Thus, Roche-Molina et al. (2015) hypothesized that injection of AAV-PCSK9D374Y into apoE$^{-/-}$ mice would result from having similar hypercholesterolemic features to that of double apoE/Ldlr knockout mice. As expected, the doubled size of lesions was measured in apoE$^{-/-}$ AAV-PCSK9^{D374Y} mice compared to wild-type mice fed the same diet. However, no significant difference was observed in their lipoprotein profile (Roche-Molina et al., 2015).

Overall, AAV-PCSK9 mouse model is an appropriate model of atherosclerosis due to the stable expression of PCSK9 after a single administration of AAV-PCSK9, no reported adverse effect concerning AAV administration, and fast development of atherosclerosis plaques in aorta upon AAV-PCSK9 injection in combination with western-type diet (Roche-Molina et al., 2015). We used this mice model in our second study to investigate the effect of PCSK9 gene down-regulation on preventing the development of atherosclerosis disease.

1.4.2 PCSK9 as a potential therapeutic target for reducing atherosclerosis

The loss-of-function (LOF) mutations of PCSK9 in healthy individuals were shown to decrease plasma level of LDL-C by about 30% and risk of CHD by up to

88% (Cohen et al., 2005; Cohen et al., 2006). In addition, two healthy women were found to have PCSK9 LOF mutations on both alleles resulting in no functional PCSK9 and very low level of LDL-C in the blood (~85% less LDL-C than average; ≤ 15 mg/dL) (Hooper et al., 2007; Zhao et al., 2006). Altogether, these findings have made PCSK9 an attractive target for the treatment of hypercholesterolemia. Inhibition of PCSK9 would be a useful therapy for hypercholesterolemia either alone or in combination with statins. Statins inhibit HMG-CoA reductase, the rate-controlling enzyme for cholesterol synthesis, which induces SREBP2 activity and increases liver LDLR expression and plasma LDL-C clearance (Istvan, 2002; Dubuc et al., 2004; Dong et al. 2010). Using monoclonal antibodies or mimetic peptides to disrupt the PCSK9-LDLR interaction, and PCSK9 gene silencing using RNA interference or antisense oligonucleotides are different approaches to inhibit PCSK9 functions as reviewed recently (Hess et al., 2018). Monoclonal antibodies and mimetic peptides target the extracellular function of circulating PCSK9, while both intra- and extracellular functions of PCSK9 can be affected by gene silencing and small molecule inhibitors (Table 1.3).

Table 1.2 A summary of PCSK9-inhibiting drugs under-development

PCSK9 inhibitor	Agent	Company	Stage
Antibody	Alirocumab	Sanofi/Regeneron	Approved
	Evolocumab	Amgen	Approved
	Bococizumab	Pfizer/Rinat	Terminated
	MPSK 3169A/RG7652	Genentech/Roche	Terminated
	LGT209	Novartis	Terminated
	LY3015014	Eli Lilly	Terminated
	RG-7652	Roche	Terminated
	ALD-306	Alder	Terminated
siRNA	ALN-PCS02	Alnylam Pharmaceuticals	Phase 3

Small protein (adnectin)	BMS-962476	Bristol-Myers Squibb/Adnexus	Terminated
Small molecule inhibitor	SX-PCK9	Serometrix LLC	Terminated
	TBD	Shifa-Biomedical corporation	Terminated
	PF-06446846	Pfizer	Terminated
Synthetic compound	K-312	Kowa Research Ins.	Terminated
Mimetic Peptides	A peptide mimicking LDLR-EGF A domain	Genetech, Inc	Terminated
	A peptide that mimics part of PCSK9 that binds to LDLR	Genetech, Inc	Terminated
Antisense oligonucleotide	SPC-5001	Santaris Pharma A/S	Terminated
	-	Idera Pharmaceutical	Terminated
Vaccine	-	Pfizer	Preclinical
	ATH05, ATH06, ATH07	Affiris AG	Preclinical

*adapted from (Mombelli et al., 2015 and Mullard and Asher 2017)

Monoclonal antibodies: To date, the most effective PCSK9 inhibitors are monoclonal antibodies raised against the catalytic domain of PCSK9, which is responsible for interacting with LDLR. They prevent LDLR degradation by disrupting the interaction between PCSK9 and LDLR proteins (Chan et al., 2009). Among these antibodies, Evolocumab (Repatha, Amgen Inc.) and Alirocumab (Praluent, Sanofi/Regeneron Pharmaceuticals Inc.) are commercially available. PCSK9 antibodies were approved in 2015 by the United States Food and Drug Administration and Health Canada to be used by patients that were unable to achieve an optimal plasma level of LDL-C, and have been diagnosed with atherosclerotic CVD or FH (Food and Administration, 2015a; Food and Administration, 2015b). Using approved monoclonal antibodies against PCSK9 in

high-risk patients largely reduced atherogenic lipid particles such as LDL-C, apoB and lipoprotein a, and demonstrated protective effects on CVD, MI, and stroke compared to the control (placebo) group (Schmidt et al., 2018). After using PCSK9 antibodies, no increase in the risk of adverse events such as cancer and neurocognitive events were observed compared to the control group. However, their long-term efficacy and safety need to be followed (Schmidt et al., 2018). Since the efficiency of these antibodies depends on frequent subcutaneous administration (every 2 or 4 weeks) over a long time (Li et al., 2015a), their high production cost is still an important issue. Furthermore, reactions at the injection site and autoantibody production would be other possible limitations of this therapy.

Small interfering RNA (siRNA) against PCSK9: RNA interference (RNAi) is a novel promising approach for the development of therapeutic gene silencing (Whitehead et al., 2009). Reduction in PCSK9 transcription using small interfering RNA (siRNA) led to a decrease in mRNA level of PCSK9 by 50-70% in the liver of mice and rats, which led to a decrease (~60%) in plasma level of cholesterol (Frank-Kamenetsky et al., 2008). In addition, a single intravenous injection of siRNA resulted in PCSK9 gene silencing for up to 3 weeks, which suggest the potential of this new class of drugs for the treatment of hypercholesterolemia (Frank-Kamenetsky et al., 2008). Phase-I clinical trial of PCSK9 siRNA (0.4 mg/kg; ALN-PCS siRNA, Alnylam Co., MA, USA) was performed on 32 healthy volunteers with a baseline level of LDL-C (~3 mmol/L), which was reduced by 41% upon PCSK9 siRNA injection (Fitzgerald et al., 2014). This study was pushed to a phase-II clinical trial, and its results were presented in November 2016 at a meeting of the American Heart Association (AHA). Their results demonstrated that single subcutaneous

injection of ALN-PCS (Inclisiran) to the patients with high plasma level of LDL reduced the average level of LDL-C by 51% three-month post siRNA injection (Ray et al., 2017). Moreover, the second injection of the same dose of inclisiran reduced the level of LDL-C by 57% after 180 days (Ray et al., 2017). After monoclonal antibodies, inclisiran is considered as the most promising PCSK9 inhibitor. However, several shortcomings limit the utility of siRNA as a therapeutic method. These limitations are mainly:

- Unfavorable physicochemical properties such as negative charges, massive molecular weight, and size (Takahashi et al., 2009; Whitehead et al., 2009).
- Low effectiveness as lysosomal degradation of siRNA after endocytosis may reduce its therapeutic activity (Tseng et al., 2009).
- Safety as competition between siRNA and endogenous RNA can lead to the saturation of the microRNA processing pathways and cause toxicity and liver damage (Grimm et al., 2006).
- Stimulation of innate immune responses (Akhtar and Benter, 2007)
- Off-target silencing (Schiffelers et al., 2004)

Antisense oligonucleotides (ASOs): Antisense oligonucleotides (ASOs) are short nucleic acid sequences that reduce the levels of the targeted mRNA *via* RNase H1-dependent degradation (Vickers and Crooke, 2014). ISIS 394814 is an ASO that is targeting the mRNA of mouse PCSK9. ISIS 394814 was well tolerated in mice, and its administration led to a sharp (92%) reduction in mRNA expression of PCSK9 in mouse liver and lower level of total cholesterol and LDL-C in mouse plasma (Graham et al., 2007). Also, a higher protein level of LDLR was observed in

mouse hepatocytes six weeks after ISIS 394814 administration (Graham et al., 2007). However, the company stopped working on the drug because of injection site reactions and safety concerns (van Poelgeest et al., 2015). Another ASO against PCSK9 corresponds to the second generation ASO (locked nucleic acid, LNA) that target PCSK9 with more specificity and higher affinity (Gupta et al., 2010). Its administration to mice decreased PCSK9 mRNA by 60% and increased protein level of LDLR ~3-fold in mouse liver (Gupta et al., 2010). In addition, treating the non-human primates with the LNA ASO SPC5001 reduced plasma level of PCSK9 and LDL-C by 85% and 50%, respectively (Lindholm et al., 2012). However, the development of second-generation ASOs (SPC5001 and BMS-844421) is not proceeding anymore because of undisclosed reasons.

Mimetic peptides: A synthetic peptide, mimicking the EGF-A domain of the LDLR, has been developed to inhibit the PCSK9-LDLR interaction (Shan et al., 2008). Shan et al. (2008) demonstrated that EGF-A peptide could inhibit LDLR degradation in the presence of exogenous recombinant PCSK9 in HepG2 cells. Then, a comparative study of a truncated 26 amino acid EGF-A analog led to the finding of the most potent peptide capable of inhibiting PCSK9 function and reduce LDLR degradation (Schroeder et al., 2014). The hydrogen bond between Tyr-306 in EGF-A variant (H306Y) of LDLR and Asp-374 (D374) in PCSK9 increases the affinity of the receptor to PCSK9 at neutral pH. Thus, LDLR-EGF-A (H306Y) sub-fragments were generated to enhance the potency of these peptides (McNutt et al., 2009). Upon addition of inhibitory peptides to the medium of hepatic cells stably overexpressing WT PCSK9 or GOF variants (D374Y or S127R), LDLR levels recovered to those of control cells. However, the affinity of these peptides for PCSK9

is lower than anti-PCSK9 monoclonal antibodies, and peptides with higher affinity are still needed to potentially inhibit PCSK9 binding to LDLR. Another option instead of using the analog of the EGF-A domain from LDLR was to use small peptides from pro- and catalytic domains of PCSK9 that compete with full-length PCSK9 for LDLR binding (Palmer-Smith and Basak, 2010). In this study, two catalytic domain peptides hPCSK9 (181-200) and hPCSK9 (368-390) were shown to increase PCSK9-functional activity and reduce LDLR level. *In vitro* and *in vivo* analysis demonstrated that a discrete PCSK9 C-terminal domain protein could compete with full-length PCSK9 for binding to the LDLR and reduce degradation of LDLR by PCSK9 (Du et al., 2011). Also, two groups of phage-displayed peptide libraries, Linear-lib and Cyclic-lib, were constructed by Zhang et al. (2014). Their study resulted in the identification of a 13-amino acid linear peptide (Pep2-8) that specifically bound to PCSK9 and inhibited LDLR and EGF (A) domain binding to PCSK9 (Zhang et al., 2014). Although *in vitro* and preliminary *in vivo* analysis demonstrated a promising therapeutic effect of peptide-based PCSK9-inhibitors, the critical impediments to their successful clinical use cannot be ignored. The limitations of developing PCSK9 inhibitory peptides are due to their stability in oral delivery since they can be degraded in the gastrointestinal system before exhibiting any therapeutic benefit.

We also studied whether peptide inhibitors could protect LDLR from being degraded through the PCSK9 extracellular pathway. We found a 22 amino acids peptide, based on a modified sequence of PCSK9 that inhibits LDLR degradation, without directly binding to the LDLR, possibly by impeding the receptor from reaching the lysosomes.

Adnectins (Monobodies): Adnectins are small proteins (~12 kDa) based on fibronectin and their structure, β-sheet with branched-out loops, can be engineered to increase their affinity for binding to a specific therapeutic target (Koide et al., 1998; Wojcik et al., 2010). For *in vivo* trials, it is required to perform pharmacokinetic enhancement modification to prevent the rapid filtration by kidney due to their small size. Interaction of PCSK9 to the EGFA domain of LDLR suggests that LDLR-EGFA is the most suitable target to develop PCSK9-centric lipid-lowering therapy (Zhang et al., 2007). A progenitor adnectin clone, targeting the LDLR-EGFA domain-binding site of the PCSK9 surface, was prepared using mRNA display (Mitchell et al., 2014). A maximal dose (1mg/kg) administration of an adnectin inhibitor of PCSK9, BMS-962476, on 64 healthy subjects reduced free PCSK9 by >90% and level of LDL-C by 48% (Stein et al., 2014). Moreover, this study demonstrated that BMS962476 was well tolerated over a trial period of 43 days (Stein et al., 2014). However, more studies with a more significant number of subjects and longer time duration are required to get a better insight into the effect of BMS962476 on safety, tolerability, and pleiotropic functions of PCSK9.

Small molecule inhibitors of PCSK9: Small molecules (< 900 daltons) are compounds that bind to the DNA, RNA or protein targets and inhibit their biological function. Inhibition of PCSK9 using small-molecules has attracted considerable attention, which has been recently reviewed by Xu et al. (2018). Oral administration and low preparation cost of these molecules are advantages over mAbs and siRNAs. However, low stability and bioavailability of the small molecules in the blood (Williams et al., 2013), and difficulties in designing a small molecule targeting the

large LDLR-binding site on the surface of PCSK9 (Surdo et al., 2011) might limit the production of these molecules.

Despite all difficulties, Cameron et al. (2008) found a plant-derived substance that inhibits the function of PCSK9. This small molecule is called Berberine (Cameron et al., 2008). Also, Shifa Biomedical (PA, USA) developed small molecules that either prevent the interaction of PCSK9 to the LDLR or prevent the secretion of PCSK9 by blocking the autocatalytic cleavage of PCSK9 (Crunkhorn, 2012). However, these molecules have low potency that makes them unusable for clinical trials (Crunkhorn, 2012). Pfizer screened 2.5 million anti-PCSK9 small molecules over 5 years and ended up with a single compound, PF-06446846, which was highly selective for PCSK9, but they never advanced into clinical phases because of off-target effect and low potency (Lintner et al., 2017; Mullard and Asher, 2017).

PCSK9-vaccine: A recent work demonstrated that peptide-based anti-PCSK9 vaccines are efficient tools for long-term LDL-C management through inducing the generation of antibodies, which remain functional for more than a year (Galabova et al., 2014). The rationale behind vaccine-immune therapy is to elicit high-affinity and long-lasting antibodies by stimulating the immune system (Schneeberger et al., 2010). Based on the mechanism of molecular mimicry, three different peptide-based vaccine candidates, ATH04, ATH05, and ATH06 were selected to produce PCSK9-specific antibodies in humans (Galabova et al., 2014). Preclinical studies in a period of ten months on wild-type mice, *Ldlr+/−* mice, and rats demonstrated a significant reduction in the level of LDL-C (50-55%) following three to four vaccination using the identified vaccine candidates (Galabova et al.,

2014). Furthermore, it has been demonstrated that immunization of atherosclerotic APOE*3Leiden-CETP mice with the AT04A anti-PCSK9 vaccine, led to a decrease in plasma level of PCSK9 as well as the number and the area of atherosclerotic lesions in the aortic wall (Landlinger et al., 2017; Ummarino, 2017). More studies are needed to find the optimal immunization dosage of candidate PCSK9 vaccines and investigate their long-term effect on safety, tolerability, and induction of a humoral immune response. If the results of the future studies were promising and successful, then the annual administration of anti-PCSK9 vaccine could count as an innovative therapy for atherosclerosis treatment.

Genome editing technique with CRISPR-Cas9: CRISPR (clustered regularly interspaced short palindromic repeats) is an adaptive immune system that is found in various species of bacteria and archaea (Sander and Joung, 2014). Approaches based on this mechanism helped to develop new therapies based on genome editing and facilitates the generation of cell lines and mice with altered alleles (Wright and Doudna, 2016). However, this therapy strategy is not yet appropriate for human use. Therefore, a mouse model with a humanized liver was used to investigate further the efficacy of this strategy (Strom et al., 2010).

Administration of an adenovirus expressing Cas9 and a CRISPR guide RNA targeting PCSK9 in hepatocytes resulted in high mutagenesis rate of PCSK9 (>50%) in mouse liver 3-4 days post virus injection (Ding et al., 2014). Consequently, the plasma level of PCSK9 was reduced, which led to an increase in the level of LDLR and ~40% decrease in plasma level of total cholesterol. This study suggested that *in vivo* use of CRISPR-Cas9 genome editing might modify *PCSK9* alleles permanently and function as a one-time cure (Ding et al., 2014). However, to test

this hypothesis and determine if there are off-targets, the CRISPR-Cas9 needs to be examined over an extended period.

Initiation of the inflammatory response in humans upon administration of an adenovirus, as well as difficulty in infecting the human hepatocytes with the strains of adenoviruses, are the major roadblocks in using the CRISPR/Cas system (Ding et al., 2014). Therefore, more research is needed to solve the safety and delivery problems prior to its application in human subjects.

1.5 Golgi Glycoprotein 1 (GLG1) and atherosclerosis

Golgi Glycoprotein 1 (GLG1) is a cysteine-rich membrane sialoglycoprotein located at the medial cisternae in neurons of the Golgi apparatus (Ahn et al., 2005). It has other aliases such as E-Selectin Ligand-1 (ESL-1) (Steegmaler et al., 1995), Golgi Sialoglycoprotein MG-160 (Stieber et al., 1995), Cysteine-rich fibroblast growth factor receptor-1 (CFR-1) (Burrus et al., 1992), and latent transforming growth factor-β complex protein 1 (LTCP-1) (Olofsson et al., 1997). GLG1 is a multifunctional protein but mainly function as a cell adhesion ligand of E-selectin and mediate leukocyte-endothelial interactions (Steegmaler et al., 1995). GLG1 is also an essential protein in mouse embryonic development. The study of Miyaoka et al. (2010) demonstrated that deficiency of GLG1 results in perinatal mortality and ~90% early postnatal death. In the study of Luo et al. (2012), none of the *Glg1*$^{-/-}$ mouse embryos survived. However, some other studies have shown that surviving homozygous *Glg1*-deficient mice survived for at least 40 weeks, but with reduced body weight, skeletal malformation (Yang et al., 2013; Yang et al., 2010), splenomegaly, and higher numbers of blood neutrophil and monocyte

(Sreeramkumar et al., 2013). The gene encoding the GLG1 protein, known as *GLG1* gene, has been assigned to human chromosome 16q22-q23 (Mourelatos et al., 1995).

1.5.1 GLG1 structure

The cDNA sequence of human *GLG1* (isoform 3) encodes the mRNA transcript of 3,513 base pairs, and a polypeptide with 1,179 amino acids, which is targeted to the cell-surface (Gonatas et al., 1995).

GLG1 comprises an N-terminal cleavable signal peptide (26-residue), followed by a proline-glycine-rich section (amino acids 31-99), 16 cysteine-rich repeats (~60 amino acids each), and five NXT glycosylation sites in its extracellular domain. Following the transmembrane domain (22 residues), the cytosolic C-terminal domain is composed of a cytoplasmic tail of 13 residues (Gonatas et al., 1995). The molecular weight of the primary translational product of GLG1, unglycosylated precursor of GLG1, is about 130 kDa (Gonatas et al., 1995; Johnston et al., 1994), which increases to 150 KDa upon its posttranslational glycosylation (Gonatas et al., 1989; Johnston et al., 1994). GLG1-glycoprotein undergoes a maturation process leading to a sialylated and fucosylated carbohydrate structures with ~160 kDa (Gonatas et al., 1989; Johnston et al., 1994). Finally, proteolytic cleavage in the extracellular domain of GLG1 (Olofsson et al., 1997), *via* furin-like proprotein convertase and metalloproteases, leads to the production of two secreted polypeptides with the molecular weight of 150 kDa and 55 kDa (Antoine et al., 2009a). The secreted glycoprotein, which is cleaved in the extracellular domain, is highly sialylated and N-glycosylated (Köhl et al., 2000).

Alternative splicing of *GLG1* gene (isoform 2) encodes a polypeptide with 1,192 amino acids, 24 extra amino acid residues at its C-terminal domain compared to isoform 3 of GLG1, which is expressed in Golgi (Ahn et al., 2005). It has been suggested that production of GLG1 is species-specific since its expression has been observed in human but not murine (Ahn et al., 2005) or chicken (Antoine et al., 2009b).

1.5.2 GLG1 localization and functions

GLG1 is widely distributed throughout the body within various organs and could induce pleiotropic effects depending on its subcellular localization (Gonatas et al., 1989). GLG1 is localized in the medial cisternae of the Golgi apparatus in neurons (Gonatas et al., 1989), at the cell surface in mouse myeloid cells, and its posttranslational modification, C-terminal tail truncation, in 32Dc13 cells, K46 lymphoma cell line, and mouse neutrophils mediate its displacement to the plasma membrane and filopodia (Steegmaier et al., 1997; Gonatas et al., 1998).

Different aliases of GLG1 are MG160 identified in rat brain (Gonatas et al., 1998), ESL-1 at the cell-surface of murine myeloid cells (Steegmaler et al., 1995), and CFR-1 in chick embryos (Burrus and Olwin, 1989).

The structure of CFR-1 contains 16 cysteine-rich repeats in the intraluminal domain, two potential proteolytic cleavage sites of 2-3 amino acid residues close to the transmembrane domain, and a short cytoplasmic tail (Olofsson et al., 1997).

Although GLG1 lacking the short cytosolic tail is preferentially expressed at the cell surface, artificial constructs of GLG1 without cysteine-rich repeats are extremely unstable (Miyaoka et al., 2011). This short half-life of the truncated GLG1

constructs, lacking the C-terminal domain, is not due to the proteolytic cleavage, nor lysosome or proteasome degradation pathways (Miyaoka et al., 2011). Instead, mutation analysis determined that Cfr repeats are specific for protein destabilization, and cleaved proteins are destabilized at the cell surface due to less number of cysteine-rich repeats (Miyaoka et al., 2011).

Immunofluorescence staining demonstrated GLG1 accumulation in a juxtanuclear position in COS-1 cells (Antoine et al., 2009b). Furthermore, the experimental analysis demonstrated that addition of heparin to the media of the cells resulted in an increase in GLG1 translocation to the cell-medium due to the high GLG1-heparin binding affinity (Antoine et al., 2009b). This suggests that GLG1 could mediate different physiological functions through its binding with a variety of molecular targets.

1.5.3 GLG1 interacting partners

Interaction of GLG1 with different proteins (depending on the experimental cell types), has been found in the secretory pathway and demonstrated different functions. So far, it is known that GLG1 plays a role in processing and targeting the fibroblast growth factor (FGF), and latent TGF-β complex in cells. Also, the function of GLG1 in E-selectin adhesion/signaling ligand is identified. However, all interacting proteins and functions of GLG1 are not yet known, and their identifications require further research.

1.5.3.1 GLG1 interacts with FGF

Interaction of GLG1 with FGFs was discovered by Burrus and Olwin in 1989. FGFs are a family of growth factors with at least 22 members. They mediate a variety

of vital functions through their interaction with FGF receptor tyrosine kinases (FGFR1-FGFR4). Essential functions regulated by FGFs are such as cell proliferation, differentiation, and migration, tissue repair, and organ development (Eswarakumar et al., 2005).

Cell-transfection experiments and biochemical analysis demonstrated the interaction of GLG1 with FGF1, FGF2 (Burrus and Olwin, 1989), FGF3 (Köhl et al., 2000), and FGF4 (Burrus et al., 1992). A similar binding site for FGF-2 is found on GLG1 and FGF receptors demonstrating that these two receptors compete for this interaction and cannot bind concomitantly with FGF-2 (Zhou et al., 1997). Additional experiments demonstrated reduced intracellular protein level of FGF-1 and FGF-2 in CHO cells upon expression of full-length GLG1 (Zuber et al., 1997). Also, co-transfection of COS-1 cells with pCFR1.1, an uncleavable construct of GLG1 (Burrus et al., 1992), and FGF-3 resulted in sequestering the FGF-3 in the Golgi apparatus and consequently reduced its secretion into cell-media (Köhl et al., 2000).

The binding site of GLG1 with FGFs was identified experimentally using different GLG1 constructs with deletion mutants. A region of GLG1 with ~200 amino acid, $GLG1^{290-496}$, showed a binding affinity to the FGFs (Zhou et al., 1997). Moreover, this study resulted in the identification of another fragment of GLG1, $GLG1^{625-740}$, as the binding site with FGFs (Zhou et al., 1997). The identified binding sites of GLG1 with FGFs indicate the importance of luminal cysteine-rich repeats of GLG1 in this interaction (Zhou et al., 1997).

Unlike the interaction between FGFs and their receptors, the presence of heparan sulfate proteoglycans is not necessarily required for the GLG1-FGFs interaction (Zhou et al., 1997) but it increases (2-3 fold) their interaction. The reason

for this increase was mainly due to the effect of heparan sulfate in increasing the ionic strength rather than through its direct association with FGFs. However, since GLG1 can also interact with heparin, two mechanisms were suggested for its interaction with FGFs. First, FGFs directly binds to the cysteine-rich repeats of GLG1. Secondly, the indirect interaction between GLG1 and FGFs is mediated by heparan sulfate (Zhou et al., 1997).

Immunoprecipitation experiments revealed that there is a physical interaction between GLG1 and FGF18 in COS7 cells (Miyaoka et al., 2010). Furthermore, GLG1 is involved in regulating the signaling pathway of FGF18, which is a prerequisite growth factor for hypertrophy, differentiation/proliferation of chondrocyte (Ohbayashi et al., 2002), and vascularization of growth plates (Liu et al., 2007). Mice with disrupted FGF18 demonstrated reduced embryonic alveolar development, delayed osteogenic differentiation, and increased chondrocyte differentiation and proliferation (Liu et al., 2007). The phenotype of *Glg1*$^{-/-}$ mice resembles the phenotype of FGF18 knockout mice, in displaying growth retardation, tail malformation, and cleft palate, which caused the presence of a bloated abdomen (Miyaoka et al., 2010). Mice lacking either GLG1 or FGFs died mostly at the embryonic stage, while few survivor mice were smaller than wild-type mice and demonstrated few physical abnormalities (Miyaoka et al., 2010). Also, mice double heterozygous for GLG1, and FGF18 (*Glg1+/-* and *Fgf18+/-*) had a significantly lower weight than a control group. These mice demonstrated early onset of tail malformation at a prevalence of 83% (Miyaoka et al., 2010). In contrast, no abnormal phenotype was observed in mice with single haploinsufficiency of either GLG1 or FGF18 (Luo et al., 2012).

The interaction of GLG1 with delta-like protein (DLK) was shown by Miyaoka et al. (2010). DLK, also called preadipocyte factor 1 (Pref-1), is a transmembrane protein with six epidermal growth factor (EGF) repeats in its extracellular domain. Moon et al. (2002) demonstrated a loss of antiadipogenic action in *Pref-1*-null mice, which leads to disturbed homeostasis of triglycerides, free fatty acids, and cholesterol. Thus, knockout of *Dlk* in mice resulted in increased serum lipid metabolites, increased adiposity, and obesity phenotype (Moon et al., 2002). Immunoprecipitation and blotting experiments revealed that DLK significantly prevents GLG1/FGF18 interaction (Miyaoka et al., 2010). Thus, we can conclude that a significant reduction in GLG1/FGF18 binding reduces FGF18 signaling.

1.5.3.2 GLG1 is an E-selectin ligand

The interaction of GLG1 (or ESL-1) with E-selectin was observed at the surface of myeloid (Steegmaler et al., 1995) and neutrophil cells (Steegmaier et al., 1997). Cell-surface expression of GLG1 is required for its function as an E-selectin ligand (Antoine et al., 2009b; Steegmaier et al., 1997). The interacting proteins with E-selectin require having sialylated and fucosylated carbohydrate structures (Zöllner and Vestweber, 1996). E-selectin, a type I calcium-dependent transmembrane glycoprotein, is synthesized by endothelial cells. Its expression is inducible by tumor necrosis factor (TNF), nuclear factor κB (NF-κB), interleukin (IL)-1, and hypoxia (Russell et al., 2000). During inflammation, selectins regulate leukocyte rolling and initiate their extravasation by interacting with leucocytes on the apical surface of endothelial cells (Bevilacqua and Nelson, 1993).

Surface plasmon resonance (SPR) was used to determine the affinity of E-selectin to its ligand, ESL-1 (GLG1), which was extracted from bone marrow (Wild

et al., 2001). In this study, the dissociation and association rate constant of GLG1 to E-selectin was found to be 4.6 s^{-1} and 7.4×10^{4} M^{-1} s^{-1}, respectively. Also, the GLG1/E-selectin interaction was not altered by a change of temperature in normal physiological conditions (Wild et al., 2001). Although E-selectins are involved in leukocyte rolling and interact robustly with GLG1, the absence of GLG1 in leukocytes demonstrated only a minor alteration in the function of leukocytes *in vivo* and binding of proteins to E-selectin *in vitro* (Hidalgo et al., 2007). This effect suggested that other E-selectin binding proteins are involved in hematological homeostasis. Xia et al. (2002) reported that P-selectin glycoprotein ligand-1 (PSGL-1) is not only the primary ligand of P-selectin but also interacts with E-selectin. To better determine the contribution of PSGL-1 and GLG1 in myeloid cell trafficking, mice doubly deficient in both glycoproteins were produced, and their effect in hematological homeostasis was compared (Sreeramkumar et al., 2013). Mice lacking GLG1 and PSGL-1 demonstrated splenomegaly and morphological defects similar to single Glg1 knockout mice (Sreeramkumar et al., 2013). Sreeramkumar et al. (2013) further demonstrated that double knockout mice had a higher level of blood neutrophils and monocytes than Glg1 knockout mice, while no difference was observed in lymphocytes count between these two groups. Also, their findings demonstrated that GLG1 and PSGL1 have a role in regulating neutrophil homeostasis and clearance of myeloid leukocytes (Sreeramkumar et al., 2013). Although GLG1 was not involved in leukocyte rolling velocity, its effect was dominant for binding to the E-selectin and migration of immature hematopoietic cells (Sreeramkumar et al., 2013).

Werneburg et al. (2016) reported that GLG1, a Golgi-localized polysialylated protein, is a novel carrier of polysialic acid (polySia), which is also stored in the Golgi

apparatus of mouse microglia. GLG1 is involved in the regulation of microglial activity and human THP-1 macrophages in the inflammatory progress. PolySia is released in response to lipopolysaccharide (LPS) or injury to control pro-inflammatory process (Werneburg et al., 2016). Secretion of GLG1-PolySia is dependent on metalloproteinase-mediated protein ectodomain shedding (Antoine et al., 2009b) and shedding of GLG1-PolySia complex act as a negative feedback regulator of NO and cytokine production (Werneburg et al., 2016).

1.5.3.3 GLG1 is a latent TGF-β-binding protein

Transforming growth factor-β (TGF-β), a family of 25-kDa dimeric proteins having different isoforms (i.e., TGF-β1, -β2 and -β3 with distinct biological activities) (Sporn and Roberts, 1990), are secreted in a complex with latency-associated peptides (LAP) from various cell types (Miyazono et al., 1993). TGF-β can be produced in the skeletal system, where it is involved in regulating the cartilage and bone plate homeostasis (Annes et al., 2003). Moreover, its signaling is an essential factor in the regulation of various cellular processes such as cell growth, differentiation, proliferation, migration, adhesion, and apoptosis (Sporn and Roberts, 1990; Ten Dijke et al., 2002), as well as specification of developmental fate, in embryos and mature tissues, in various types of species including flies, worms and mammals (Massagué and Chen, 2000 ; Patterson and Padgett, 2000).

The inactive precursor of TGF-β (pro–TGF-β), the initial form of TGF-β in the secretory pathway, undergoes posttranslational cleavage/maturation process by a furin-like protease to become active. This maturation process occurs in the Golgi apparatus at a site of TGF-β, that is between the latency domain and ligand domain (Annes et al., 2003; Dubois et al., 1995; Janssens et al., 2005; Miyazono et al.,

1992). Yang et al. (2010) demonstrated that GLG1 could inhibit TGF-β maturation by downregulating the activity of furin-like protease in murine chondrocytes and HEK293 cells. They further explained that direct interaction of GLG1 with TGF-β in Golgi apparatus prevents TGF-β maturation and thereby limiting its bioavailability (Yang et al., 2010).

Latent TGF-β complexes, composed of mature TGF-β, LAP and latent TGF-β binding protein-1 (LTBP1) (Dallas et al., 1994; Miyazono et al., 1991; Olofsson et al., 1992), have been identified in human platelets (Miyazono et al., 1988; Wakefield et al., 1988), and rat platelets (Okada et al., 1989). The disulfide interaction between LTBP-1 and LAP forms complexes with a molecular weight around 230 kDa. Interaction of TGF-β with different proteins depending on the cell type might change its functional properties. Olofsson et al. (1997) demonstrated that TGF-β could also interact with GLG1 apart from its interaction with LAP in latent TGF-β complexed protein-1 (LTCP-1). Olofsson et al. (1997) purified LTCP-1 from the conditioned medium of Chinese hamster ovary (CHO) cells that were transfected with TGF-β1 cDNA. Moreover, their results demonstrated high mRNA expression of LTCP-1 in the ovary, placenta, and testis compared to other tissues (Olofsson et al., 1997).

Binding of TGF-β ligand to the assembled type I and II receptor serine/threonine kinases at the cell surface results in phosphorylation of receptor I *via* receptor II and initiation of TGF-β signaling. TGF-β signaling leads to phosphorylation and thereby, activation of Smad proteins. Then, activated Smad proteins translocate to the nucleus and associate with other nuclear cofactors to regulate the transcription of target genes (Shi and Massagué, 2003). It has been demonstrated that high expression of GLG1 inhibits TGF-β/Smad signaling (Yang et

al., 2010), while its deficiency in *Glg1*$^{-/-}$ mice led to an increased level of TGF-β signaling (Yang et al., 2010). Dysregulation in the signaling of TGF-β inhibits growth plate homeostasis and is the leading cause of skeletal dysplasia (Kronenberg, 2003; Kronenberg, 2007). Severe shortening of all structural elements in Xenopus laevis embryo, which was injected with GLG1 mRNA, was due to the reduced level of TGF-β signaling (Yang et al., 2010). Also, increased TGF-β signaling in *Glg1*$^{-/-}$ mice, led to an increase in TGF-β downstream factors such as a parathyroid hormone-related peptide (PTHrP), which resulted in reduced chondrocyte proliferation, chondrocyte cell-density and, shortening of the growth plates (Yang et al., 2010). Yang et al. (2013) later confirmed that the absence of GLG1 in primary culture osteoblasts led to a delayed differentiation, mineralization, and stimulation of osteoclastogenesis. The absence of difference in bone homeostasis in primary culture of *Glg1*$^{-/-}$ osteoclasts suggested that GLG1 primarily acts in osteoblasts for bone hemostasis. Their investigations further clarified the effect of increased TGF-β signaling in differentiation and coupling of osteoclasts-osteoblasts and abnormal phenotypes of *Glg1*$^{-/-}$ mice (Yang et al., 2013).

1.5.4 GLG1 role in cancer

Activation of hepatic stellate cells (HSC), pericytes of liver sinusoidal endothelial cells, and consequently their transdifferentiation into myofibroblasts are the essential steps for the repair of injured hepatic tissue, angiogenesis of hepatic metastases and liver regeneration (Balabaud et al., 2004; Friedman, 2003). Antoine et al. (2009b) showed a functional E-selectin binding activity for GLG1 and α·(1,3)-fucosyltransferases VII (FucT7) on the cell surface of HSC. This binding was

reduced under hypoxic conditions, while the expression level of GLG1 remained constant. They further explained that the loss in cell surface GLG1 binding activity might be due to the increased level of cleaved and secretory form of GLG1 in oxygen-deficient HSC, which consequently could affect liver metastasis and inflammatory liver diseases.

It has been shown that GLG1 is involved in prostate cancer metastasis (Yasmin-Karim et al., 2014). In cancer metastases, primary tumor cells attach to bone marrow endothelial cells and undergo morphogenetic changes to become circulating tumor cells (CTCs) (He et al., 2010). Rolling of CTC on the endothelial cell surfaces that express E-selectin, subsequently cause a bone metastasis (Dimitroff et al., 2004). Yasmin-Karim et al. (2014) reported that elevated level of E-selectin ligands in prostate tumor metastasis (Dimitroff et al., 2004), and more specifically ESL-1 (GLG1) upregulates adhesion of circulating prostate cancer (PCa) cells to bone marrow vascular epithelium cells by activating RAS-MAP signaling kinase pathway, which subsequently induces oncogenicity and cancer cell metastasis. The authors confirmed their observations by demonstrating impaired rolling and low level of cancer aggressiveness in Glg1-knockdown cells (Yasmin-Karim et al., 2014).

1.5.5 GLG1 role in atherosclerosis

Despite clinical improvements in cardiac therapy, cardiovascular disease is still one of the predominant causes of death (Mathers et al., 2001). Several large epidemiological studies have consistently reported that atherosclerosis is one of the most common forms of cardiovascular diseases (Feigin et al., 2016). Two major

conditions in atherosclerotic disease are ischemic heart disease and cerebrovascular disease, mainly ischemic stroke. The mortality from these two conditions was 248 per 100,000 in 2013, representing 84.5% of cardiovascular deaths and 28.2% of all-cause mortality (Barquera et al., 2015). Atherosclerosis is a complex disease that could be caused by multiple factors including genetic, environment and lifestyle. Other events, such as endothelial dysfunction, inflammation, abnormal lipoprotein metabolism, dysfunctional coagulation, and fibrinolysis, play a key role in the Pathogenesis of Atherosclerosis. Epidemiological studies, as well as animal studies have shown that there are number of genes in which mutations are associated with the incidence of atherosclerosis disease. Some of these candidate genes are LDLR, apoB, apoE, ATP Binding Cassette Transporter 1 and scavenger receptor class B type 1. Identification and characterization of new genes that might be involved in atherosclerotic cardiovascular disease are highly valuable.

Luo et al. (2012) reported that deficiency of GLG1 in atherosclerosis mouse model (*apoe*$^{-/-}$), increased atherosclerotic plaque stability. They observed that heterogenous deficiency of GLG1 in *apoe* knockout mice (*apoe*$^{-/-}$/*Glg1*$^{+/-}$) led to a reduction in liver macrophage content and increase in collagen deposition to the atherosclerotic lesions compared to the control (*apoe*$^{-/-}$/*Glg1*$^{+/+}$) group.

The association of GLG1 with coronary artery disease was further verified due to its interaction with adiponectin (APN) on cell adhesion (Yamamoto et al., 2016). APN is an adipocyte-derived hormone, which is expressed with high specificity in adipose tissue (Ukkola and Santaniemi, 2002). APN is involved in anti-

atherogenic mechanisms and pleiotropic biological processes such as inflammation and vascular homeostasis (Luo et al., 2017). Also, a lower concentration of APN in patients suffering from coronary artery disease further confirmed its protective role in the development of atherosclerosis (Ukkola and Santaniemi, 2002). More recently, Yamamoto et al. (2016) indicated that the interaction of GLG1 with APN induces anti-atherogenic mechanisms by blocking GLG1/E-selectin binding. These data provide a strong rationale for targeting GLG1 pathways in lipid-lowering therapies and atherosclerosis research.

1.6 Hypothesis and objectives

First Study Hypothesis: ***An endogenous PCSK9 interactor could regulate PCSK9 function in cholesterol metabolism:*** Through co-immunoprecipitation, mass spectrometry, western blot assays, and confocal immunofluorescence microscopy in cells and animal models, a new PCSK9 interacting protein will be discovered that could help to bring a new potential therapeutic approach to inhibit PCSK9 function and reduce circulating LDL.

Objectives:

- Investigate the role of this endogenous PCSK9 modulator on PCSK9 function and on other main PCSK9 binding partners.
- Characterize its underlying mechanisms in cholesterol regulation.

Second Study Hypothesis: ***Developing an atherosclerotic mouse model will advance our understanding of the PCSK9 effect on aortic lesions.*** The link between PCSK9 and regression of atherosclerotic plaques can be investigated, using genetically modified relevant mouse models, atherogenic diet, tetracycline-inducible gene expression system, and PCSK9 GOF mutation.

Objectives:

- Identify the most suitable mouse model for studying PCSK9 role in atherosclerosis.
- Investigate the effect of PCSK9 gene overexpression on atherosclerotic plaques development in mice fed a Western-type diet (WTD).
- Study the effect of PCSK9 gene downregulation on atherosclerotic plaques in our selected atherosclerosis mice model.

CHAPTER 2

2 PCSK9 and GLG1

CHAPTER 2: PCSK9 and GLG1

ARTICLE A: Loss of hepatic GLG1 reduces apolipoprotein B-100 secretion via promoting its aggregation and degradation by autophagy

AUTHORS: Samaneh Samami[1,2,3], Maya Mamarbachi[1], Mahmood Hussain[4], Eric Rhéaume[2,5], Jean-Claude Tardif[2,5], Steve Poirier[1], Gaétan Mayer[1,3,6,*]

Laboratory of [1] Molecular Cell Biology, & [2]Atherosclerosis, Montreal Heart Institute.

[3]Department of Pharmacology, Faculty of Medicine, Université de Montréal.

[4] Diabetes and Obesity Research Center, New York University Winthrop Hospital, Mineola, NY, USA

[5]Department of Medicine, Faculty of Medicine, Université de Montréal.

[6]Faculty of Pharmacy, Université de Montréal

* Corresponding author; email gaetan.mayer@icm-mhi.org

Short title: **Golgi glycoprotein 1 regulates the secretion of apolipoprotein B-100**

CURRENT STAGE: Under Preparation

Authors' contributions

SS and GM designed the study. SS carried out the experiment. SS and GM analyzed the data and wrote the paper. MM helped in building expression constructs, MH

helped in MTP activity experiment. SP, EC, JT, and GM advised on the study and provided laboratory support. GM supervised the study.

2. Foreword

PCSK9 binds the LDLR at the cell surface of hepatocytes induces its internalization and its degradation in lysosomes. However, these two proteins co-exist within the secretory pathway without leading to complete LDLR degradation. This might be due to the presence of endogenous inhibitors of PCSK9-induced LDLR degradation. Therefore, studying PCSK9-interacting proteins that might modulate its function may lead to better insight into the function of PCSK9 and outcome of using PCSK9 inhibitors in the future.

In the following article, we identified Golgi glycoprotein 1 (GLG1) as a new binding partner of PCSK9. We found that GLG1 also binds with apoB and LDLR. Binding of GLG1 to three proteins for which corresponding genetic defect cause FH prompted us to investigate its regulatory role on cholesterol. Our results demonstrated that GLG1 downregulation reduces MTP activity, secretion of apoB-containing lipoproteins, and PCSK9. We further demonstrated that GLG1 deficiency leads to impairment of apoB trafficking to the lipid droplets, which thereby induces apoB-aggregation and its autophagic degradation. Thus, preventing the interaction of GLG1 with apoB might pave the way towards the development of a new treatment of hypercholesterolemia.

2.1 Abstract

Proprotein convertase subtilisin kexin-like 9 (PCSK9) protein is involved in the regulation of low-density lipoprotein receptor (LDLR) and apolipoprotein B (apoB) levels, thereby, plays a major role in cholesterol metabolism. Some endogenous PCSK9 binding partners may exist that regulate circulatory cholesterol level. Mass spectrometry analyses of PCSK9-interacting proteins revealed that Golgi apparatus protein 1 (GLG1), is a novel PCSK9 interactor. Co-immunoprecipitation and confocal immunofluorescence microscopy confirmed that GLG1 interacts with PCSK9 and LDLR in Huh7 cells. Our results also demonstrated that GLG1 binds with apoB in cells and mouse liver. Therefore, we assessed whether GLG1 affects PCSK9 function and is involved in the regulation of cholesterol metabolism. Knockdown of GLG1 decreased apoB, LDLR, PCSK9 and increased P62, a marker of aggresome formation, protein levels in Huh7 cells and mouse liver. Moreover, deficiency of GLG1 in Huh7 cells induced perinuclear aggregation of apoB, and reduced apoB secretion in media. Cyto-ID autophagy detection assay determined more autophagic vacuoles formation post Glg1 knockdown in Huh7 cells. Glg1-knockdown mice demonstrated reduced body weight and a substantial reduction in circulating cholesterol (VLDL-C and LDL-C), PCSK9 and triglycerides (TG) in mouse plasma compared to the control group. Electron microscopy analysis demonstrated abnormal morphological changes, including the presence of swollen endoplasmic reticulum (ER) and double-membraned autophagosome structure in mouse liver upon Glg1-knockdown. Western blot and confocal microscopy analysis revealed that autophagy inhibitors prevented reduction of apoB secretion upon knockdown of Glg1

and induced accumulation of aggregated apoB in the perinuclear region. Our results demonstrate for the first time that GLG1 is involved in the regulation of cholesterol metabolism through the regulation of TG-rich lipoprotein secretion and expression of PCSK9, LDLR, and apoB. Taken together, our results show that GLG1 could represent a new target for hypercholesterolemia treatment.

Keywords: PCSK9, LDLR, apoB, GLG1, autophagy.

2.2 Introduction

High plasma level of low-density lipoprotein (LDL) cholesterol (LDL-C) is a known risk factor for coronary heart disease (CHD) (Zhang et al., 2007), which accounts for nearly one-third of all deaths throughout the world (Roth et al., 2017). LDL receptor (LDLR) plays an essential role in the plasma clearance of LDL particles through the lysosomal degradation pathway (Twisk et al., 2000). Apolipoprotein B (apoB) is the main component of potentially atherogenic particles, including LDL, very-low-density lipoprotein (VLDL), and intermediate-density lipoprotein (IDL) particles. Therefore, increased concentration of apoB is a significant predictor of CHD (Sniderman et al., 2010).

apoB is involved in 1) maintaining the overall integrity of the lipoprotein assembly, 2) facilitating the lipoprotein uptake by acting as a ligand for lipoprotein receptors and 3) modulating the activity of enzymes that act on lipoproteins. ApoB has two isoforms, apoB-100, synthesized in the liver, and apoB48, synthesized in the small intestine. ApoB-100 is the major protein of LDL and VLDL and is responsible for their formation and secretion. Apo48 plays the same role in chylomicrons. The newly synthesized apoB can be degraded by the proteasome

upon ubiquitination in lipid-poor conditions or the absence of microsomal triglyceride transfer protein activity (Zhou et al., 1998). Autophagy is the other possible mechanism that can induce apoB degradation in late-stage protein quality control (Ohsaki et al., 2006; Zhong et al., 2010). In the autophagy process, accumulated apoB in autophagosomes, membrane structures near cytosolic lipid droplets (Ohsaki et al., 2006), are delivered to lysosomes for their disposal (Glick et al., 2010).

The LDLR and apoB are two main interacting partners of proprotein convertase subtilisin kexin-like 9 (PCSK9), a protein mostly expressed in the liver (Seidah et al., 2003). PCSK9 has different functions depending on its target proteins. PCSK9-LDLR binding induces LDLR degradation in lysosomes, thereby, increasing plasma LDL-cholesterol (LDL-C) level and risk of CHD (Zhang et al., 2007). PCSK9-apoB binding increases secretion of apoB by inhibiting intracellular apoB degradation through the autophagosome/lysosome pathway (Sun et al., 2012), which increases the level of circulating apoB and LDL-C (Sniderman et al., 2010).

The important function of PCSK9 on the cellular degradation of the LDLR and increased plasma level of LDL-C raised a high interest in the development of pharmacologically PCSK9 inhibitors that were reviewed recently (Hess et al., 2018). In addition, critical functions of LDLR in the clearance of plasma LDL-C, while circulatory PCSK9 induces LDLR degradation, suggest the presence of endogenous PCSK9-inhibitors that modulate the PCSK9 function to maintain the optimal blood lipid levels (Surdo et al., 2011). Our team pioneered the hypothesis that some endogenous PCSK9-interacting proteins might be involved in modulating the function of PCSK9. We have identified annexin A2 (Mayer et al., 2008; Seidah et al., 2012), and GRP94 (Poirier et al., 2015) as endogenous PCSK9-binding proteins.

Annexin A2 is an extrahepatic inhibitor of PCSK9-enhanced LDLR degradation (Seidah et al., 2012), and GRP94 protects LDLR from early degradation by PCSK9 within the ER (Poirier et al., 2015). PCSK9 undergoes an autocatalytic cleavage within the ER (Seidah et al., 2003), resulting in the formation of a heterodimer complex of mature PCSK9 bound to its prosegment, which exits and is secreted from the ER (Cunningham et al., 2007). So far, no other endogenous PCSK9 inhibitor has been identified at the cell surface or within the secretory pathway of hepatocytes.

In the present study, we found that the Golgi apparatus protein 1 (GLG1) (Ahn et al., 2005), is a novel PCSK9 interactor protein. Haploinsufficiency of GLG1 decreases atherosclerotic plaque macrophage content, whereas its complete absence leads to early embryonic lethality (Luo et al., 2012). GLG1 is a multifunctional protein, widely tissue-distributed, and induces pleiotropic effects depending on its subcellular localization and additional protein interactions. Therefore, we assessed whether GLG1 is involved in regulating the function of PCSK9 and its interacting partners, as well as cholesterol metabolism.

2.3 Experimental procedures

Antibodies

The following antibodies were used for western blot, immunocytochemistry (ICC) and immunohistochemistry (IHC) analysis: goat anti human or mouse LDLR (1:3000; catalog no. AF2148 or 1:1000; catalog no. A2255, R&D Systems), rabbit anti-human (amino acids 31-454) or mPCSK9 (1:3000; in-house or catalog no. AF3985, R&D system), goat anti-human apo-B100/48 (1:5000; catalog no. 20A-G1b,

Academy biomedical company), mouse monoclonal anti-apoB (1:3000; clone 2G11 , Cat. No. MABS2046, EMD Millipore), goat anti-mouse/human-Albumin (1:6000; catalog no. AF3329, R&D system), mouse anti-V5-tag (1:5000; catalog no. A01724-100, GenScript), mouse anti-P62 (1:200; catalog no. Sc-28359, Santa Cruz) or rabbit anti-P62 (1:10,000; Cat no. EPR 4844, Abcam), rabbit anti-GLG1 (1:3000; catalog no. AP9839b, ABGENT), rabbit anti-LC3B (1:1000; catalog no. NB100-2220, NovusBio), mouse anti-ubiquitin (FK2, 1:3000, Catalog no. PW8810; Enzo), mouse monoclonal LPL (F-1, 1:200; catalog no. Sc-373759, Santa Cruz), rabbit anti-actin (1:5000; catalog no. A2066, Sigma-Aldrich), Rabbit anti-Pan-Cadherin (1:10000; catalog no. 717100, Life Technologies), Golgin-97 (1:1000; catalog no. A-21270, Invitrogen Corporation), rat anti-GRP94 (1:30,000; Cat.#ADI-SPA-850, Enzo Life Sciences), rabbit anti-GRP78 (1:2500; Cat. #ab21685, Abcam), Rabit anti-apoA1 (1:1000; catalog no. ab20453, Abcam), Mouse monoclonal perilipin (G-2, Sc-390169, 1:200; Santa Cruz), mouse monoclonal anti-Calnexin (AF18, 1:200; catalog no. sc23954, Santa Cruz), rabbit anti- ANGPTL3 (1:5000; catalog no. ab154009, Abcam), Horseradish peroxidase (HRP)-conjugated goat anti-human albumin (1:7000; catalog no. AL10H-G1a, Academy Bio-medical), rabbit anti-HA (1:5000, product no. H 6908, Sigma), rabbit anti-mouse MTP antibody (kind gift from Dr. Laurie Swift, Vanderbilt University Medical Center).

Reagents

3-Methyladenine (3-MA; catalog no. M9281), ammonium chloride (NH_4Cl; Catalog no. 254134), Tyloxapol (catalog no. T0307), cycloheximide (CHX; catalog no. C7698) and oleate (OA; Catalog no. O7501) were purchased from Sigma-

Aldrich. Brefeldin A (BFA; Catalog no. 159027, 194802) was purchased from MP Biochemical. MG-132 (Catalog no. 474790) was obtained from EMD Millipore. ApoB detection kit (LSBIO, Catalog no. LS-F9541-1L), Mouse PCSK9 ELISA kit (Cyclex; Catalog no. Cy-8078), cyto-ID autophagy detection kit (ENZO, Catalog no. ENZ-51031-0050), Lipoprotein Lipase (LPL) Activity Assay Kit (Cell Biolabs, catalog no. STA-610), T-cholesterol (Wako, catalog no. TP898) and Triglyceride (CEDARLANE, Lot# EBG6547) assay kits were used according to the manufacturer protocol. MTP activity was assessed using related vesicles that were a nice gift from Dr. Mahmood Hussain from NYU Winthrop Hospital.

Cell Culture, cDNA/siRNA transfection, and Cell Treatments

Hepatocellular carcinoma (Huh7) cells were cultured in Dulbecco's Modified Eagle's Medium (DMEM; catalog no. 319-005-CL, Wisent) containing 10% fetal bovine serum (FBS; catalog no. 080-350, Wisent) in a 5% CO_2 atmosphere at 37 °C. Cells were used for different experiments at about 70-90% confluency.

Approximately 120,000 Huh7 cells with different passage number stocks were plated in 12-well culture plates. Huh7 cells were either transfected with plasmids using Lipofectamine 3000 (Cat. #L3000008, Life Technologies) or reverse transfected with small interfering RNAs (siRNA) using Lipofectamine RNAiMax reagent (Cat. #13778075, Life Technologies) according to the manufacturer's instructions. siGLG1 (Cat No.M-010597-01-0005, Dpharmacon), siPCSK9 (Cat No.s48694, Life technologies) or a negative control siRNA with no known targets (Cat No. D-001206-14, GE HealthCare Dharmacon) was used for reverse transfection in Huh7 cells.

To ascertain whether Glg1-knockdown could affect the half-life of GLG1, apoB, LDLR, and PCSK9 proteins, the protein translation inhibitor CHX was used. Huh7 cells, 72-hours post-reverse-transfection, were incubated with complete growth medium containing CHX (25 µg/mL) analyzed at 0, 3, 6, and 8 h. Protein samples were subjected to SDS/PAGE, and immunoblots were evaluated using corresponding antibodies. ImageJ software version 1.50b (National Institutes of Health, Bethesda, Maryland) was used for densitometry calculations on scanned immunoblots.

To clarify the mechanisms underlying Glg1-knockdown-induced apoB degradation, different inhibitors including ammonium chloride (NH_4Cl, endosome/lysosome neutralizing agent), MG-132 (proteasome inhibitor) and 3-MA (an autophagy inhibitor) were used. Also, brefeldin A (BFA) was used as an inhibitor of the trafficking vesicles from the endoplasmic reticulum to the Golgi apparatus. Huh7 cells, 48 h post-reverse transfection, were washed and incubated at 37°C with conditioned medium supplemented either with NH_4Cl (10mM), MG132 (5 µM) or BFA (5 µg/ml) for 16 hours or with 3-MA (10 mM) for 3 to 4 hours.

To stimulate lipid synthesis, Huh7 cells were treated for 4 hours with oleate (OA; solubilized in anhydrous methanol, 1.5 mM). Cells were used 72 h after reverse transfection for protein/RNA extraction, or microscopy experiments.

For a selection of stable derivatives of transduced cells, Huh7 Cells were seeded in 6-well culture dishes at 150,000–250,000 cells per well. Cells were then transfected with GFP-LC3 using Lipofectamine 3000 (Cat. #L3000008, Life Technologies) according to the manufacturer's recommendations. Fluorescent cells were identified 48 h after transfection, confirming GFP activity, and next incubated

with DMEM containing 500 mg/ml Geneticin (G418, Life Technologies) at 37°C. Untransfected Huh7 cells were cultured under the same conditions as a negative control. Transfected cells were selected after 5-7 passages in the presence of the antibiotic G418.

Expression Constructs

Human V5-tagged PCSK9 and LDLR (C-terminal V5-tag) was PCR amplified and subcloned into the BglII/AgeI-digested pIRES vector (Invitrogen). The construct pIRES-human PCSK9-V5 was used as a template to generate cDNAs coding human PCSK9 mutants (pIRES-PCSK9-S127R-V5). This construct lacks the prodomain of PCSK9. pIRES-CHRD-V5 and pIRES-prodomain-V5 and removal of the vector sequence encoding the fluorescent proteins were also performed by site-directed mutagenesis using partially overlapping primers. pIRES-PCSK9-CHRD-V5 mutant constructs were generated by PCR mutagenesis using the pIRES-PCSK9-V5 cDNA template. All constructs contained a V5 tag at the C terminus. The siRNA against GLG1 and the control siRNA were purchased from Dharmacon (Lafayette, CO, USA) and the EGFP-tagged LC3 (plasmid No.11546) was purchased from Addgene Inc. (Cambridge, MA, USA). mGlg1 (GB NM_009149 nucleotides 2033-2054) was PCR amplified and subcloned into pcDNA3.0 vector. Human influenza hemagglutinin (HA) epitope tag (YPYDVPDYA) was introduced into pcDNA3.0-mGLG1 vector after the signal peptide using overlapping PCR1 and PCR2 primer pairs. Amplicons of the 2 PCR were gel purified, mixed and used as a template for third PCR. Final purified amplicons were digested and ligated to pcDNA3.0 mGlg1 at EcoRI/ SbfI-restriction sites. Mature antisenses mGlg1 (5'-GTATATCCTCGGACTCTAACT) and mLDLR

(5’-TATTAAGGGAGAATGGCGACT) targeting mGlg1 (GB NM_009149 nucleotides 2033-2054) and mLDLR (GB NM_010700 nucleotides 3425-3445) were generated by PCR. The sequence of the control shRNA (Scramble) was taken from Addgene (plasmid 1864).

Single-stranded cDNA (sscDNA) of mGLG1 (5’-TAACCCTCACTAAAGGGACTCAAGCTTTTCCAAAAAAAAGTTAGAGTCCGAGGATATACCTCTTGAGTATATCCTCGGACTCTAACTCGGGATCCATCGAGCCCTATAGTGAGTCGTATT), mLDLR (5’-TAACCCTCACTAAAGGGACTCAAGCTTTTCCAAAAAAAGTCGCCATTCTCCCTTAATACTCTTGATATTAAGGGAGAATGGCGACTCGGGATCCATCGAGCCCTATAGTGAGTCGTATTA) and Control (Scramble, 5’-TAACCCTCACTAAAGGGACTCAAGCTTTTCCAAAAAACCTAAGGTTAAGTCGCCCTCGCTCTTGACGAGGGCGACTTAACCTTAGGCGGGATCCATCGAGCCCTATAGTGAGTCGTATTA) containing different short hairpin RNA (shRNA)-flanked by HindIII/BamHI sites were purchased from Integrated DNA Technologies (IA, USA).

Briefly, the recombinant adeno-associated virus serotype 8 (AAV8)–shRNA against mGLG1, mLDLR, and scramble were generated by PCR amplification of sscDNAs. Double-stranded amplicons were digested with the 2 restriction sites and loaded on 1% agarose gel. Digested-PCR products were gel-purified and ligated in pU6 ITR (kind donation from Dr. N. Bousette from Montreal Heart Institute), followed by transformation in Stbl3 bacteria. All used clones were confirmed by sequencing and purified by Maxiprep (Qiagen, Catalog No. D4202). All PCR primer pairs are described in Table 2.1.

Mass Spectrometry and Protein Identification

To identify novel PCSK9 interactors, Huh-7 cells were transiently transfected without (empty vector; pIRES-V5) or with pIRES-hPCSK9- V5 using Lipofectamine 2000 (Cat. #11668027; ThermoFisher Scientific). Forty-eight hours post-transfection, cells were washed three times with phosphate-buffered saline (PBS) and incubated with 1 mM dithiobis[succinimidylpropionate] (DSP; Cat. #22585, ThermoFisher Scientific) and a thiol-cleavable cross-linking reagent for 30 min at room temperature. Cells were then incubated with a stop solution (15 min; 15 mM Tris/HCl, pH 7.5), and lysed in a complete radio-immune precipitation assay (RIPA) buffer (50 mM Tris/HCl, pH 8.0, 1% (v/v) Nonidet P40, 0.5% sodium deoxycholate, 150 mM NaCl and 0.1% (v/v) sodium dodecyl sulfate (SDS)) supplemented with a complete protease inhibitor mixture, passed 25 times through a 22-gauge needle and centrifuged at 11,000 g for 15 min at 4°C. Supernatants were incubated and rotated overnight with mouse anti-V5- tag (mAb: V5, 1:500; Cat. #R960-25, ThermoFisher Scientific) and 50 µl protein A/G PLUS-agarose (Cat. #sc-2003, Santa Cruz), washed six times with RIPA buffer and resuspended in Laemmli sample buffer. Co-IP proteins were separated by SDS-PAGE and visualized using the Pierce silver stain kit (Cat. #24600, ThermoFisher Scientific). Following electrophoresis, selected bands were excised from the gel, cut into ~1-2 mm 3 pieces and proteins were eluted and identified by LC-MS/MS as described previously (Poirier et al., 2015).

Briefly, excised gel chips were extensively washed, destained and re-hydrated at 4°C for 40 min in trypsin solution (6 ng/µl; Cat. #V5111, Promega, 25

mM ammonium bicarbonate). Protein digestion with trypsin was performed at 58°C for 1 h and stopped with 1% formic acid/2% acetonitrile (ACN) solution. Peptides were extracted from the gel and dried in a vacuum centrifuge. For LC-MS/MS analysis, peptides were dissolved in 1% formic acid/50% ACN and then loaded onto a C18 reversed-phase column mounted on a nanoLC-2D system (Eksigent) coupled to the LTQ Orbitrap (ThermoFisher Scientific). LC-MS/MS acquisitions were accomplished using a four-scan event cycle enabling high resolution/high mass accuracy. Proteins were identified from peptide sequences by searching the human NCBInr protein database with Mascot 2.1 (Matrix Science).

Animals

Wild-type C57BL/6 eight-weeks-old male mice were obtained from Charles River and maintained on a standard rodent diet in a 12 h light/12 h dark cycle for acclimatization. They were tail-vein injected with AAV-shRNA against mGLG1, mLDLR or scrambled virus (control) at 1×10^{11} VG/ml. Two weeks post-virus injection, mice were anesthetized by inhalation of 2% isoflurane and oxygen flow of 0.8 liters/minute in the induction chamber. Blood was collected by cardiac puncture using a 21-gauge needle mounted on a 1-mL syringe. Liver tissues were dissected, embedded in OCT medium or snap-frozen in liquid nitrogen and stored at −80 °C for further analyses. The Montreal Heart Institute Animal Care and the Ethical committee approved all animal experiments.

Co-immunoprecipitation

For the co-immunoprecipitation assay, proteins were extracted either from transfected cells or homogenized mouse liver using Ripa lysis buffer (-SDS) containing protease inhibitors as explained below. Part of the supernatants was kept for input, and the remaining part was mixed overnight at 4°C with 40 µl of protein A/G agarose beads (catalog no. sc-2003, Santa Cruz Biotechnology, Inc.) and 1 µg of anti-GLG1 antibodies. After incubation, samples were centrifuged at 2500 rpm for 5 min at 4°C, and the beads were washed by resuspension in cell lysis buffer three times and centrifugation. After the last wash, the immunoprecipitated proteins were eluted in 50 µl of Sample loading buffer and heated for 5 min before western blotting.

Western Blotting

Immunoblotting analysis was performed following standard procedures. Cells or piece of the mouse liver was homogenized with ice-cold Ripa buffer (50 mM Tris/HCl, pH 8.0, 150 mM NaCl, 0.1% (v/v) SDS, 1% (v/v) Nonidet P40, and 0.5% sodium deoxycholate) containing protease inhibitor mixture (Roche Applied Science). Samples were then centrifuged (12,000 g) for 30 min at 4 °C. Briefly, 30–60 µg of protein were resolved on 5–8% SDS-PAGE and transferred onto a nitrocellulose membrane (Bio-Rad). Membranes were blocked with 5% nonfat milk, probed with primary and appropriate HRP-conjugated secondary antibodies (1:10,000; GE healthcare). Bands were detected using western Lightning Ultra chemiluminescence kit (catalog no. NEI112001EA, PerkinElmer Life Sciences), BioFlex EC Films (catalog no. CLEC810, InterScience) and were developed using enhanced chemiluminescence method (Pierce). Band intensity was quantified using ImageJ.

Immunocytochemistry (ICC), Immunohistochemistry (IHC) and Lipid droplet staining

Huh-7 cells were grown on glass coverslips (MAtTek Corp) coated with 50 µg/ml laminin (Sigma, MO, USA) to image the colocalization of either transfected or endogenous genes. To examine the colocalization of PCSK9 and GLG1, cells were transiently co-transfected with cDNA of pIRES-hPCSK9- V5 and GLG1 plasmids 24 h after cell seeding using Lipofectamine 3000 (Life Technologies) according to the manufacturer's recommendations. For intracellular immunolabelings, cells either nontransfected or 48 hours post-transfection, fixed with 3.5% paraformaldehyde in PBS for 5 min at room temperature and permeabilized with 0.1% Triton-X 100/PBS for 15 min. Cell surface LDLR labeling was carried out under non-permeabilizing conditions. Afterward, the cells were incubated with 150 mM glycine for 5 min to neutralize the aldehydes and then incubated with blocking buffer containing 1% BSA (Fraction V; Cat. #BP1605, Sigma) in PBS at room temperature for 1 hour. The cells were then incubated with the indicated primary antibody diluted in blocking buffer; anti-GLG1 (1:200), anti-hPCSK9 (1:200), anti-hLDLR (1:500), anti-hapoB (1:200) or Golgin-97 (1:200) overnight at 4 °C. For LDLR staining of mouse liver, a piece of the tissue was cold-embedded in OCT medium and frozen at -20 °C. Cryosections (10 µm) were fixed in methanol/acetone (1:1) for 5 min, washed with PBS, blocked and then incubated with goat anti-mouse LDLR (1:200) as explained above. Following 4 washes, either cells or mouse liver cryosections were subsequently incubated with 1:500 dilution of corresponding species-specific secondary antibodies conjugated to Alexa Fluor 488,

555 or 647 (Invitrogen) for 1 h. After which they were washed with PBS, counterstained with DAPI (4=,6-di-amidino-2-phenylindole) and mounted with 90% glycerol supplemented with 5% diazabicyclo[2.2.2]octane (DABCO, Sigma).

For neutral lipids staining, Huh7 cells (48-hours post reverse transfection) and mouse liver cryosections (10-µm-thick sections from OCT-embedded tissue samples) were fixed in 4% paraformaldehyde for 5 min and then were incubated with 1 µM Bodipy-conjugated palmitate (BODIPY 493/503, Life Technologies) for 30 min at room temperature. After washing, cells or cryosections were mounted in Vectashield (Vector Laboratories). Olympus Fluoview FV10i confocal microscope was used to image the cells. Colocalization analysis and quantification of the number and size of the LDs were performed with ImageJ program from 10-15 randomly captured images. Each result presented is the mean ± SD.

Electron Microscopy (EM)

Samples of mouse liver tissue were fixed in 4% paraformaldehyde (freshly made from paraformaldehyde) for 15 min and stored in Ringer solution at 4 °C for overnight. Samples were embedded in Lowicryl K4M, as previously described (Bendayan, 1995). Lowicryl K4M was a kind gift from Dr. Moïse Bendayan from the Department of Pathology and Cell Biology at the Université de Montréal. Ultrathin sections of Lowicryl K4M-embedded tissues were examined using a Philips CM120 electron microscope equipped with a digital camera.

Measurement of plasma lipids

Blood samples were collected into EDTA-tubes, and plasma was separated by centrifugation at 2000g for 15 min and stored at -80°C. Total cholesterol was measured using an assay kit (Wako Pure Chemical Industries, Osaka, Japan) according to the manufacturer's protocol. The total plasma lipoprotein classes were fractionated by gel filtration chromatography using a superose 6 column, run at a flow rate of 0.5 ml/min. Pooled plasma from each group (100 µl) was subjected to fast performance liquid chromatography (FPLC) for lipoprotein analysis, and 45 fractions (300 µl each) were collected. Total cholesterol content was measured in each fraction (100 µl from each fraction) using the enzymatic assays by fluorimetry.

To determine the distribution of apoB within the lipoprotein fractions, equal aliquots (200 µl) of each three consecutive FPLC fractions were pooled and delipidated with 10 ml of ethanol/ether (1:1). Centrifugation of the delipidated apolipoproteins at 1000g for 15 min resulted in forming precipitated apolipoproteins which were dissolved with nonreducing protein loading buffer and subjected to 5% SDS-gel electrophoresis. Mouse monoclonal anti-apoB (1:3000; clone 2G11) was probed by Western blotting to measure apoB secretion in different lipoproteins.

Measurement of triglycerides in the liver

Snap-frozen liver pieces (100 mg) were washed with cold PBS and homogenized in 500 µl of 5% (W/V) NP-40 in water, heated to 90 °C in the water bath for 2-5 min until NP-40 appeared cloudy, and cooled down to room temperature. Heating and cooling steps were repeated one more time to solubilize all triglycerides, and then samples were centrifuged at 14000 g for 2 min to remove insoluble material. Total triglyceride concentrations were measured using a

colorimetric/fluorometric assay kit (Abcam, San Francisco, CA) according to the manufacturer's protocol.

VLDL secretion

C57BL/6 mice (8-weeks old) were infected with recombinant adeno associated virus expressing shRNA against mouse GLG1 and control virus (three mice per group). Two weeks after virus injection, mice were fasted for 6 hours and injected from a tail vein with 500 mg/kg body weight of TRITON WR 1339 (Tyloxapol, Sigma-Aldrich) diluted in 200 µl of sterile saline to block lipoprotein lipase (LPL) activity. Blood samples were collected before injection, and then after 40, 80, 120 and 240 min post-injection in EDTA-coated tubes from the facial vein. TG content in blood samples was measured using an assay kit (Abcam, San Francisco, CA).

MTP activity

MTP activity was measured by a rapid and sensitive fluorescent assay in mouse liver as described previously (Athar et al., 2004; Rava et al., 2005) with slight modifications. Small pieces (0.1 g) of liver were homogenized in 500 µL low-salt buffer K (1 mM Tris-HCl (pH 7.6), 1.0 mM EGTA, 1.0 mM $MgCl_2$) containing protease inhibitor mixture (Roche Applied Science). Homogenized samples were then centrifuged (12,000 g) for 30 min at 4 °C, and protein concentrations were determined in supernatants using Bio-Rad Protein Assay (Bio-Rad, Hercules, CA). MTP assay was performed in triplicate in black plates (Optiplate-96, F, New, 50B, Perkin-Elmer Instruments) using 5 µL of vesicles containing quenched fluorescent lipids (Chylos Inc., NY) and 20-40 µg of the protein samples. The MTP-mediated

transfer is quantified by measuring the increase in fluorescence intensity as determines the removal of the neutral lipids from the quenched donor vesicles. Plates were incubated at room temperature and read at 5, 15, 30 and 45 minutes post-addition of vesicles in a fluorescence plate reader (Fusion B, Packard Bioscience Company) using excitation and emission wavelengths of 460-470 and 530-550 nm, respectively. Blank values were determined by adding 90 µL water and 5 µL homogenization buffer to 5 µL of vesicles. To determine the total fluorescence of donor vesicles, we added 95 µL isopropanol to 5 µL vesicles. Then, following equation was used to calculate MTP activity (percentage transfer), (fluorescence units=FU):

$$\%\text{Transfer} = (\text{Sample}_{FU} - \text{Blank}_{FU}) / (\text{Total}_{FU} - \text{Blank}_{FU}) \times 100.$$

Analysis of autophagy by flow cytometry

Flow cytometric analysis of Cyto-ID Autophagy Detection Kit (Enzo Life Sciences) was used to monitor stained cells according to the manufacturer's protocol. In brief, cells were harvested 72 hours post-reverse transfection and washed with PBS, stained with Cyto-ID diluted in the serum-free culture medium for 30 min at 37°C. Then cells were washed and resuspended with 1× Assay Buffer. Data were acquired immediately by cell quantification on a FACSCanto (Becton Dickinson) flow cytometer.

LPL activity

Lipoprotein Lipase (LPL) activity was assayed by a Fluorometric kit (Cat No STA-610, Cell Biolabs INC, USA) in pre- and post-heparin plasma. Blood was

collected before and 10 min after tail vein injection of heparin (0.1 U/g body weight) and then centrifuged at 1000 x g at 4°C for 10 minutes to collect plasma supernatant. Diluted plasma in 1X LPL Assay Buffer (1:100) was used for assaying following the manufacturer's protocol.

RNA extraction and RT-PCR

Total RNA was isolated from cultured human hepatocytes (Huh7) and mouse liver using Trizol reagent (Cat. #15596026, Invitrogen) according to the manufacturer's recommendations and resolved in sterilized RNase-free water. NanoDrop spectrophotometer (Thermo Scientific Inc., Waltham, MA) was used to determine the RNA concentration, and the purified RNA was stored at -80 °C. The integrity of the RNA samples was confirmed by agarose gel electrophoresis. One µg of total RNA was used for cDNA synthesis using the iScript cDNA synthesis kit (cat. # 170-8891, BioRad) for PCR with reverse transcription.

Quantitative PCR

Real-time PCR was performed using the PerfeCTa SYBR Green SuperMix, UNG, Low ROX (Cat. #95070-100, Quanta Biosciences) and with the MX3000p real-time thermal cycler (Agilent). Dissociation curves and agarose gel electrophoresis were performed for each gene of interest to confirm the specificity of PCR products. The levels of expression of individual genes were determined from PCR duplicates and normalized to the glyceraldehyde 3-phosphate dehydrogenase (GAPDH) or the TATA box binding protein (TBP). The values show the fold change of expression of

each gene relative to the value of the control sample. Oligonucleotide sequences are listed in Table 1.

AAV vector production

Human embryonic kidney 293T (HEK293T) cells were cultivated in complete DMEM without sodium pyruvate (catalog no. 319-015-CL, Wisent) containing 10% fetal bovine serum (FBS; catalog no. 080-350, Wisent). HEK293T cells were plated into 16 X100-mm culture plates ($5.0x10^6$ cells) to reach 70–80% confluence on the day of transfection for virus production. Co-transfection of the cells with a mixture of plasmids and linear polyethylenimine (PEI) MW 25,000 (PEI; 46 µl/plate, Cat No.23966, Polysciences) produced AAV serotype 8 vectors. The plasmids mixture contained packaging plasmid PDG8 (8.6 µg/plate) (Grimm and Kleinschmidt, 1999) and constructed plasmid (2.9 µg/plate). Three days after transfection, cells were harvested and pelleted by centrifugation (1140 g for 10 min at room temperature). The cells were resuspended in 4.5 ml of lysis buffer (50 mM Tris, 150 mM NaCl, pH 8.5) and the virus was released from the cells by three rounds of freeze and thaw in Ethanol/dry ice bath for 5 min and 37°C water bath for 2 min respectively. Per ml of Crude lysates were treated with 250 units of Benzonase nuclease (Sigma, E1014-5KU) and 1mM $MgCl_2$, mixed and incubated for 45 min at 37℃. After pelleting the cell debris for 20 min at 6000 g, the supernatant was used for further purification.

An iodixanol step density gradient was prepared as described previously (Zolotukhin et al., 1999) with slight modifications: Briefly, 60% iodixanol (OptiPrep; Sigma D1556) was diluted to 40, and 25% in 5X PBS-MK (5X PBS, 5 mM $MgCl_2$,12.5 mM KCl). To facilitate distinguishing the phase boundaries within the gradients, 2.5

µl of 0.5% phenol red (Bioshop PHE600.5/5g) was added per milliliter to the of 25 and 60% iodixanol. One milliliter of 60, 40, and 25 % iodixanol solutions was successively underlaid in a 5-ml Beckman ultracentrifuge tube (catalog No# 326819), and 1.5 to 2 ml of the processed cell lysate was gently overlaid onto the gradients and centrifuged in a 55Ti rotor for 3 hr at 33,000 rpm at 4℃. After centrifugation, the tubes were punctured between the 60 and 40% interphase (bottom and middle layers), using an 18-gauge needle, to collect ~1-ml/tube of the fraction containing the virus. A pool of collected iodixanol containing virus was diluted with PBS-0.001% Tween to reach a total volume of 15ml and concentrated to ~1ml by passage through Amicon Ultra-15 centrifugal filter unit (MWCO, 100 kDa; Merck Millipore). The concentrator was filled up to 10 ml and concentrated the virus again to 1 ml. This step was repeated two more times. Viral titers in terms of viral genomes (VG)/ml were determined by Real-Time qPCR with four different dilutions of the virus relative to standards using following primer pair: BGH-F; 5=TGCCTTCCTTGACCCT and BGH-R; 5=CCTTGCTGTCCTGCCC. Finally, viral batches were aliquoted and stored at -80℃.

Statistical Analysis

Statistical analysis was performed using GraphPad Prism Version 5 (Prism Software Inc., La Jolla, CA, USA). Unpaired two-tail Student's t-test was measured to determine P-value. Statistically, the significance of the difference between groups was set at $P < 0.05$ and indicated by *. Distribution of the continuous variables between groups of each experiment was expressed as mean ± SD and represented the result of at least three independent experiments. N indicates the number of

replicates in each group of the experiment. Protein bands from SDS-PAGE were quantified and normalized using ImageJ version 1.50b software (NIH).

Table 2.1. Oligonucleotides used for plasmid constructions and quantitative PCR

Name	Forward (5'->3')	Reverse (5'->3')
Constructs		
pcDNA3.0-mGlg1-HA	PCR1:TAGAATTCATGGCGGTGTG TGGACGTGTACGG PCR2:ACGTCCCAGACTACGCGCA GAATGGTCACGGTCAGG PCR3:TTAGAATTCATGGCGGTGT GTGGACGTGTACGG	PCR1:GGGACGTCGTATGGGTAGGCCCC TGCTGCCGCGAG PCR2:TGATTGCAGTCTGAAGAAATCTC PCR3:TGATTGCAGTCTGAAGAAATCTC
pcDNA3.0-mGlg1- HAΔ1169	GCCTTGGACATTAAACACCACT	GTCTGTACACTATCTCTTGGTGATCCGTC CACACAT
pcDNA3.1 mGlg1-HA+24aa (Cterm, hGlg1)	PCR1:CAGCATGTGCCTTGGACAT T PCR2:AGGACAGGCTACAATACAG GTCA PCR3:CAGCATGTGCCTTGGACAT T	PCR1:GACCTGTATTGTAGCCTGTCCTTC AGCTCTCGTG PCR2:TTATGTACAAAGTTTGTCTGGAGTG TGCAGAA PCR3:TTATGTACAAAGTTTGTCTGGAGTG TGCAGAA
pcDNA3.1-mGlg1-HA-GPI	PCR1:CAGCATGTGCCTTGGACAT T PCR2:GTGATGACATCTCCCTCAA AGAACPCR3: CAGCATGTGCCTTGGACATT	PCR1:GTTCTTTGAGGGAGATGTCATCAC T PCR2:CGGTGTACATTAAAGAACATTCATA PCR3:CGGTGTACATTAAAGAACATTCATA
ShmGLG1, ShmLDLR, ShScramble	TAACCCTCACTAAAGGGACTC	TAATACGACTCACTATAGGGCTC
Quantitative PCR		
hHMGCR (NM_000859)	GTCACATGATTCACAACAGG	GTCCTTTAGAACCCAATGC
hLDLR (NM_000527)	AGGAGACGTGCTTGTCTGTC	CTGAGCCGTTGTCGCAGT
hTBP(NM_001172085)	CGAATATAATCCCAAGCGGTTT	GTGGTTCGTGGCTCTCTTATCC
mHmgcr (NM_008255)	GTACGGAGAAAGCACTGCTGAA	TGACTGCCAGAATCTGCATGTC
mLldlr (NM_010700)	GTATGAGGTTCCTGTCCATC	CCTCTGTGGTCTTCTGGTAG
hapoB100(NM_00038.2)	TGCCTGAGCAGACCATTGAG	TGTGTGTTCCCAAAACATTTAGTT
hBeclin (XM_017025264)	CCAGATGCGTTATGCCCAGA	TCCATTCCACGGGAACACTG
mLC3B(NM_026160.4)	AGTCAGATCGTCTGGCTCGG	AGCCGGACATCTTCCACTCT
hLC3B((NM022818.4)	AACGGGCTGTGTGAGAAAAC	AGTGAGGACTTTGGGTGTGG
hATG7(NM_001349236.1)	TCCTGGGCTCATCGCTTTTT	AGTCCTGGACGACTCACAGT
mBeclin(XM_006533784.3)	AGCTGGAGTTGGATGACGAA	ATTGTGCCAAACTGTCCGCT
mATG7(XM_006506710.3)	AACGAGTACCGCCTGGACGA	GCGTGGAGGCACTCATGTCA
mP62(NM_001290769.1)	GCTCCACCAGAAGATCCCAAT	GTGTCAGGCGGCTTCTCTTC
mMTTP(NM_008642.2)	CTCTTGGCAGTGCTTTTTCT	GAGCTTGTATAGCCGCTCT

mGLG1 (NM_009149)	TCGGGATTGGAAGTTGGACC	CCTCTGGACTTCAGCTCGAC
mPCSK9 (NM_153565)	TGCAAAATCAAGGAGCATGGG	CAGGGAGCACATTGCATCC
hGLG1 (NM-001145666.1)	TTCTCGTCTTTGCCACACC	ATCCTTTGGACTTCAGCTCG
hMTTP(NC_018915.2)	ATACCTGCAGCCTGACAACC	AGGTCTGAGCAGAGGTGACA
mAlbumin (NM_009654)	GCTGAGACCTTCACCTTCCA	CTTGTGCTTCACCAGCTCAG
mapoB(NM_009693.2)	CTACTTCCACCCACAGTCCC	TAGCCTTAGAAGCCTTGGGC

2.4 Results

Identification of GLG1 as an endogenous PCSK9, LDLR, and apoB-binding protein

To identify PCSK9-interacting proteins, PCSK9 was immunoprecipitated (IP) under overexpressed conditions from human hepatic Huh-7 cells. Co-interacting proteins were resolved by SDS-PAGE and visualized by silver staining. Mass spectrometry of excised gel bands identified a 150-kD band, the most enriched migrating protein complex with PCSK9, as human GLG1 (Figure 2.1A). Also, immunoblotting confirmed that endogenous GLG1 was co-immunoprecipitated explicitly with PCSK9-V5, a truncated PCSK9 lacking the C-terminal domain (PCSK9-L455X-V5) and LDLR-V5 under overexpressed conditions (Figure 2.1B). The intracellular interaction of the PCSK9 and apoB (Sun et al., 2012), prompted us to test whether GLG1 could physically interact with apoB. Co-immunoprecipitation experiments showed that apoB was explicitly pulled down with GLG1 in mouse liver (Figure 2.1C) and Huh7 cells (Figure 2.1D). Co-immunoprecipitation of apoB with GLG1, in either the absence or presence of PCSK9, indicates that GLG1 interaction with apoB is PCSK9-independent (Figure 2.1D).

As a first approach to gain insight into the GLG1-localization in the medial cisternae of the Golgi apparatus (Gonatas et al., 1989), Huh7 cells were double-immunolabeled with an antibody against GLG1 and a Golgi marker, Golgin-97, following GLG1-overexpression. Our confocal microscopy analysis demonstrated the co-localization of GLG1 (red) and Golgin-97 (Green) in the juxta-nuclear region of Huh7 cells (Supp. Figure 2.1A). In agreement with co-IP experiments, the colocalization pattern of endogenous GLG1 with overexpressed PCSK9-V5 was found in the Golgi apparatus (Figure 2.1E). The GLG1 co-localization with either apoB (Figure 2.1A F) or LDLR (Figure 2.1G) in physiological conditions of Huh7 cells was visualized by confocal microscopy and analyzed quantitatively (Figure 2.1H).

Knockdown of GLG1 reduced apoB, PCSK9 and LDLR protein stabilization in Huh7 cells and resulted in lower protein expression in mouse liver and human hepatic cell lines

Transfection of Huh7 cells with a specific small interfering RNA (siRNA) or intravenous injection of mice with the AAV8-expressing short hairpin RNA against GLG1 resulted in a significant decrease of RNA level of GLG1 in cells (Supp. Figure 2.1B) and mouse liver (Supp. Figure 2.1C). We observed a significant reduction in mRNA expression of LDLR (~51%) in Huh7 cells (Supp. Figure 2.1B), mRNA level of LDLR (~47%) and apoB (~57%) in mouse liver (Supp. Figure 2.1C) upon Glg1-knockdown compared to the control group. In addition, downregulation of GLG1 resulted in 35% less mRNA expression of HMGCR in mouse liver (Supp. Figure 2.1C). Moreover, GLG1-deficient mice gained 11.64% less weight than the control group over 2 weeks of virus injection (Supp. Figure 2.1D). Knockdown of GLG1 in

Huh7 cells using siRNA reduced the half-life of apoB (Figure 2.2A), and PCSK9 (Figure 2.2B) by ~37%. Similarly, there was a statistically significant ($p<0.05$) decrease in protein half-life of LDLR in cells with Glg1 knockdown compared to the control cells (Figure 2.2C). Next, we investigated whether the protein expression of apoB, LDLR, and PCSK9 were altered by knockdown of endogenous GLG1 in either Huh7 cells or mouse liver. Western blotting results demonstrated that Glg1-knockdown in Huh7 cells (Figure 2.2D) and mouse liver (Figure 2.2E) caused a robust decrease in apoB, LDLR, and PCSK9 protein levels. Also, Glg1 knockdown in Huh7 cells decreased the secretion of apoB in the media by about 37% (Figure 2.2D). However, knockdown of Glg1 in mouse liver increased apoB accumulation in plasma by about 46% (Figure 2.2E) and reduced the amount of secreted PCSK9 protein by ~58% compared to the control (scramble) group (Figure 2.2F). The postoperative confocal analysis confirmed that Glg1 knockdown reduced cell surface expression of LDLR in Huh7 cells (Figure 2.2G) and mouse liver (Figure 2.2H). Lower apoB secretion in Glg1-knockdown cells suggested that GLG1 might be involved in the regulation of cholesterol and apoB-lipoprotein secretion.

Glg1 knockdown altered plasma apoB-containing lipoproteins, HDL-cholesterol, and triglycerides regulation.

Our observations of the effect of mouse hepatic Glg1-knockdown on the protein level of apoB, LDLR, and PCSK9 prompted us to test whether GLG1-deficiency could change total cholesterol level and apoB distribution within plasma lipoproteins. Plasma total cholesterol (Figure 2.3A), including LDL- and HDL-cholesterol (Figure 2.3B) were sharply reduced by downregulation of GLG1 in mouse

liver compared to the control (scramble) group. We further analyzed the distribution of apoB48 and -100 among fractionated lipoproteins. The pattern of apoB48 and -100 distribution in the lipoprotein fractions were different between the two groups of mice. In the control (scramble) group, the plasma level of apoB48 was higher than apoB-100 in VLDL particles, as previously described (Plump et al., 1992). However, these apolipoproteins were no longer visible in VLDL fractions by knockdown of Glg1.

The abundant amounts of apoB that appeared in the HDL fraction upon Glg1-knockdown might be related to the accumulation of aggregated-apoB in mouse plasma (Figure 2.3B; bottom). Accumulation of apoB in plasma of Glg1 knockdown mice was also supported by an apoB ELISA kit (Figure 2.3C). Also, a sharp reduction of HDL-cholesterol by Glg1 knockdown suggested us to test the effect of GLG1 downregulation on apolipoprotein A1 (apoA1), a major protein component of HDL. Western blotting (Figure 2.3D, left panel) and quantification (Figure 2.3D, right panel) analysis indicated that protein level of apoA1 was highly suppressed (4.24-fold) in mouse liver samples following knockdown of Glg1.

In addition, a substantial reduction of plasma total cholesterol level upon Glg1 knockdown suggested a possible GLG1 role in VLDL synthesis and secretion. In a time-course experiment, the rate of hepatic lipid export (VLDL secretion) was measured after injecting the mice with tyloxapol, an inhibitor of lipoprotein lipase (LPL) activity, to inhibit VLDL catabolism. Plasma triglyceride measurements demonstrated lower VLDL secretion over time in mice with Glg1 knockdown compared to the control virus-treated mice (Figure 2.3E). We next examined whether hepatic triglyceride content could be influenced by lower plasma triglyceride content

induced by Glg1-knockdown. Our analysis demonstrated ~2-fold increase in the liver triglyceride storage by knockdown of the GLG1 compared to the control group (Figure 2.3F). The hepatic assembly and secretion of VLDL require microsomal triglyceride transfer protein (MTP) (Bakillah et al., 2000). Thus, we assessed MTP activity and expression by knockdown of Glg1.

Our mouse liver analysis demonstrated a significant reduction in MTP activity (Figure 2.3G) upon Glg1-knockdown. Moreover, the mRNA level of MTP was reduced by 38% without reaching statistical significance (Supp. Figure 2.2A). No significant difference was observed in the protein level of MTP upon Glg1 knockdown (Supp. Figure 2.2B). In addition, mRNA (Supp. Figure 2.2C) and protein (Supp. Figure 2.2D) level of MTP did not change significantly after GLG1 downregulation in Huh7 cells.

Another potential factor that may influence lipoprotein secretion by Glg1 knockdown is Angiopoietin-like3 (ANGPTL3). Angptl3, a hepatic secretory factor, suppresses lipoprotein lipase (LPL) activity and increases VLDL secretion by decreasing hydrolysis of triglycerides and phospholipids,(Koishi et al., 2002; Shan et al., 2009; Shimizugawa et al., 2002). Moreover, ANGPTL3 plays an essential role in the regulation of plasma HDL cholesterol via a heparin-dependent mechanism acting as an endothelial lipase (EL) inhibitor (Shimamura et al., 2007). Therefore, we tested a hypothesis that deficiency of GLG1 might decrease ANGPTL3 secretion thereby increasing LPL and EL activity. In addition, ANGPTL3 may explain the decrease in plasma level of TG-rich lipoproteins and HDL cholesterol-induced upon the Glg1 knockdown. Contrary to our hypotheses, a small increase in the protein level of both endogenous (Supp. Figure 2.2E) and overexpressed (Supp. Figure

2.2F) ANGPTL3 was observed in cell lysates and conditioned medium of Glg1-knockdown cells compared to the control group. However, the difference was not statistically significant (Supp. Figure 2.2F; right panel).

We also analyzed the LPL- activity in mouse plasma samples before and after heparin injection. Our results demonstrated that LPL activity did not change in pre-heparin plasma and slightly decreased in post-heparin plasma of the mice injected with shGLG1 (Supp. Figure 2.2G). Also, no difference was observed in the protein level of LPL in mouse liver of the same animal groups (Supp. Figure 2.2H).

Knockdown of GLG1 increased lipid droplets in Huh7 cells and changed the morphology of the endoplasmic reticulum in mouse liver

Accumulation of triglycerides in the liver by Glg1-knockdown, suggests a potential role for GLG1 in the regulation of hepatic lipid content. Neutral lipid staining of Huh7 cells indicated a remarkable increase in the intensity of the lipid droplets by knockdown of Glg1 over the control group (Figure 2.4A). Quantitative analyses of the confocal microscopy images showed a significant increase by 1.7-fold in the number of lipid storage droplets per cell (Figure 2.4B) and no change in droplet sizes (Figure 2.4C) upon Glg1 knockdown compared to the control group. Immunoblotting of protein samples (Figure 2.4D) and postoperative confocal analysis (Figure 2.4E) from mouse liver, further confirmed our observations by detecting a ~4-fold increase in the amount of perilipin, lipid droplet coat protein, and high bodipy staining by Glg1-knockdown. In line with these results, electron microscopy analysis revealed abnormal morphological changes including the presence of large vesicles containing lipid droplets (Figure 2.4F) and dilated or distorted (swollen) endoplasmic reticulum

(ER) (Figure 2.4G) in liver of the AAV8/shGLG1-treated mice compared to the regular liver of the control (scramble) group. ER is the primary site of protein folding and assembly. Ultrastructural abnormalities of the ER might represent ER-stress, which in turn leads to the Unfolded Protein Response (UPR) to restore normal ER function (Ron and Walter, 2007). IB and quantification (right panel) results indicated no changes in the protein level of Glucose-regulated protein 78/BiP (GRP78) and Grp94 (the ER Hsp90 paralog), early respondent of ER stress signal transduction (Tabas and Ron, 2011), by knockdown of Glg1 in mouse liver (Figure 2.4H).

Glg1-knockdown induced autophagosome/aggresome formation and apoB-100 degradation in a pre-Golgi compartment

It is well established that the export of the proteins from the ER depends on proper protein folding (Hurtley and Helenius, 1989). A vesicle trafficking inhibitor brefeldin A (BFA) (Fujiwara et al., 1988) was used to examine whether Glg1-knockdown induced apoB-degradation requires the transport of apoB out of the ER. WB analysis demonstrated a similar intracellular accumulation of apoB, GLG1, and PCSK9 in Huh7 cells treated with BFA, While it did not affect Glg1 knockdown induced lower apoB or PCSK9 protein levels (Figure 2.5A). The lack of BFA effect on preventing lower apoB expression upon Glg1-knockdown, suggests that GLG1 is required for the transit of apoB from the ER to the secretory pathway and its knockdown induces apoB-degradation by excluding apoB from existing transport vesicles. Thus, Glg1-knockdown may cause improper folding of apoB, its aggregation, and translocation to the autophagosome/aggresome compartment for degradation. Therefore, we investigated the effect of Glg1-knockdown on RNA and

protein level of P62 (SQSTM1/sequestosome), a standard component of protein aggregates (Ravikumar et al., 2002; Ravikumar et al., 2004; Zatloukal et al., 2002).

The protein level of P62 was remarkably increased in the liver of the mice (Figure 2.5B) and Huh7 cells (Figure 2.5C) after GLG1 downregulation. In addition, the confocal microscopic analysis further supported our result by showing enhanced protein expression of P62 in GLG1 deficient Huh7 cells (Figure 2.5D). Upon completion of folding, ER constitutes a major source/scaffold of the autophagic isolation membrane (Hayashi-Nishino et al., 2009). Autophagic destruction is late-stage quality control, activated when newly synthesized apoB escapes other ER-degradation systems (Pan et al., 2008). Autophagic degradation is highly active for apoB-degradation in primary hepatocytes (Qiu et al., 2011). The fact that apoB can be degraded through autophagosome/lysosome degradation pathway (Ohsaki et al., 2006), and the effect of GLG1 downregulation on increased level of P62 (Figure 2.5B-D), and reduced level of apoB secretion (Figure. 2.1A), suggest a potential role of GLG1-deficiency in the apoB autophagy-lysosomal degradation pathway.

The most common method used to show increased autophagy is the detection of LC3-II by immunofluorescence or immunoblotting (Klionsky et al., 2008). Thus, we established Huh7 cells stably expressing GFP-LC3 to monitor the formation of autophagic vesicles in the presence or deficiency of GLG1. We observed that GFP-LC3-positive dots tend to be incorporated into perinuclear structures, hallmark features of aggresomes, upon Glg1 knockdown (Figure 2.5E). In principle, GFP-LC3-positive protein aggregates are degraded by autophagy (Szeto et al., 2006). We next sought to investigate the effect of Glg1 knockdown on autophagy flux using LC3B immunoblotting assay. Unpredictably, the level of

endogenous LC3B was slightly reduced by downregulation of GLG1 in either cells (Supp. Figure 2.3A) or mouse liver (Supp. Figure 2.3B). However, since autophagy degrades LC3, immunoblotting assay might not be a suitable method to distinguish activated autophagy from impaired autophagy flux (Guo et al., 2015; Mizushima and Yoshimori, 2007). Then we compared protein level of LC3-II in the presence and absence of lysosomal inhibitor (NH_4Cl) to measure the quantity of delivered LC3-II into lysosomes with/without GLG1. Our results demonstrated an increase in protein level of LC3-II in GLG1-deficient Huh7 cells in the presence of NH_4Cl (Supp. Figure 2.3C).

We also used electron microscopy analysis and Cyto-ID assay with a cationic amphilic fluorescent tracer dye (Chan et al., 2012) to better clarify the effect of Glg1 knockdown on autophagy flux. Electron microscope observations demonstrated that deficiency of GLG1 induces autophagic vacuoles (double or multi membrane-bound structures) formation in mouse liver (Figure 2.5F). Consistent with this result, the flow cytometry analysis of 4 independent experiments detected higher fluorescence intensity of the cationic amphilic tracer dye upon knockdown of Glg1 (Figure 2.5G). Following Glg1-knockdown in cells and mouse liver, we measured mRNA levels of key molecules in autophagy pathways. Our qPCR analysis showed mRNA level of Beclin, LC3B, and ATG7 remain unchanged in cells (Supp. Figure 2.3D) and mouse liver (Supp. Figure 2.3E).

Glg1-knockdown decreased circular staining of apoB in CLDs (apoB-crescents) and induced accumulation of apoB in aggresomal structures

Mobilization of lipids to the cytoplasmic lipid droplets (CLD) is required for VLDL assembly (Gibbons et al., 2000). The decrease in VLDL secretion by knockdown of Glg1 in mouse liver prompted us to monitor the association of apoB with CLDs. For this reason, we treated Huh7 cells, with or without Glg1-knockdown, for 4 hours with oleic acid (OA; 1.5 mM) to stimulate lipid synthesis. Fluorescence confocal microscopy analysis revealed that apoB was labeled around CLDs (apoB-crescent) in control cells (Figure 2.6A). ApoB underwent a profound conformational change with no localization around CLDs in the siGLG1-treated cells (Figure 2.6A). To further investigate the role of Glg1-knockdown in autophagy degradation of apoB and the characteristic shape of apoB, we treated the cells with an autophagy inhibitor, 3-methyladenine (3MA; 10 mM), for 3 hours. Circular double labeling of apoB and CLDs was observed in control cells that were treated with 3-MA. Conversely, no association of undegraded apoB (gross aggregation) with CLDs was observed in Glg1-knockdown cells that were treated with 3-MA (Figure 2.6A).

Quantification of fluorescence intensity of apoB demonstrated a significant decrease of apoB staining by knockdown of Glg1, but the decrease was blocked by 3-MA (Figure 2.6B). Based on the characteristic shape, the frequency of apoB-crescents was decreased, mostly diffused, and partially aggregated by Glg1-knockdown. Also, Inhibition of autophagy in Huh7 cells post knockdown of Glg1 caused a cytosolic accumulation of apoB in large aggregates and a decrease in the number of apoB-crescents (Figure 2.6C).

Since P62 plays an essential role in the autophagic degradation of ubiquitinated cytoplasmic proteins (Ichimura et al., 2008), we analyzed the effect of Glg1 knockdown on the correlation between apoB, P62, and ubiquitin, (Pankiv et al.,

2007). Immunofluorescence staining demonstrated a robust increase in cytoplasmic accumulation of P62 and a minimal increase of nuclear ubiquitin staining by knockdown of Glg1 (Figure 2.6D). Accumulation of aggregated apoB and P62 in the perinuclear region was observed in cells with Glg1 knockdown following treatment with an autophagy inhibitor. Moreover, redistribution of nuclear ubiquitin to the perinuclear region indicated impaired autophagy and GLG1 deficiency together induced ubiquitination of undegraded apoB (Figure 2.6D).

Increase in P62 staining upon GLG1 deficiency was confirmed by quantification analysis (Figure 2.6E). A significant increase in ubiquitin immunofluorescence staining was observed in GLG1 deficient Huh7 cells that were treated with an autophagy inhibitor (3-MA) (Figure 2.6F). Our further quantification analysis demonstrated a significant increase in apoB co-localization with P62 by Glg1 knockdown with/without an autophagy inhibitor. This suggests that co-localization of apoB with P62 by Glg1 knockdown is autophagy-independent (Figure 2.6G). These observations further verified that Glg1 knockdown alters the processing of apoB, via the autophagosome/aggresome pathway.

Autophagy inhibition upon Glg1 knockdown compromises degradation of ubiquitinated apoB aggregates

To further investigate the contribution of autophagy in apoB degradation upon downregulation of GLG1, we performed immunofluorescence staining of apoB and marker of autophagy (LC3), in Huh7 cells that were treated with OA (1.5 mM; 4 hours) in presence or absence of 3-MA (10 mM; 3 hours). Our confocal microscopy analysis demonstrated a decrease in apoB expression and change in the localization

of endogenous apoB and LC3 upon knockdown of Glg1 (Figure 2.7A). Incubating the GLG1 deficient cells with 3-MA prevented the decrease of apoB expression and induced aggregation of apoB and LC3 in the perinuclear region (Figure 2.7A). To better understand the role of Glg1-knockdown on intracellular trafficking of apoB, Huh7 cells (with or without Glg1 knockdown) were treated with 3-MA either in the absence (Figure 2.7B) or presence (Figure 2.7C) of OA. OA stimulates apoB secretion by preventing proteasomal apoB degradation in HepG2 cells (Dixon et al., 1991).

Western blot analysis indicated that knockdown of Glg1 reduced protein level of apoB in cell lysates and caused a robust decrease in apoB secretion in cells that were treated with (Figure 2.7B) or without (Figure 2.7C) OA. Treating the cells with 3-MA, blocked the intracellular degradation of apoB in Glg1-knockdown cells. However, a marked decrease of apoB secretion was detected in either control or Glg1-knockdown cells (Figure 2.7B). We next changed our experimental strategy to examine whether inhibition of autophagy could block reduction of apoB secretion in GLG1-deficient cells. For this purpose, we treated the cells with OA to induce apoB secretion and 3-MA to inhibit autophagy degradation. Prevention of the dramatic decrease of apoB secretion in Glg1-knockdown cells was observed by immunoblotting analysis of the conditioned medium (Figure 2.7C). Together, these data argue strongly that Glg1-knockdown requires autophagosome/lysosomes pathway to induce degradation of aggregated apoB.

2.5 Discussion

The observation that PCSK9 and LDLR co-exist within the secretory pathway, and that PCSK9 induces LDLR degradation, while there are some remaining LDLR at the cell-surface for clearance of LDL, raised the possibility of the presence of some modulators that might change the capacity of PCSK9 for LDLR degradation (Surdo et al., 2011). We began this study with a desire to find a new PCSK9 interacting protein that may change the function of PCSK9 on LDLR degradation. The data presented in this work revealed that GLG1 is an endogenous PCSK9 intracellular binding protein that can also interact with apoB and LDLR in physiological conditions. GLG1 is also known as E-selectin ligand-1 (ESL-1) (Steegmaler et al., 1995), Golgi sialoglycoprotein (MG-160) (Stieber et al., 1995), cysteine-rich fibroblast growth factor receptor (CFR) (Burrus et al., 1992), homocysteine-rich fibroblast growth factor receptor (CGR-1)(Burrus et al., 1992), and latent transforming growth factor-β complex protein 1 (LTCP-1) (Olofsson et al., 1997).

The interaction of GLG1 with a truncated PCSK9 lacking the C-terminal domain (PCSK9-L455X-V5) as well as pro- and mature- forms of PCSK9 suggest that GLG1 interacts with the catalytic domain of PCSK9 via intracellular trafficking of the PCSK9 to the cell surface. Given that interaction of GLG1 with PCSK9, LDLR, and apoB might have a crucial role in the regulation of plasma cholesterol homeostasis, our work focused on the specific role of GLG1 in regulating the expression of PCSK9, LDLR, apoB-lipoproteins, and cholesterol homeostasis.

Our results demonstrated that knockdown of Glg1 decreased RNA (Supp. Figure 2.1C) and protein (Figure 2.2D) expression of LDLR in Huh7 cell lysates.

Moreover, downregulation of Glg1 decreased protein level of PCSK9 in lysates and apoB in media and lysates of Huh7 cells (Figure 2.2D). The decrease of apoB in the media of Huh7 cells following the Glg1 knockdown, in conditions where there are less LDLR at the cell surface for its clearance; suggest that GLG1 might be required for the secretion of apoB-lipoproteins to the cell surface. Ligand-receptor interaction, within the trafficking pathway of proteins from the ER to the cell surface, is an important mechanism to regulate protein secretion, in a way that receptor modulates the export of its ligands from the ER to the cell surface (Gillian-Daniel et al., 2002). In our study, a decrease in LDLR protein expression (Figure 2.2D and E) and its interactions with its ligands (PCSK9, and apoB) might decrease the trafficking pathway of apoB, PCSK9, and LDLR to the cell-surface and, in consequence, induce their degradation pathway.

Genetic defects in LDLR (Brown and Goldstein, 1986), apoB (Soria et al., 1989), and PCSK9 (Abifadel et al., 2003) are associated with autosomal dominant hypercholesterolemia (ADH), an inherited disorder characterized by elevated plasma levels of low LDL particles (Nordestgaard et al., 2013). A study on ADH-families without any mutations in these three genes has indicated the existence of other ADH genes. A genome-wide scan analysis of this family mapped a fourth ADH gene at 16q22.1 locus containing 154 genes, including GLG1 gene (Marques-Pinheiro et al., 2010).

To better characterize the importance of GLG1 in cholesterol regulation, we analyzed tissue samples from C57BL/6 mice after two-weeks of Glg1-knockdown. Our data revealed that knockdown of Glg1 in mouse liver decreases intracellular protein level of LDLR, PCSK9, and apoB (Figure 2.2E). Moreover, it led to marked

reductions in PCSK9 secretion (Figure 2.2F) and plasma cholesterol level (Figure 2.3A). To our knowledge, there has been no previous report on the importance of GLG1 in the regulation of PCSK9, apoB, and LDLR proteins. Furthermore, the effect of GLG1 on cholesterol regulation has not been reported before. The assembly and secretion of apoB-containing lipoproteins from hepatocytes depend on the amount of apoB that is loaded with TG through the activity of MTP. In contrast, poorly lipidated apoB cannot fold properly and therefore is more likely to be delivered to ubiquitination machinery for degradation. Hence, the availability of apoB, TG, and MTP is important in determining the plasma cholesterol level and its substantial influences on the risk of cardiovascular disease (Polonovski and Beucler, 1983).

Thus, we further characterized the decrease of the circulatory level of cholesterol observed in Glg1-knockdown mice using FPLC analysis and TG measurements. Our results showed a significant decrease in LDL, HDL (Figure 2.3B) and TG secretion (Figure 2.3E) in plasma of Glg1-knockdown mice. The decrease in TG secretion into the plasma resulted in TG accumulation (Figure .23G) and more lipid droplet formation (Figure 2.4E-F) in mouse liver upon Glg1-knockdown. In contrast to our results with Huh7 cells, apoB accumulated in the plasma of the Glg1-knockdown mice (Figure 2.3E). The reason for this discrepancy in our results is not well understood. This could be due to physiological differences between growing cells in flat layers and in vivo state as well as different lipid profile between mouse and human hepatocytes. Mouse has a high level of atheroprotective HDL, whereas human has high level of atherogenic LDL (Vergeer et al., 2010). We also speculate that the apoB accumulation in plasma of Glg1-knockdown mice is due to the long-term low expression of cell surface LDLR and reduced level of MTP activity, two

effects that were previously reported in the $Ldlr^{-/-}$ $Mtp^{\Delta/\Delta}$ mice (Larsson et al., 2004). Accumulation of apoB, while there are less VLDL and LDL in plasma, brought the idea that apoB lipidation was inadequate in Glg1 knockdown mice. This led us to propose that GLG1 downregulation decreases MTP activity in transferring neutral lipids into the core of primordial lipoprotein particles for mature VLDL synthesis. Our data supported this hypothesis by showing a remarkable decrease of MTP activity in liver of the GLG1- knockdown mice (Figure 2.3G). The present results are consistent with the study of Larsson et al. (2004) suggesting that low levels of MTP activity and cell surface LDLR can lead to apoB accumulation in mouse plasma. ApoB and neutral lipids are the known substrates for MTP activity. Reduction in mRNA level of apoB in mouse liver (Figure 2.1 C), and no significant change in mRNA and protein level of MTP (Supp. Figure 2.2 A-B), while there is a decrease in MTP activity (figure 2.3G) may suggest that decrease in MTP activity is simply due to the less availability of apoB for lipidation.

A decrease in HDL secretion following Glg1 knockdown might be explained by the decrease of MTP activity as demonstrated in a study with liver-specific MTP-knockout mice (Raabe et al., 1999). MTP is essential for transferring triglycerides into the ER lumen for VLDL assembly. Inactivating the MTP gene in the liver reduces VLDL triglycerides and subsequently decreases the availability of substrates for the generation of HDL (Raabe et al., 1999). Moreover, fine mapping and association studies on patients with low levels of HDL-C have shown that a region on chromosome 16 is likely to harbor a gene for the low circulatory level of HDL, which is not identified yet (Dastani et al., 2010). The extreme decrease in the circulatory level of HDL by GLG1-downregulation and the fact that GLG1 gene is located at the

16q22.1 locus (Mourelatos et al., 1995), suggest that the sequencing of GLG1 in these patients (individuals with low levels of HDL-C) might help to identify the causal gene that is responsible for severe low plasma level of HDL.

Immunoblotting for apoB of FPLC fractions demonstrated a darkly stained smear overlapping with small HDL that might correspond to aggregated apoB and poorly lipidated lipoproteins because of Glg1 knockdown (Figure 2.3B). We also showed that downregulation of Glg1 altered apoB distribution within different lipoprotein fractions and reduced apoB secretion in VLDL containing lipoproteins (Figure 2.3B). The decrease of apoB concentration in VLDL lipoproteins might be a consequence of the decrease in MTP activity and lower apoB secretion from the liver (Raabe et al., 1999), or it could be because of the increase in apoB degradation by inducing the autophagy pathway (Boström et al., 1986; Davis et al., 1990). However, there is no direct evidence to identify which of these two concepts is a primary cause of reduced apoB secretion in plasma.

To investigate whether downregulation of Glg1 induces the degradation of apoB100 in a pre- or post-Golgi compartment, we treated Huh7 cells with BFA. Our results demonstrated that knockdown of Glg1 significantly decreases the protein level of apoB-100 that was retained in the ER (Figure 2.5A). These results suggested that GLG1 is required for the transit of apoB from the ER to the post-ER compartments. This explains that GLG1 would be required for substantial interaction with apoB and probably some other proteins that cannot be regained by its knockdown and contributes to the different fate of these proteins.

A number of potential mechanisms, including ER-associated and post-ER proteolysis, exist to transfer apoB from the ER to the degradation compartments

(PERPP) (Fisher and Ginsberg, 2002; Fisher et al., 2001). Proteasomal and autophagic degradation systems are early and late quality control mechanisms for apoB-degradation, respectively (Qiu et al., 2011). It has previously been reported that apoB-crescents are formed by lipidated apoB in hepatocytes with regular MTP activity, and their amount is reduced by inhibition of MTP activity in Huh7 cells (Ohsaki et al., 2008). If newly synthesized apoB lipoproteins are not correctly lipidated, they will be removed from the secretory pathway by apoB-proteasomal or autophagosomal degradation (Qiu et al., 2011). Poorly lipidated apoB tend to form irreversible aggregates (Williams and Tabas, 1995) and autophagy plays a major role in the elimination of aggregated proteins (Komatsu et al., 2005).

It has been shown that degradation of apoB in Huh7 cells is mainly through autophagy (Ohsaki et al., 2006). Our confocal microscopy analysis demonstrated a significant decrease in the number of apoB-crescents and an increase of apoB aggregation in Glg1-knockdown cells. This data can be explained by our in-vivo observation that MTP activity was reduced in mouse liver upon Glg1 knockdown. In contrast to the studies supporting the idea that aggregation is toxic (Goldsteins et al., 2008; Pasinelli et al., 2004), some reports have suggested that aggregation is not toxic but maybe rather protective (Prudencio et al., 2009; Witan et al., 2008). P62, a common component in protein aggregates, has a protective role in cell survival by recruiting autophagosomal components to the polyubiquitinylated protein aggregates (Arrasate et al., 2004). Our data showed an increase in the protein level of P62 expression in Glg1 knockdown cells and mouse liver. In our results, knockdown of Glg1 in Huh7 cells led to the aggregation of autophagy marker, either endogenous LC3 or overexpressed LC3-GFP. In addition, an increase in

colocalization of aggregated apoB with P62 was observed in GLG1-deficient Huh7 cells. We observed the formation of autophagic vacuoles in the liver of Glg1 knockdown mice by electron microscopy images. Our flow cytometry analysis also demonstrated an increase in the amount of autophagy fluorescent marker by downregulation of Glg1 in Huh7 cells (Figure 2.5G). Altogether, our results suggest that downregulation of Glg1 in Huh7 cells or mouse liver led to impairment of apoB trafficking to the LDs and decreased secretion of apoB, which in turn resulted in the formation of apoB aggregates and their translocation to the autophagosome/aggresome compartment for degradation.

To further evaluate the effect of Glg1 knockdown on autophagy degradation of apoB, Huh7 cells (with or without Glg1-knockdown) were treated with an autophagy inhibitor. Our results demonstrated that inhibition of autophagy in control cells decreased apoB secretion into media (Figure 2.7B). Since proteasomal and autophagic degradative pathways are linked together for apoB degradation (Ohsaki et al., 2006), and apoB secretion depends on the rate of apoB degradation (Borchardt and Davis, 1987), we concluded that autophagy inhibition induced proteasomal degradation of apoB and thereby decreased apoB secretion into media. An earlier study in HepG2 cells showed that OA inhibits the proteasomal apoB degradation, and stimulates apoB secretion (Dixon et al., 1991). Moreover, Qiu et al. (2005) suggested a stimulatory role of OA in MTP gene transcription with increased protein level and activity of MTP in HepG2 cells. Therefore, we analyzed the effect of 3-MA upon Glg1 knockdown in cells that were treated with OA to prevent accelerated proteasomal degradation of apoB. Our western blot analysis demonstrated that intracellular apoB degradation was partly blocked by 3-MA in

Glg1-knockdown cells and induced apoB secretion. Preventing disposal of aggregated apoB by 3-MA in OA treated Glg1-knockdown cells, led to apoB ubiquitination and formation of large apoB-aggregates. Further aggregation of endogenous LC3 by autophagy inhibition in Glg1 knockdown cells might indicate the stuffed autophagosome from aggregated apoB.

Glg1-knockdown mice demonstrated reduced body weight (Supp. Figure 2.1D). GLG1 interacts with many proteins, including fibroblast growth factors (FGFs). FGFs are a family of at least 22 growth factors with essential functions such as cell proliferation and differentiation, tissue repair, and organ development (Eswarakumar et al., 2005). It has been shown that phenotype of $Glg1^{-/-}$ mice is similar to the phenotype of FGF18 knockout mice, in showing growth retardation (Miyaoka et al., 2010). In a study by Yang et al. (2013), loss of GLG1 resulted in severe osteopenia and decreased bone formation in mice. These results most likely help to explain why mouse body weight was lower in our Glg1-knockdown group.

While we have shown strong findings, there are some limitations to our experiments. Although HuH7 cell line retained many of the primary hepatocyte functions, they come with limitations. The monolayer culture of human hepatic cell lines may result in a loss of hepatocyte morphology and liver-specific functions (Bachmann et al. 2015). The human liver secretes apoB100 mainly associated with VLDL particles, unlike the HuH7 cells that secrete predominately LDL, and higher density apoB100-containing particles. Thus, using an alternative model such as human primary grown in 3D organoids may more closely resemble hepatocyte biology. In this study, we focused on the effect of GLG1 on circulatory and degradation pathway of apoB. However, the effect of GLG1 on trafficking pathways

of apoA1, PCSK9, and LDLR is not yet entirely studied. We proposed that GLG1 is required for their transit from the ER to the post-ER compartments. Systematic experiments to determine and validate the underlying pathways of the interrelationship between GLG1, PCSK9, apoA1, and LDLR will have to be performed.

In summary, we provided evidence that the interaction of GLG1 with apoB is important, for apoB-lipoprotein secretion and cholesterol regulation. Figure 2.8 is a graphical abstract, summarizing the major features of different trafficking pathways of apoB in presence or knockdown of Glg1 implied by our data. This study opened up a proposed mechanism of how Glg1 knockdown decreases apoB lipidation and TG secretion. Our results raised many unexpected questions related to the regulatory role of GLG1 on intracellular trafficking of PCSK9, LDLR, and probably some other lipoproteins such as apoA1. Therefore, it would be interesting to elucidate the function of GLG1 on other GLG1-interacting proteins. Taken together, our results suggest that blocking the interaction of GLG1 with apoB might be a promising therapeutic approach to decrease the production of atherogenic apoB-containing lipoproteins and thus prevent the development of atherosclerosis.

2.6 Figures

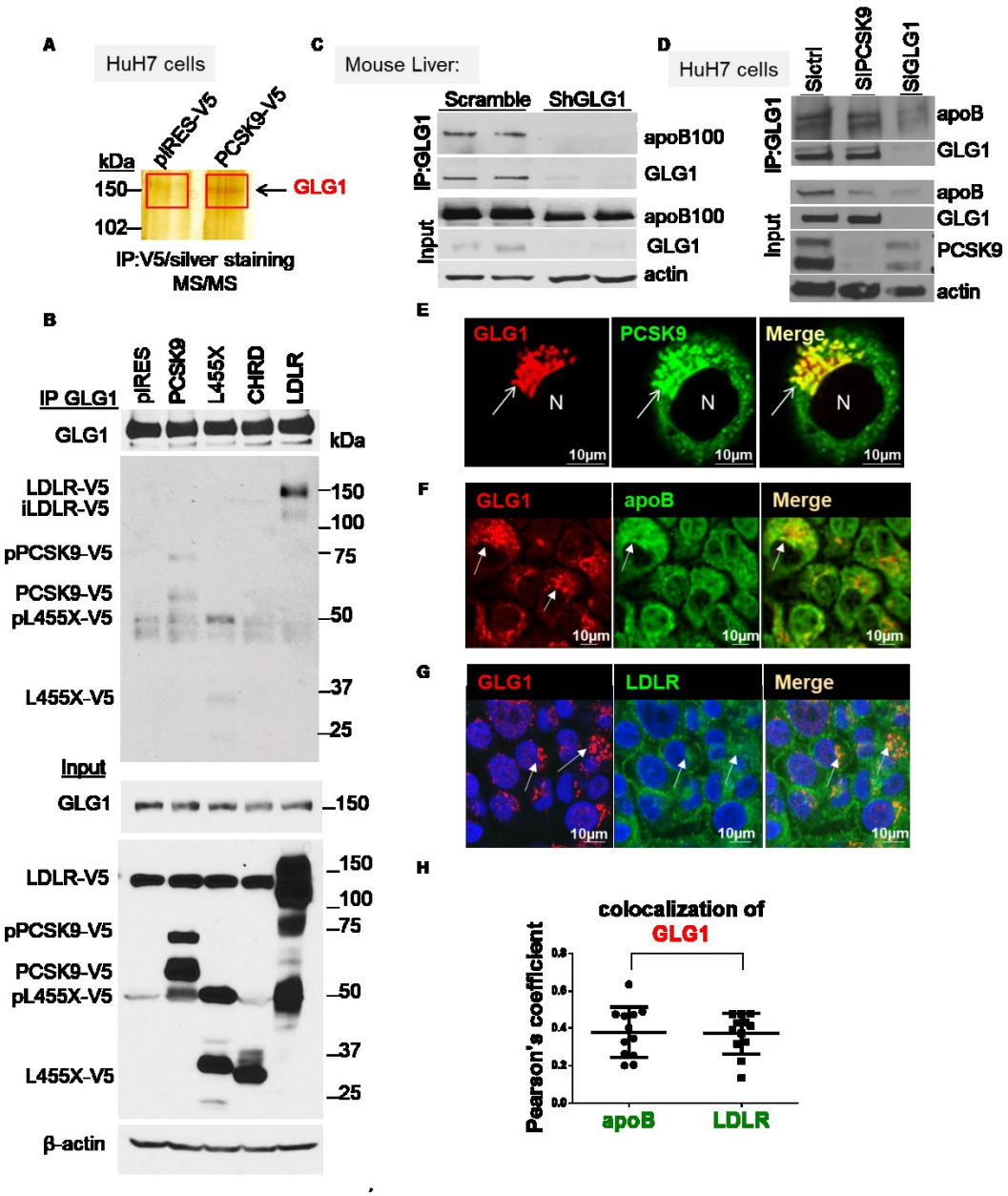

Figure 2.1 Identification of GLG1 as an endogenous PCSK9, LDLR, and apoB-binding protein

(A) Silver staining of proteins immunoprecipitated (IP) with overexpressed V5-tagged PCSK9 in Huh7 cells. The indicated protein by an arrow at 150 kDa was identified by mass spectrometry. (B) Immunoblot (IB) showing coIP of endogenous

GLG1 with indicated constructs of PCSK9 and LDLR (overexpressed V5-tagged plasmids) in Huh-7 cells. (C-D) IB showing coIP of endogenous GLG1 with apoB in (C) liver of the mice injected with AAV8-shRNA against GLG1 or control scramble virus (D) or in Huh-7 cells transfected with siRNAs against PCSK9 or GLG1 (E-G) Confocal immunofluorescence microscopy of endogenous GLG1 with (E) overexpressed PCSK9, or endogenous (F) apoB or (G) LDLR in Huh-7 cells. Arrows point to regions of partial co-localization. Scale bar: 10 μm. (H) Colocalization between GLG1 and apoB or GLG1 and LDLR was quantified by measuring the overlap between the red and the green channels and calculated by Pearson's correlation coefficient (r) value. Graph H represent means ±SD ($*p < 0.05$).. All data are representative of at least two independent experiments.

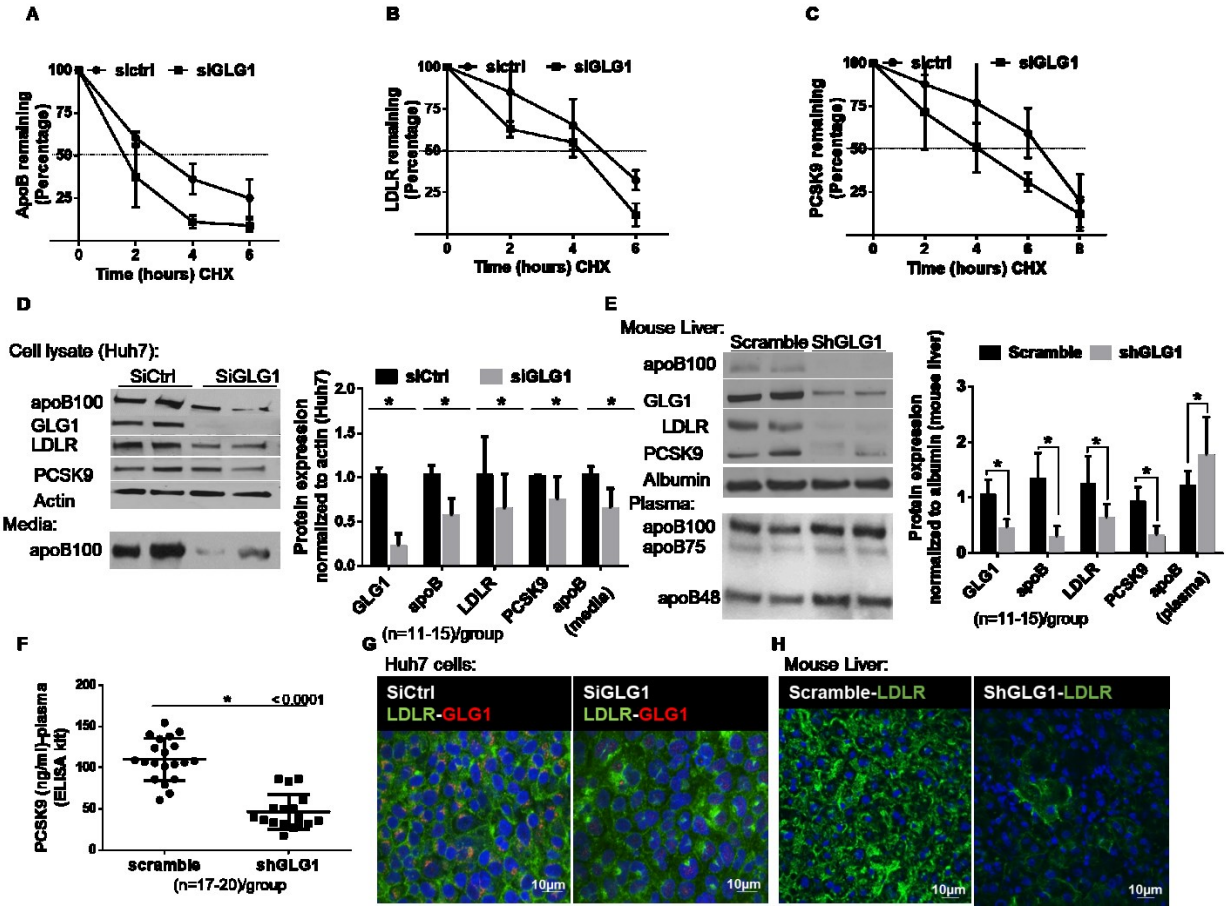

Figure 2.2 Knockdown of GLG1 reduced apoB, PCSK9 and LDLR protein expression in Huh7 cells and in mouse liver

(A-C) Huh7 cells, 72-hours post reverse transfection with siRNAs against GLG1 and control, were incubated with complete media + Cycloheximide (CHX; 25 µg/mL), analyzed by IB (data not shown), quantified and normalized over β-actin. Graphs represent the percentage of remaining protein of (A) apoB (B) PCSK9 (C) and LDLR after incubation of cells with CHX at indicated time points from two independent experiments. Graphs represent means ±SD ($*p < 0.05$). (D) Huh7 cells were transfected with siCtrl or siRNA against GLG1. Protein levels of GLG1, LDLR, PCSK9 (lysates) and apoB (lysates and an equal volume of conditioned media) were analyzed by IB, quantified, and normalized over β-actin (right panel). Graphs show

means ±SD of at least three independent experiments (∗p < 0.05). (E) IB and quantification analysis (right panel) of apoB-100, GLG1, LDLR, PCSK9, albumin in mouse liver and apoB-100 and apoB48 in plasma of control and Glg1-knockdown mice. Graphs represent means ±SD from four independent experiments (∗p < 0.05). (F) Plasma level of PCSK9 (ng/ml) from mice treated with AAV8-shGLG1 or AAV8-scramble in four independent experiment; error bars: SD; n= (17-20)/group; (∗∗∗p < 0.001). (G) Huh7 cells (H) or mouse liver cryosections were fixed with 4% formaldehyde and immunostained for LDLR (green) in control and Glg1 knockdown groups. DAPI is shown in blue. Scale bar: 10 μm.

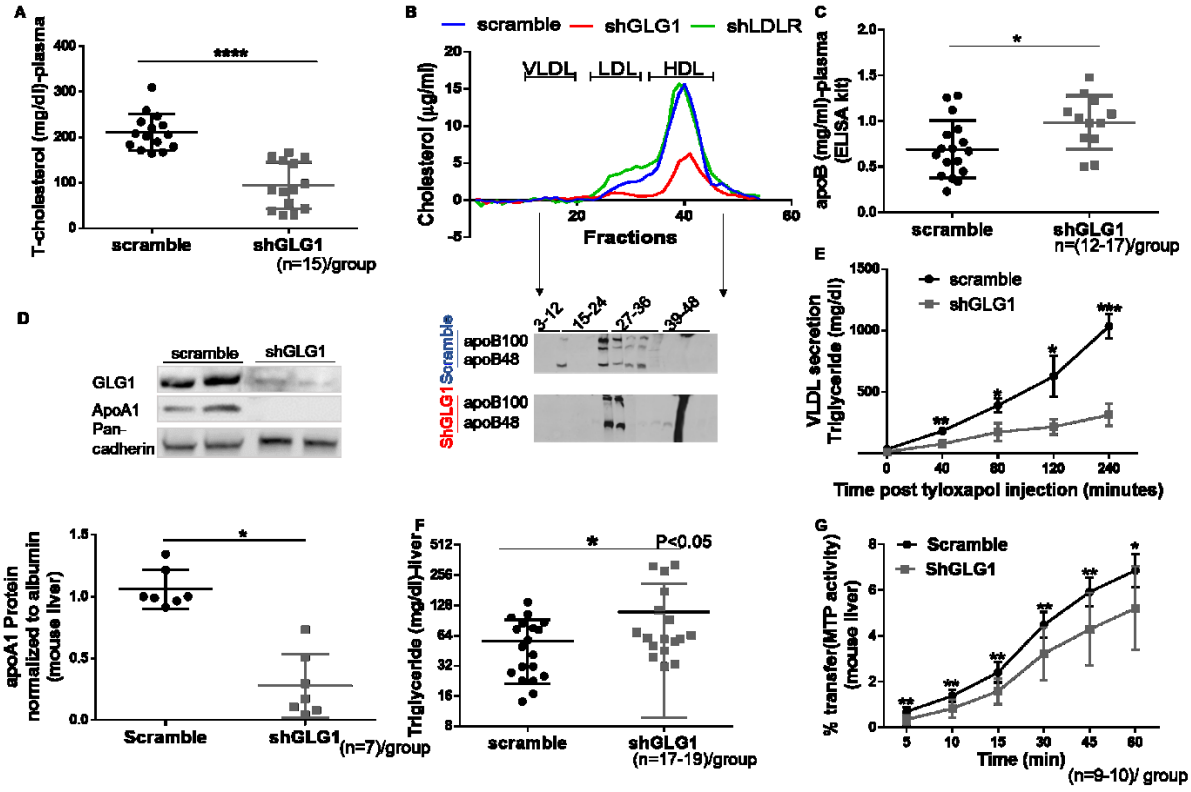

Figure 2.3 Regulation of plasma apoB-containing lipoproteins, HDL-cholesterol, and triglycerides upon Glg1 knockdown.

(A-G) C57BL/6 mice (8-wk-old) were injected with AAV8 expressing either control shRNA (scramble) or shRNA against GLG1. All treated mice were sacrificed after 2-weeks of virus injection, and plasma and liver samples were collected. (A) Total cholesterol in mouse plasma was measured using a commercial kit (Wako) from four independent experiments; error bars: SD; (n=15)/group; (****p<0.0001). (B) Distribution of cholesterol and apoB in lipoprotein fractions. Pooled plasma samples (from five mice/group) were size-fractionated by gel filtration chromatography using a Superose 6 column, and aliquots of the FPLC fractions were used for cholesterol determination (enzymatically) and IB analysis. (C) Total plasma apoB from each group of mice was measured using an ELISA kit (LSBIO)

from four independent experiments; error bars: SD; (n=12-17)/group; (*p<0.05). (D) IB and quantification (right panel) analysis of apoA1 in mouse liver from two independent experiments. Protein samples were separated on 10% polyacrylamide gel. Error bars: SD; (n=7)/group; (*p<0.05). (E) Hepatic secretion of VLDL-triglycerides in fasting mice (6 hours) after i.v. administration of tyloxapol (500 mg/kg body weight). Blood samples were taken from both groups of mice (control and Glg1 knockdown) at indicated time points after tyloxapol injection. TG concentration was analyzed using an Elisa kit (CEDARLANE), and VLDL secretion rate (mg/dl) was calculated using the slopes of the curves. Error bars: SD; (n=3)/group; (*p<0.05; ∗∗p < 0.01; ∗∗∗p < 0.001). (F) Hepatic triglyceride concentration (mg/dl) was evaluated in mouse liver, using 100 mg of tissue samples and the triglyceride quantification kit (CEDARLANE). All results are presented as the mean ± SD from at least three independent experiments. n= (17-19)/group; (*p<0.05). (G) MTP activity in mouse liver tissue from four independent experiment; error bars: SD; n= (9-10)/group; (*p<0.05; ∗∗p < 0.01).

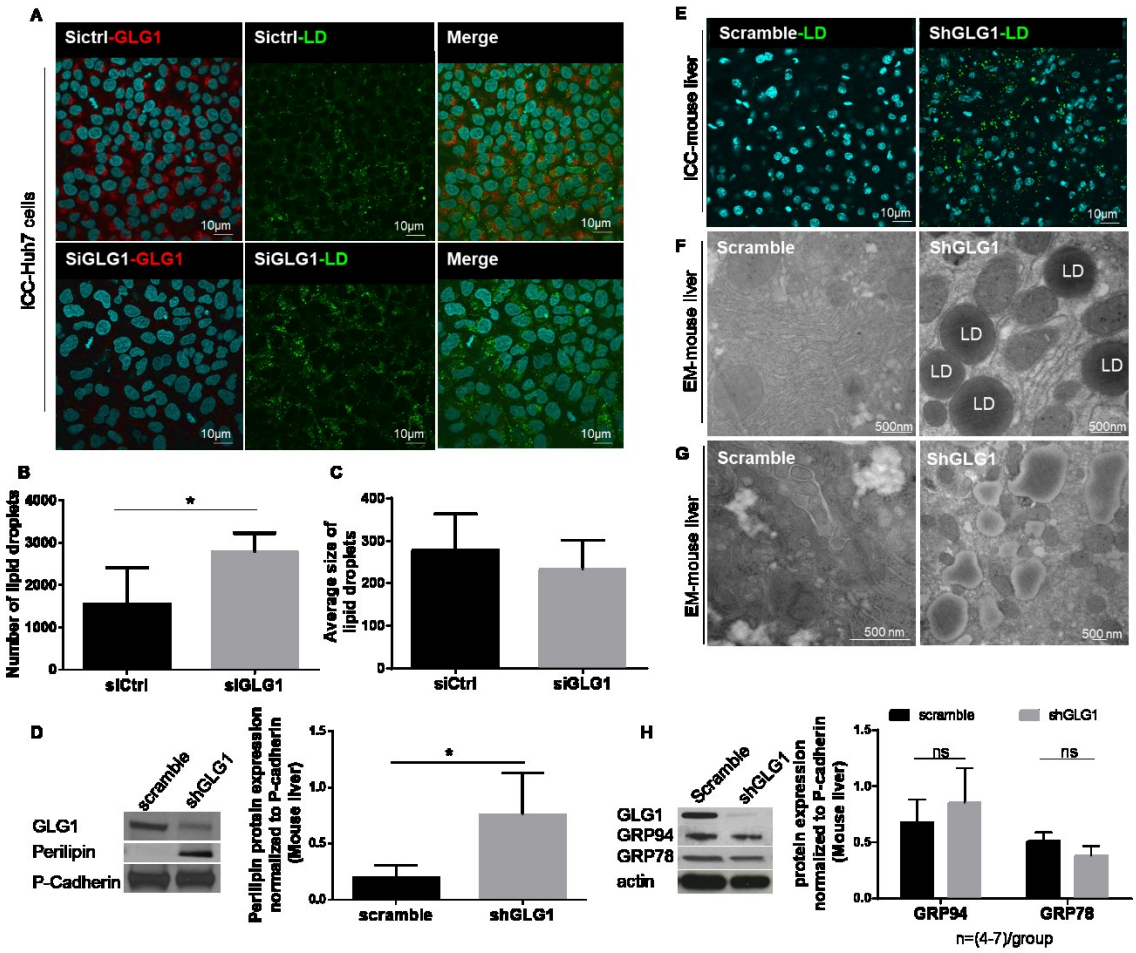

Figure 2.4 Knockdown of GLG1 increased lipid droplets numbers in Huh7 cells and changed the morphology of the endoplasmic reticulum in mouse liver.

(A) Huh7 cells were fixed with 4% paraformaldehyde for confocal microscopy analysis, 72-hours post reverse transfection with either siCtrl or siGLG1. Fat bodies were stained with Bodipy 493/503 (green) to visualize LDs and apoB with the anti-apoB antibody (blue). Scale bar: 10 μm. (B) Quantification of LDs number (C) and LDs size distribution of each group of transfected cells. More than 100 cells were counted in each condition from three independent experiments. Error bars: SD ;(*p<0.05). (D-H) Mouse livers were collected 2-weeks after injection with AAV8-shGLG1 or scramble for IB, IHC, and electron microscopy analysis. (D) IB and

quantification (right panel) analysis of perilipin, a lipid droplet-associated protein, in mouse liver upon Glg1 knockdown. P-cadherin was used for loading control. Error bars: SD; n= (7-9)/group from two independent experiments; (*p<0.05) (E) BODIPY staining (green) on 10 μm mouse liver cryosections. BODIPY-positive LDs are abundant in hepatocytes from mouse group with the Glg1 knockdown. Scale bar: 10 μm. (F, G) Conventional thin-section electron microscopy images of mouse liver demonstrate (F) lipid droplets, (G) and morphological changes in the Endoplasmic reticulum (ER). Scale bar: 500 nm. (H) IB and quantification (right panel) analysis from two different markers of ER-stress (GRP94 and GRP78) in mouse liver. Error bars=SD; n= (4-7)/group from two independent experiments; (ns=not significant).

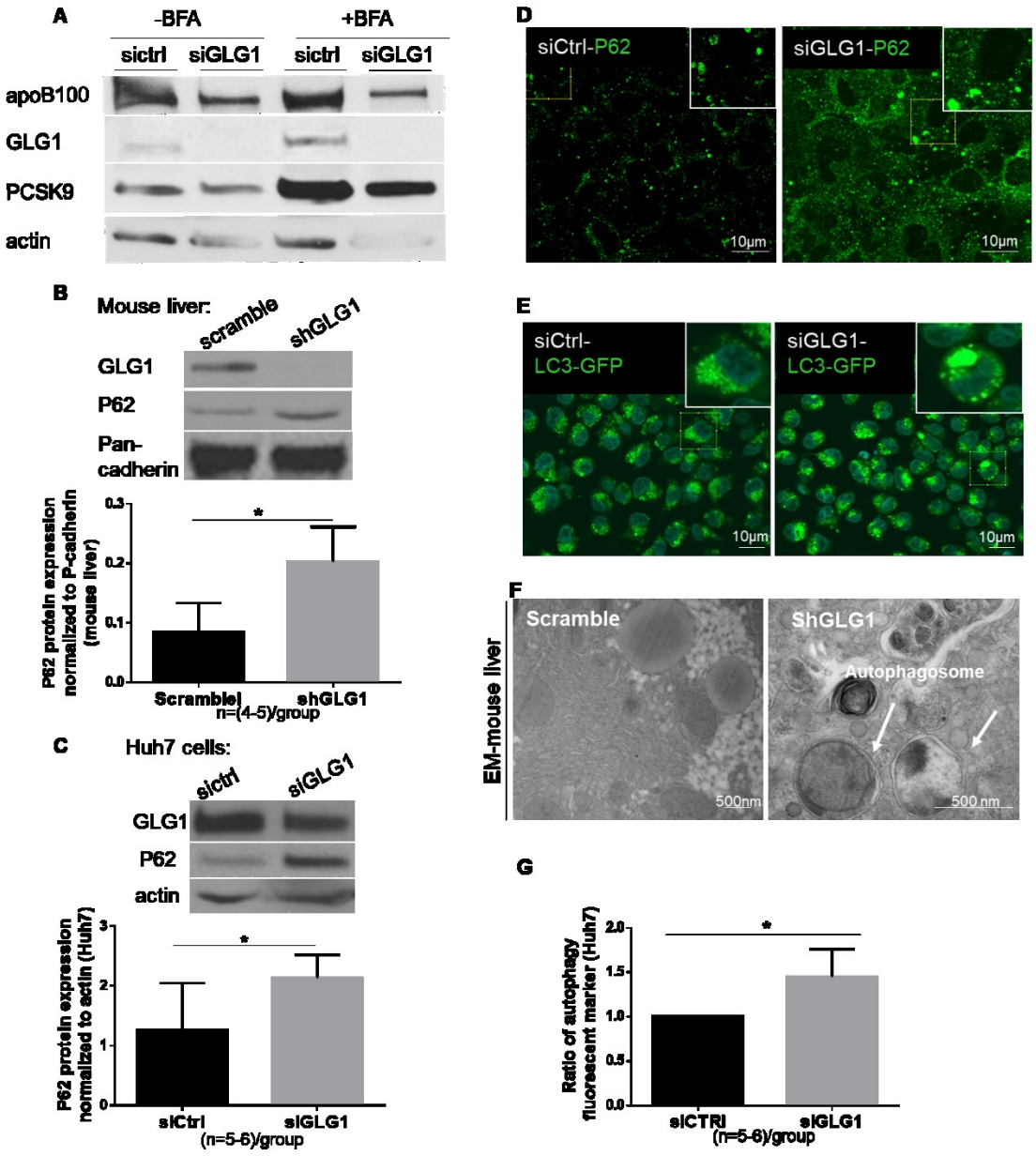

Figure 2.5 Glg1-knockdown induced autophagosome/aggresome formation and apoB-100 degradation.

(A) Huh7 cells were treated with or without the vesicular trafficking inhibitor brefeldin A (BFA; 5 μg/ml), 48 hours after reverse transfection with siCtrl or siGLG1, for 16 hours. IB analysis of apoB-100, GLG1, PCSK9, and β-actin, in protein extracts from treated cells; n=2. (B-C) IB and quantification (bottom panel) analysis of P62

protein expression (B) in mouse liver, two-weeks after injection with AAV8 expressing either shGLG1 or scramble (control); n= (4-5)/group from two independent experiments. Error bars=SD; ($*p < 0.05$) (C) Or in lysates of Huh7 cells, 72-hours after reverse transfection with siCtrl or siGLG1. n= (5-6)/group from three different experiments. Error bars=SD; ($*p < 0.05$). (D) Huh7 cells, 72-hours post-reverse transfection with siCtrl or siGLG1 were fixed with 4% paraformaldehyde and immunostained for P62 (green). DAPI is shown in blue. Scale bar: 10 μm. Images are representative of three independent experiments. (E) Confocal immunofluorescence microscopy of Huh7 cells stably overexpressing GFP-LC3 with or without a Glg1 knockdown. Scale bar: 10 μm; n=3. (F) Mouse liver samples from both groups of mice (scramble and shGLG1) were processed for EM. Arrows show autophagosomes. Scale bar: 500 nm. (G) Autophagy flux was determined in Huh7 cells using Cyto-ID assay with a fluorescent, cationic amphilic tracer dye. Fluorescence intensity of the dye was detected by flow cytometry analysis in three independent experiments. n= (5-6)/group. Error bars=SD; ($*p < 0.05$).

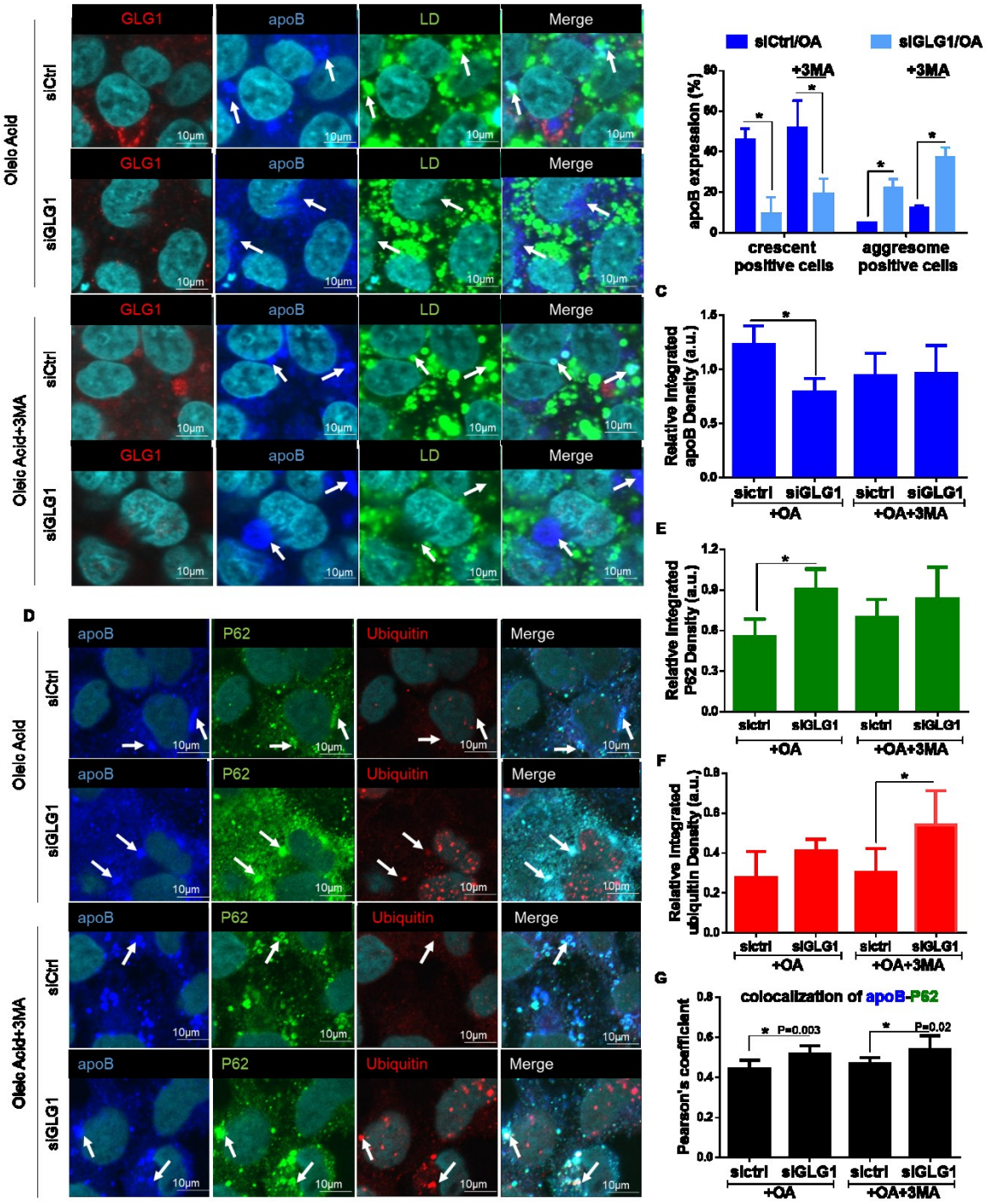

Figure 2.6 Glg1-knockdown decreased staining of apoB (apoB-crescents) and induced accumulation of apoB in aggresomes.

Huh7 cells were reverse transfected with siCtrl or siGLG1 and 72-hours post reverse transfection, the normal culture medium was supplemented with oleic acid

(OA; 1.5 mM) ± 3-methyladenine (3-MA; 5 mM), an autophagy inhibitor, for 4 hours. (A) Huh7 cells were fixed with 4% paraformaldehyde and immunostained for GLG1 (red) and apoB (blue). LDs (green) were stained with BODIPY and nuclei (cyan) were stained with DAPI. Arrows demonstrate apoB distributed throughout the LDs in control cells (first row), but a conspicuous concentration of apoB around LDs disappeared after Glg1 knockdown (second row). Addition of 3-MA into complete media after Glg1 knockdown reduced crescent shape of apoB and induced its perinuclear aggregation. Scale bars:10 μm. n=3 (B) The integrated fluorescence intensity associated with the antibody against apoB. More than 100 cells were counted per experiment. n=3; errors=SD; ($*p < 0.05$) (C) The numbers of apoB-crescent–positive cells and apoB-aggresome–positive cells were counted in confocal microscopy images. The percentage was calculated by dividing the counts by the total number of cells in each field. More than 100 cells were counted per experiment. n=3. Error bars=SD; ($*p < 0.05$). (D) Huh7 cells were fixed with 4% paraformaldehyde and immunolabeled for apoB (blue), P62 (green) and ubiquitin (red). In Glg1-knockdown cells, increased level of P62 and ubiquitin expression were detected. Arrows demonstrated a conformational change of apoB and increased colocalization of apoB with P62 and ubiquitin by Glg1 knockdown compared to the control cells. Scale bar: 10 μm (E-F) Integrated fluorescence intensity of (E) P62 or (F) ubiquitin was quantified using Image J program. More than 100 cells were counted per experiment. n=2; errors=SD; ($*p < 0.05$). (G) Colocalization of apoB with P62 was analyzed by means of Pearson's correlation coefficients in randomly chosen fields. n=2. Error bars=SD; ($*p < 0.05$).

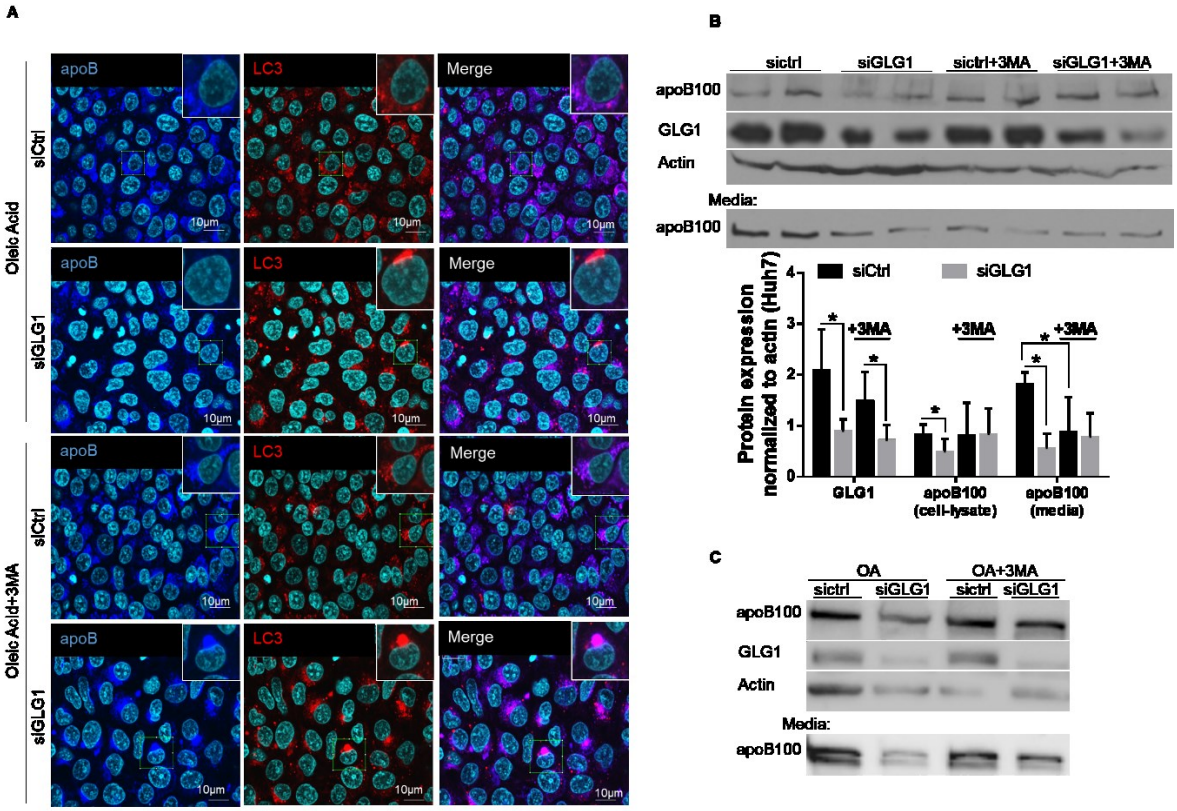

Figure 2.7 Autophagy inhibition upon Glg1 knockdown compromises degradation of apoB aggregates.

(A) Huh7 cells were reverse transfected with either siCtrl or siGLG1 and, 72 hours post-transfection; they were treated with OA (1.5 mM) in the absence/presence of 3MA (5 mM) for 4 hours. Cells were fixed with 4% paraformaldehyde and immunolabeled for apoB (blue) and a marker of endogenous LC3 (red). Confocal microscopy images showing colocalization of apoB with LC3 (red) in control cells (first row). Knockdown of GLG1 led to the formation of aggregated LC3 and diffused apoB (second row). Incubating of cells with 3-MA post Glg1 knockdown (fourth row), demonstrating further LC3 aggregation and colocalization with large apoB-aggregates. Scale bar: 10 μM. (B) IB and quantification (bottom panel) analysis to determine the effect of autophagy inhibition

(3-MA; 5 mM; 4 hours) on protein level of apoB (lysates and conditioned media) following Glg1 knockdown compared to the control cells. n=3, ($*p < 0.05$). (C) Immunoblotting of lysates and conditioned media from Huh7 cells, with or without GLG1knockdown. Cells were treated with OA (1.5 mM) in the absence or presence of 3-MA (5 mM); n=3.

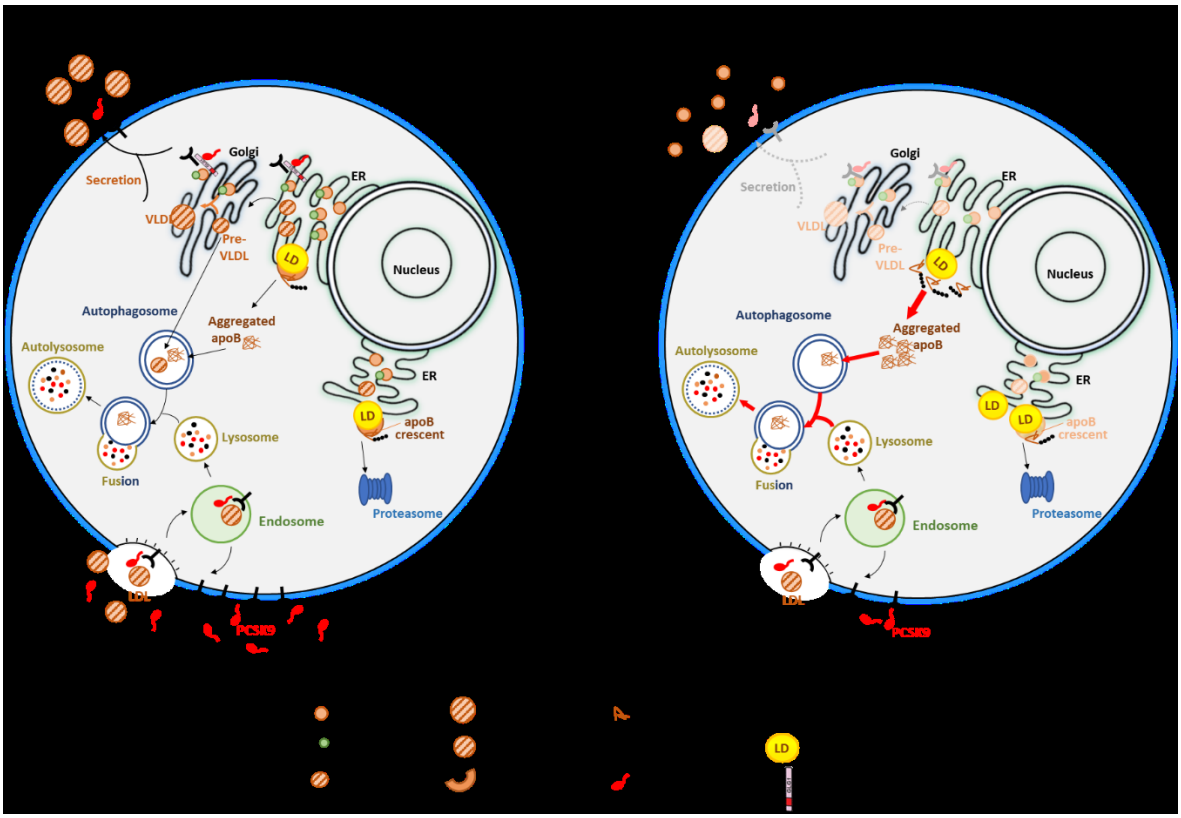

Figure 2.8 Schematic diagram showing proposed pathways of apoB secretion or degradation in the presence (left) or absence of GLG1 (right).

In control hepatocytes (left diagram), GLG1 interacts with apoB, PCSK9, and LDLR in the pre-Golgi compartment and regulates their cell-surface expression. ApoB, after its translation, could undergo a degradational pathway or a pathway that leads to its secretion. ApoB-VLDL secretion depends on the amount of apoB that is degraded in hepatocytes. Lipidation of apoB by MTP results in the pre-VLDL formation, and VLDL-TG secretion. poorly-lipidated apoB or misfolded apoB is translocated to the cytoplasm, ubiquitinated and targeted for proteasomal or autophagosomal degradation. Lipid droplets (LDs) serve as a platform for apoB accumulation. Accumulation of apoB in a crescent-shaped structure around LDs is

named apoB-crescent. ApoB-crescents and LDs are in close proximity to proteasomes. Impairment in degradation of misfolded apoB via ubiquitin-proteasome pathway leads to apoB aggregation, and then aggregates are degraded by an autophagic process.

In Glg1-knockdown hepatocytes (right diagram), the intracellular trafficking of PCSK9 and LDLR to the cell-surface is disrupted, which result in a decrease in their cell-surface expression. Moreover, a decrease in MTP activity was observed in Glg1-knockdown hepatocytes which led to decrease in apoB-lipidation and secretion. Also, impaired trafficking of misfolded apoB to apoB-crescent structures was observed in GLG1-deficient hepatocytes, which resulted in an increase in the formation of apoB-aggregates and their autophagosomal degradation. Here, we have depicted accumulation of poorly lipidated apoB by Glg1 knockdown in mouse hepatocyte but based on our *in vitro* data in Huh7 cells we cannot exclude that the total level of apoB was reduced in the medium of cells with GLG1 deficiency.

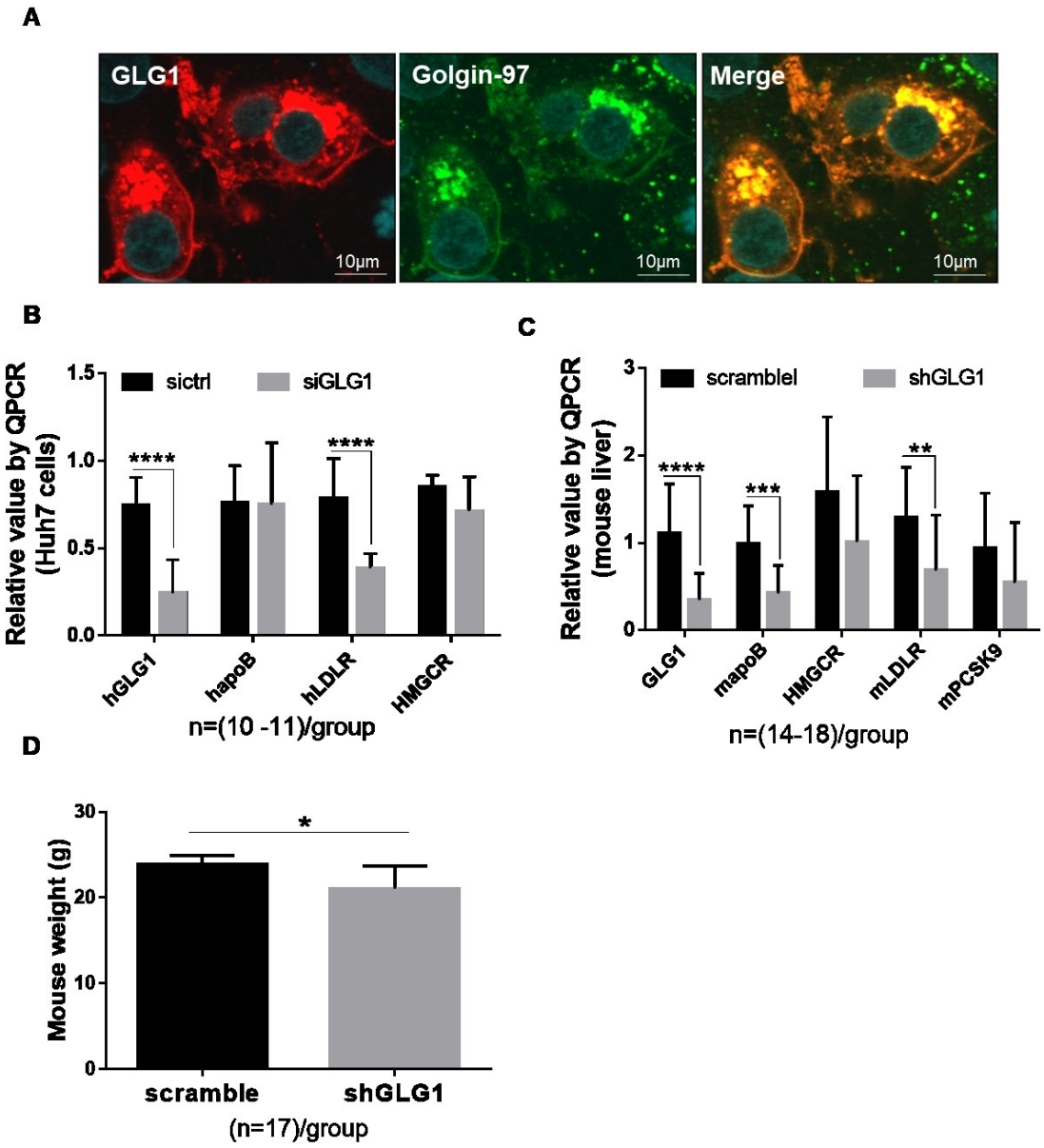

Supplementary Figure 2.1. Effect of GLG1 deficiency on RNA expression of genes that are involved in cholesterol regulation

(A) Huh7 cells were fixed with 4% paraformaldehyde and double immunolabeled for GLG1 (red) and Golgi apparatus (green) using anti-GLG1 and Golgin-97 (a marker of Golgi staining) primary antibodies and appropriate secondary antibodies. Scale bar: 10 μM. (B) RNA was harvested from Huh7 cells, seventy-two

hours after reverse transfection with sictrl or siGLG1. Then, mRNA levels of GLG1, apoB, LDLR, 3-Hydroxy-3-methylglutaryl-CoA reductase (HMGCR), TBP (TATA box binding protein) and albumin were assessed by RT-qPCR and normalized to TBP and albumin expression levels. Data represent the means of three independent experiments analyzed in duplicate ± SD (****$p < 0.0001$). (C) RNA was harvested from the liver of the mice, two-weeks after tail-vein injection of AAV8-shGLG1 or scramble. Expressions of genes were measured by RT-qPCR in duplicates from four independent experiments and normalized to TBP (TATA box binding protein) and albumin. Error bars=SD (**$p < 0.01$, ***$p < 0.001$, ****$p < 0.0001$). (D) Comparison of mouse body weight between the control group (scramble) and the group of the mice with 2-weeks of Glg1 knockdown.

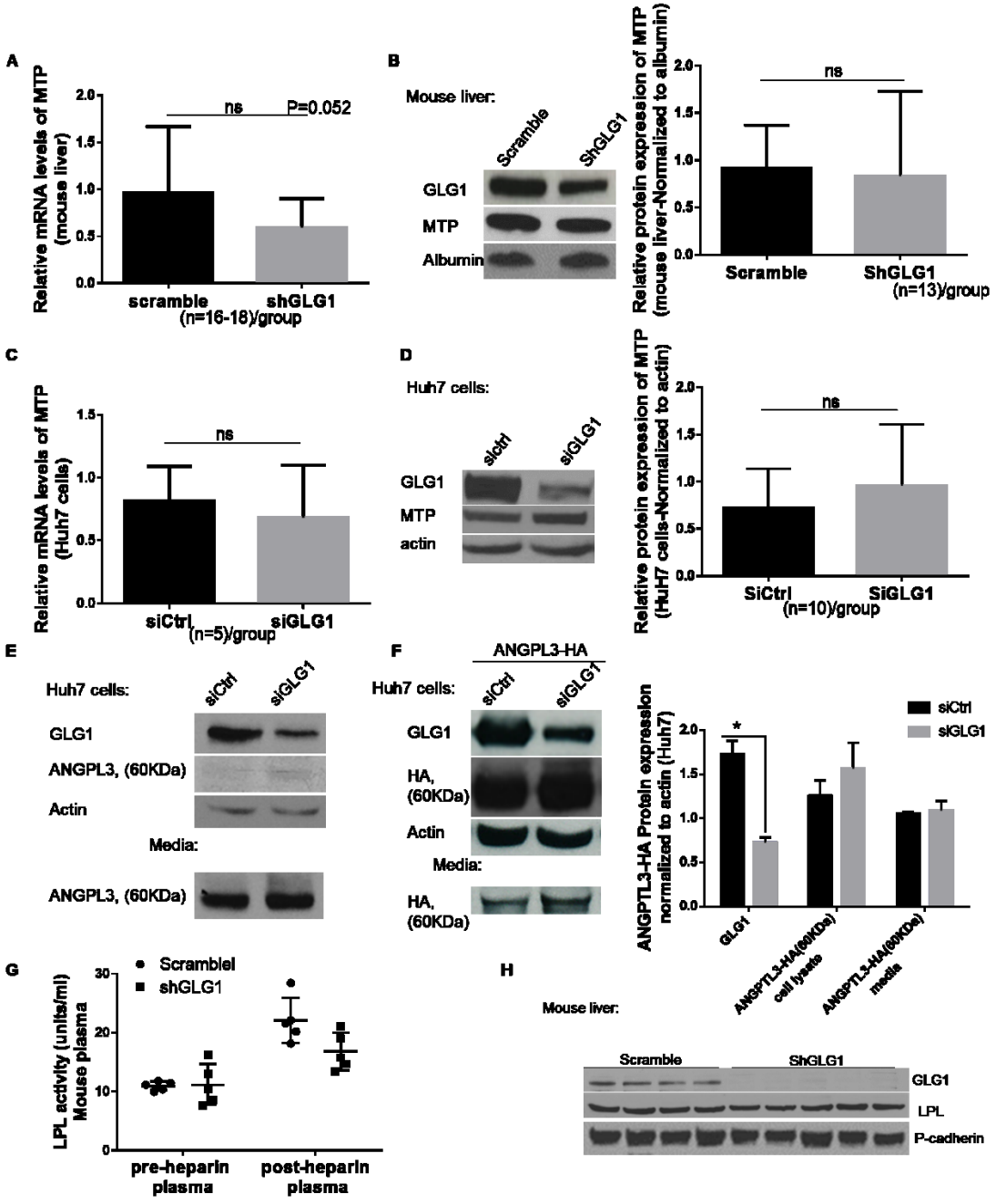

Supplementary Figure 2.2. Effect of Glg1 knockdown on potential factors that may influence lipoprotein secretion

(A-B) C57BL/6 mice (8-wk-old) were injected with AAV8 expressing either control shRNA (scramble) or shRNA against GLG1. All treated mice were sacrificed after 2-weeks of virus injection, and liver samples were collected for (A) RNA, and

(B) protein analysis. (A) RNA levels of MTP, TBP (TATA box binding protein) and albumin were assessed by RT-qPCR and normalized to TBP and albumin expression levels. Data represent means of three independent experiments analyzed in duplicate ± SD; n=(16-18)/group, (ns=non significant). (B) IB and quantification analysis (right panel) of MTP and albumin in lysates of liver samples from control and Glg1 knockdown mice. The protein level of MTP was normalized to albumin. Graphs represent means ±SD from four independent experiments; (n=13)/group; (ns=non significant). (C) RNA, and (D-F) protein was harvested from Huh7 cells, seventy-two hours after reverse transfection with sictrl or siGLG1. (C) mRNA levels of MTP and TBP (TATA box binding protein) were assessed by RT-qPCR and normalized to TBP expression levels. Data represent the means of three independent experiments analyzed in duplicate ± SD; (n=5)/group (ns=non significant). (D) Protein levels of MTP and actin were analyzed by IB, quantified, and normalized over β-actin (right panel). Graphs show means ±SD of three independent experiments. (n=10)/group; (ns=non significant). (E) IB analysis of protein levels of ANGPTL3 and actin in cell lysates and ANPTL3 in conditioned media; n=3. (F) Cells were transfected with the plasmid of ANGPTL3-HA using Lipofectamine 3000 , 48-hours after reverse transfection with either sictrl or siGLG1. Lysates and conditioned media underwent Western blotting for GLG1, ANGPTL3-HA, and actin in lysates and ANGPTL3-HA in media. Intensities of signal were quantified by densitometry (right panel), n=3; (ns=non significant). (G) Plasma lipoprotein lipase activity before and 10 min after tail vein injection of heparin (0.1 U/g body weight) in the scramble (control) and the shGLG1 mice. Heparin increased LPL activity in both groups ($p<0.001$), but this effect was not different between the

scramble and shGLG1 (P>0.05). Values are means ± s.e.m. (N=9). (G-H) C57Bl/6 mice (8-wk-old) were injected with AAV8 expressing either control shRNA (scramble) or shRNA against GLG1. (G) Blood samples were collected before and 10 min after heparin (0.1 U/g body weight) administration, 2-weeks after virus injection. Plasma lipoprotein lipase (LPL) activity was measured in mouse plasma using the Fluorometric kit (Cell Biolabs INC). Heparin increased LPL activity in both groups ($p<0.0001$), though this effect was not different between control (scramble) and the group of the mice that were injected with shGLG1 (ns=non significant). Data represent mean±SD; (n=5)/group. (H) IB analysis of LPL and P-cadherin in lysates of liver samples from control and Glg1 knockdown mice. P-cadherin was used for loading control.

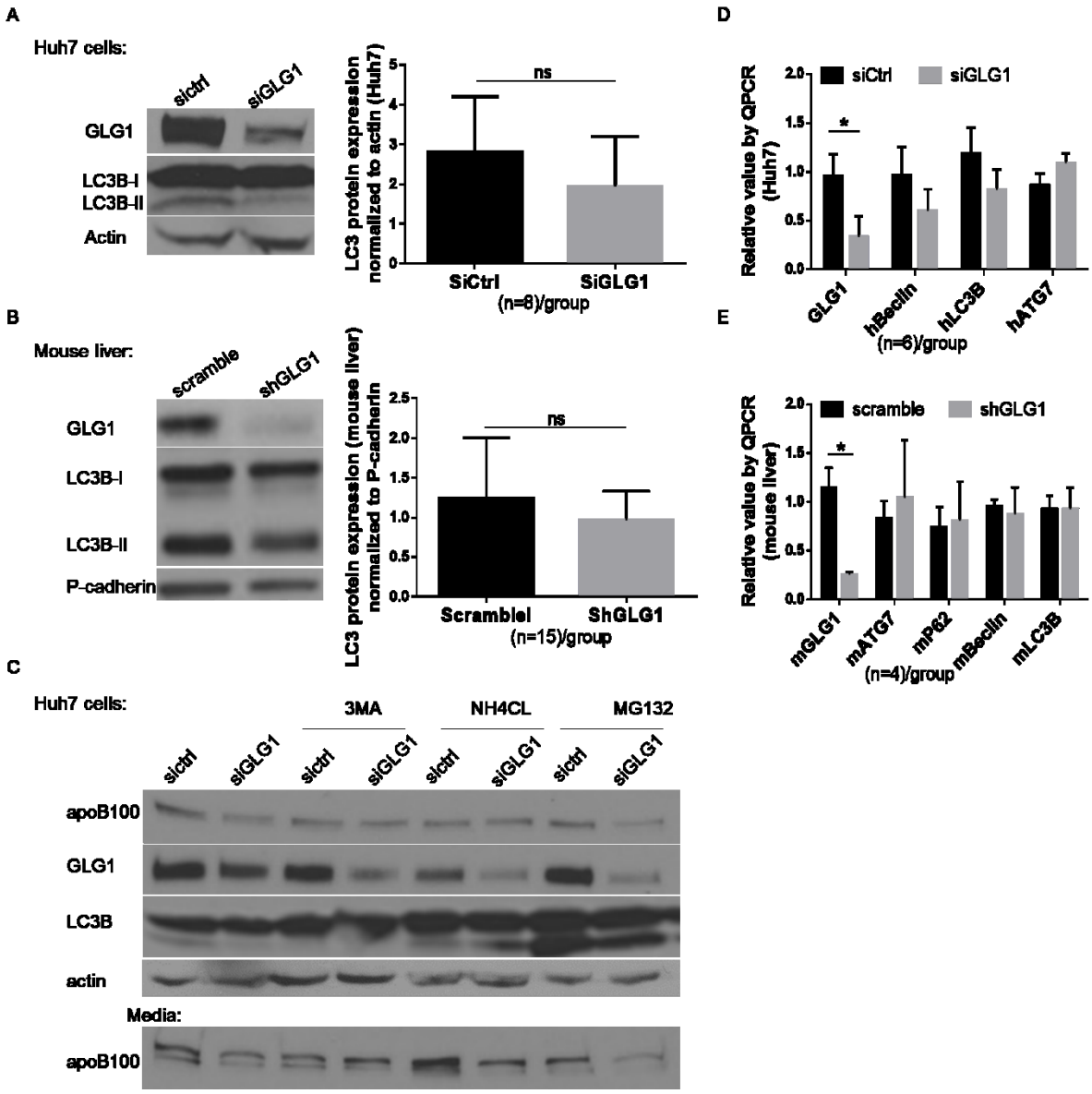

Supplementary Figure 2.3. The protein level of LC3-II is increased in GLG1-deficient Huh7 cells in the presence of lysosomal inhibitor (NH4Cl)

(A) IB analysis and densitometry quantification (right panel) of LC3B and actin in protein extract from Huh7 cells transfected with either sictrl or siGLG1. The protein level of LC3 was normalized to actin levels. n=8. Error bars: SD; (ns=non significant). (B) IB and quantification (right panel) analysis of LC3B and actin in liver protein extracts from mouse liver with or without Glg1 knockdown. n=15, Error bars:

SD; (ns=non significant). (C) Huh7 cells, 48 h post-reverse transfection with sictrl or siGLG1, were treated with NH_4Cl (10 mM) or MG132 (5 μM) for 16 hours or with 3-MA (10 mM) for 3 to 4 hours. Media and protein lysates were subjected to immunoblotting analysis. Actin and albumin were used for loading control in lysates and media, respectively. (D) The expression levels of different autophagy-related genes in Huh7 cells (with or without Glg1 knockdown) were measured by RT-qPCR in duplicates and normalized to TBP (TATA box binding protein). (n=6)/group; (*P<0.05). (E) qPCR analysis of autophagic-target genes expression in liver samples isolated from C57BL/6 mice, 2-weeks post virus (AAV8-shGLG1 or -scramble) injection. (n=4)/group; (*P<0.05).

2.7 References

Abifadel, M., J.P. Rabès, M. Devillers, A. Munnich, D. Erlich, C. Junien, M. Varret, and C. Boileau. 2009. Mutations and polymorphisms in the proprotein convertase subtilisin kexin 9 (PCSK9) gene in cholesterol metabolism and disease. Human mutation. 30:520-529.

Abifadel, M., M. Varret, J.-P. Rabès, D. Allard, K. Ouguerram, M. Devillers, C. Cruaud, S. Benjannet, L. Wickham, and D. Erlich. 2003. Mutations in PCSK9 cause autosomal dominant hypercholesterolemia. Nature genetics. 34:154-156.

Arrasate, M., S. Mitra, E.S. Schweitzer, M.R. Segal, and S. Finkbeiner. 2004. Inclusion body formation reduces levels of mutant huntingtin and the risk of neuronal death. Nature. 431:805-810.

Athar, M., C. Li, X. Tang, S. Chi, X. Zhang, A.L. Kim, S.K. Tyring, L. Kopelovich, J. Hebert, and E.H. Epstein. 2004. Inhibition of smoothened signaling prevents ultraviolet B-induced basal cell carcinomas through regulation of Fas expression and apoptosis. Cancer research. 64:7545-7552.

Bakillah, A., N. Nayak, U. Saxena, R.M. Medford, and M.M. Hussain. 2000. Decreased Secretion of apoB Follows Inhibition of apoB− MTP Binding by a Novel Antagonist. Biochemistry. 39:4892-4899.

Bendayan, M. 1995. Colloidal gold post-embedding immunocytochemistry. Progress in histochemistry and cytochemistry. 29:III1-VIII159.

Borchardt, R., and R. Davis. 1987. Intrahepatic assembly of very low density lipoproteins. Rate of transport out of the endoplasmic reticulum determines rate of secretion. Journal of Biological Chemistry. 262:16394-16402.

Boström, K., M. Wettesten, J. Boren, G. Bondjers, O. Wiklund, and S.-O. Olofsson. 1986. Pulse-chase studies of the synthesis and intracellular transport of apolipoprotein B-100 in Hep G2 cells. Journal of Biological Chemistry. 261:13800-13806.

Brown, M.S., and J.L. Goldstein. 1986. A receptor-mediated pathway for cholesterol homeostasis. Science. 232:34-47.

Chan, L.L.-Y., D. Shen, A.R. Wilkinson, W. Patton, N. Lai, E. Chan, D. Kuksin, B. Lin, and J. Qiu. 2012. A novel image-based cytometry method for autophagy detection in living cells. Autophagy. 8:1371-1382.

Dastani, Z., P. Pajukanta, M. Marcil, N. Rudzicz, I. Ruel, S.D. Bailey, J.C. Lee, M. Lemire, J. Faith, and J. Platko. 2010. Fine mapping and association studies of a high-density lipoprotein cholesterol linkage region on chromosome 16 in French-Canadian subjects. European Journal of Human Genetics. 18:342.

Davis, R.A., R. Thrift, C. Wu, and K. Howell. 1990. Apolipoprotein B is both integrated into and translocated across the endoplasmic reticulum

membrane. Evidence for two functionally distinct pools. Journal of Biological Chemistry. 265:10005-10011.

Dixon, J.L., S. Furukawa, and H. Ginsberg. 1991. Oleate stimulates secretion of apolipoprotein B-containing lipoproteins from Hep G2 cells by inhibiting early intracellular degradation of apolipoprotein B. Journal of Biological Chemistry. 266:5080-5086.

Eswarakumar, V., I. Lax, and J. Schlessinger. 2005. Cellular signaling by fibroblast growth factor receptors. Cytokine & growth factor reviews. 16:139-149.

Fisher, E.A., and H.N. Ginsberg. 2002. Complexity in the secretory pathway: the assembly and secretion of apolipoprotein B-containing lipoproteins. Journal of Biological Chemistry. 277:17377-17380.

Fisher, E.A., M. Pan, X. Chen, X. Wu, H. Wang, H. Jamil, J.D. Sparks, and K.J. Williams. 2001. The triple threat to nascent apolipoprotein B Evidence for multiple, distinct degradative pathways. Journal of Biological Chemistry. 276:27855-27863.

Fujiwara, T., K. Oda, S. Yokota, A. Takatsuki, and Y. Ikehara. 1988. Brefeldin A causes disassembly of the Golgi complex and accumulation of secretory proteins in the endoplasmic reticulum. Journal of Biological Chemistry. 263:18545-18552.

Gibbons, G.F., K. Islam, and R.J. Pease. 2000. Mobilisation of triacylglycerol stores. Biochimica et Biophysica Acta (BBA)-Molecular and Cell Biology of Lipids. 1483:37-57.

Gillian-Daniel, D.L., P.W. Bates, A. Tebon, and A.D. Attie. 2002. Endoplasmic reticulum localization of the low density lipoprotein receptor mediates presecretory degradation of apolipoprotein B. Proceedings of the National Academy of Sciences. 99:4337-4342.

Goldsteins, G., V. Keksa-Goldsteine, T. Ahtoniemi, M. Jaronen, E. Arens, K. Åkerman, P.H. Chan, and J. Koistinaho. 2008. Deleterious role of superoxide dismutase in the mitochondrial intermembrane space. Journal of Biological Chemistry. 283:8446-8452.

Gonatas, J., S. Mezitis, A. Stieber, B. Fleischer, and N. Gonatas. 1989. MG-160. A novel sialoglycoprotein of the medial cisternae of the Golgi apparatus [published eeratum appears in J Biol Chem 1989 Mar 5; 264 (7): 4264]. Journal of Biological Chemistry. 264:646-653.

Grimm, D., and J.A. Kleinschmidt. 1999. Progress in adeno-associated virus type 2 vector production: promises and prospects for clinical use. Human gene therapy. 10:2445-2450.

Guo, S., Y. Liang, S.F. Murphy, A. Huang, H. Shen, D.F. Kelly, P. Sobrado, and Z. Sheng. 2015. A rapid and high content assay that measures cyto-ID-stained autophagic compartments and estimates autophagy flux with potential clinical applications. Autophagy. 11:560-572.

Hayashi-Nishino, M., N. Fujita, T. Noda, A. Yamaguchi, T. Yoshimori, and A. Yamamoto. 2009. A subdomain of the endoplasmic reticulum forms a cradle for autophagosome formation. Nature cell biology. 11:1433-1437.

Hurtley, S.M., and A. Helenius. 1989. Protein oligomerization in the endoplasmic reticulum. Annual review of cell biology. 5:277-307.

Ichimura, Y., T. Kumanomidou, Y.-S. Sou, T. Mizushima, J. Ezaki, T. Ueno, E. Kominami, T. Yamane, K. Tanaka, and M. Komatsu. 2008. Structural basis for sorting mechanism of p62 in selective autophagy. Journal of Biological Chemistry. 283:22847-22857.

Klionsky, D.J., H. Abeliovich, P. Agostinis, D.K. Agrawal, G. Aliev, D.S. Askew, M. Baba, E.H. Baehrecke, B.A. Bahr, and A. Ballabio. 2008. Guidelines for the use and interpretation of assays for monitoring autophagy in higher eukaryotes. Autophagy. 4:151-175.

Koishi, R., Y. Ando, M. Ono, M. Shimamura, H. Yasumo, T. Fujiwara, H. Horikoshi, and H. Furukawa. 2002. Angptl3 regulates lipid metabolism in mice. Nature genetics. 30:151-157.

Komatsu, M., S. Waguri, T. Ueno, J. Iwata, S. Murata, I. Tanida, J. Ezaki, N. Mizushima, Y. Ohsumi, and Y. Uchiyama. 2005. Impairment of starvation-induced and constitutive autophagy in Atg7-deficient mice. J Cell Biol. 169:425-434.

Lagace, T.A. 2014. PCSK9 and LDLR degradation: regulatory mechanisms in circulation and in cells. Current opinion in lipidology. 25:387.

Larsson, S.L., J. Skogsberg, and J. Björkegren. 2004. The low density lipoprotein receptor prevents secretion of dense apoB100-containing lipoproteins from the liver. Journal of Biological Chemistry. 279:831-836.

Luo, W., H. Wang, C. Guo, J. Wang, J. Kwak, K.L. Bahrou, and D.T. Eitzman. 2012. Haploinsufficiency of E-selectin ligand-1 is associated with reduced atherosclerotic plaque macrophage content while complete deficiency leads to early embryonic lethality in mice. Atherosclerosis. 224:363-367.

Marques-Pinheiro, A., M. Marduel, J.-P. Rabès, M. Devillers, L. Villéger, D. Allard, J. Weissenbach, M. Guerin, Y. Zair, and D. Erlich. 2010. A fourth locus for autosomal dominant hypercholesterolemia maps at 16q22. 1. European Journal of Human Genetics. 18:1236.

Mayer, G., J. Hamelin, M.-C. Asselin, A. Pasquato, E. Marcinkiewicz, M. Tang, S. Tabibzadeh, and N.G. Seidah. 2008. The regulated cell surface zymogen activation of the proprotein convertase PC5A directs the processing of its secretory substrates. Journal of Biological Chemistry. 283:2373-2384.

Mizushima, N., and T. Yoshimori. 2007. How to interpret LC3 immunoblotting. Autophagy. 3:542-545.

Nordestgaard, B.G., M.J. Chapman, S.E. Humphries, H.N. Ginsberg, L. Masana, O.S. Descamps, O. Wiklund, R.A. Hegele, F.J. Raal, and J.C. Defesche.

2013. Familial hypercholesterolaemia is underdiagnosed and undertreated in the general population: guidance for clinicians to prevent coronary heart disease: consensus statement of the European Atherosclerosis Society. European heart journal. 34:3478-3490.

Ohsaki, Y., J. Cheng, A. Fujita, T. Tokumoto, and T. Fujimoto. 2006. Cytoplasmic lipid droplets are sites of convergence of proteasomal and autophagic degradation of apolipoprotein B. Molecular biology of the cell. 17:2674-2683.

Ohsaki, Y., J. Cheng, M. Suzuki, A. Fujita, and T. Fujimoto. 2008. Lipid droplets are arrested in the ER membrane by tight binding of lipidated apolipoprotein B-100. Journal of cell science. 121:2415-2422.

Pan, M., V. Maitin, S. Parathath, U. Andreo, S.X. Lin, C.S. Germain, Z. Yao, F.R. Maxfield, K.J. Williams, and E.A. Fisher. 2008. Presecretory oxidation, aggregation, and autophagic destruction of apoprotein-B: a pathway for late-stage quality control. Proceedings of the National Academy of Sciences. 105:5862-5867.

Pankiv, S., T.H. Clausen, T. Lamark, A. Brech, J.-A. Bruun, H. Outzen, A. Øvervatn, G. Bjørkøy, and T. Johansen. 2007. p62/SQSTM1 binds directly to Atg8/LC3 to facilitate degradation of ubiquitinated protein aggregates by autophagy. Journal of Biological Chemistry. 282:24131-24145.

Pasinelli, P., M.E. Belford, N. Lennon, B.J. Bacskai, B.T. Hyman, D. Trotti, and R.H. Brown. 2004. Amyotrophic lateral sclerosis-associated SOD1 mutant proteins bind and aggregate with Bcl-2 in spinal cord mitochondria. Neuron. 43:19-30.

Plump, A.S., J.D. Smith, T. Hayek, K. Aalto-Setälä, A. Walsh, J.G. Verstuyft, E.M. Rubin, and J.L. Breslow. 1992. Severe hypercholesterolemia and atherosclerosis in apolipoprotein E-deficient mice created by homologous recombination in ES cells. Cell. 71:343-353.

Poirier, S., M. Mamarbachi, W.-T. Chen, A.S. Lee, and G. Mayer. 2015. GRP94 regulates circulating cholesterol levels through blockade of PCSK9-induced LDLR degradation. Cell reports. 13:2064-2071.

Polonovski, J., and I. Beucler. 1983. Structure and metabolism of plasma lipoproteins. Pathologie-biologie. 31:225-234.

Prudencio, M., A. Durazo, J.P. Whitelegge, and D.R. Borchelt. 2009. Modulation of mutant superoxide dismutase 1 aggregation by co-expression of wild-type enzyme. Journal of neurochemistry. 108:1009-1018.

Qiu, W., C. Taghibiglou, R.K. Avramoglu, S.C. Van Iderstine, M. Naples, H. Ashrafpour, S. Mhapsekar, R. Sato, and K. Adeli. 2005. Oleate-mediated stimulation of microsomal triglyceride transfer protein (MTP) gene promoter: implications for hepatic MTP overexpression in insulin resistance. Biochemistry. 44:3041-3049.

Qiu, W., J. Zhang, M.J. Dekker, H. Wang, J. Huang, J.H. Brumell, and K. Adeli. 2011. Hepatic autophagy mediates endoplasmic reticulum stress–induced degradation of misfolded apolipoprotein B. Hepatology. 53:1515-1525.

Raabe, M., M.M. Véniant, M.A. Sullivan, C.H. Zlot, J. Björkegren, L.B. Nielsen, J.S. Wong, R.L. Hamilton, and S.G. Young. 1999. Analysis of the role of microsomal triglyceride transfer protein in the liver of tissue-specific knockout mice. The Journal of clinical investigation. 103:1287-1298.

Rava, P., H. Athar, C. Johnson, and M.M. Hussain. 2005. Transfer of cholesteryl esters and phospholipids as well as net deposition by microsomal triglyceride transfer protein. Journal of lipid research. 46:1779-1785.

Ravikumar, B., R. Duden, and D.C. Rubinsztein. 2002. Aggregate-prone proteins with polyglutamine and polyalanine expansions are degraded by autophagy. Human molecular genetics. 11:1107-1117.

Ravikumar, B., C. Vacher, Z. Berger, J.E. Davies, S. Luo, L.G. Oroz, F. Scaravilli, D.F. Easton, R. Duden, and C.J. O'Kane. 2004. Inhibition of mTOR induces autophagy and reduces toxicity of polyglutamine expansions in fly and mouse models of Huntington disease. Nature genetics. 36:585-595.

Ron, D., and P. Walter. 2007. Signal integration in the endoplasmic reticulum unfolded protein response. Nature reviews Molecular cell biology. 8:519-529.

Rusiñol, A.E., H. Jamil, and J.E. Vance. 1997. In vitro reconstitution of assembly of apolipoprotein B48-containing lipoproteins. Journal of Biological Chemistry. 272:8019-8025.

Seidah, N.G., S. Benjannet, L. Wickham, J. Marcinkiewicz, S.B. Jasmin, S. Stifani, A. Basak, A. Prat, and M. Chrétien. 2003. The secretory proprotein convertase neural apoptosis-regulated convertase 1 (NARC-1): liver regeneration and neuronal differentiation. Proceedings of the National Academy of Sciences. 100:928-933.

Seidah, N.G., S. Poirier, M. Denis, R. Parker, B. Miao, C. Mapelli, A. Prat, H. Wassef, J. Davignon, and K.A. Hajjar. 2012. Annexin A2 is a natural extrahepatic inhibitor of the PCSK9-induced LDL receptor degradation. PloS one. 7:e41865.

Shan, L., X.-C. Yu, Z. Liu, Y. Hu, L.T. Sturgis, M.L. Miranda, and Q. Liu. 2009. The angiopoietin-like proteins ANGPTL3 and ANGPTL4 inhibit lipoprotein lipase activity through distinct mechanisms. Journal of Biological Chemistry. 284:1419-1424.

Shimamura, M., M. Matsuda, H. Yasumo, M. Okazaki, K. Fujimoto, K. Kono, T. Shimizugawa, Y. Ando, R. Koishi, and T. Kohama. 2007. Angiopoietin-like protein3 regulates plasma HDL cholesterol through suppression of endothelial lipase. Arteriosclerosis, thrombosis, and vascular biology. 27:366-372.

Shimizugawa, T., M. Ono, M. Shimamura, K. Yoshida, Y. Ando, R. Koishi, K. Ueda, T. Inaba, H. Minekura, and T. Kohama. 2002. ANGPTL3 decreases very low density lipoprotein triglyceride clearance by inhibition of lipoprotein lipase. Journal of Biological Chemistry. 277:33742-33748.

Soria, L.F., E.H. Ludwig, H. Clarke, G.L. Vega, S.M. Grundy, and B.J. McCarthy. 1989. Association between a specific apolipoprotein B mutation and familial defective apolipoprotein B-100. Proceedings of the National Academy of Sciences. 86:587-591.

Sun, H., A. Samarghandi, N. Zhang, Z. Yao, M. Xiong, and B.-B. Teng. 2012. Proprotein convertase subtilisin/kexin type 9 interacts with apolipoprotein B and prevents its intracellular degradation, irrespective of the low-density lipoprotein receptor. Arteriosclerosis, thrombosis, and vascular biology. 32:1585-1595.

Surdo, P.L., M.J. Bottomley, A. Calzetta, E.C. Settembre, A. Cirillo, S. Pandit, Y.G. Ni, B. Hubbard, A. Sitlani, and A. Carfí. 2011. Mechanistic implications for LDL receptor degradation from the PCSK9/LDLR structure at neutral pH. EMBO reports. 12:1300-1305.

Szeto, J., N.A. Kaniuk, V. Canadien, R. Nisman, N. Mizushima, T. Yoshimori, D.P. Bazett-Jones, and J.H. Brumell. 2006. ALIS are stress-induced protein storage compartments for substrates of the proteasome and autophagy. Autophagy. 2:189-199.

Tabas, I., and D. Ron. 2011. Integrating the mechanisms of apoptosis induced by endoplasmic reticulum stress. Nature cell biology. 13:184-190.

Twisk, J., D.L. Gillian-Daniel, A. Tebon, L. Wang, P.H.R. Barrett, and A.D. Attie. 2000. The role of the LDL receptor in apolipoprotein B secretion. Journal of Clinical Investigation. 105:521.

Varret, M., M. Abifadel, J.P. Rabès, and C. Boileau. 2008. Genetic heterogeneity of autosomal dominant hypercholesterolemia. Clinical genetics. 73:1-13.

Vergeer, M., A.G. Holleboom, J.J. Kastelein, and J.A. Kuivenhoven. 2010. The HDL hypothesis: does high-density lipoprotein protect from atherosclerosis? Journal of lipid research. 51:2058-2073.

Williams, K.J., and I. Tabas. 1995. The response-to-retention hypothesis of early atherogenesis. Arteriosclerosis, thrombosis, and vascular biology. 15:551-561.

Witan, H., A. Kern, I. Koziollek-Drechsler, R. Wade, C. Behl, and A.M. Clement. 2008. Heterodimer formation of wild-type and amyotrophic lateral sclerosis-causing mutant Cu/Zn-superoxide dismutase induces toxicity independent of protein aggregation. Human molecular genetics. 17:1373-1385.

Yang, T., I. Grafe, Y. Bae, S. Chen, Y. Chen, T.K. Bertin, M.-M. Jiang, C.G. Ambrose, and B. Lee. 2013. E-selectin ligand 1 regulates bone remodeling by limiting bioactive TGF-β in the bone microenvironment. Proceedings of the National Academy of Sciences. 110:7336-7341.

Zatloukal, K., C. Stumptner, A. Fuchsbichler, H. Heid, M. Schnoelzer, L. Kenner, R. Kleinert, M. Prinz, A. Aguzzi, and H. Denk. 2002. p62 Is a common component of cytoplasmic inclusions in protein aggregation diseases. The American journal of pathology. 160:255-263.

Zhang, D.-W., T.A. Lagace, R. Garuti, Z. Zhao, M. McDonald, J.D. Horton, J.C. Cohen, and H.H. Hobbs. 2007. Binding of proprotein convertase subtilisin/kexin type 9 to epidermal growth factor-like repeat A of low density lipoprotein receptor decreases receptor recycling and increases degradation. Journal of Biological Chemistry. 282:18602-18612.

Zhong, S., A.L. Magnolo, M. Sundaram, H. Zhou, E.F. Yao, E. Di Leo, P. Loria, S. Wang, M. Bamji-Mirza, and L. Wang. 2010. Nonsynonymous Mutations within APOB in Human Familial Hypobetalipoproteinemia EVIDENCE FOR FEEDBACK INHIBITION OF LIPOGENESIS AND POSTENDOPLASMIC RETICULUM DEGRADATION OF APOLIPOPROTEIN B. Journal of Biological Chemistry. 285:6453-6464.

Zhou, M., E.A. Fisher, and H.N. Ginsberg. 1998. Regulated Co-translational ubiquitination of apolipoprotein B100 A new paradigm for proteasomal degradation of a secretory protein. Journal of Biological Chemistry. 273:24649-24653.

Zolotukhin, S., B. Byrne, E. Mason, I. Zolotukhin, M. Potter, K. Chesnut, C. Summerford, R. Samulski, and N. Muzyczka. 1999. Recombinant adeno-associated virus purification using novel methods improves infectious titer and yield. Gene therapy. 6.

CHAPTER 3

3 PCSK9 and Atherosclerosis

CHAPTER 3: PCSK9 and Atherosclerosis

ARTICLE B: Development of an atherosclerosis mouse model to evaluate the regression of aortic root lesions following PCSK9 gene downregulation

AUTHORS: Samaneh Samami[1,2], Teodora Mihalache-Avram[1], Eric Rhéaume[1,3], Jean-Claude Tardif[1,3], Gaétan Mayer[1,2,4],

[1] Centre de Recherche de l'Institut de Cardiologie de Montréal, Départements de [2]Pharmacologie & [3]Médecine, Faculté de médecine, Université de Montréal.

[4]Faculty of Pharmacy, Université de Montréal

* Corresponding author; email gaetan.mayer@icm-mhi.org

CURRENT STAGE: Under Preparation

Authors' contributions

SS and GM designed the study. SS carried out the experiment. SS and GM analyzed the data and wrote the paper. TM helped in with the animal work, EC, JT, and GM advised on the study and provided laboratory support. GM supervised the study

Foreword

While LDLR$^{-/-}$ and apoE$^{-/-}$ are the most common used atherosclerosis mice models, they are not efficient for studying the effect of PCSK9 as both genes are required for PCSK9 function. Another atherosclerosis mice model is APOE*3Leiden.CETP mice that express LDLR and apoE genes but their use is

limited by high cost, several timely backcrosses, and limited accessibility. Thus, the magnitude of the association between plasma level of PCSK9 and atherosclerosis is not well known due to the lack of appropriate and easy accessible murine atherosclerosis model.

This study was undertaken to identify a suitable atherosclerosis mice model to study the effect of PCSK9 gene modulation on atherosclerosis. Our data indicate that overexpression of gain-of-function mutated $PCSK9^{D377Y}$ in C57BL/6 mice fed WTD induced development of atherosclerotic lesions in the aortic root, which was then reduced by inducing PCSK9 downregulation using DOX reversible system. Having appropriate animal models and applicable techniques will facilitate the examination of new treatments for atherosclerosis disease.

3.1 Abstract

Various atherosclerosis mouse models have been developed to investigate atherosclerotic aortic lesions. However, these models are mostly dependent on the absence of either LDLR or apoE genes, which are both required for the PCSK9 mode of action. Our objective was to develop an atherosclerosis mouse model, harboring LDLR and apoE genes, to investigate the association between PCSK9 and atherosclerotic lesions. We measured atherosclerotic lesions and circulating cholesterol level in the ATX [$LDLR^{-/-}$;Tg ($apoB^{+/+}$)] mice fed either a chow diet or a Western-type diet (WTD) and compared them with our developed ATX-HZ [$LDLR^{-/+}$; Tg ($apoB^{-/+}$)] mice fed a WTD, and C57BL/6 mice overexpressing gain-of-function mutant $PCSK9^{D377Y}$ (AAV8-Teton-$PCSK9^{D377Y}$) fed a WTD. ATX-HZ mice did not develop plaque, indicating that only one allele of LDLR is sufficient to protect mice against atherosclerosis. In contrast, significant atherosclerotic lesions were observed in the aortic root of the $PCSK9^{D377Y}$ overexpressed group similar to the levels found in the ATX mice. Doxycycline regulatable Tet-ON system was used to downregulate PCSK9 gene expression following its overexpression. The level of all circulating lipoproteins and the number of plaques in the aortic root were significantly reduced by inducing DOX reversible system. Thus, the C57BL/6 mice that overexpress $PCSK9^{D377Y}$ in an inducible manner is a useful mouse model for understanding the molecular role of PCSK9 on atherosclerotic plaques development.

Keywords: Atherosclerosis, mice model, PCSK9, LDLR.

3.2 Introduction

Atherosclerosis is characterized by the accumulation of fatty materials and plaque in artery walls. It can lead to heart attacks, strokes, and peripheral vascular disease, which are the principal causes of death worldwide (Mathers and Loncar, 2006; Weber and Noels, 2011). The etiology of atherosclerosis is multifactorial such as heredity, high levels of plasma low-density lipoprotein cholesterol (LDL-C), high blood pressure, smoking, obesity, and lack of physical activity. Among these factors, elevated plasma LDL cholesterol level is a major risk factor that alone is sufficient to induce atherosclerotic plaque formation (Wilson et al., 1998). High level of plasma LDL can be the result of heterozygous mutations in LDL receptor (LDLR) (Brown and Goldstein, 1986a), and less frequently in apolipoprotein B-100 (APOB) (Soria et al., 1989) and proprotein convertase subtilisin/kexin type 9 (PCSK9) (Abifadel et al., 2003). Therefore, LDL clearance, which is mediated by the liver through the LDL receptor (LDLR), represents an essential mechanism to maintain vascular health (Brown and Goldstein, 1986a).

PCSK9, a liver-secreted glycoprotein, was identified as an extracellular ligand of LDLR. It enhances the LDLR lysosomal degradation and thereby increases plasma LDL concentrations. PCSK9 gain-of-function (GOF) mutations greatly increase LDLR degradation, which results in high blood LDL and an increase in the risk of coronary heart disease (CHD) (Abifadel et al., 2003; Timms et al., 2004). The endeavor for atherosclerosis plaque regression has met considerable resistance over the years (Blankenhorn and Hodis, 1994; Stein and Stein, 2001). Very low plasma level of LDL and 88% lower risk of CHD in individuals by PCSK9 loss-of-

function (LOF) mutations (Cohen et al., 2005) suggests that reducing the function of PCSK9 might be a therapeutic approach for atherosclerosis disease. This idea was further supported by observing a higher level of LDLR and 25% to 50% decrease in plasma cholesterol of PCSK9 knockout mice (Rashid et al., 2005). Although the functional roles of PCSK9 in atherosclerosis has been studied before, the *in vivo* relevance of PCSK9 inhibition on protection against atherosclerosis is not yet fully understood. A proper atherosclerotic animal model is required to define the detailed mechanism of PCSK9 effect on atherosclerotic lesions.

The most frequent murine atherosclerotic models are the apoE$^{-/-}$ (Piedrahita et al., 1992) or LDLR$^{-/-}$ mice models (Ishibashi et al., 1994). Previous studies demonstrated that inhibiting PCSK9 function has a minimal atheroprotective effect either with LDLR$^{-/-}$ or apoE$^{-/-}$ background (Ason et al., 2014). In addition, no differences or very low impact on aortic cholesterol ester accumulation was found by knockout or overexpression of PCSK9 in LDLR or apoE deficient mice (Denis et al., 2012). Therefore, both apoE and LDLR genes play critical roles in the PCSK9 mode of action. ApoE*3-Leiden (E3L). Cholesteryl ester transfer protein (CETP) transgenic mice provide an alternative model. In this model, using a monoclonal antibody against PCSK9 (Alirocumab, Sanofi & Regeneron) has shown atheroprotective effects (Kühnast et al., 2014). Although E3L.CETP mice express both LDLR and apoE genes; they have limited accessibility and need several time-consuming and costly backcrosses. The scarcity of a suitable atherosclerosis murine model for studying the effect of PCSK9 inhibition prompted us to establish and evaluate other genetically modified mice models.

To overcome the limitations of current mice models, we aimed to develop an easily accessible model to study the PCSK9 role in atherosclerosis. We evaluated atherosclerotic plaque formation in ATX [LDLR$^{-/-}$; Tg (apoB$^{+/+}$)] mice fed either a chow diet or a Western-type diet (WTD) and compared them with our developed ATX-HZ [LDLR$^{-/+}$; Tg (apoB$^{-/+}$)] mice fed a WTD, and C57BL/6 mice overexpressing PCSK9 gain-of-function mutation (D377Y) (AAV8-Teton-PCSK9^{D377Y}) fed a WTD.

To modulate PCSK9 expression, we tested the use of Short hairpin RNA (shRNA) against PCSK9 in mice overexpressing PCSK9^{D377Y}, and the use of the Tet-on system to induce and then block PCSK9^{D377Y} overexpression in C57BL/6 mice. Lastly, we assessed the efficiency of each model in PCSK9 gene modulation, cholesterol regulation, and atherosclerotic plaque regression.

3.3 Experimental procedures

Animals and diets

ATX [LDLR$^{-/-}$; Tg (human apoB$^{+/+}$)] mice which are hybrids of the 129Sv/Ev, C57BL/6, and SJL strains, were obtained from the Eric Thorin laboratory (Institut de Cardiologie de Montreal, QC, Canada). They were divided into two groups; the first group fed a normal (chow) diet and kept for ~36 weeks of age. The second group of ATX mice fed a WTD (34% sugar, 21% fat, and 0.2% cholesterol) for 11-15 weeks, and kept for ~30 weeks of age.

ATX-HZ mice were produced by breeding four 8-week old C57Bl/6 females with four 8-week old ATX male mice. Five ATX-HZ pups were obtained from each breeding. Mice were weaned at 3 to 4 weeks of age and fed a WTD for 29 weeks to

develop atherosclerotic plaques rich in foam cells (~50% macrophage content). C57BL/6 mice (8-week old) from Charles River Laboratories (Montreal, Quebec) were used to generate AAV-PCSK9^{D377Y} mice. Briefly, C57BL/6 mice were intravenously injected with 1.66*10^{11} genome copies of a viral vector (rAAV8) expressing hPCSK9^{D377Y} and then fed a WTD for 12-13 weeks.

To study the effect of PCSK9 absence on aortic plaque regression, an aortic transplantation technique was tried. The abdominal aorta of donor ATX mice was perfused with chilled heparinized-saline and a 10–15 mm segment of donor descending abdominal aorta was taken. Age-and sex-matched PCSK9$^{-/-}$ mice were used as a recipient mouse, and its abdominal aorta was proximally and distally clamped and transected. A tube graft of the aorta part of the donor mice was inserted into the recipient mice; an end-to-end microsurgical anastomosis was done by an 11-0 monofilament nylon sutures (Ethicon, Somerville, New Jersey). The abdominal wall was closed by 7-0 prolene sutures. The handling time of complete grafting procedure was around 50–70 minutes. One week post-surgery, the recipient animals were sacrificed by exsanguination under anesthesia. Formation of atherosclerotic lesions in the abdominal aorta of donor mice and the viability of the mice after transplantation was assessed in a pilot experiment.

For PCSK9 downregulation following its overexpression, either 1.66 x 10^{11} genome copies of AAV8 expressing shRNA against PCSK9 or TetOn inducible/reversible system were used. TetOn inducible/reversible system requires simultaneous microinjection of two individual viral constructs (AAV8-EF1a-rtTA and AAV8-mCMV-hPCSK9^{D377Y}). The same day of virus injection, inducing agent Doxycyclin (Dox; 1 mg/ml; Sigma D-9891) was added to the mouse drinking water. Adding DOX (1

mg/ml) to the drinking water leads to binding of rtTA to tetO sequences, which in turn activates mCMV-PCSK9^{D377Y} gene transcription and reaches to its maximal induction level within 2-weeks. Drinking water was supplemented with DOX, kept in the dark, and changed every three days. To prevent PCSK9^{D377Y} transcription, DOX was removed from drinking water. In the absence of DOX, rtTA does not bind or binds weakly to tetO sequences; thus, the targeted gene (PCSK9^{D377Y}) is no longer transcribed.

All mice were kept in a conventional, non-germ-free animal house with free access to food and water (Table 3.1). All animal care and experimental procedures were approved by the animal care committee of the Institut de Cardiologie de Montreal.

Table 3.1 Mice body weight, age and duration of WTD in different groups of mice*

Genotype	WT	PCSK9^{D377Y}	ATX		ATX-HZ
Diet type	Chow	WTD	Chow	WTD	WTD
Diet duration (wks)	8	12-13	36	11-15	29
Age (wks)	8	21	36	30	32
Weight (g)	23	41	35	40	46

* From each genotype,six male mice were compared. WT: C57Bl/6 mice fed a chow diet (8 weeks old). AAV-PCSK9^{D377Y}: C57Bl/6 mice that were injected with AAV-PCSK9^{D377Y} at eight weeks of age and fed WTD for 12-13 weeks post-virus injection. ATX**:** ATX mice fed a chow diet (36 weeks old) or WTD (30 weeks old) for 11-15 weeks. ATX-HZ mice fed WTD for 29 weeks (32 weeks old),

Cell Culture and cDNA transfection

The AML12 (alpha mouse liver 12) mouse hepatocytes were cultured in Dulbecco's Modified Eagle's Medium (DMEM/F-12; Gibco) containing insulin, transferrin,

selenium (ITS; Gibco) and dexamethasone (DEX) (40 ng/ml; Sigma) in a 5% CO_2 atmosphere at 37 °C. Cells were used at about 70-90% confluency, and approximately 120,000 AML-12 cells were plated in 12-well culture plates. To test the efficiency of different shRNA sequences against PCSK9 (Kysenius et al., 2012), AML-12 cells were transiently transfected with shRNA-cassettes using Lipofectamine 2000 (Invitrogen) according to the manufacturer's instructions. These protein samples were extracted from cells 48-hours post-transfection and subjected to SDS/PAGE for immunoblot analysis.

PCSK9 immunoprecipitation

To detect the level of plasma PCSK9 in a wild-type mouse, 40 µl of plasma was mixed with 40 µl of protein A/G agarose beads (catalog no. sc-2003, Santa Cruz Biotechnology, Inc.) and 1 µg of anti-mPCSK9 antibody. After incubation, samples were centrifuged at 2500 rpm for 5 min at 4°C, and the beads were washed by resuspension in cell lysis buffer three times and centrifugation. After the last wash, the immunoprecipitated proteins were eluted in 50 µl of sample loading buffer and heated at 95 °C for 5 min before western blotting.

Plasmid and viral production

A viral vector in serotype eight capsids (rAAV8) with efficient liver-specific (HCR/apoE-hAAT) promoter was constructed to encode GOF mutation form of murine $PCSK9^{D377Y}$. For replacement of TRE pTight by TRE 3G in backbone plasmid pAAV-TRE-HTG (Addgene 27437), the TRE 3G seq flanked by 5'MluI and 3'EcoRI

sites was cloned in a plasmid pMK-RQ-Bb. An intermediate clone was generated by purification and ligation of both vector and insert (TRE3G) digested MluI and EcoRI.

The shRNAs sequence against PCSK9 was F12:5'-TTCTGGTGGCAGTGGACATGG-3' and G2: 5'-TTGGTAGAGAAGTGGATCAGC-3' (Kysenius et al., 2012) and the sequence of control shRNA (Scramble) was taken from addgene (plasmid 1864). Mature antisenses were generated by PCR. Briefly, single-stranded cDNAs containing different shRNA flanked by HindIII and BamHI sites and two linkers were purchased from IDT (Integrated DNA Technologies,IA, USA) and amplified by PCR using forward (fwd: 5' TAACCCTCACTAAAGGGACTC) and reverse (rev: 5' TAATACGACTCACTATAGGGCTC) linker primers. Double-stranded amplicons were digested with the two restriction sites, gel purified and ligated in pU6 ITR (graceful donation from Dr. N. Bousette) followed by the transformation in Stbl3 bacteria.

To obtain pAAV hEF1 alpha prom Tet-on 3G: two individual viral constructs, 1) a transcription regulatory unit linked to EF1alpha promoter (AAV8-EF1a-rtTA), which is a mutant Tet repressor fused to VP16 to form rtTA (transcription activator), and 2) the responsive element tet operator (tetO) sequences linked to a minimal CMV promoter-driven target gene (AAV8-mCMV-hPCSK9^{D377Y}) were produced.

Two viral constructs for the TetOn inducible/Reversible system were used. 1) Replacement of HTG by Tet on 3G (Clonetech) in plasmid pAAV-TRE-HTG (Addgene 27437): Minimal CMV Tet-on 3G sequence (clonetech) flanked by 5' EcoRI and 3'BglII was synthesized (Generate themofisher) and cloned in vector backbone (pMK-RQ; kanR). The clone was cut using both restriction sites, and the purified insert was ligated in pAAV-TRE-HTG vector (using same restriction

enzymes for linearization). This, in turn, resulted in pAAV TRE3G Tet-on 3G formation (an intermediate clone). 2) Replacement of TRE3G with EF1alpha promoter: EF1alpha promoter was generated by PCR using pEF GFP (Addgene 11154) as a template and primers forward 5'TATACGCGTGACTAGATCATCGCGTGAGGC and reverse 5'GGGCACCACCCCGGTGAACA. An amplicon (1303 bps) was cloned in pDrive (Qiagen) for sequencing purpose. Intermediate pAAV TRE3G tet on 3G vector was digested at MluI and EcoRI sites, gel purified and ligated with pDrive EF1alpha insert at the same restriction sites of the vector and gel purified. All used clones were confirmed by sequencing and purified by Maxiprep (Qiagen, Catalog No. D4202).

AAV vector production

Human embryonic kidney 293T (HEK293T) cells were cultivated in complete DMEM without sodium pyruvate (catalog no. 319-015-CL, Wisent) containing 10% fetal bovine serum (FBS; catalog no. 080-350, Wisent). HEK293T cells were plated into 16 X100-mm culture plates ($5.0x10^6$ cells) to reach 70–80% confluence on the day of transfection for virus production. Cells were co-transfected with a mixture of plasmids using linear polyethylenimine (PEI) MW 25,000 (PEI; 46 µl/plate, Cat No.23966, Polysciences) to produce AAV serotype eight vectors. The plasmids mixture contained packaging plasmid PDG8 (8.6 µg/plate) (Grimm and Kleinschmidt, 1999) and constructed plasmid(s) (2.9 µg/plate). Three days after transfection, cells were harvested and pelleted by centrifugation (1140 g for 10 min at room temperature). The cells were resuspended in 4.5 ml of lysis buffer (50 mM Tris, 150 mM NaCl, pH 8.5) and the virus was released from the cells by three rounds of freeze

and thaw in ethanol/dry ice bath for 5 min and 37°C water bath for 2 min, respectively. Crude lysates were treated with 250 units of Benzonase nuclease (Sigma, E1014-5KU) and 1mM $MgCl_2$ to each ml of lysate, and the mix was incubated for 45 min at 37°C. After pelleting the cell debris for 20 min at 6000 g, the supernatant was used for further purification.

An iodixanol step density gradient was prepared as described previously (Zolotukhin et al., 1999) with slight modifications: Briefly, 60% iodixanol (OptiPrep; Sigma D1556) was diluted to 40, and 25% in 5X PBS-MK (5X PBS, 5 mM $MgCl_2$,12.5 mM KCl). To distinguish of the phase boundaries within the gradients, 2.5 µl of 0.5% phenol red (Bioshop PHE600.5/5g) was added per milliliter of 25 and 60% iodixanol. One milliliter of 60, 40, and 25 % iodixanol solutions was successively underlaid in a 5-ml Beckman ultracentrifuge tube (catalog No# 326819), and 1.5 to 2 ml of the processed cell lysate was gently overlaid onto the gradients and centrifuged in a 55Ti rotor for 3 hr at 33,000 rpm at 4℃. After centrifugation, the tubes were punctured between 60 and 40% interphase (bottom and middle layers), using an 18-gauge needle, to collect ~1-ml/tube of the fraction containing the virus. A pool of collected iodixanol containing virus was diluted with PBS-0.001% Tween 20 to reach a total volume of 15 ml and concentrated to ~1 ml by passage through Amicon Ultra-15 centrifugal filter unit (MWCO, 100kDa; Merck Millipore). The concentrator was filled up to 10 ml to concentrate the virus again to 1 ml. This step was repeated two more times. Viral titers in terms of viral genomes (VG)/ml were determined by Real-Time qPCR with four different dilutions of the virus relative to standards using primer pairs in Table 3.2.

Table 3.2 Oligonucleotides used for quantitative PCR

Gene	Primer Sequences (5'→3')
Mouse PCSK9	F: TGCAAAATCAAGGAGCATGGG R: CAGGGAGCACATTGCATCC
BGH	F: TGCCTTCCTTGACCCT R: CAGGGAGCACATTGCATCC

Animal euthanasia and dissection

Mice were anesthetized by inhalation of 2% isoflurane and oxygen flow of 0.8 liters/minute in the induction chamber. Blood was taken using a 21-gauge needle mounted on a 1-mL syringe. Liver tissues were dissected, snap-frozen in liquid nitrogen, and stored at −80 °C. Aortas were dissected from the heart down to the iliac branches, and further removal of the adventitia was performed under a microscope.

Analysis of plasma PCSK9 and lipoprotein profile

Blood samples were collected into tubes containing EDTA. Plasma was isolated by centrifugation at 3000 ×g for 15 min and stored at -80°C. Mouse plasma PCSK9 concentration was determined using an ELISA kit (Cyclex Co, #CY-8078, Japan). Total cholesterol and LDL cholesterol levels were measured using a colorimetric enzymatic assay (Wako Pure Chemical Industries, Osaka, Japan) according to the manufacturer's protocol. A pooled plasma sample from six mice of each genotype (100 µl) was subjected to fast performance liquid chromatography (FPLC) for lipoprotein analysis, and 54 fractions (300 µl each) were collected. Superose 6 column of FPLC gel filtration (flow rate of 0.5 ml/min) was used for

separating of plasma lipoprotein fractions. Fifty-two fractions (300 µl each) were collected, and cholesterol content was eluted and measured in each fraction (100 µl from each fraction) using the fluorometric enzyme assays (Horton et al., 1999).

Quantification of atherosclerotic lesions on the whole aorta (*En Face*) and cross-sectional quantification of the aortic root

The upper part of the heart was separated from the ascending aorta, excised and pinned-out from the aortic arch to the iliac bifurcation. Heart and pinned-out aorta were fixed with 4% paraformaldehyde (PFA) in PBS for 1 to 3 days and then aortas were stained for 1 hour with a solution of 0.7% oil red O (Sigma-Aldrich), which followed by aorta counterstaining using 0.05% Nuclear Fast Green (Sigma-Aldrich, F7258) to optimize contrast. Images were captured using a Digital Camera (MC170 HD, Leica Microsystem). Image-Pro premier 9.2 (Media Cybernetics, Inc, Rockville, MD) was used to quantify atherosclerotic lesions from the aortic root down to the iliac artery bifurcation.

The heart was embedded in paraffin and sliced into 10-µm sections from the beginning of the valves to the aortic root (420 µm). Plaque analysis was performed using hematoxylin-phloxine-saffron (HPS) staining. Afterward, the sections were placed under a microscope, and images were captured by a trained observer who was blinded to mouse genotypes and treatments. Atherosclerosis lesions were quantified using Image-Pro Premier 9.2.

Western Blot Analysis

Cells or piece of the mouse liver was homogenized with ice-cold Ripa buffer (50 mM Tris/HCl, pH 8.0, 150 mM NaCl, 0.1% (v/v) SDS, 1% (v/v) Nonidet P40, and 0.5% sodium deoxycholate) containing protease inhibitor mixture (Roche Applied Science). Samples were then centrifuged at 13,000 g at 4°C for 15 min. The concentration of each sample was determined using a Bradford assay. Protein samples were then diluted with standard loading buffer (6X Laemmli) and dH_2O and then mixed and heated at 95°C for 5 minutes. Prepared samples (60 µg) and molecular weight marker (Invitrogen) were resolved on 8% SDS-polyacrylamide gels. Proteins were separated for one h at 175 V at room temperature and transferred to a nitrocellulose membrane for two h (100 V, 4 °C). Nitrocellulose membrane was blocked for 1 h at room temperature in 5% blocking buffer (10 mmol/L Tris, pH 7.4, 150 mmol/L NaCl, 0.1% Tween-20 (TBST) containing 5% skimmed milk). After blocking, membranes were probed with goat anti-mouse LDLR (1:1000; catalog no. A2255, R&D Systems), goat anti-mouse/human-Albumin (1:6000; catalog no. AF3329, R&D system), rabbit anti-mPCSK9 (1:3000; in-house or catalog no. AF3985, R&D system) or rabbit anti-actin (1:5000; catalog no. A2066, Sigma-Aldrich) primary antibodies in TBST-1% milk overnight at room temperature. Albumin and actin were used to confirm equal loading. Then, the blots were washed three times (10 min each) with TBST. After washing, blots were incubated for 1h with corresponding HRP-conjugated secondary antibodies (1:10,000), washed in TBST (3 times, 10 min each), developed with ECL reagent and exposed to x-ray films. Band intensities were determined and quantified by Image J software (NIH).

Statistical analysis

GraphPad Prism Version 5 (Prism Software, Inc., La Jolla, CA, USA) was used to assess statistical significance for PCSK9, T-cholesterol, and aortic lesion area measurements. Unpaired two-tail Student's t-test was used to compare between two groups with unequal variances, and P values were determined. Significance was set at $P < 0.05$ for all tests. Significant effects are indicated by * for comparison between the specified groups. Mean values in each group of different experiments were determined and given as mean ± SD. All reported replicates were biological replicates or pooled samples from biological replicates. N indicates the number of mice. Error bars represent SD in all figures. LDLR level of the indicated genotypes was quantified using Image J software (NIH). Histology pictures were quantified by a blind person to our experimental groups.

3.4 Results

ATX-HZ mice did not develop atherosclerotic plaque in the aortic root regardless of high plasma level of LDL-C

ATX mice fed a chow diet showed high levels of cholesterol in plasma, mainly accumulated in the LDL fraction and low plasma levels of HDL-C (Figure 3.1A-B). To study plaque formation, the histochemical analysis was performed. HPS and en face oil Red O staining were used in a subset of animals from each genotypic group to study lesion development in the aortic root or elongated aortas. Lesions appear to be localized to the root of the aorta in association with the aortic valves in the absence of both alleles of LDLR (Figure 3.1C). Moreover, atherosclerotic lesions were visible in en face aortas of ATX mice (Figure 3.1D).

Thus, according to our results (Figure 3.1A-D) and previous reports (Sanan et al., 1998), ATX mice were highly susceptible to atherosclerosis when fed a standard chow diet. To determine if this susceptibility to atherosclerosis is preserved in human apoB transgenic mice lacking one allele of LDLR, C57Bl/6 female mice (8 weeks old) were bred with age-matched ATX males. To accelerate lesion development, generated ATX-HZ mice were fed WTD after the weaning period. Formation of atherosclerotic plaques was assessed in ATX-HZ mice fed WTD (29 weeks) and compared with ATX mice with and without consuming WTD.

Separation of plasma lipoproteins by FPLC confirmed that lacking one allele of LDLR in ATX-HZ mice results in a dramatic increase in the LDL cholesterol content and a decrease in the cholesterol of the HDL fraction compared to wild-type (WT) mice (Figure 3.1F). However, no plaque was formed neither in the aortic root (Figure 3.1G) nor in the entire aorta (Figure 3.1H) of ATX-HZ mice after 29 weeks of exposure to WTD.

Our FPLC analysis from pooled plasma of ATX mice fed WTD (Figure 3.1I) demonstrated a dramatic increase in plasma level of VLDL (Figure 3.1J). Oil Red O staining displayed the extent of lesion formation in the entire aorta of ATX fed WTD mice (Figure 3.1K). Representative examples are taken from the mid-range of aortic involvement with plaque formation in each genotype.

AAV-PCSK9^{D377Y} overexpression induced hyperlipidemia and atherosclerotic lesions

Then, we attempted to develop an atherosclerosis mice model using a single tail-vein injection of a recombinant adeno-associated virus serotype-8 expressing $PCSK9^{D377Y}$ (5×10^{11} viral particles) into eight weeks old C57Bl/6 mice fed a Western-type diet for 12-13 weeks (Figure 3.2A). Our results demonstrated a constant increase of $PCSK9^{D377Y}$ in mouse plasma during 13 weeks post virus injection (Figure 3.2B). PCSK9 overexpression led to an increase in the plasma level of LDL, which remained stable at all post-injection times that were analyzed (Figure 3.2C). Total plasma cholesterol in mice was highly increased ($p<0.01$) after eight-weeks post-virus injection (~500 versus 120 mg/dl), which continued to increase ($p<0.05$, ~700 mg/dl) in 21-weeks old mice (Figure 3.2D). As expected from the increase in the level of total cholesterol and increase in the level of LDL in plasma, high level of VLDL and LDL were observed in relevant FPLC fractions from the pooled plasma of 21-weeks old treated mice (Figure 3.2E).

We compared plaque size in the aortic root of C57BL/6 mice fed WTD at 8 and 13 weeks post virus injection. $PCSK9^{D377Y}$ overexpression in C57BL/6 mice resulted in atheroma plaques development at 16-weeks old mice, which was further increased in 21-weeks old mice (Figure 3.2F). For detection of neutral lipids on the entire aorta of 21-weeks old mice, en face Oil Red O staining was performed. The appearance of no plaque in the whole aorta demonstrated lesion formation requires a more extended period of PCSK9 overexpression in C57Bl/6-WTD fed mice (Figure 3.2G). Different slices of aortic root were prepared and used for plaque cross-sectional area quantification. Quantification analysis showed a significant (P value< 0.01) increase (about six-fold) in plaque area in 21-weeks old mice compared with 16-weeks old mice (~40 vs. ~250 mm^2) (Figure 3.2H).

Comparison of different atherosclerosis mice models

Six male mice in each group of the following 4 genotypes were compared: 1) ATX mice fed chow diet (36 weeks old), 2) ATX-HZ mice fed WTD for 29 weeks (32 weeks old), 3) ATX mice fed WTD for 11-15 weeks (30 weeks old), and 4) C57Bl/6 mice that were injected with AAV-PCSK9^{D377Y} at 8 weeks of age and fed WTD for 12-13 weeks post-virus injection. Also, C57Bl/6 (WT) mice fed a chow diet (8 weeks old) was used in some analysis as a control (Table 3.1).

The genotype of each group of mice and the efficiency of AAV-PCSK9^{D377Y} injection for LDLR degradation were confirmed with WB analysis using anti-mouse LDLR antibody (1:1000; catalog no. A2255, R&D Systems). Injection of AAV-PCSK9^{D377Y} led to degradation of almost all LDL receptors in mouse liver compared to ATX-HZ ($p< 0.05$) and WT mice. No LDLR was detected in ATX mice (Figure 3.3A-B). A plasma level of PCSK9 was significantly higher in mice that were injected with AAV-PCSK9^{D377Y} compared with all other groups. In addition, the absence of LDLR in ATX mice led to more PCSK9 accumulation in plasma compare to ATX-HZ mice ($p< 0.05$). No difference in plasma level of PCSK9 was observed between ATX mice fed either chow or WTD (Figure 3.3C).

The mean level of plasma cholesterol in the ATX mice fed WTD was significantly ($p<0.01$) higher than all other groups. ATX mice-fed WTD demonstrated 2.5-fold higher level of total cholesterol in plasma than ATX mice-fed with chow diet. Circulatory level of cholesterol in AAV-PCSK9^{D377Y} transduced mice was similar to the ATX mice fed chow diet, while it was significantly ($p<0.01$) higher than plasma cholesterol level in the ATX-HZ mice. The expression of one allele of LDLR in the

ATX-HZ mice fed WTD led to a 4-fold decrease ($p< 0.01$) in the level of plasma cholesterol compared to the ATX mice fed WTD (3.3D).

To examine the efficiency of ATX-HZ and AAV-PCSK9^{D377Y} mice on the development of atherosclerosis plaques, plaque volume in the aortic root of mice was analyzed and compared with the same analysis in known atherosclerosis mice model (ATX mice). Our results confirmed that 36 weeks old chow-fed ATX mice develop large atherosclerotic lesions in aortic root (Figure 3.3E) as well as in whole aorta surface (Figure 3.3F). Our quantifications of aortic lesion area indicated higher ($p<0.05$) level of plaques in the aortic root of AAV-PCSK9^{D377Y} injected mice compared to chow-fed ATX mice (189908 vs. 66484 μm^2) (Figure 3E). The ATX-HZ mice had no plaques either in the aortic root or in the entire aorta (Figure 3E-F).

Effect of PCSK9 deficiency on atherosclerosis plaque formation

To investigate the effect of PCSK9 gene deficiency in slowing down the progression of atherosclerosis, various approaches were tested. We initially proposed to transplant a segment of abdominal aorta containing plaques from hyperlipidemic ATX mice into PCSK9$^{-/-}$ mice. Atherosclerosis ATX mice have been described previously (Sanan et al., 1998) as well as in our study. The results of our pilot study demonstrated that abdominal transplantation and grafting procedure were successfully carried out, and animals were alive one week after transplantation. However, the level of developed plaques in the segment of the abdominal aorta of donor mice was not sufficient to study plaque regression after transplantation. The atherosclerosis plaques in the abdominal aorta of 36-weeks old ATX mice fed chow-diet and 30-weeks old fed WTD for 15-weeks were quantified (Supplementary Fig

3.1). Thus, we evaluated two other alternative approaches, shRNA against PCSK9 and TetOn inducible/reversible system, to study the effect of reduction in plasma level of PCSK9 on atherosclerosis disease. Although shPCSK9 was efficient to reduce the level of PCSK9 in mouse hepatocytes (AML-12 cells) and plasma of wild-type mice, it was not effective in reducing the extremely elevated plasma level of PCSK9 after 15-weeks of PCSK9 overexpression.

The efficiency of the autoregulated Tet-inducible system in PCSK9 overexpression and atherosclerotic plaque formation, as well as its reversible effect on preventing of PCSK9 overexpression and plaque regression, was examined. First, we tested PCSK9 overexpression after intravenous administration of AAV8 vectors. The expression of $PCSK9^{D377Y}$ fused CMV minimal (CMVm) promoter linked to tetO sequences was under the control of the transcription regulatory unit (a mutant Tet repressor fused to VP16) linked to EF1alpha promoter. Absence or presence of DOX inducing agent in mice drinking water prevents or induces $PCSK9^{D377Y}$ transcription by regulating rtTA interaction with tetO sequences. Schematic of AAV8 vectors and their function in Dox-inducible/reversible system is presented in Fig 3.4A.

In a first longitudinal study, both AAV8 vectors (AAV8-EF1a-rtTA and AAV8-mCMV- $PCSK9^{D377Y}$ were simultaneously injected in six 8-weeks old C57BL/6 mice. DOX (1 mg/ml) was added to mice drinking water on the same day. In the progression group, drinking water was supplemented with DOX throughout the experiment (17 weeks). In the regression group, DOX was removed from the drinking water of 10-weeks old mice for two weeks. After that, the water of 12-weeks old mice was supplemented with DOX again for 8-more weeks. All six mice fed WTD from the

age of 12-weeks and sacrificed at 25-weeks (Fig 3.4B). Our results demonstrated that Dox-inducible system was sufficient to reduce the overexpressed level of PCSK9 to background values within two weeks. These cycles of activation and inactivation of the PCSK9 gene expression by switching gene expression on and off was repeated one more time with the same animals. The outcome of our study demonstrated abolished level of PCSK9 in mouse plasma was fully restored and remained constant for 8-weeks upon supplying the animals drinking water with DOX (1 mg/ml). However, withdrawal of the antibiotic for the second time did not reduce plasma level of PCSK9 further (Figure 3.4C).

Visualization of the lipoprotein profile by chromatography analysis from the pooled plasma of three mice in each group showed that activation of PCSK9 expression in 8-weeks old mice in the progression group strongly increased the plasma level of LDL-C. In addition, inactivation and re-inactivation of PCSK9 gene expression robustly reduced level of LDL-C in plasma of 12- (Figure 3.4D) and 25- (Figure 3.4E) weeks old mice in the regression group. Both progression and regression groups demonstrated similar profile in HDL particles. The lower level of total cholesterol in plasma of mice in the regression group prompted us to test whether modulation in PCSK9 expression could change the degree of atherosclerotic plaques in the aortic sinus. The HPS staining and quantification analysis demonstrated a reduction in the level of atherosclerotic plaques in the aortic root of two out of three mice in the regression group (Figure 3.4F).

For the second and more comprehensive experiment, twenty-one 8-weeks old C57BL/6 mice were used, seven each for the baseline, continued overexpression of PCSK9 (progression) and reducing the overexpressed level of PCSK9 in (24-28)-

weeks old mice in regression group. DOX was added or removed from mice drinking water as indicated in the schema. Mice in the baseline group were sacrificed at the age of 24 to 28 weeks to have a control for the level of atherosclerosis plaques to compare its level with the level of plaques in mice with continued PCSK9 overexpression (progression) and downregulated level of PCSK9 (regression). Mice in progression and regression groups were sacrificed at the age of 30 to 34 weeks (Figure 3.5A). At sacrifice, the plasma level of PCSK9, plasma lipoprotein profile, and atherosclerotic lesions in aortic root were compared among the three experimental groups. The levels of the analytes showed released PCSK9 protein in the bloodstream highly increased 2-weeks post virus+DOX administration (data not are shown) and remained constant for 26-30 weeks (Figure 3.5B). Although the plasma level of PCSK9 was not reduced significantly upon six weeks of DOX withdrawal from mice drinking water, a tendency to decrease with less variation between animals was observed in 30-34-weeks old mice in the regression group (Figure 3.5B).

Plasma lipoproteins from pooled samples in each group were separated by FPLC. Our results demonstrated a sharp decrease in the plasma level of LDL in the regression group compared to the baseline. However, no clear difference was observed between the lipoprotein profile of progression and regression groups (Figure 3.5C). This observation supported the expected association of plasma level of PCSK9 with LDL particles. To evaluate the effect of PCSK9 and LDL reduction on atherosclerotic lesion development, HPS staining in cross-sections of the aortic root area was performed. We then quantified the plaque volume in each section all along the aortic root. Representative images of HPS-stained atherosclerotic lesions in the

aortic root area (Figure 3.5E) and quantification analysis (Figure 3.5F) demonstrated a similar level of plaques in the aortic root of baseline and regression groups, though mice in regression group consumed WTD for six weeks more than baseline.

3.5 Discussion

The goal of this study is to develop a practical, fast, and low-cost methodology to understand the association between PCSK9 gene downregulation and atherosclerotic lesion development. In this study, we developed a tetracycline-inducible AAV8 vector expressing GOF mutant form of mouse PCSK9^{D377Y} (AAV8-tetON- PCSK9^{D377Y}) in mice, and DOX (1 mg/ml) in the drinking water. We found that 1 mg/ml DOX promotes a significant increase in PCSK9^{D377Y} expression levels and induces atherosclerosis in mice fed WTD for 17 weeks. In the absence of DOX, the level of all circulating lipoproteins and the number of plaques in the aortic root were reduced.

Knockout or overexpression of PCSK9 in most common atherosclerosis mice models, LDLR$^{-/-}$ or apoE$^{-/-}$, has shown no difference or shallow impact on aortic cholesterol ester accumulation (Denis et al., 2012). Also, PCSK9 deficiency in mice with LDLR and apoE knockout background resulted in a minimal atheroprotective effect (Ason et al., 2014). E3L.CETP mice is another model developed for studying atherosclerosis disease (Westerterp et al., 2006). Inhibiting PCSK9 by a monoclonal antibody (Alirocumab) in E3L.CETP model led to atheroprotective effects (Kühnast et al., 2014). In summary, lack of LDLR and apoE in LDLR$^{-/-}$ or apoE$^{-/-}$ mice models, limited accessibility of E3L.CETP mice and the high cost of monoclonal antibodies pose potential limitations for studying the effect of PCSK9 inhibition on reducing the

atherosclerotic lesions. Thus, development of a novel strategy for studying the association between PCSK9 absence/reduction and atherosclerotic lesions is highly valuable.

It has been reported that ATX mice develop extensive and complex atherosclerotic lesions without using any type of high cholesterol/fat diet (Sanan et al., 1998). Thus, we asked whether transplanting a segment of the abdominal aorta, containing atherosclerotic lesions of ATX mice to PCSK9$^{-/-}$ mice would be a potential approach for this study. The data of our pilot study demonstrated that ATX mice fed either a chow diet (36 wks) or a high-fat diet (11 to 15 wks) do not develop sufficient percentage of plaques in the abdominal aorta. Since transplantation of the abdominal aorta to the aortic arch is preferred due to difficulties in ligation of branches such as the carotid and subclavian arteries in the aortic arch, we concluded that these mice are not an appropriate transplantation model for studies on regression of atherosclerotic lesions.

We then evaluated the development of atherosclerosis plaques in ATX-HZ mice. Unexpectedly, our results demonstrated that ATX-HZ mice do not display apparent atherosclerotic lesion formation either in the aortic root or in the entire aorta even after 29 weeks consuming WTD. Our result indicates that only one allele of LDLR is sufficient to protect mice against atherosclerosis.

As an alternative approach, we induced atherosclerosis by a single AAV8–mediated transfer of mouse PCSK9^{D377Y} in wild-type mice fed WTD. Two recent studies have demonstrated that transfer of AAV expressing GOF mutant form of either mouse PCSK9^{D377Y} (Bjoerklund et al., 2014b) or human PCSK9^{D374Y} (Roche-Molina et al., 2015a) induced and sustained atherosclerosis lesions in aortic roots of

high-fat diet fed wild-type mice. Our results demonstrated that downregulation of PCSK9 using an shRNA against PCSK9 in this model was not efficient despite its high efficiency in PCSK9 gene downregulation in wild-type mice. A possible explanation may be that the AAV8 binding site on its receptor was already occupied by the first virus injection because we also used AAV8 for PCSK9 overexpression and re-injected the same animals with AAV8-shRNA for PCSK9 downregulation.

AAV is a non-pathogenic virus (Nakai et al., 2005) and considered as a promising delivery system in gene therapy due to their safety, lack of toxicity and rare immune response (Ratko et al., 2003). AAVs are practical tools for long-term modulation of gene expression and can be preferentially targeted to different organs by replacing capsids among different AAV serotypes. AAV8 has been reported to have higher transfection efficiency in the liver compared with other AAV serotypes (Gao et al., 2005; Nakai et al., 2005). The receptor of AAV8 in host hepatocytes is known as the laminin receptor (LamR) (Akache et al., 2006). A single injection of recombinant AAV8 can result in long-term hepatic expression of a transgenic protein or shRNA without toxicity in mice (Ho et al., 2008).

AAV8-PCSK9^{D377Y} mice can speed discoveries in studying the effect of PCSK9 on atherosclerosis disease due to the presence of both apoE and LDLR genes as well as its easy accessibility by avoiding time-consuming and costly crossing of mouse strains with different genetic backgrounds. Thus, we established AAV8-mediated atherosclerosis in C57Bl/6 mice overexpressing PCSK9^{D377Y} adapted from DOX-inducible TetOn system (AAV8-tetON- PCSK9^{D377Y}) to regulate PCSK9 expression activity. In TetOn system, mutant reverse transactivators (rtTAs)

bind to the TRE in the presence of DOX to drive transgene expression, which does not occur in the absence of DOX (Gossen and Bujard, 1995).

In a proof-of-principle study, we found that inducible Tet system was an effective methodology for $PCSK9^{D377Y}$ overexpression, which resulted in atherosclerotic plaque formation after 17 weeks in WTD fed mice (progression group). In light of the observed high efficiencies of inducible Tet system in PCSK9 overexpression, we assessed whether reversible Tet system could be used to downregulate PCSK9 gene expression (regression group) in the developed atherosclerosis mice model. Both groups were sacrificed at 25 weeks old. Quantification of atherosclerotic plaques in aortic root demonstrated that mice in the progression group (+DOX) had ~4-fold higher level of plaques compared with baseline. Baseline and regression groups (-DOX) displayed similar levels of atherosclerotic plaques in aortic roots. Our results illustrated the capability of the Tet-inducible system in gaining better insights into the effect of PCSK9 gene downregulation on atherosclerosis disease. However, long-term exposure to DOX increased the variations in plasma level of PCSK9 between different animals, which thus requires having more mice in each group to overcome this limitation.

A possible reason that we did not detect any change in PCSK9 level after removing DOX from water (Fig 3.5B) may be related to PCSK9 turnover. LDLR is the main regulator for PCSK9 turnover. Under normal conditions, PCSK9 shows a very rapid turnover, with an estimated half-life of about 5 minutes. In the absence of LDLR, the PCSK9 half-life is about 3 to 10 times over normal (Grefhorst et al., 2008). We confirmed the efficiency of DOX inducible system in reducing the overexpressed level of PCSK9 after two weeks washout. However, under the condition of our study,

an extremely high level of PCSK9 during 24-28 weeks over-expression may result in all LDLRs degradation and increased PCSK9 half-life. Therefore, a longer washout period after PCSK9 overexpression may help to see the difference in PCSK9 clearance.

To quantify the enormous increase in PCSK9 level in plasma, a very high dilution of plasma was required. This might affect the efficiency and accuracy of the ELISA kit to quantify the actual concentration of PCSK9. The reason that there is a decrease in plasma level of LDL in both progression and regression groups compared to the baseline (figure 3.5C) might be explained by the potential resistance to DOX in mice after long exposure to it. Therefore the actual level of PCSK9 was not increased anymore (figure 3.5B). Also, ELISA does not distinguish between the cleaved and uncleaved form of PCSK9. Although autocleavage of endogenous PCSK9 is required for its secretion, we assumed that long-term consuming DOX (24-28 weeks) might induce secretion of the uncleaved form of overexpressed PCSK9. Uncleaved form of PCSK9 is unable to degrade LDLR (McNutt et al. 2007), leading to more LDL clearance in both experimental groups (figure 3.5C). Another reason that PCSK9 was not reduced in the regression group when DOX was removed from water may be related to the inhalation of DOX by animals (Tata et al., 2013). Although the addition of DOX to the water was stopped in the regression group, they were still in the same environment as another mouse in the progression group. We were adding DOX to the water of the progression group every 2-3 days. Finally, long-term DOX exposure induced high variation in PCSK9 protein, and consequently, cholesterol levels between animals in the progression group. This might be due to the different level of water consumption among animals. Thus, increasing the

number of animals in each group could help us to see a more clear difference between our experimental groups.

Other transcription-based regulation systems that can be used in gene therapy vectors in animal models are Ecdysone (No et al., 1996), mifepristone/RU-486 (Wang et al., 1994) and rapamycin (Rivera et al., 1996). Also, a translational regulation system was developed by Rivera et al. (2000) to control protein secretion. It has been reported that the Tet-inducible system and rapamycin are the most appropriate approaches for long-term regulatable expression (Rendahl et al., 2002). Also, FDA approval of DOX as a transcriptional regulator implies a lack of significant immune response, which is the main advantage of this system.

To our knowledge, our results demonstrate for the first time that regulation of PCSK9 gene expression by DOX-inducible system directly regulates plasma level of cholesterol and atherosclerotic lesion size in the aortic root area. Taken together, we showed in our study that the C57BL/6 mice, overexpressing $PCSK9^{D377Y}$ in an inducible manner, is a useful mouse model for understanding the molecular role of PCSK9 on atherosclerotic plaques development.

3.6 Figures

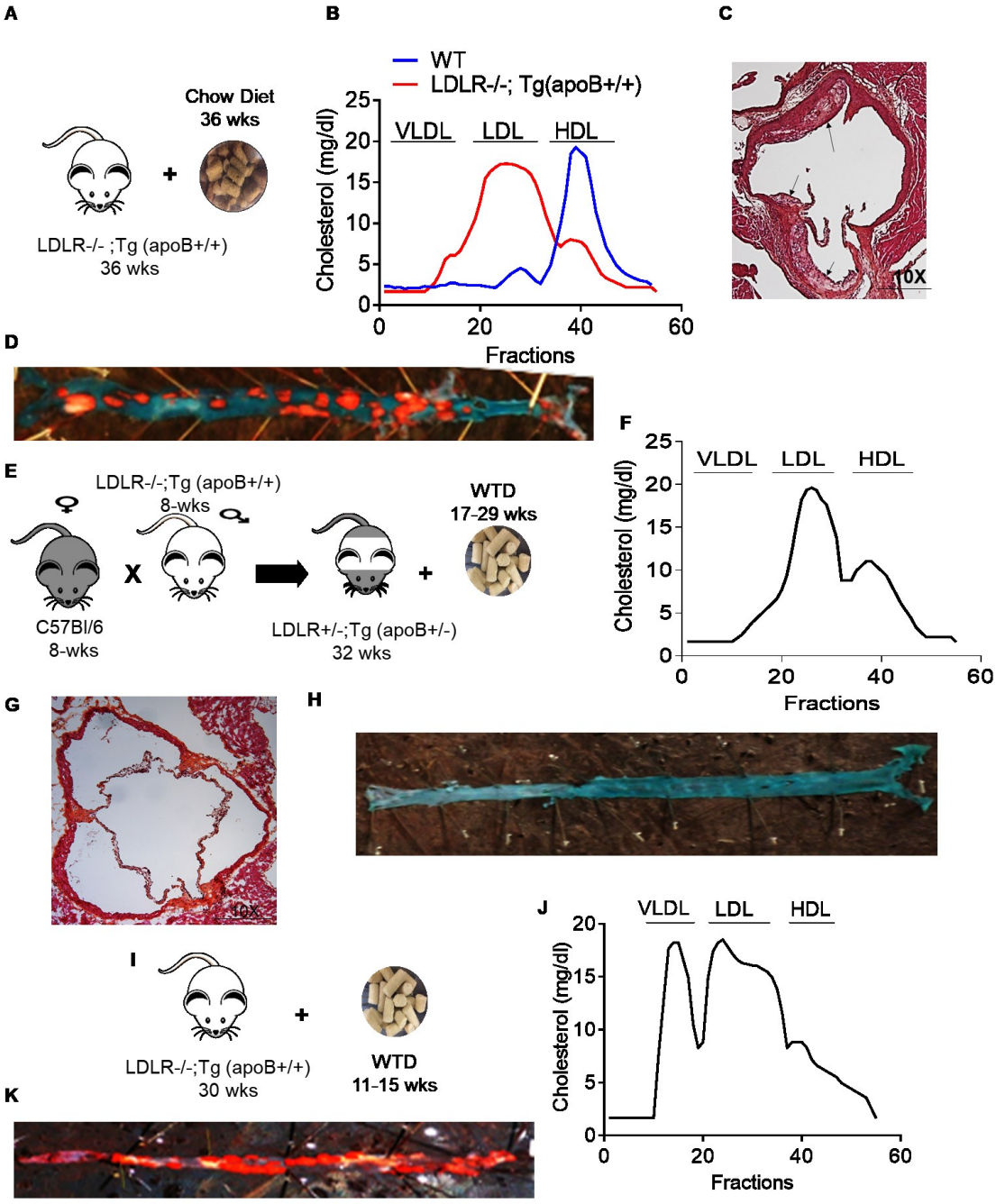

Figure 3.1 Generation of a potential mouse model of atherosclerosis and its comparison with known atherosclerosis mice model.

(A) Scheme depicting ATX [LDLR$^{-/-}$;Tg (apoB$^{+/+}$)] mice fed a chow diet for 36 weeks. (B) 36-weeks old ATX mice fed chow diet were sacrificed, and blood was

obtained. Total plasma cholesterol profiles were assayed by fast performance liquid chromatography (FPLC). (C) Representative images of an HPS-stained cross-section of the aortic root area. (D) Aorta pinned out and stained with Oil Red O, which stains neutral lipids (red). (E) ATX-HZ [LDLR+/-; Tg (apoB+/-)] mice were produced by breeding four 8-week old females (C57Bl/6) with four age-matched ATX male mice. ATX-HZ generated mice model were fed a western-type diet for a maximum of 29 weeks. (F) 32 weeks old ATX-HZ mice were sacrificed, and total plasma cholesterol profiles were assayed by FPLC from pooled plasma of 6 mice. (G) Different cross-sections of the aortic root were stained with HPS. (H) Aorta pinned out and stained with Oil-Red-O. (I) 30-weeks old ATX mice fed WTD for 11-15 weeks. (J) FPLC analyzes from pooled plasma of six 30-weeks old ATX mice. (K) Neutral lipids were stained in red with Oil-Red-O in the pinned out aorta.

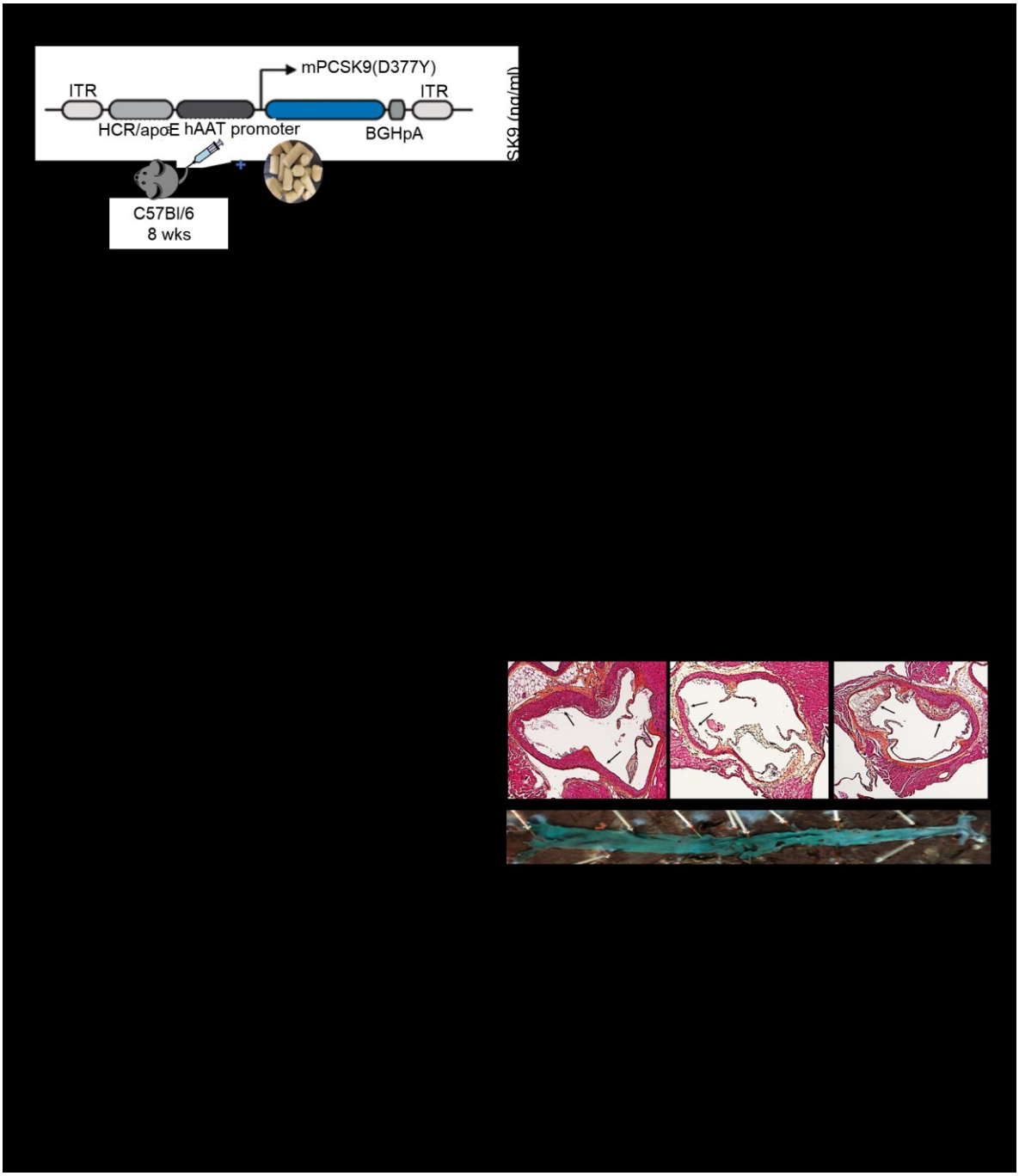

Figure 3.2 Plasma and plaque analysis in the aortic root of C57Bl/6 mice injected with AAV8-mPCSK9-DY and fed a Western-type diet.

(A) Structure of the adeno-associated virus (AAV) vector encoding the mouse PCSK9 gain-of-function (GOF) mutant D377Y under control of the liver-specific HRC/apoE-hAAT promoter. Scheme depicting the methodology used to generate

the atherosclerosis mice model. Overexpression of PCSK9^{D377Y} GOF mutant achieved through a single tail-vein injection of a recombinant AAV8. (B-D) Blood was obtained from 8-weeks old mice before and at equal intervals after injection. (B) Plasma levels of PCSK9 (C) LDL cholesterol and (D) total cholesterol. (E) Total plasma cholesterol profiles were assayed by FPLC in 21-weeks old mice (13-weeks post-virus injection). (F) Representative images of hematoxylin-phloxine-saffron (HPS)-stained cross-section of the aortic root area of mice fed WTD before (8 wks old mice), and 8- (16 wks old mice) and 13 wks (21 wks old mice) after AAV8-mPCSK9^{D377Y} injection. (G) Oil Red O staining of Neutral lipids in the pinned-out aorta of 21-weeks old mice. (H) Quantitative analysis of atherosclerotic lesion size in HPS-stained aortic sections at 8 and 13 weeks post AAV8-mPCSK9-DY injection. (*P < 0.05; **p < 0.01, ****P < 0.0001, ns=non-significant (Unpaired t-test). Data are presented as mean ± SD.

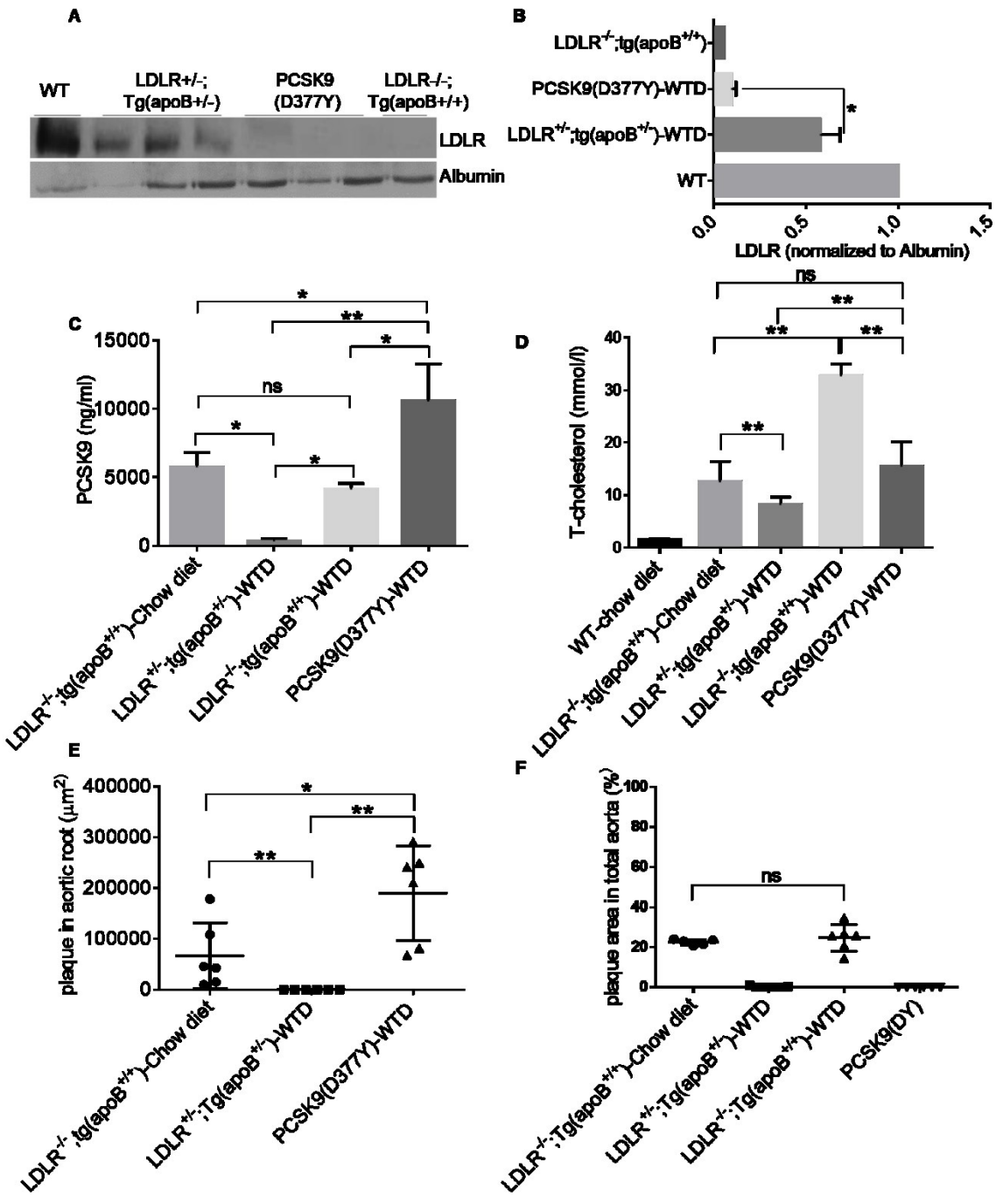

Figure 3.3 Plasma and plaque analysis of ATX, ATX-HZ, and AAV8-tetON-PCSK9D377Y mice models.

(A) Western blot analysis of LDLR in lysates of mouse liver. Albumin was used as a loading control. (B) Expression of LDLR relative to the loading control

(Albumin) was quantified using Image J software (NIH) and expressed as percent relative to controls. (C) Plasma levels of mPCSK9 protein were measured by ELISA. (D) Plasma total cholesterol and (E) Quantification of lesion area in different cross-sections of the aortic root (F) Plaque quantification (%) in the total aorta in different groups of mice (*P < 0.05; **p < 0.01, ns=non-significant (Mann-Whitney test). Data are presented as mean ± SD.

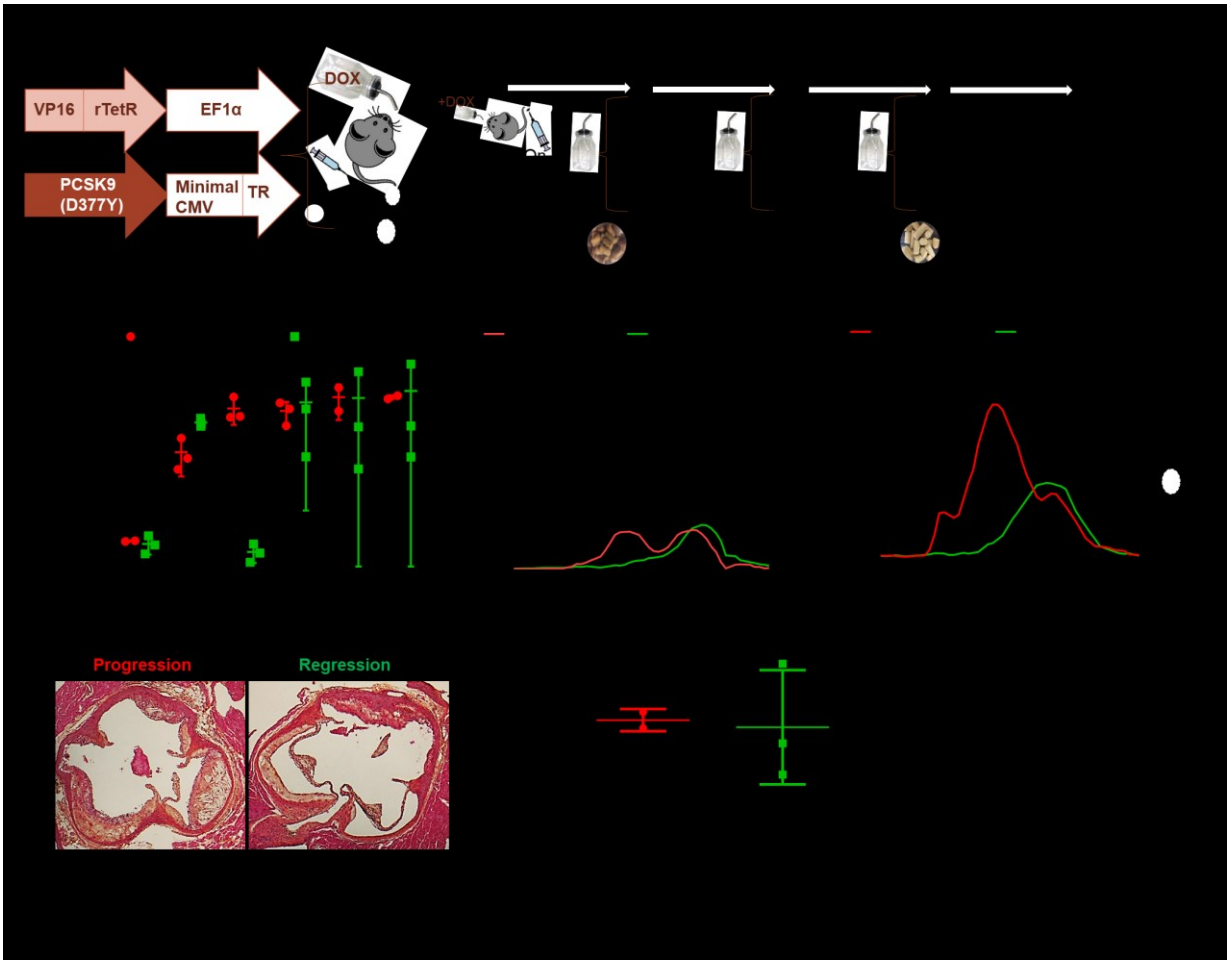

Figure 3.4 Regulation of PCSK9 gene expression using an inducible/reversible Tet system.

(A) Schematic representation of the mechanism of tetracycline (tet)-on controlled transcriptional regulation system and structure of the adeno-associated virus (AAV) vector encoding the mouse PCSK9^{D377Y} under control of CMV minimal promoter and tet-operator (tetO) sequence. The tetracycline repressor protein (TetR) binds to the tetO in the presence of DOX to induce transcription of PCSK9 under control of the tet promoter. In contrast, in the absence of Dox, rTetR cannot bind to the tetO; thus, the PCSK9^{D377Y} expression does not occur. (B) Scheme depicting the methodology used to evaluate the efficiency of the DOX-inducible system for regulating PCSK9 protein expression and atherosclerotic plaque formation by

overexpressing $PCSK9^{D377Y}$ in WTD-fed wild-type mice. (C) Plasma PCSK9 levels before injection of the virus in 8-weeks old mice and at 2, 4, 8, 12, and 17 weeks after injection. (D-E) FPLC analysis of plasma lipoprotein fractions from (D) 12-weeks old and (E) 25-weeks old mice. Collected plasma from three wild-type mice in each group was pooled, size-fractionated by gel filtration chromatography using a superose 6 column and total cholesterol profiles were determined enzymatically in FPLC fractions. HDL, high-density lipoprotein; LDL, low-density lipoprotein; VLDL, very low-density lipoprotein. (F) Images represent hematoxylin–phloxine–saffron (HPS)-stained and quantification analysis of atherosclerotic lesions in cross-sections of the aortic root in 25-weeks old mice (progression and regression groups) after 17-weeks of treatment. ***p=0.0003 (Multiple t-tests). Data are presented as mean ± SD.

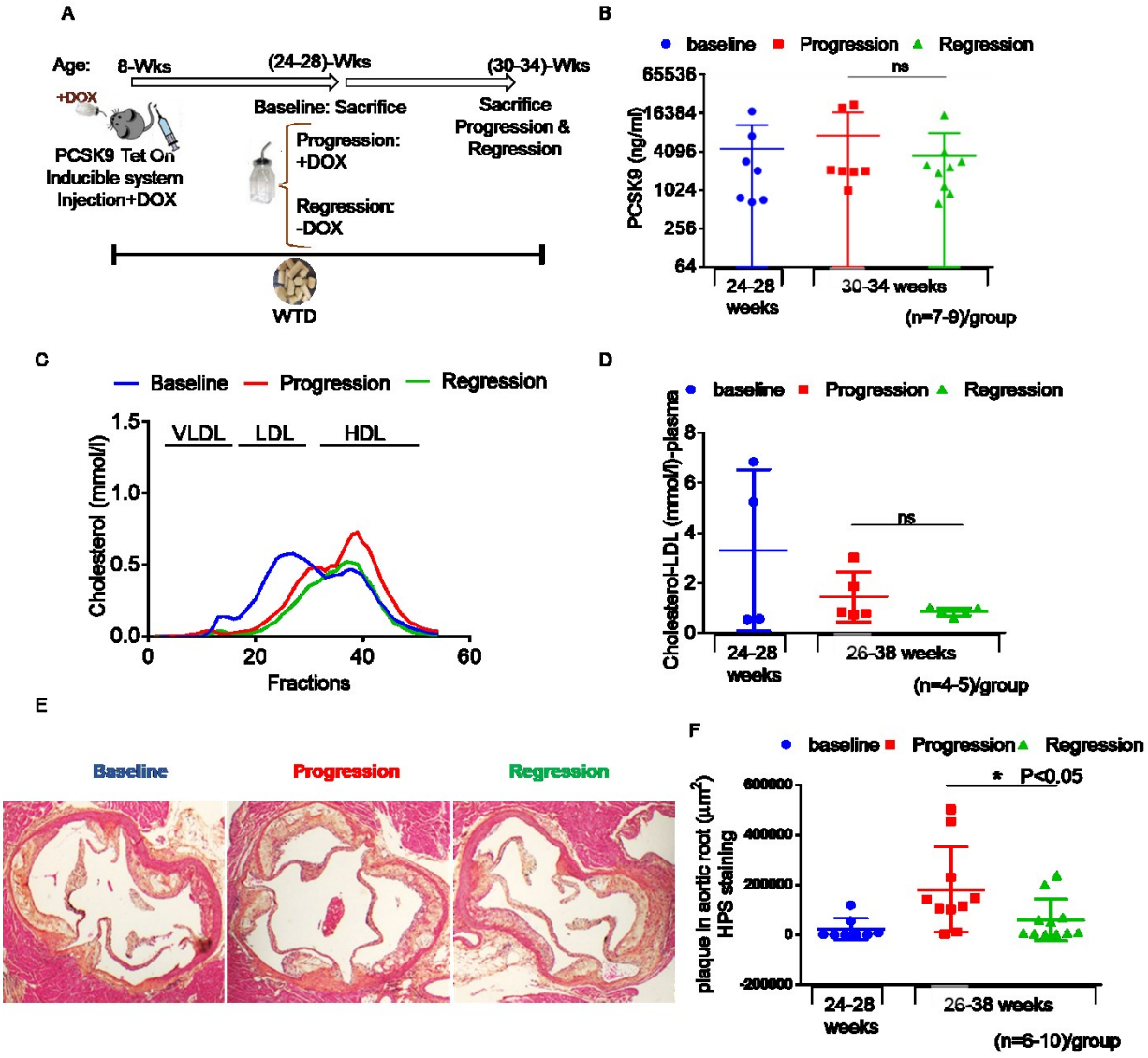

Figure 3.5 PCSK9 down-regulation rescues AAV-PCSK9D377Y mice from atherosclerosis disease.

(A) Study design. (B) Plasma PCSK9, (C) total plasma level of cholesterol and (D) plasma level of LDL were quantified at the day of sacrifice. Plasma from seven C57Bl/6 mice in each group was pooled, size-fractionated by gel filtration chromatography using a superose 6 column and total cholesterol profiles were determined in FPLC fractions enzymatically. HDL, high-density lipoprotein; LDL, low-

density lipoprotein; VLDL, very-low-density lipoprotein. (E) Representative images and (F) quantification analysis of hematoxylin–phloxine–saffron (HPS)-stained atherosclerotic lesions in cross-sections of the aortic root in C57Bl/6 mice. Mice in each group were treated as demonstrated in A. ns=non-significant (Unpaired t-test). Data are presented as mean ± SD.

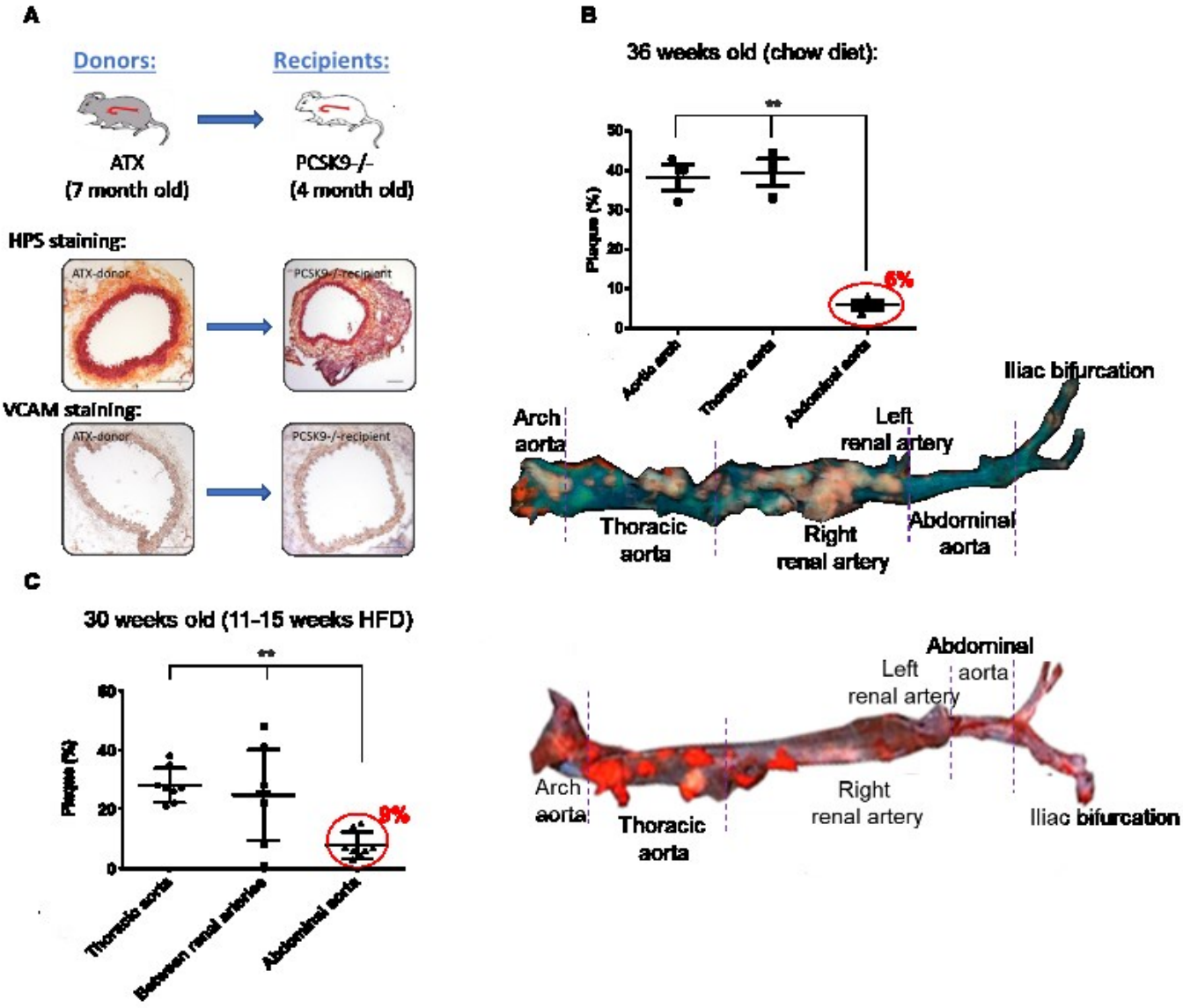

Supplementary Figure 3.1 Transplantation of atherosclerotic arch aorta.

(A) Schematic setup of the aorta transplantation model. A segment of the abdominal aorta (4 mm) from donor mice was interposition with the thoracic aorta in the recipient mice. Different cross-sections of the aortic root were stained with HPS or VCAM. (B) Aorta of ATX [LDLR-/-; Tg (apoB+/+)] mice fed a chow diet for 36 weeks, Top: Quantitative analysis of the percentage of presented plaque in different parts of aorta, Bottom: Aorta was pinned out and stained with Oil Red O to have

neutral lipid staining (red). (C) Aorta of 30-weeks old ATX [LDLR-/-; Tg (apoB+/+)] mice fed WTD for 15-weeks, Left: Quantitative analysis of the percentage of presented plaque in different parts of aorta, Right: Aorta was pinned out and stained with Oil Red O to have neutral lipid staining (red).

3.7 References

Abifadel, M., M. Varret, J.-P. Rabès, D. Allard, K. Ouguerram, M. Devillers, C. Cruaud, S. Benjannet, L. Wickham, and D. Erlich. 2003. Mutations in PCSK9 cause autosomal dominant hypercholesterolemia. Nature genetics. 34:154-156.

Akache, B., D. Grimm, K. Pandey, S.R. Yant, H. Xu, and M.A. Kay. 2006. The 37/67-kilodalton laminin receptor is a receptor for adeno-associated virus serotypes 8, 2, 3, and 9. Journal of virology. 80:9831-9836.

Ason, B., J.W. van der Hoorn, J. Chan, E. Lee, E.J. Pieterman, K.K. Nguyen, M. Di, S. Shetterly, J. Tang, and W.-C. Yeh. 2014. PCSK9 inhibition fails to alter hepatic LDLR, circulating cholesterol, and atherosclerosis in the absence of apoE. Journal of lipid research. 55:2370-2379.

Blankenhorn, D.H., and H.N. Hodis. 1994. George Lyman Duff Memorial Lecture. Arterial imaging and atherosclerosis reversal. Arteriosclerosis, thrombosis, and vascular biology. 14:177-192.

Brown, M.S., and J.L. Goldstein. 1986. A receptor-mediated pathway for cholesterol homeostasis. Science. 232:34-47.

Cohen, J., A. Pertsemlidis, I.K. Kotowski, R. Graham, C.K. Garcia, and H.H. Hobbs. 2005. Low LDL cholesterol in individuals of African descent resulting from frequent nonsense mutations in PCSK9. Nature genetics. 37:161-165.

cNutt, M.C., T. Lagace and J. Horton. 2007. Catalytic activity is not required for secreted PCSK9 to reduce low density lipoprotein receptors in HepG2 cells. Journal of Biological Chemistry. 282:20799-20803.

Denis, M., J. Marcinkiewicz, A. Zaid, D. Gauthier, S. Poirier, C. Lazure, N.G. Seidah, and A. Prat. 2012. Gene inactivation of proprotein convertase subtilisin/kexin type 9 reduces atherosclerosis in miceclinical perspective. Circulation. 125:894-901.

Gao, G., L.H. Vandenberghe, and J.M. Wilson. 2005. New recombinant serotypes of AAV vectors. Current gene therapy. 5:285-297.

Grefhorst, A., M.C. McNutt, T.A. Lagace, and J.D. Horton. 2008. Plasma PCSK9 preferentially reduces liver LDL receptors in mice. Journal of lipid research. 49:1303-1311.

Gossen, M., and H. Bujard. 1995. Efficacy of tetracycline-controlled gene expression is influenced by cell type: commentary. Biotechniques. 19:213-216; discussion 216-217.

Grimm, D., and J.A. Kleinschmidt. 1999. Progress in adeno-associated virus type 2 vector production: promises and prospects for clinical use. Human gene therapy. 10:2445-2450.

Ho, K.J., C.E. Bass, A.H. Kroemer, C. Ma, E. Terwilliger, and S.J. Karp. 2008. Optimized adeno-associated virus 8 produces hepatocyte-specific Cre-

mediated recombination without toxicity or affecting liver regeneration. American Journal of Physiology-Gastrointestinal and Liver Physiology. 295:G412-G419.

Horton, J.D., H. Shimano, R.L. Hamilton, M.S. Brown, and J.L. Goldstein. 1999. Disruption of LDL receptor gene in transgenic SREBP-1a mice unmasks hyperlipidemia resulting from production of lipid-rich VLDL. The Journal of clinical investigation. 103:1067-1076.

Ishibashi, S., J. Herz, N. Maeda, J.L. Goldstein, and M.S. Brown. 1994. The two-receptor model of lipoprotein clearance: tests of the hypothesis in" knockout" mice lacking the low density lipoprotein receptor, apolipoprotein E, or both proteins. Proceedings of the National Academy of Sciences. 91:4431-4435.

Kühnast, S., J.W. van der Hoorn, E.J. Pieterman, A.M. van den Hoek, W.J. Sasiela, V. Gusarova, A. Peyman, H.-L. Schäfer, U. Schwahn, and J.W. Jukema. 2014. Alirocumab inhibits atherosclerosis, improves the plaque morphology, and enhances the effects of a statin. Journal of lipid research. 55:2103-2112.

Kysenius, K., P. Muggalla, K. Mätlik, U. Arumäe, and H.J. Huttunen. 2012. PCSK9 regulates neuronal apoptosis by adjusting apoER2 levels and signaling. Cellular and molecular life sciences. 69:1903-1916.

Mathers, C.D., and D. Loncar. 2006. Projections of global mortality and burden of disease from 2002 to 2030. PLoS medicine. 3:e442.

Nakai, H., X. Wu, S. Fuess, T.A. Storm, D. Munroe, E. Montini, S.M. Burgess, M. Grompe, and M.A. Kay. 2005. Large-scale molecular characterization of adeno-associated virus vector integration in mouse liver. Journal of virology. 79:3606-3614.

No, D., T.-P. Yao, and R.M. Evans. 1996. Ecdysone-inducible gene expression in mammalian cells and transgenic mice. Proceedings of the National Academy of Sciences. 93:3346-3351.

Piedrahita, J.A., S.H. Zhang, J.R. Hagaman, P.M. Oliver, and N. Maeda. 1992. Generation of mice carrying a mutant apolipoprotein E gene inactivated by gene targeting in embryonic stem cells. Proceedings of the National Academy of Sciences. 89:4471-4475.

Rashid, S., D.E. Curtis, R. Garuti, N.N. Anderson, Y. Bashmakov, Y. Ho, R.E. Hammer, Y.-A. Moon, and J.D. Horton. 2005. Decreased plasma cholesterol and hypersensitivity to statins in mice lacking Pcsk9. Proceedings of the National Academy of Sciences of the United States of America. 102:5374-5379.

Ratko, T.A., J.P. Cummings, J. Blebea, and K.A. Matuszewski. 2003. Clinical gene therapy for nonmalignant disease. The American journal of medicine. 115:560-569.

Rendahl, K.G., D. Quiroz, M. Ladner, M. Coyne, J. Seltzer, W.C. Manning, and J.A. Escobedo. 2002. Tightly regulated long-term erythropoietin expression in vivo

using tet-inducible recombinant adeno-associated viral vectors. Human gene therapy. 13:335-342.

Rivera, V.M., T. Clackson, S. Natesan, R. Pollock, J.F. Amara, T. Keenan, S.R. Magari, T. Phillips, N.L. Courage, and F. Cerasoli Jr. 1996. A humanized system for pharmacologic control of gene expression. Nature medicine. 2:1028.

Rivera, V.M., X. Wang, S. Wardwell, N.L. Courage, A. Volchuk, T. Keenan, D.A. Holt, M. Gilman, L. Orci, and F. Cerasoli. 2000. Regulation of protein secretion through controlled aggregation in the endoplasmic reticulum. Science. 287:826-830.

Sanan, D., D. Newland, R. Tao, S. Marcovina, J. Wang, V. Mooser, R. Hammer, and H. Hobbs. 1998. Low density lipoprotein receptor-negative mice expressing human apolipoprotein B-100 develop complex atherosclerotic lesions on a chow diet: no accentuation by apolipoprotein (a). Proceedings of the National Academy of Sciences. 95:4544-4549.

Soria, L.F., E.H. Ludwig, H. Clarke, G.L. Vega, S.M. Grundy, and B.J. McCarthy. 1989. Association between a specific apolipoprotein B mutation and familial defective apolipoprotein B-100. Proceedings of the National Academy of Sciences. 86:587-591.

Stein, Y., and O. Stein. 2001. Does therapeutic intervention achieve slowing of progression or bona fide regression of atherosclerotic lesions? Arteriosclerosis, thrombosis, and vascular biology. 21:183-188.

Tata, P.R., A. Pardo-Saganta, M. Prabhu, V. Vinarsky., Law, B.M., Fontaine, B.A., Tager, A.M. and J. Rajagopal. 2013. Airway-specific inducible transgene expression using aerosolized doxycycline. American journal of respiratory cell and molecular biology, 49:1048-1056

Timms, K.M., S. Wagner, M.E. Samuels, K. Forbey, H. Goldfine, S. Jammulapati, M.H. Skolnick, P.N. Hopkins, S.C. Hunt, and D.M. Shattuck. 2004. A mutation in PCSK9 causing autosomal-dominant hypercholesterolemia in a Utah pedigree. Human genetics. 114:349-353.

Wang, Y., B.W. O'Malley, and S.Y. Tsai. 1994. A regulatory system for use in gene transfer. Proceedings of the National Academy of Sciences. 91:8180-8184.

Weber, C., and H. Noels. 2011. Atherosclerosis: current pathogenesis and therapeutic options. Nature medicine. 17:1410.

Westerterp, M., C.C. van der Hoogt, W. de Haan, E.H. Offerman, G.M. Dallinga-Thie, J.W. Jukema, L.M. Havekes, and P.C. Rensen. 2006. Cholesteryl ester transfer protein decreases high-density lipoprotein and severely aggravates atherosclerosis in APOE* 3-Leiden mice. Arteriosclerosis, thrombosis, and vascular biology. 26:2552-2559.

Wilson, P.W., R.B. D'Agostino, D. Levy, A.M. Belanger, H. Silbershatz, and W.B. Kannel. 1998. Prediction of coronary heart disease using risk factor categories. Circulation. 97:1837-1847.

Zolotukhin, S., B. Byrne, E. Mason, I. Zolotukhin, M. Potter, K. Chesnut, C. Summerford, R. Samulski, and N. Muzyczka. 1999. Recombinant adeno-associated virus purification using novel methods improves infectious titer and yield. Gene therapy. 6.

CHAPTER 4

4 Closing Remarks

4.1 General Discussion

While the pathways of LDLR endocytosis, recycling, and trafficking have been well documented (Goldstein and Brown, 2009), the mechanism of PCSK9-induced LDLR degradation is increasingly revised (Hess et al., 2018). PCSK9 undergoes an autocatalytic cleavage and exits the ER to reach the Golgi for further modulation and secretion. PCSK9 induces LDLR degradation by two separated pathways. It can bind with LDLR in an intracellular pathway and directs the complex to the lysosome for degradation (Poirier et al., 2009). Alternatively, secreted PCSK9 binds to the EGF-A domain of LDLR at the cell surface, and the complex is internalized into the endosome (Lagace et al., 2006; Zhang et al., 2007). Despite the presence of PCSK9 and LDLR together within the secretory pathway and the function of PCSK9 on LDLR degradation, LDL clearance by LDLR remains operational. This suggests the presence of some endogenous inhibitors, which could specifically interact with PCSK9 and prevent complete LDLR degradation.

Our team has previously identified Annexin A2 (Mayer et al., 2008; Seidah et al.,2012), and GRP94 (Poirier et al., 2015) as new endogenous PCSK9-binding proteins that regulate LDLR degradation and LDL levels. Here, we explored PCSK9-interacting proteins and characterized another endogenous modulator of PCSK9 function (Chapter 2). These proteins may be used as therapeutic targets to inhibit PCSK9 functions and, hence, reducing LDL and the risk of CVD. In addition, we attempted to identify an accessible and practical approach to study the effect of PCSK9 on atherosclerosis (Chapter 3). Apart from the advanced progress in understanding the therapeutic efficacy of PCSK9-monoclonal antibodies, there is

very little known about the effect of PCSK9 inhibition on atherosclerosis disease. This is mainly due to the limited availability and high cost of monoclonal antibodies, and the scarcity of a suitable atherosclerosis murine model for studying the effect of PCSK9 inhibition.

The methodological approach used combined mass spectrometry, co-immunoprecipitation, western blotting, real-time PCR, confocal and electron microscopy in relevant cells and mouse model to find and characterize the functions of a new PCSK9-binding protein (Chapter 2) followed by development of a murine model of atherosclerosis (Chapter 3) to assess the association between PCSK9 reduction and atherosclerotic plaque lesions.

In our first study, we demonstrated that GLG1 is a new PCSK9-interacting protein, which also binds with LDLR and apoB. Our results showed that deficiency of GLG1 in either hepatocytes or mouse liver reduces the intracellular protein level of PCSK9, LDLR, and apoB as well as the circulatory level of PCSK9 and apoB-containing particles. The absence of PCSK9 was shown to reduce apoB, atherogenic LDLs, atherosclerosis, independent of LDLR in an LDLR $^{-/-}$/apoBec$^{-/-}$/PCSK9$^{-/-}$ mouse model (Sun et al., 2017). Haploinsufficiency of GLG1 was previously shown to be associated with reduced atherosclerotic plaque macrophage (Luo et al., 2012), but its mechanisms were not understood.

We studied the mechanism of action of GLG1 on cholesterol regulation, apoB secretion, and degradation pathways. Plasma level of cholesterol is mainly dependent on the availability of apoB, TG, and MTP (Polonovski and Beucler, 1983). Active synthesis and more importantly, the availability of neutral-lipids (TG and CE), are key factors regulating the amount of nascent apoB that are secreted or

degraded. In the presence of free fatty acids, apoB availability and apoB lipidation are increased due to enhanced apoB stability during co- and posttranslational process. MTP is a key factor in hepatic VLDL assembly by transferring TGs into the apoB (Aggerbeck et al., 1992). In the absence of neutral-lipids or when MTP activity is reduced, apoB fails to be translocated into the lumen of the ER. Consequently, apoB becomes ubiquitinated and targeted for degradation pathways (Dixon et al., 1991; Dixo and Ginsberg, 1993). ApoB degradation is accomplished by both proteasomal and nonproteasomal (autophagy/lysosomal) pathways (Olofsson and Boren, 2012). Both pathways occur around lipid droplets (LDs) which provide a surface for convergence of the two degradation systems (Ohsaki et al., 2006). Our *in vivo* analysis showed that knockdown of Glg1 results in lower MTP activity in mouse liver, a significant reduction in plasma TGs level and reduced apoB levels in VLDL fractions of mouse plasma. Thus, a reduction in apoB levels of VLDL lipoproteins in plasma of *Glg1* deficient mice is most likely due to lower MTP activity and apoB secretion from the liver (Raabe et al., 1999), or higher apoB degradation (Boström et al., 1986; Davis et al., 1990).

The LDLR and PCSK9 are coordinately regulated by intracellular cholesterol level via SREBP2 (Edwards et al., 2000; Maxwell et al., 2003). Intracellular cholesterol level is controlled by three major sources: cholesterol synthesis, uptake, and degradation pathways that are all involved in SREBP2 regulation. Knockdown of GLG1 in our study induced accumulation of TG and lipid droplets in mouse liver, an effect that may require activation of SREBP-1c and/or SREBP2. It has been reported that SREBP2 also activates autophagy genes during cellular cholesterol depletion (Seo et al., 2011). In addition, SREBP-2 regulates transcription of HMGCR,

which is an important gene in cholesterol homeostasis (Horton et al. 1998). Upon Glg1 knockdown in our study, mRNA level of LDLR was reduced, but no change was observed in PCSK9, HMGCR (Supp. Figure 2.1C) and autophagy genes expression (Supp. Figure 2.3E). Considering this, other non-sterol mediators such as growth hormone, hepatocyte growth factor, or cytokines that have been shown to regulate LDLR transcription could play a role in GLG function.

Treating cells with brefeldin A, an inhibitor of trafficking vesicles from the ER to the Golgi apparatus, helped us to understand that reduction in the protein level of apoB in Glg1-knockdown hepatocytes occurs in ER and pre-Golgi compartment. Poorly lipidated apoB that cannot exit from the ER needs to be removed from the secretory pathway by apoB-proteasomal or autophagosomal degradation. Our confocal microscopy analysis demonstrated that knockdown of Glg1 in Huh7 cells led to impairment of apoB proteasomal degradation, which in turn directed apoB towards autophagosome/aggresome compartments. An autophagy inhibitor (3-MA) restored apoB expression, which was reduced by Glg1 knockdown in hepatocytes. These findings suggest that reduced apoB level following GLG1 deficiency is autophagy-dependent. Thus, inhibiting GLG1-apoB interaction may decrease the production of atherogenic apoB-containing lipoproteins and prevent the development of atherosclerosis.

We suggested a possibility of developing a small molecule/peptide to inhibit the GLG1-apoB interaction as a drug to reduce plasma cholesterol level. However, it is first essential to identify the binding site and the mechanism by which GLG1 interacts with apoB in order to develop an inhibitor for GLG1-apoB interaction. More studies using this potential inhibitor under different conditions will help to

understand how GLG1-apoB inhibition functions *in vivo* and evaluate its potential side effects. There are several limitations in the direct administration of small molecules such as rapid elimination of drugs, low bioavailability, nonspecific cytotoxicity, and adverse side effects. Given the ubiquitous expression profile of GLG1, there is a need to develop a suitable targeted drug delivery system to distribute the therapeutically active drug molecule only in the liver, site of lipoprotein formation, without affecting other tissue or organs. Systems with carrier-based delivery, such as metal nanoparticles (NPs), liposomes, ceramic materials, and polymeric micelles help to enhance the targeting of the drug and reduce its side effects compared with free drugs.

Aside from the regulatory role of GLG1 on intracellular trafficking of PCSK9 and lipid metabolism, the importance of GLG1 and PCSK9 activity in metabolic disorders such as diabetes remains to be discussed. It has been shown that GLG1 interacts with APN, an adipocyte-derived hormone with anti-diabetic properties (Yamamoto et al., 2016). A decreased level of APN in serum is considered as a risk factor for the progression of type 2 diabetes (Daimon et al. 2003). GLG1-APN interaction has also been shown to block GLG1-E-selectin binding and induced anti-atherogenic response such as inflammation. PCSK9 and GLG1 may also play a role in the development of the central nervous system. It has been reported that PCSK9 interacts with the β-site amyloid precursor protein-cleaving enzyme 1 (Jonas et al. 2008) and by inducing its degradation is involved in reducing the risk of Alzheimer disease (Ko and Puglieli 2019). Therefore, in the early stages of GLG1-PCSK9 based drug development for hypercholesterolemia, it is essential to perform more investigations to understand GLG1 functions beyond lipid metabolism.

Modulating GLG1 function as a way to reduce cholesterol level may have potential benefits in other disorders. For example, binding of GLG1 to E-selectin on the surface of hepatic stellate cells is important in regulating the functional activity of these cells. Hepatic stellate cells are involved in the repair of injured hepatic tissue, liver regeneration, and angiogenesis of hepatic metastasis (Antoine et al., 2009). It was shown that causes of inflammatory liver disease and liver metastasis in hypoxic conditions might be due to the increased cleaved and secretory form of GLG1, which results in less cell surface GLG1-binding activity (Antoine et al., 2009). Furthermore, the role of GLG1 in prostate cancer metastasis and reducing cancer aggressiveness has been reported (Yasmin-Karin et al. 2010).

Lack of an ideal animal model of atherosclerosis, suitable for studying PCSK9 function, is one of the main limitations that researchers in this field have faced. In our second study, we measured atherosclerotic lesions and circulating cholesterol level in the ATX [*Ldlr*$^{-/-}$;Tg (apoB$^{+/+}$)] mice fed either a chow diet or a Western-type diet (WTD) and compared them with our developed ATX-HZ [*Ldlr*$^{-/+}$; Tg (apoB$^{+/+}$)] mice fed a WTD, and C57BL/6 mice overexpressing gain-of-function mutant PCSK9^{D377Y} (AAV8-tetON-PCSK9^{D377Y}) fed a WTD. Our results demonstrated that 12-weeks overexpression of PCSK9^{D377Y} in C57BL/6 mice fed WTD led to the development of large atherosclerotic lesions, while ATX-HZ mice developed no plaque in their aortic root after 29-weeks exposure to WTD. This indicates the potency of one allele of LDLR in protecting mice against atherosclerosis. Thus, we aimed to study the effect of PCSK9 gene silencing on atherosclerosis using C57BL/6 mice overexpressing PCSK9^{D377Y}. Our results demonstrated that the long-term gene

expression ability of the DOX-inducible system in AAV8-tetON-PCSK9^{D377Y} mice induced and sustained atherosclerosis lesions in aortic roots, which were then significantly reduced by blocking PCSK9^{D377Y} overexpression in C57BL/6 mice. Our results suggest that the C57BL/6 mice that overexpress PCSK9^{D377Y} in an inducible manner are a useful mouse model for understanding the molecular role of PCSK9 on atherosclerotic plaques development.

4.2 General Conclusion

Although the progress made in understanding the PCSK9 role in lipoprotein regulation and development of atherosclerosis, prevention of atherosclerosis by modulating PCSK9 expression and function remains an unresolved topic. PCSK9 endogenous interacting proteins seem to be potential targets for inhibition of PCSK9-induced LDLR degradation, reducing plasma cholesterol level and formation of atherosclerotic plaques. Here, we showed for the first time that Golgi apparatus protein 1 (GLG1), a protein encoded by the GLG1 gene, interacts with PCSK9, apoB, and LDLR, and hence regulate cholesterol homeostasis. Most importantly, we demonstrated that GLG1 deficiency reduces apoB lipidation and TG secretion through an autophagy-dependent pathway. Thus, preventing the interaction of GLG1 with apoB might pave the way towards the development of a new treatment of hypercholesterolemia and atherosclerosis.

Animal models have been extensively used to study atherosclerosis disease in human. ApoE knockout and LDLR-deficient models are two major mice models, exhibit significant hypercholesterolemia, that are served as valuable tools to understand atherosclerosis development. However, these two genes are required

for studying the molecular mechanisms underlying PCSK9 function. Here, we developed an AAV8-tetON-PCSK9^{D377Y} mice model which we found to be well-suited to study the effect of PCSK9 gene modulation on atherosclerosis. An advantage of using this mice model is the development of atherosclerotic plaques in the presence of both LDLR and apoE genes. Moreover, using an inducible expression system facilitates studying the effect of plasma PCSK9 level on atherosclerosis lesions. Our mice model will advance our understanding of atherosclerotic plaque development and help to validate treatment options using PCSK9-related therapies.

Taken together, this thesis provides novel insights into the PCSK9 regulation and identifies a new PCSK9 interacting protein, GLG1, that reduces apoB-100 secretion and modulates lipid metabolism. We provide a new foundation upon which future studies on cholesterol hemostasis may be undertaken, to translate this knowledge into new therapeutic approaches for the atherosclerosis disease.

4.3 Future Perspectives

Based on our findings, many questions and ideas have been proposed:

- We observed the accumulation of poorly lipidated-apoB in mouse plasma 2-weeks post Glg1-knockdown, whereas deficiency of GLG1 in Huh7 cells reduced apoB secretion in media. The reason for this discrepancy in our results is not well understood. However, because of apoB accumulation in plasma of mice with double Ldlr and Mtp deficiency in the liver (Ldlr$^{-/-}$ Mtp$^{\Delta/\Delta}$) (Larsson et al., 2004), we hypothesized that accumulation of apoB in plasma of Glg1-knockdown mice might be due to the long-term low expression of LDLR at the surface of hepatocytes and reduced level of MTP activity.

Larsson et al. (2004) suggested that normal level of MTP is required for mediating the second step of VLDL assembly, while low levels of MTP is sufficient for apoB100 synthesis and the initial step of VLDL assembly. Degradation of dense apoB100-containing lipoproteins that escape co-translational degradation is mainly via intracellular hepatic LDLR. Thus, the presence of an insufficient level of LDLR and MTP may lead to the accumulation of apoB in mouse plasma.

According to our results, presenting a low level of LDLR at the cell surface after two weeks of Glg1-knockdown might be due to the defective LDLR-transport to the cell surface, while lysosomal degradation of cell-surface LDLR is still ongoing. Thus, during a short-term deficiency of GLG1, we hypothesize that some LDLR would still be present at the cell surface for the clearance of plasma apoB. To evaluate our hypothesis, measuring the protein level of apoB in mouse plasma 2 to 7 days after Glg1-knockdown could be tested. This experiment will help to clarify the reason for increased level of apoB in mouse plasma post Glg1-knockdown.

- We detected an intracellular binding between endogenous GLG1 and apoB in mouse liver and cultured hepatocytes. Moreover, we found that GLG1 downregulation results in reduced plasma level of cholesterol. However, the sequences of GLG1 and apoB proteins that are required for their interaction are not identified yet. Also, it is not yet clear whether any interaction between GLG1 and apoB exist in the circulatory pathway. Clarifying the details of GLG1-apoB binding might help to synthesize a peptide, based on the

identified sequence of GLG1 that interacts with apoB, to block the GLG1-apoB binding and consequently reduce the secretion of apoB-containing lipoproteins. GLG1 contains a large extracellular (16 repeats of a Cfr motif), and a short intracellular (13 aa residues) domains (Zhou et al., 1997). Constructing the clones of GLG1 with mutations in different regions and the mammalian two-hybrid system can be used to determine the minimal length of GLG1 that is required for the interaction with apoB. Also, setting up the same type of experiments with apoB constructs would help to delineate the region(s) of apoB (lipid-binding domain, RNA editing region, and LDL receptor-binding domain) that is(are) required for the interaction with GLG1.

- In the GLG1 study, we focused on the effect of GLG1 on circulatory and degradation pathway of apoB. However, the effect of GLG1 on trafficking pathways of apoA1, PCSK9, and LDLR is not yet entirely studied. We proposed that GLG1 is required for their transit from the ER to the post-ER compartments. Systematic experiments to determine and validate the underlying pathways of the interrelationship between GLG1, PCSK9, apoA1, and LDLR will have to be performed. We need to investigate whether GLG1 interacts with either intracellular or circulating apoA1. Moreover, we need to delineate whether the interaction of GLG1 with apoB, PCSK9, and LDLR is through direct or indirect binding using co-IP and double knock-out experiments in hepatic cell lines or mouse liver.

- PCSK9, LDLR, and apoB are three major proteins for which genetic defect causes ADH, which is characterized by elevated plasma level of LDL.

Marques-Pinheiro et al. (2010) reported that the fourth gene that is involved in ADH is located at a 16q22.1 locus, which contains 154 genes. Regulatory role of GLG1, located at the16q22.1 locus, on PCSK9, LDLR and apoB suggests that it would be interesting to screen FH negative-LDLR/APOB/PCSK9 cohorts for GLG1 mutations.

- Herein, we observed that deficiency of GLG1 led to a sharp reduction in plasma level of HDL. This observation might be due to the lower level of MTP activity as it was reported previously in *Mtp*-knockout mice (Raabe et al., 1999). Furthermore, Dastani et al. (2010) reported that a region on chromosome 16 is likely to harbor a gene for the low circulatory level of HDL. Thus, we hypothesized that the sequencing of GLG1 in patients with low levels of HDL-C might help to confirm the role of GLG1 in cholesterol metabolism.

- We found an unexpected decrease in the endogenous protein level of LC3-II upon downregulation of Glg1 in either cells or mouse liver. The decrease in the protein level of LC3II was restored in the presence of a lysosomotropic reagent (NH_4Cl), which means LC3II was degraded through lysosome-autophagy pathways (Mizushima and Yoshimori, 2007). Electron microscopy analysis demonstrated the increased formation of autophagy vacuoles in the liver of the *Glg1* deficient mice. Also, flow cytometry analysis demonstrated an increase in the number of autophagy fluorescent marker in GLG1-deficient cells. Confocal microscopy analysis further confirmed that Glg1 knockdown in Huh7 cells led to the aggregation of autophagy marker (either endogenous

LC3B or overexpressed LC3-GFP). Thus, as it was suggested before (Mizushima et al., 2010), we used a combination of various independent experiments to evaluate the level of autophagic flux in the presence and absence of GLG1. However, to further confirm our results it would be interesting to determine the effect of Glg1-knockdown in autophagy-deficient mice (Rubinsztein et al., 2011) or use long-lived protein degradation approach (Dupont et al., 2017) to measure the effect of GLG1-deficiency on the autophagy pathway in cultured cells. The long-lived protein degradation approach is an effective assay for quantification of the autophagic flux of endogenous proteins in adherent cell lines (Luhr et al., 2018).

- In the present study, we found that GLG1-downregulation induces autophagy clearance of apoB. An earlier study by Luo et al. (2012) demonstrated that haploinsufficiency of GLG1 is associated with reduced atherosclerotic plaque macrophage content. However, the detailed process of this observation was not verified. Ouimet et al. (2011) reported that the autophagy process is involved in regulating the level of macrophages. Razani et al. (2012) indicated that oxidized-LDL could be cleared through autophagosome/lysosome pathway in human vascular endothelial cells. Thus, it would be interesting to investigate the association of GLG1 with autophagy clearance of plaque macrophage content and therapeutic effect of Glg1-knockdown on atherosclerosis development.

- We found that GLG1 is a new LDLR and PCSK9-interacting protein and the effect of GLG1 on atherosclerosis (Luo et al., 2012) might be through the

LDLR/PCSK9 mode of action, which needs to be elucidated. It is important to focus on delineating the physiological and biochemical mechanisms underlying the protective role of LDLR, PCSK9, and GLG1 inhibition/downregulation in the development of atherosclerosis. The AAV8-tetON-PCSK9^{D377Y} atherosclerosis mice model, developed in our second study, can be used to verify the LDLR/PCSK9-dependency of GLG1 effect on atherosclerosis and the related process by altering the PCSK9 expression using DOX system and GLG1 gene expression using CRISPR/Cas9 (Sander and Joung, 2014).

- It would be useful to determine the effect of GLG1 or PCSK9 knockdown on the morphology of plaques. Immunohistochemistry and quantification analyses of CD68-positive macrophages/foam-cells and chemokine receptors (CCR2, CCR7, and CX3CR1) can be used to determine atherosclerotic plaque inflammation, and Verhoeff-Van Gieson staining to analyze the elasticity of the fibers by detecting foam cells and smooth muscle cells (Daugherty and Whitman, 2003)

5 Reference

Abifadel, M., J.P. Rabès, M. Devillers, A. Munnich, D. Erlich, C. Junien, M. Varret, and C. Boileau. 2009. Mutations and polymorphisms in the proprotein convertase subtilisin kexin 9 (PCSK9) gene in cholesterol metabolism and disease. Human mutation. 30:520-529.

Abifadel, M., M. Varret, J.-P. Rabès, D. Allard, K. Ouguerram, M. Devillers, C. Cruaud, S. Benjannet, L. Wickham, and D. Erlich. 2003. Mutations in PCSK9 cause autosomal dominant hypercholesterolemia. Nature genetics. 34:154-156.

Abumrad, N.A., M.R. El-Maghrabi, E. Amri, E. Lopez, and P. Grimaldi. 1993. Cloning of a rat adipocyte membrane protein implicated in binding or transport of long-chain fatty acids that is induced during preadipocyte differentiation. Homology with human CD36. Journal of Biological Chemistry. 268:17665-17668.

Aggerbeck, L. P., Bouma, M. E., Eisenberg, C., Munck, A., Hermier, M., Schmitz, J., ... & Gregg, R. E. 1992. Absence of microsomal triglyceride transfer protein in individuals with abetalipoproteinemia. Science. 258(5084), 999-1001.

Ahn, J., M. Febbraio, and R.L. Silverstein. 2005. A novel isoform of human Golgi complex-localized glycoprotein-1 (also known as E-selectin ligand-1, MG-160, and cysteine-rich fibroblast growth factor receptor) targets differential subcellular localization. J Cell Sci. 118:1725-1731.

Akhtar, S., and I.F. Benter. 2007. Nonviral delivery of synthetic siRNAs in vivo. The Journal of clinical investigation. 117:3623-3632.

Ali, Z., N. Alp, H. Lupton, N. Arnold, D. Greaves, Y. Hu, J. Gunn, and K. Channon. 2006. Increased in-stent stenosis, in apoE-Knockout mice: A novel mouse model of angioplasty and stenting.

Annes, J.P., J.S. Munger, and D.B. Rifkin. 2003. Making sense of latent TGFβ activation. Journal of cell science. 116:217-224.

Antoine, M., R. Köhl, C.G. Tag, A.M. Gressner, C. Hellerbrand, and P. Kiefer. 2009a. Secreted cysteine-rich FGF receptor derives from posttranslational processing by furin-like prohormone convertases. Biochemical and biophysical research communications. 382:359-364.

Antoine, M., C.G. Tag, A.M. Gressner, C. Hellerbrand, and P. Kiefer. 2009b. Expression of E-selectin ligand-1 (CFR/ESL-1) on hepatic stellate cells: implications for leukocyte extravasation and liver metastasis. Oncology reports. 21:357-362.

Ason, B., JW. van der Hoorn, J. Chan, E. Lee, EJ. Pieterman, KK. Nguyen, M. Di, S. Shetterly, J. Tang, WC. Yeh, M. Schwarz. 2014. PCSK9 inhibition fails to alter

hepatic LDLR, circulating cholesterol, and atherosclerosis in the absence of apoE. Journal of lipid research.1;55(11):2370-9.

Awan, Z., K. Alrasadi, G. Francis, R. Hegele, R. McPherson, J. Frohlich, D. Valenti, B. De Varennes, M. Marcil, and C. Gagne. 2008. Vascular calcifications in homozygote familial hypercholesterolemia. Arteriosclerosis, thrombosis, and vascular biology. 28:777-785.

Baker, B.F., S.S. Lot, T.P. Condon, S. Cheng-Flournoy, E.A. Lesnik, H.M. Sasmor, and C.F. Bennett. 1997. 2′-O-(2-Methoxy) ethyl-modified anti-intercellular adhesion molecule 1 (ICAM-1) oligonucleotides selectively increase the ICAM-1 mRNA level and inhibit formation of the ICAM-1 translation initiation complex in human umbilical vein endothelial cells. Journal of Biological Chemistry. 272:11994-12000.

Bakillah, A., N. Nayak, U. Saxena, R.M. Medford, and M.M. Hussain. 2000. Decreased Secretion of apoB Follows Inhibition of apoB− MTP Binding by a Novel Antagonist. Biochemistry. 39:4892-4899.

Balabaud, C., P. Bioulac-Sage, and A. Desmoulière. 2004. The role of hepatic stellate cells in liver regeneration. Journal of hepatology. 40:1023-1026.

Barquera, S., A. Pedroza-Tobías, C. Medina, L. Hernández-Barrera, K. Bibbins-Domingo, R. Lozano, and A.E. Moran. 2015. Global overview of the epidemiology of atherosclerotic cardiovascular disease. Archives of medical research. 46:328-338.

Bauriedel, G., R. Hutter, U. Welsch, R. Bach, H. Sievert, & B. Lüderitz, B. 1999. Role of smooth muscle cell death in advanced coronary primary lesions: implications for plaque instability. Cardiovascular research. 41(2), 480-488.

Bachmann A, M. Moll, E. Gottwald, C. Nies, R. Zantl, H. Wagner, B. Burkhardt, J. Sánchez, R. Ladurner, W. Thasler, G. Damm. 2015. 3D cultivation techniques for primary human hepatocytes. Microarrays. 4:64-83.

Bengoechea-Alonso, M. T., & J. Ericsson. 2009. A phosphorylation cascade controls the degradation of active SREBP1. Journal of Biological Chemistry. 284(9), 5885-5895.

Benjannet, S., D. Rhainds, R. Essalmani, J. Mayne, L. Wickham, W. Jin, M.-C. Asselin, J. Hamelin, M. Varret, and D. Allard. 2004. NARC-1/PCSK9 and its natural mutants zymogen cleavage and effects on the low density lipoprotein (LDL) receptor and LDL cholesterol. Journal of Biological Chemistry. 279:48865-48875.

Benjannet, S., D. Rhainds, J. Hamelin, N. Nassoury, and N.G. Seidah. 2006. The proprotein convertase (PC) PCSK9 is inactivated by furin and/or PC5/6A functional consequences of natural mutations and post-translational modifications. Journal of Biological Chemistry. 281:30561-30572.

Benoist, F., and T. Grand-Perret. 1997. Co-translational Degradation of apolipoprotein B100 by the Proteasome Is Prevented by Microsomal Triglyceride Transfer Protein SYNCHRONIZED TRANSLATION STUDIES

ON HepG2 CELLS TREATED WITH AN INHIBITOR OF MICROSOMAL TRIGLYCERIDE TRANSFER PROTEIN. Journal of Biological Chemistry. 272:20435-20442.

Bevilacqua, M.P., and R.M. Nelson. 1993. Selectins. The Journal of clinical investigation. 91:379-387.

Bjoerklund, M.M., A.K. Hollensen, M.K. Hagensen, F. Dagnaes-Hansen, C. Christoffersen, J.G. Mikkelsen, and J.F. Bentzon. 2014. Induction of atherosclerosis in mice and hamsters without germline genetic engineering. Circulation research:CIRCRESAHA. 113.302937.

Björkerud, B., S. Björkerud. 1996. Contrary effects of lightly and strongly oxidized LDL with potent promotion of growth versus apoptosis on arterial smooth muscle cells, macrophages, and fibroblasts. Arteriosclerosis, thrombosis, and vascular biology. 16(3):416-24.

Blasiole, D.A., A.T. Oler, and A.D. Attie. 2008. Regulation of apoB secretion by the low density lipoprotein receptor requires exit from the endoplasmic reticulum and interaction with apoE or apoB. Journal of Biological Chemistry. 283:11374-11381.

Bonthu, S., D.D. Heistad, D.A. Chappell, K.G. Lamping, and F.M. Faraci. 1997. Atherosclerosis, vascular remodeling, and impairment of endothelium-dependent relaxation in genetically altered hyperlipidemic mice. Arteriosclerosis, Thrombosis, and Vascular Biology. 17:2333-2340.

Boström, K., M. Wettesten, J. Boren, G. Bondjers, O. Wiklund, SO. Olofsson. 1986. Pulse-chase studies of the synthesis and intracellular transport of apolipoprotein B-100 in Hep G2 cells. Journal of Biological Chemistry. 261(29):13800-6.

Bottomley, M.J., A. Cirillo, L. Orsatti, L. Ruggeri, T.S. Fisher, J.C. Santoro, R.T. Cummings, R.M. Cubbon, P.L. Surdo, and A. Calzetta. 2009. Structural and biochemical characterization of the wild type PCSK9-EGF (AB) complex and natural familial hypercholesterolemia mutants. Journal of Biological Chemistry. 284:1313-1323.

Braun, M., P. Pietsch, S. Felix, and G. Baumann. 1995. Modulation of intercellular adhesion molecule-1 and vascular cell adhesion molecule-1 on human coronary smooth muscle cells by cytokines. Journal of molecular and cellular cardiology. 27:2571-2579.

Brown, M., and J. Goldstein. 1983. Lipoprotein receptors in the liver. Control signals for plasma cholesterol traffic. The Journal of clinical investigation. 72:743-747.

Brown MS, P. Kovanen, and J. Goldstein. 1981 Regulation of plasma cholesterol by lipoprotein receptors. Science. 212:628–635

Brown, M.S., and J.L. Goldstein. 1975. Regulation of the activity of the low density lipoprotein receptor in human fibroblasts. Cell. 6:307-316.

Brunham, L.R., J.K. Kruit, J. Iqbal, C. Fievet, J.M. Timmins, T.D. Pape, B.A. Coburn, N. Bissada, B. Staels, and A.K. Groen. 2006. Intestinal ABCA1 directly contributes to HDL biogenesis in vivo. The Journal of clinical investigation. 116:1052-1062.

Burnett, J.R., L.J. Wilcox, D.E. Telford, S.J. Kleinstiver, P.H.R. Barrett, R.S. Newton, and M.W. Huff. 1999. Inhibition of ACAT by avasimibe decreases both VLDL and LDL apolipoprotein B production in miniature pigs. Journal of lipid research. 40:1317-1327.

Burnett, J. R., Wilcox, L. J., Telford, D. E., Kleinstiver, S. J., Barrett, P. H. R., & Huff, M. W. 1998. Inhibition of cholesterol esterification by DuP 128 decreases hepatic apolipoprotein B secretion in vivo: effect of dietary fat and cholesterol. Biochimica et Biophysica Acta (BBA)-Lipids and Lipid Metabolism. 1393: 63-79.

Burrus, L.W., and B. Olwin. 1989. Isolation of a receptor for acidic and basic fibroblast growth factor from embryonic chick. Journal of Biological Chemistry. 264:18647-18653.

Burrus, L.W., M.E. Zuber, B.A. Lueddecke, and B.B. Olwin. 1992. Identification of a cysteine-rich receptor for fibroblast growth factors. Molecular and Cellular Biology. 12:5600-5609.

Butkinaree, C., M. Canuel, R. Essalmani, S. Poirier, S. Benjannet, M.-C. Asselin, A. Roubtsova, J. Hamelin, J. Marcinkiewicz, and A. Chamberland. 2015. Amyloid precursor-like protein 2 and sortilin do not regulate the PCSK9 convertase-mediated low density lipoprotein receptor degradation but interact with each other. Journal of Biological Chemistry. 290:18609-18620.

Caligiuri, G., B. Levy, J. Pernow, P. Thorén, and G.K. Hansson. 1999. Myocardial infarction mediated by endothelin receptor signaling in hypercholesterolemic mice. Proceedings of the National Academy of Sciences. 96:6920-6924.

Cameron, J., T. Ranheim, M.A. Kulseth, T.P. Leren, and K.E. Berge. 2008. Berberine decreases PCSK9 expression in HepG2 cells. Atherosclerosis. 201:266-273.

Cannon, C.P., M.A. Blazing, R.P. Giugliano, A. McCagg, J.A. White, P. Theroux, H. Darius, B.S. Lewis, T.O. Ophuis, and J.W. Jukema. 2015. Ezetimibe added to statin therapy after acute coronary syndromes. New England Journal of Medicine. 372:2387-2397.

Canuel, M., X. Sun, M.-C. Asselin, E. Paramithiotis, A. Prat, and N.G. Seidah. 2013. Proprotein convertase subtilisin/kexin type 9 (PCSK9) can mediate degradation of the low density lipoprotein receptor-related protein 1 (LRP-1). PloS one. 8:e64145.

Cenarro, A., A.L. García-Otín, M. Tejedor, M. Solanas, E. Jarauta, C. Junquera, E. Ros, P. Mozas, J. Puzo, and M. Pocovi. 2011. A presumptive new locus for autosomal dominant hypercholesterolemia mapping to 8q24. 22. Clinical genetics. 79:475-481.

Cerrone, M., M. Noorman, X. Lin, H. Chkourko, F.-X. Liang, R. Van Der Nagel, T. Hund, W. Birchmeier, P. Mohler, and T.A. Van Veen. 2012. Sodium current deficit and arrhythmogenesis in a murine model of plakophilin-2 haploinsufficiency. Cardiovascular research. 95:460-468.

Cesarman, G.M., C.A. Guevara, and K.A. Hajjar. 1994. An endothelial cell receptor for plasminogen/tissue plasminogen activator (t-PA). II. Annexin II-mediated enhancement of t-PA-dependent plasminogen activation. Journal of Biological Chemistry. 269:21198-21203.

Chan, JC., DE. Piper, Q. Cao, D. Liu, C. King, W. Wang, J. Tang, Q. Liu, J. Higbee, Z. Xia, Y. Di. 2009. A proprotein convertase subtilisin/kexin type 9 neutralizing antibody reduces serum cholesterol in mice and nonhuman primates. Proceedings of the National Academy of Sciences. 106(24):9820-5.

Chen, X.-W., H. Wang, K. Bajaj, P. Zhang, Z.-X. Meng, D. Ma, Y. Bai, H.-H. Liu, E. Adams, and A. Baines. 2013. SEC24A deficiency lowers plasma cholesterol through reduced PCSK9 secretion. Elife. 2.

Chen, Y.-C., A.L. Huang, T.S. Kyaw, A. Bobik, and K. Peter. 2016. Atherosclerotic plaque rupture: identifying the straw that breaks the camel's back. Arteriosclerosis, thrombosis, and vascular biology. 36:e63-e72.

Chen, Z.-Y., A. Ieraci, H. Teng, H. Dall, C.-X. Meng, D.G. Herrera, A. Nykjaer, B.L. Hempstead, and F.S. Lee. 2005. Sortilin controls intracellular sorting of brain-derived neurotrophic factor to the regulated secretory pathway. Journal of Neuroscience. 25:6156-6166.

Choudhury, RP., V. Fuster, ZA. Fayad. 2004. Molecular, cellular and functional imaging of atherothrombosis. Nature reviews Drug discovery. 3(11):913.

Cohen, J., A. Pertsemlidis, I.K. Kotowski, R. Graham, C.K. Garcia, and H.H. Hobbs. 2005. Low LDL cholesterol in individuals of African descent resulting from frequent nonsense mutations in PCSK9. Nature genetics. 37:161-165.

Cohen, J.C., E. Boerwinkle, T.H. Mosley Jr, and H.H. Hobbs. 2006. Sequence variations in PCSK9, low LDL, and protection against coronary heart disease. New England Journal of Medicine. 354:1264-1272.

Cohen, J.D., E.A. Brinton, M.K. Ito, and T.A. Jacobson. 2012. Understanding Statin Use in America and Gaps in Patient Education (USAGE): an internet-based survey of 10,138 current and former statin users. Journal of clinical lipidology. 6:208-215.

Costandi, J., M. Melone, A. Zhao, and S. Rashid. 2011. Human Resistin Stimulates Hepatic Overproduction of Atherogenic apoB-Containing Lipoprotein Particles by Enhancing apoB Stability and Impairing Intracellular Insulin SignalingNovelty and Significance. Circulation research. 108:727-742.

Costet, P., B. Cariou, G. Lambert, F. Lalanne, B. Lardeux, AL. Jarnoux, A. Grefhorst, B. Staels, M. Krempf. 2006. Hepatic PCSK9 expression is regulated by nutritional status via insulin and sterol regulatory element-binding protein 1c. Journal of Biological Chemistry. 281(10):6211-8.

Couture, P., J. Morissette, D. Gaudet, M.-C. Vohl, C. Gagné, J. Bergeron, J.-P. Després, and J. Simard. 1999. Fine mapping of low-density lipoprotein receptor gene by genetic linkage on chromosome 19p13. 1-p13. 3 and study of the founder effect of four French Canadian low-density lipoprotein receptor gene mutations. Atherosclerosis. 143:145-151.

Crunkhorn, S. 2012. Trial watch: PCSK9 antibody reduces LDL cholesterol. Nature Publishing Group.

Cuchel, M., E. Bruckert, H.N. Ginsberg, F.J. Raal, R.D. Santos, R.A. Hegele, J.A. Kuivenhoven, B.G. Nordestgaard, O.S. Descamps, and E. Steinhagen-Thiessen. 2014. Homozygous familial hypercholesterolaemia: new insights and guidance for clinicians to improve detection and clinical management. A position paper from the Consensus Panel on Familial Hypercholesterolaemia of the European Atherosclerosis Society. European heart journal. 35:2146-2157.

Cunningham, D., D.E. Danley, K.F. Geoghegan, M.C. Griffor, J.L. Hawkins, T.A. Subashi, A.H. Varghese, M.J. Ammirati, J.S. Culp, and L.R. Hoth. 2007. Structural and biophysical studies of PCSK9 and its mutants linked to familial hypercholesterolemia. Nature Structural and Molecular Biology. 14:413.

Curtiss, L.K., and W.A. Boisvert. 2000. Apolipoprotein E and atherosclerosis. Current opinion in lipidology. 11:243-251.

Dallas, S.L., S. Park-Snyder, K. Miyazono, D. Twardzik, G.R. Mundy, and L.F. Bonewald. 1994. Characterization and autoregulation of latent transforming growth factor beta (TGF beta) complexes in osteoblast-like cell lines. Production of a latent complex lacking the latent TGF beta-binding protein. Journal of Biological Chemistry. 269:6815-6821.

Dastani, Z., P. Pajukanta, M. Marcil, N. Rudzicz, I. Ruel, S.D. Bailey, J.C. Lee, M. Lemire, J. Faith, and J. Platko. 2010. Fine mapping and association studies of a high-density lipoprotein cholesterol linkage region on chromosome 16 in French-Canadian subjects. European Journal of Human Genetics. 18:342.

Daugherty, A., and S.C. Whitman. 2003. Quantification of atherosclerosis in mice. In Transgenic Mouse. Springer. 293-309.

Davis, R., R. Thrift, C. Wu, K. Howell. 1990. Apolipoprotein B is both integrated into and translocated across the endoplasmic reticulum membrane. Evidence for two functionally distinct pools. Journal of Biological Chemistry. 265:10005-11.

Day, I., R. Whittall, S. O'dell, L. Haddad, M. Bolla, V. Gudnason, and S. Humphries. 1997. Spectrum of LDL receptor gene mutations in heterozygous familial hypercholesterolemia. Human mutation. 10:116-127.

Daya, S., and K.I. Berns. 2008. Gene therapy using adeno-associated virus vectors. Clinical microbiology reviews. 21:583-593.

Defesche, J.C. 2004. Low-density lipoprotein receptor-its structure, function, and mutations. In Seminars in vascular medicine. Vol. 4. Copyright© 2004 by

Thieme Medical Publishers, Inc., 333 Seventh Avenue, New York, NY 10001, USA. 5-11.

Demers, A., B. Lauzier, C. Des Rosiers, and G. Mayer. 2013. Proprotein convertase subtilisin/kexin type 9 (PCSK9) targets the CD36 receptor for degradation. Am Heart Assoc.

Demers, A., S. Samami, B. Lauzier, C. Des Rosiers, E.T.N. Sock, H. Ong, and G. Mayer. 2015. PCSK9 induces CD36 degradation and affects long-chain fatty acid uptake and triglyceride metabolism in adipocytes and in mouse liver. Arteriosclerosis, thrombosis, and vascular biology:ATVBAHA. 115.306032.

Denis, M., J. Marcinkiewicz, A. Zaid, D. Gauthier, S. Poirier, C. Lazure, N.G. Seidah, and A. Prat. 2012. Gene inactivation of proprotein convertase subtilisin/kexin type 9 reduces atherosclerosis in miceclinical perspective. Circulation. 125:894-901.

DeVay, R.M., D.L. Shelton, and H. Liang. 2013. Characterization of proprotein convertase subtilisin/kexin type 9 (PCSK9) trafficking reveals a novel lysosomal targeting mechanism via amyloid precursor-like protein 2 (APLP2). Journal of Biological Chemistry. 288:10805-10818.

Dewpura, T., A. Raymond, J. Hamelin, N.G. Seidah, M. Mbikay, M. Chrétien, and J. Mayne. 2008. PCSK9 is phosphorylated by a Golgi casein kinase-like kinase ex vivo and circulates as a phosphoprotein in humans. The FEBS journal. 275:3480-3493.

Daimon M, Oizumi, T., Saitoh, T., Kameda, W., Hirata, A., Yamaguchi, H., Ohnuma, H., Igarashi, M., Tominaga, M. and Kato, T. 2003. Decreased serum levels of adiponectin are a risk factor for the progression to type 2 diabetes in the Japanese Population: the Funagata study. Diabetes care. 26(7):2015-20.

Dietschy, J.M., S.D. Turley, and D. K. Spady. 1993. Role of liver in the maintenance of cholesterol and low density lipoprotein homeostasis in different animal species, including humans. Journal of lipid research. 34.10: 1637-1659.

Dimitroff, C.J., M. Lechpammer, D. Long-Woodward, and J.L. Kutok. 2004. Rolling of human bone-metastatic prostate tumor cells on human bone marrow endothelium under shear flow is mediated by E-selectin. Cancer research. 64:5261-5269.

Ding, Q., A. Strong, K.M. Patel, S.-L. Ng, B.S. Gosis, S.N. Regan, C.A. Cowan, D.J. Rader, and K. Musunuru. 2014. Permanent Alteration of PCSK9 With In Vivo CRISPR-Cas9 Genome EditingNovelty and Significance. Circulation research. 115:488-492.

Dixon, J.L., S. Furukawa, and H. Ginsberg. 1991. Oleate stimulates secretion of apolipoprotein B-containing lipoproteins from Hep G2 cells by inhibiting early intracellular degradation of apolipoprotein B. Journal of Biological Chemistry. 266:5080-5086.

Dixon, J.L. & H. N. Ginsberg. 1993. Regulation of hepatic secretion of apolipoprotein B-containing lipoproteins: Information obtained from cultured liver cells. J. Lipid Res. 34:167–179.

Dong, B., M. Wu, H. Li, F. B. Kraemer, K. Adeli, N.G. Seidah, ... & J. Liu. 2010. Strong induction of PCSK9 gene expression through HNF1α and SREBP2: mechanism for the resistance to LDL-cholesterol lowering effect of statins in dyslipidemic hamsters. Journal of lipid research. jlr-M003566.

Du, F., Y. Hui, M. Zhang, M.F. Linton, S. Fazio, and D. Fan. 2011. Novel domain interaction regulates secretion of proprotein convertase subtilisin/kexin type 9 (PCSK9) protein. Journal of Biological Chemistry. 286:43054-43061.

Dubois, C.M., M.-H. Laprise, F. Blanchette, L.E. Gentry, and R. Leduc. 1995. Processing of transforming growth factor 1 precursor by human furin convertase. Journal of Biological Chemistry. 270:10618-10624.

Dupont, N., C. Leroy, A. Hamaï, and P. Codogno. 2017. Long-Lived Protein Degradation During Autophagy. In Methods in enzymology. Vol. 588. Elsevier. 31-40.

Dubuc, G., A. Chamberland, H. Wassef, J. Davignon, N.G Seidah, L. Bernier & A. Prat. 2004. Statins upregulate PCSK9, the gene encoding the proprotein convertase neural apoptosis-regulated convertase-1 implicated in familial hypercholesterolemia. Arteriosclerosis, thrombosis, and vascular biology. 24(8), 1454-1459.

Eberlé, D., K. Clément, D. Meyre, M. Sahbatou, M. Vaxillaire, A. Le Gall & F. Foufelle 2004. SREBF-1 gene polymorphisms are associated with obesity and type 2 diabetes in French obese and diabetic cohorts. Diabetes. 53: 2153-2157.

Edwards, P. A., D. Tabor, H. R. Kast, & A. Venkateswaran. 2000. Regulation of gene expression by SREBP and SCAP. Biochimica et Biophysica Acta (BBA)-Molecular and Cell Biology of Lipids. 1529: 103-113.

Ellison, R.C., Y. Zhang, L.E. Wagenknecht, J.H. Eckfeldt, P.N. Hopkins, J.S. Pankow, L. Djoussé, and J.J. Carr. 2005. Relation of the metabolic syndrome to calcified atherosclerotic plaque in the coronary arteries and aorta. American Journal of Cardiology. 95:1180-1186.

Eswarakumar, V., I. Lax, and J. Schlessinger. 2005. Cellular signaling by fibroblast growth factor receptors. Cytokine & growth factor reviews. 16:139-149.

Ettehad, D., C.A. Emdin, A. Kiran, S.G. Anderson, T. Callender, J. Emberson, J. Chalmers, A. Rodgers, and K. Rahimi. 2016. Blood pressure lowering for prevention of cardiovascular disease and death: a systematic review and meta-analysis. The Lancet. 387:957-967.

Fairoozy, R. H., J. Cooper, J. White, C. Giambartolomei, L. Folkersen, S. G. Wannamethee, and M. Kivimaki. 2017. Identifying low density lipoprotein cholesterol associated variants in the Annexin A2 (ANXA2) gene. Atherosclerosis. 261: 60-68.

Feigin, V. L., G. Roth, M. Naghavi, P. Parmar, R. Krishnamurthi, S. Chugh, G. Mensah, B. Norrving, I. Shiue, M. Ng, K. Estep. 2016. Global burden of stroke and risk factors in 188 countries, during 1990–2013: a systematic analysis for the Global Burden of Disease Study 2013. The Lancet Neurology. 15:913-24.

Fernandez, A.B., R. Soufer, D. Collins, A. Soufer, H. Ranjbaran, and M.M. Burg. 2010. Tendency to angry rumination predicts stress-provoked endothelin-1 increase in patients with coronary artery disease. Psychosomatic medicine. 72:348.

Ferri, N., and M. Ruscica. 2016. Proprotein convertase subtilisin/kexin type 9 (PCSK9) and metabolic syndrome: insights on insulin resistance, inflammation, and atherogenic dyslipidemia. Endocrine. 54:588-601.

Filmus, J., and S.B. Selleck, S. B. 2001. Glypicans: proteoglycans with a surprise. J. Clinical Investgation. 108:497–501

Fisher, E.A., M. Pan, X. Chen, X. Wu, H. Wang, H. Jamil, J.D. Sparks, and K.J. Williams. 2001. The triple threat to nascent apolipoprotein B Evidence for multiple, distinct degradative pathways. Journal of Biological Chemistry. 276:27855-27863.

Fisher, T.S., P. Surdo, S. Pandit, M. Mattu, Santoro, J.C., Wisniewski, D., Cummings, R.T. Calzetta, A., Cubbon, R.M., P. Fischer, and A. Tarachandani . 2007. Effects of pH and low density lipoprotein (LDL) on PCSK9-dependent LDL receptor regulation. Journal of Biological Chemistry. 282:20502-20512.

Fitzgerald, K., M. Frank-Kamenetsky, S. Shulga-Morskaya, A. Liebow, B.R. Bettencourt, J.E. Sutherland, R.M. Hutabarat, V.A. Clausen, V. Karsten, and J. Cehelsky. 2014. Effect of an RNA interference drug on the synthesis of proprotein convertase subtilisin/kexin type 9 (PCSK9) and the concentration of serum LDL cholesterol in healthy volunteers: a randomised, single-blind, placebo-controlled, phase 1 trial. The Lancet. 383:60-68.

Foley, E.M. and J.D. Esko. 2010. Hepatic heparan sulfate proteoglycans and endocytic clearance of triglyceride-rich lipoproteins. In Progress in molecular biology and translational science. 93:213-233.

Food, U., and D. Administration. 2015a. FDA approves Praluent to treat certain patients with high cholesterol: first in a new class of injectable cholesterol-lowering drugs. Press release. July 24, 2015.

Food, U., and D. Administration. 2015b. FDA approves Repatha to treat certain patients with high cholesterol. Press release. August 27, 2015.

Foretz, M., C. Guichard, P. Ferré, and F. Foufelle. 1999. Sterol regulatory element binding protein-1c is a major mediator of insulin action on the hepatic expression of glucokinase and lipogenesis-related genes. Proceedings of the National Academy of Sciences. 96: 12737-12742.

Francke, U., M.S. Brown, and J.L. Goldstein. 1984. Assignment of the human gene for the low density lipoprotein receptor to chromosome 19: synteny of a

receptor, a ligand, and a genetic disease. Proceedings of the National Academy of Sciences. 81:2826-2830.

Frank-Kamenetsky, M., A. Grefhorst, N.N. Anderson, T.S. Racie, B. Bramlage, A. Akinc, D. Butler, K. Charisse, R. Dorkin, and Y. Fan. 2008. Therapeutic RNAi targeting PCSK9 acutely lowers plasma cholesterol in rodents and LDL cholesterol in nonhuman primates. Proceedings of the National Academy of Sciences. 105:11915-11920.

Fredrickson, D.S. 1971. Mutants, hyperlipoproteinaemia, and coronary artery disease. British Medical Journal. 2:187.

Fredrickson, D.S., R.I. Levy, and R.S. Lees. 1967. Fat transport in lipoproteins—an integrated approach to mechanisms and disorders. New England Journal of Medicine. 276:34-44.

Friedman, S.L. 2003. Liver fibrosis–from bench to bedside. Journal of hepatology. 38:38-53.

Fruchart, J.-C., F. Sacks, M.P. Hermans, G. Assmann, W.V. Brown, R. Ceska, M.J. Chapman, P.M. Dodson, P. Fioretto, and H.N. Ginsberg. 2008. The Residual Risk Reduction Initiative: a call to action to reduce residual vascular risk in patients with dyslipidemia. The American journal of cardiology. 102:1K-34K.

Fuster, J.J., A.I. Castillo, C. Zaragoza, B. Ibáñez, and V. Andrés. 2012. Animal models of atherosclerosis. In Progress in molecular biology and translational science. Vol. 105. Elsevier. 1-23.

Gagliardi, A., N.P. Mullin, Z.Y. Tan, D. Colby, A.I. Kousa, F. Halbritter, J.T. Weiss, A. Felker, K. Bezstarosti, and R. Favaro. 2013. A direct physical interaction between Nanog and Sox2 regulates embryonic stem cell self-renewal. The EMBO journal. 32:2231-2247.

Galabova, G., S. Brunner, G. Winsauer, C. Juno, B. Wanko, A. Mairhofer, P. Lührs, A. Schneeberger, A. von Bonin, and F. Mattner. 2014. Peptide-based anti-PCSK9 vaccines-an approach for long-term LDLc management. PLoS One. 9:e114469.

Garcia, C.K., K. Wilund, M. Arca, G. Zuliani, R. Fellin, M. Maioli, S. Calandra, S. Bertolini, F. Cossu, and N. Grishin. 2001. Autosomal recessive hypercholesterolemia caused by mutations in a putative LDL receptor adaptor protein. Science. 292:1394-1398.

Gauthier, M.-S., J.R. Pérusse, Z. Awan, A. Bouchard, S. Tessier, J. Champagne, B. Krastins, G. Byram, K. Chabot, and P. Garneau. 2015. A semi-automated mass spectrometric immunoassay coupled to selected reaction monitoring (MSIA–SRM) reveals novel relationships between circulating PCSK9 and metabolic phenotypes in patient cohorts. Methods. 81:66-73.

Genest, J.J., S.S. Martin-Munley, J.R. McNamara, J.M. Ordovas, J. Jenner, R.H. Myers, S.R. Silberman, P.W. Wilson, D.N. Salem, and E.J. Schaefer. 1992. Familial lipoprotein disorders in patients with premature coronary artery disease. Circulation. 85:2025-2033.

Getz, G.S., and C.A. Reardon. 2009. Apoprotein E as a lipid transport and signaling protein in the blood, liver, and artery wall. Journal of lipid research. 50:S156-S161.

Getz, G.S., and C.A. Reardon. 2012. Animal models of atherosclerosis. Arteriosclerosis, thrombosis, and vascular biology. 32:1104-1115.

Gijbels, M.J., M. van der Cammen, L.J. van der Laan, J.J. Emeis, L.M. Havekes, M.H. Hofker, and G. Kraal. 1999. Progression and regression of atherosclerosis in APOE3-Leiden transgenic mice: an immunohistochemical study. Atherosclerosis. 143:15-25.

Gillian-Daniel, D.L., P.W. Bates, A. Tebon, and A.D. Attie. 2002. Endoplasmic reticulum localization of the low density lipoprotein receptor mediates presecretory degradation of apolipoprotein B. Proceedings of the National Academy of Sciences. 99:4337-4342.

Giugliano, R.P., and M.S. Sabatine. 2015. Are PCSK9 inhibitors the next breakthrough in the cardiovascular field? Journal of the American College of Cardiology. 65:2638-2651.

Giunzioni, I., H. Tavori, R. Covarrubias, A.S. Major, L. Ding, Y. Zhang, R.M. DeVay, L. Hong, D. Fan, and I.M. Predazzi. 2016. Local effects of human PCSK9 on the atherosclerotic lesion. The Journal of pathology. 238:52-62.

Goettsch, C., J.D. Hutcheson, S. Hagita, M.A. Rogers, M.D. Creager, T. Pham, J. Choi, A.K. Mlynarchik, B. Pieper, and M. Kjolby. 2016. A single injection of gain-of-function mutant PCSK9 adeno-associated virus vector induces cardiovascular calcification in mice with no genetic modification. Atherosclerosis. 251:109-118.

Goldberg, I.J. 1996. Lipoprotein lipase and lipolysis: central roles in lipoprotein metabolism and atherogenesis. Journal of lipid research. 37:693-707.

Goldstein, J.L. 1989. Familial hypercholesterolemia. The metabolic basis of inherited disease:1215-1250.

Goldstein, J.L. 2001. Familial hypercholesterolemia.

Goldstein, J.L., and M.S. Brown. 1987. Regulation of low-density lipoprotein receptors: implications for pathogenesis and therapy of hypercholesterolemia and atherosclerosis. Circulation. 76:504-507.

Goldstein JL, and M.S. Brown. 2009. The LDL receptor. Arteriosclerosis, thrombosis, and vascular biology. 29(4):431-8.

Goldstein, J.L., M.S. Brown, R.G. Anderson, D.W. Russell, and W.J. Schneider. 1985. Receptor-mediated endocytosis: concepts emerging from the LDL receptor system. Annual review of cell biology. 1:1-39.

Goldstein, J.L., S.E. Dana, and M.S. Brown. 1974. Esterification of low density lipoprotein cholesterol in human fibroblasts and its absence in homozygous familial hypercholesterolemia. Proceedings of the National Academy of Sciences. 71:4288-4292.

Gonatas, J., S. Mezitis, A. Stieber, B. Fleischer, and N. Gonatas. 1989. MG-160. A novel sialoglycoprotein of the medial cisternae of the Golgi apparatus [published eeratum appears in J Biol Chem 1989 Mar 5; 264 (7): 4264]. Journal of Biological Chemistry. 264:646-653.

Gonatas, J.O., Y.-J. Chen, A. Stieber, Z. Mourelatos, and N.K. Gonatas. 1998. Truncations of the C-terminal cytoplasmic domain of MG160, a medial Golgi sialoglycoprotein, result in its partial transport to the plasma membrane and filopodia. Journal of Cell Science. 111:249-260.

Gonatas, J.O., Z. Mourelatos, A. Stieber, W.S. Lane, J. Brosius, and N.K. Gonatas. 1995. MG-160, a membrane sialoglycoprotein of the medial cisternae of the rat Golgi apparatus, binds basic fibroblast growth factor and exhibits a high level of sequence identity to a chicken fibroblast growth factor receptor. Journal of Cell Science. 108:457-467.

Gotto, A.M. 2002a. Lipid management in diabetic patients: lessons from prevention trials. The American journal of medicine. 112:19-26.

Gotto, A.M. 2002b. Management of dyslipidemia. The American journal of medicine. 112:10-18.

Graham, M.J., K.M. Lemonidis, C.P. Whipple, A. Subramaniam, B.P. Monia, S.T. Crooke, and R.M. Crooke. 2007. Antisense inhibition of proprotein convertase subtilisin/kexin type 9 reduces serum LDL in hyperlipidemic mice. Journal of lipid research. 48:763-767.

Grefhorst, A., M.C. McNutt, T.A. Lagace, and J.D. Horton. 2008. Plasma PCSK9 preferentially reduces liver LDL receptors in mice. Journal of lipid research. 49:1303-1311.

Grimm, D., K.L. Streetz, C.L. Jopling, T.A. Storm, K. Pandey, C.R. Davis, P. Marion, F. Salazar, and M.A. Kay. 2006. Fatality in mice due to oversaturation of cellular microRNA/short hairpin RNA pathways. nature. 441:537.

Gu, H.M., A. Adijiang, M. Mah, and D.W. Zhang. 2013. Characterization of the role of EGF-A of low density lipoprotein receptor in PCSK9 binding. Journal of lipid research. 54:3345-3357.

Guardamagna, O., F. Abello, P. Saracco, V. Baracco, E. Rolfo, and M. Pirro. 2009. Endothelial activation, inflammation and premature atherosclerosis in children with familial dyslipidemia. Atherosclerosis. 207:471-475.

Gupta, N., N. Fisker, M.-C. Asselin, M. Lindholm, C. Rosenbohm, H. Ørum, J. Elmén, N.G. Seidah, and E.M. Straarup. 2010. A locked nucleic acid antisense oligonucleotide (LNA) silences PCSK9 and enhances LDLR expression in vitro and in vivo. PloS one. 5:e10682.

Gürkan, C., SM. Stagg, P. LaPointe, WE. Balch. 2006 The COPII cage: unifying principles of vesicle coat assembly. Nature Reviews Molecular Cell Biology. 7(10):727.

Gustafsen, C., M. Kjolby, M. Nyegaard, M. Mattheisen, J. Lundhede, H. Buttenschøn, O. Mors, J.F. Bentzon, P. Madsen, and A. Nykjaer. 2014. The hypercholesterolemia-risk gene SORT1 facilitates PCSK9 secretion. Cell metabolism. 19:310-318.

Gustafsen, C., D. Olsen, J. Vilstrup, S. Lund, A. Reinhardt, N. Wellner, T. Larsen, C.B Andersen, K. Weyer, J.P. Li, and P.H. Seeberger. 2017. Heparan sulfate proteoglycans present PCSK9 to the LDL receptor. Nature communications, 8:503.

Hampton, E.N., M.W. Knuth, J. Li, J.L. Harris, S.A. Lesley, and G. Spraggon. 2007. The self-inhibited structure of full-length PCSK9 at 1.9 Å reveals structural homology with resistin within the C-terminal domain. Proceedings of the National Academy of Sciences. 104:14604-14609.

Hardy, J. 2006. A hundred years of Alzheimer's disease research. Neuron. 52:3-13.

Hartvigsen, K., C.J. Binder, L.F. Hansen, A. Rafia, J. Juliano, S. Hörkkö, D. Steinberg, W. Palinski, J.L. Witztum, and A.C. Li. 2007. A diet-induced hypercholesterolemic murine model to study atherogenesis without obesity and metabolic syndrome. Arteriosclerosis, thrombosis, and vascular biology. 27:878-885.

He, H., X. Yang, A.J. Davidson, D. Wu, F.F. Marshall, L.W. Chung, H.E. Zhau, and R. Wang. 2010. Progressive epithelial to mesenchymal transitions in ARCaPE prostate cancer cells during xenograft tumor formation and metastasis. The Prostate. 70:518-528.

Heart, N., Lung, B. Institute, N.I.o. Diabetes, Digestive, and K. Diseases. 1998. Clinical guidelines on the identification, evaluation, and treatment of overweight and obesity in adults: the evidence report. National Heart, Lung, and Blood Institute.

Heath, K.E., I.N. Day, and S.E. Humphries. 2000. Universal primer quantitative fluorescent multiplex (UPQFM) PCR: a method to detect major and minor rearrangements of the low density lipoprotein receptor gene. Journal of medical genetics. 37:272-280.

Heber, S., J. Herms, V. Gajic, J. Hainfellner, A. Aguzzi, T. Rülicke, H. Kretzschmar, C. Von Koch, S. Sisodia, and P. Tremml. 2000. Mice with combined gene knock-outs reveal essential and partially redundant functions of amyloid precursor protein family members. Journal of Neuroscience. 20:7951-7963.

Herijgers, N., M. Van Eck, P.H. Groot, P.M. Hoogerbrugge, and T.J. Van Berkel. 1997. Effect of bone marrow transplantation on lipoprotein metabolism and atherosclerosis in LDL receptor–knockout mice. Arteriosclerosis, thrombosis, and vascular biology. 17:1995-2003.

Herz, J., and H.H. Bock. 2002. Lipoprotein receptors in the nervous system. Annual review of biochemistry. 71:405-434.

Herz, J., S.-Q. Qiu, A. Oesterle, H.V. DeSilva, S. Shafi, and R.J. Havel. 1995. Initial hepatic removal of chylomicron remnants is unaffected but endocytosis is

delayed in mice lacking the low density lipoprotein receptor. Proceedings of the National Academy of Sciences. 92:4611-4615.

Hess, C.N., C.C. Low Wang, and W.R. Hiatt. 2018a. PCSK9 inhibitors: mechanisms of action, metabolic effects, and clinical outcomes. Annual review of medicine. 69:133-145.

Hess, C.N., C.C.L. Wang, and W.R. Hiatt. 2018b. PCSK9 inhibitors: mechanisms of action, metabolic effects, and clinical outcomes. Annual review of medicine. 69.

Hidalgo, A., A.J. Peired, M.K. Wild, D. Vestweber, and P.S. Frenette. 2007. Complete identification of E-selectin ligands on neutrophils reveals distinct functions of PSGL-1, ESL-1, and CD44. Immunity. 26:477-489.

Hileman, R.E., J.R. Fromm, J.M. Weiler, and R.J. Linhardt. 1998. Glycosaminoglycan-protein interactions: definition of consensus sites in glycosaminoglycan binding proteins. Bioessays, 20:156-167.

Hirano, Y., M. Yoshida, M. Shimizu, & R. Sato. 2001. Direct demonstration of rapid degradation of nuclear sterol regulatory element-binding proteins by the ubiquitin-proteasome pathway. Journal of Biological Chemistry. 276: 36431-36437.

Hobbs, H.H., M.S. Brown, and J.L. Goldstein. 1992. Molecular genetics of the LDL receptor gene in familial hypercholesterolemia. Human mutation. 1:445-466.

Hobbs, H.H., M.S. Brown, D.W. Russell, J. Davignon, and J.L. Goldstein. 1987. Deletion in the gene for the low-density-lipoprotein receptor in a majority of French Canadians with familial hypercholesterolemia. New England Journal of Medicine. 317:734-737.

Hobbs, H.H., D.W. Russell, M.S. Brown, and J.L. Goldstein. 1990. The LDL receptor locus in familial hypercholesterolemia: mutational analysis of a membrane protein. Annual review of genetics. 24:133-170.

Holla Ø.L, J. Cameron, K. Tveten, T.B. Strøm, K.E. Berge, J. K. Laerdahl, T. P. Leren. 2011. Role of the C-terminal domain of PCSK9 in degradation of the LDL receptors. Journal of lipid research. 52:1787-94.

Holmes, M.V., C.E. Dale, L. Zuccolo, R.J. Silverwood, Y. Guo, Z. Ye, D. Prieto-Merino, A. Dehghan, S. Trompet, and A. Wong. 2014. Association between alcohol and cardiovascular disease: Mendelian randomisation analysis based on individual participant data. Bmj. 349:g4164.

Hooper, A.J., A.D. Marais, D.M. Tanyanyiwa, and J.R. Burnett. 2007. The C679X mutation in PCSK9 is present and lowers blood cholesterol in a Southern African population. Atherosclerosis. 193:445-448.

Horton, J. D., Y. Bashmakov, I Shimomura, and H. Shimano. 1998. Regulation of sterol regulatory element binding proteins in livers of fasted and refed mice. Proceedings of the National Academy of Sciences. 95: 5987-5992.

Horton, J. D., J.L. Goldstein, and M.S. Brown. 2002. SREBPs: activators of the complete program of cholesterol and fatty acid synthesis in the liver. The Journal of clinical investigation. 109: 1125-1131.

Horton, J. D., N.A. Shah, J.A. Warrington, N.N. Anderson, S.W. Park, M.S. Brown, and J.L. Goldstein. 2003. Combined analysis of oligonucleotide microarray data from transgenic and knockout mice identifies direct SREBP target genes. Proceedings of the National Academy of Sciences. 100: 12027-12032.

Horton, J.D., J.C. Cohen, and H.H. Hobbs. 2009. PCSK9: a convertase that coordinates LDL catabolism. Journal of lipid research. 50:S172-S177.

Howell, B.W., and J. Herz. 2001. The LDL receptor gene family: signaling functions during development. Current opinion in neurobiology. 11:74-81.

Hu, D., Y. Yang, and D.-q. Peng. 2017. Increased sortilin and its independent effect on circulating proprotein convertase subtilisin/kexin type 9 (PCSK9) in statin-naive patients with coronary artery disease. International journal of cardiology. 227:61-65.

Hua, X., A. Nohturfft, JL. Goldstein, MS. Brown.1996. Sterol Resistance in CHO Cells Traced to Point Mutation in SREBP Cleavage–Activating Protein. Cell. 87(3):415-26.

Hua, X., C. Yokoyama, J. Wu, M.R. Briggs, M.S. Brown, J.L. Goldstein, and X. Wang. 1993. SREBP-2, a second basic-helix-loop-helix-leucine zipper protein that stimulates transcription by binding to a sterol regulatory element. Proceedings of the National Academy of Sciences. 90: 11603-11607.

Hunt, S.C., P.N. Hopkins, K. Bulka, M.T. McDermott, T.L. Thorne, B.B. Wardell, B.R. Bowen, D.G. Ballinger, M.H. Skolnick, and M.E. Samuels. 2000. Genetic localization to chromosome 1p32 of the third locus for familial hypercholesterolemia in a Utah kindred. Arteriosclerosis, thrombosis, and vascular biology. 20:1089-1093.

Innerarity, T.L., R.W. Mahley, K.H. Weisgraber, T.P. Bersot, R. Krauss, G. Vega, S. Grundy, W. Friedl, J. Davignon, and B. McCarthy. 1990a. Familial defective apolipoprotein B-100: a mutation of apolipoprotein B that causes hypercholesterolemia. Journal of lipid research. 31:1337-1349.

Innerarity, T.L., R.W. Mahley, K.H. Weisgraber, T.P. Bersot, R. Krauss, G. Vega, S. Grundy, W. Friedl, J. Davignon, and B. McCarthy. 1990b. Familial defective apolipoprotein B-100: a mutation of apolipoprotein B that causes hypercholesterolemia. Journal of lipid research. 31:1337-1349.

Innerarity, T.L., R.E. Pitas, and R.W. Mahley. 1980. Receptor binding of cholesterol-induced high-density lipoproteins containing predominantly apoprotein E to cultured fibroblasts with mutations at the low-density lipoprotein receptor locus. Biochemistry. 19:4359-4365.

Ishibashi, S., M.S. Brown, J.L. Goldstein, R.D. Gerard, R.E. Hammer, and J. Herz. 1993. Hypercholesterolemia in low density lipoprotein receptor knockout mice

and its reversal by adenovirus-mediated gene delivery. The Journal of clinical investigation. 92:883-893.

Ishibashi, S., J. Herz, N. Maeda, J.L. Goldstein, and M.S. Brown. 1994. The two-receptor model of lipoprotein clearance: tests of the hypothesis in" knockout" mice lacking the low density lipoprotein receptor, apolipoprotein E, or both proteins. Proceedings of the National Academy of Sciences. 91:4431-4435.

Istvan, E. S. 2002. Structural mechanism for statin inhibition of 3-hydroxy-3-methylglutaryl coenzyme A reductase. American heart journal. 144: S27-S32.

Janssens, K., P. Ten Dijke, S. Janssens, and W. Van Hul. 2005. Transforming growth factor-β1 to the bone. Endocrine reviews. 26:743-774.

Jawien, J., P. Nastalek, and R. Korbut. 2004. Mouse models of experimental atherosclerosis. Journal of Physiology and Pharmacology. 55:503-517.

Jeong, H. J., H. S. Lee, K. S. Kim, Y. K. Kim, D. Yoon, & S. W. Park. 2008. Sterol-dependent regulation of proprotein convertase subtilisin/kexin type 9 expression by sterol-regulatory element binding protein-2. Journal of lipid research. 49: 399-409.

Jiang, Z.G., M.N. Simon, J.S. Wall, and C.J. McKnight. 2007. Structural analysis of reconstituted lipoproteins containing the N-terminal domain of apolipoprotein B. Biophysical journal. 92:4097-4108.

Johnston, P.A., A. Stieber, and N.K. Gonatas. 1994. A hypothesis on the traffic of MG160, a medial Golgi sialoglycoprotein, from the trans-Golgi network to the Golgi cisternae. Journal of Cell Science. 107:529-537.

Jonas, M.C., C. Costantini, and L. Puglielli. 2008. PCSK9 is required for the disposal of non-acetylated intermediates of the nascent membrane protein BACE1. EMBO reports. 9:916-922.

Jonasson, L., J. Holm, O. Skalli, G. Bondjers, and G.K. Hansson. 1986. Regional accumulations of T cells, macrophages, and smooth muscle cells in the human atherosclerotic plaque. Arteriosclerosis, Thrombosis, and Vascular Biology. 6:131-138.

Jones, B., E. Jones, S. Bonney, H. Patel, A.R. Mensenkamp,... & N. Meadows. 2003. Mutations in a Sar1 GTPase of COPII vesicles are associated with lipid absorption disorders. Nature genetics. 34: 29.

Joris, I., E. Stetz, and G. Majno. 1979. Lymphocytes and monocytes in the aortic intima: An electron-microscopic study in the rat. Atherosclerosis. 34:221-231.

Kannel, W.B., T.R. Dawber, A. Kagan, N. Revotskie, and J. Stokes. 1961. Factors of risk in the development of coronary heart disease—six-year follow-up experience: the Framingham Study. Annals of internal medicine. 55:33-50.

Kannel, W. B., Dawber, T. R., Friedman, G. D., Glennon, W. E., & Mcnamara, P. M. 1964. Risk factors in coronary heart disease: an evaluation of several serum lipids as predictors of coronary heart disease: The Framingham Study. Annals of internal medicine. 61:888-899.

Kapourchali, F.R., L.C. Gangadaran Surendiran, E. Uitz, B. Bahadori, and M.H. Moghadasian. 2014. Animal models of atherosclerosis. World Journal of Clinical Cases: WJCC. 2:126.

Kessenbrock K, V. Plaks, Z. Werb. 2010. Matrix metalloproteinases: regulators of the tumor microenvironment. Cell. 141:52–67

Keys, A. 1980. Seven countries. A multivariate analysis of death and coronary heart disease. Harvard University Press.

Keys, A., H.L. Taylor, H. Blackburn, J. Brozek, J.T. Anderson, and E. Simonson. 1963. Coronary heart disease among Minnesota business and professional men followed fifteen years. Circulation. 28:381-395.

Khachadurian, A.K. 1964. The inheritance of essential familial hypercholesterolemia. The American journal of medicine. 37:402-407.

Kjolby, M., O.M. Andersen, T. Breiderhoff, A.W. Fjorback, K.M. Pedersen, P. Madsen, P. Jansen, J. Heeren, T.E. Willnow, and A. Nykjaer. 2010. Sort1, encoded by the cardiovascular risk locus 1p13. 3, is a regulator of hepatic lipoprotein export. Cell metabolism. 12:213-223.

Knott, T.J., S.C. Rall, T.L. Innerarity, S.F. Jacobson, M.S. Urdea, B. Levy-Wilson, L.M. Powell, R.J. Pease, R. Eddy, and H. Nakai. 1985. Human apolipoprotein B: structure of carboxyl-terminal domains, sites of gene expression, and chromosomal localization. Science. 230:37-43.

Knouff, C., M.E. Hinsdale, H. Mezdour, M.K. Altenburg, M. Watanabe, S.H. Quarfordt, P.M. Sullivan, and N. Maeda. 1999. Apo E structure determines VLDL clearance and atherosclerosis risk in mice. The Journal of clinical investigation. 103:1579-1586.

Knowles, J.W., and N. Maeda. 2000. Genetic modifiers of atherosclerosis in mice. Arteriosclerosis, thrombosis, and vascular biology. 20:2336-2345.

Ko, M.H., and L. Puglielli. 2009. Two endoplasmic reticulum (ER)/ER Golgi intermediate compartment-based lysine acetyltransferases post-translationally regulate BACE1 levels. Journal of Biological Chemistry. 284:2482-2492.

Kobayashi, K., K. Oka, T. Forte, B. Ishida, B. Teng, K. Ishimura-Oka, M. Nakamuta, and L. Chan. 1996. Reversal of hypercholesterolemia in low density lipoprotein receptor knockout mice by adenovirus-mediated gene transfer of the very low density lipoprotein receptor. Journal of Biological Chemistry. 271:6852-6860.

Koch, G., M. Smith, and R. Mortara. 1985. An abundant ubiquitous glycoprotein (GP100) in nucleated mammalian cells. FEBS letters. 179:294-298.

Köhl, R., M. Antoine, B.B. Olwin, C. Dickson, and P. Kiefer. 2000. Cysteine-rich fibroblast growth factor receptor alters secretion and intracellular routing of fibroblast growth factor 3. Journal of Biological Chemistry. 275:15741-15748.

Koide, A., C.W. Bailey, X. Huang, and S. Koide. 1998. The fibronectin type III domain as a scaffold for novel binding proteins1. Journal of molecular biology. 284:1141-1151.

Kolansky, D.M., M. Cuchel, B.J. Clark, S. Paridon, B.W. McCrindle, S.E. Wiegers, L. Araujo, Y. Vohra, J.C. Defesche, and J.M. Wilson. 2008. Longitudinal evaluation and assessment of cardiovascular disease in patients with homozygous familial hypercholesterolemia. American Journal of Cardiology. 102:1438-1443.

Kolodgie, F.D., J. Narula, N. Haider, and R. Virmani. 2001. Apoptosis in atherosclerosis: Does it contribute to plaque instability? Cardiology clinics. 19:127-139.

Konstantinov, I.E., and G.M. Jankovic. 2013. Alexander I. Ignatowski: a pioneer in the study of atherosclerosis. Texas Heart Institute Journal. 40:246.

Kosenko, T., M. Golder, G. Leblond, W. Weng, and T.A. Lagace. 2013. Low density lipoprotein binds to proprotein convertase subtilisin/kexin type-9 (PCSK9) in human plasma and inhibits PCSK9-mediated low density lipoprotein receptor degradation. Journal of Biological Chemistry. 288:8279-8288.

Kowal, R.C., J. Herz, J.L. Goldstein, V. Esser, and M.S. Brown. 1989. Low density lipoprotein receptor-related protein mediates uptake of cholesteryl esters derived from apoprotein E-enriched lipoproteins. Proceedings of the National Academy of Sciences. 86:5810-5814.

Kockx, M. M. (1998). Apoptosis in the atherosclerotic plaque: quantitative and qualitative aspects. Arteriosclerosis, thrombosis, and vascular biology, 18(10), 1519-1522.

Kronenberg, H.M. 2003. Developmental regulation of the growth plate. Nature. 423:332.

Kronenberg, H.M. 2007. The role of the perichondrium in fetal bone development. Annals of the New York Academy of Sciences. 1116:59-64.

Kugiyama, K., SA. Kerns, JD. Morrisett, Roberts R, PD. Henry. 1990. Impairment of endothelium-dependent arterial relaxation by lysolecithin in modified low-density lipoproteins. 344(6262):160.

Kwiterovich, P.O., D.S. Fredrickson, and R.I. Levy. 1974. Familial hypercholesterolemia (one form of familial type II hyperlipoproteinemia) a study of its biochemical, genetic, and clinical presentation in childhood. The Journal of clinical investigation. 53:1237-1249.

Kwon, H.J., T.A. Lagace, M.C. McNutt, J.D. Horton, and J. Deisenhofer. 2008. Molecular basis for LDL receptor recognition by PCSK9. Proceedings of the National Academy of Sciences. 105:1820-1825.

Lagace, T.A. 2014. PCSK9 and LDLR degradation: regulatory mechanisms in circulation and in cells. Current opinion in lipidology. 25:387.

Lagace, T.A., D.E. Curtis, R. Garuti, M.C. McNutt, S.W. Park, H.B. Prather, N.N. Anderson, Y. Ho, R.E. Hammer, and J.D. Horton. 2006. Secreted PCSK9 decreases the number of LDL receptors in hepatocytes and inlivers of parabiotic mice. The Journal of clinical investigation. 116:2995-3005.

Landlinger, C., M.G. Pouwer, C. Juno, J.W. van der Hoorn, E.J. Pieterman, J.W. Jukema, G. Staffler, H.M. Princen, and G. Galabova. 2017. The AT04A vaccine against proprotein convertase subtilisin/kexin type 9 reduces total cholesterol, vascular inflammation, and atherosclerosis in APOE* 3Leiden. CETP mice. European heart journal. 38:2499-2507.

Lardenoye, J., M. De Vries, C. Löwik, Q. Xu, C. Dhore, J. Cleutjens, V. van Hinsbergh, J. van Bockel, and P. Quax. 2002. Accelerated atherosclerosis and calcification in vein grafts: a study in APOE* 3 Leiden transgenic mice. Circulation research. 91:577-584.

Larsson, S.L., J. Skogsberg, and J. Björkegren. 2004. The low density lipoprotein receptor prevents secretion of dense apoB100-containing lipoproteins from the liver. Journal of Biological Chemistry. 279:831-836.

Law, W.M., and H. Heath. 1985. Familial benign hypercalcemia (hypocalciuric hypercalcemia): clinical and pathogenetic studies in 21 families. Annals of internal medicine. 102:511-519.

Lee, A.S. 1992. Mammalian stress response: induction of the glucose-regulated protein family. Current opinion in cell biology. 4:267-273.

Lee, A.S. 2014. Glucose-regulated proteins in cancer: molecular mechanisms and therapeutic potential. Nature reviews Cancer. 14:263.

Lee, M.C., E.A. Miller, J. Goldberg, L. Orci, and R. Schekman. 2004. Bi-directional protein transport between the ER and Golgi. Annu. Rev. Cell Dev. Biol. 20:87-123.

Leren, P. 1970. The Oslo diet-heart study: eleven-year report. Circulation. 42:935-942.

S. Yara, P. Couture, and J.-F. Beaulieu. 2013. PCSK9 plays a significant role in cholesterol homeostasis and lipid transport in intestinal epithelial cells. Atherosclerosis. 227:297-306.

Lewis, M.J., R.A. Mazzarella, and M. Green. 1986. Structure and assembly of the endoplasmic reticulum: biosynthesis and intracellular sorting of ERp61, ERp59, and ERp49, three protein components of murine endoplasmic reticulum. Archives of biochemistry and biophysics. 245:389-403.

Lewis, M.J., S. Turco, and M. Green. 1985. Structure and assembly of the endoplasmic reticulum. Biosynthetic sorting of endoplasmic reticulum proteins. Journal of Biological Chemistry. 260:6926-6931.

Li, C., L. Lin, W. Zhang, L. Zhou, H. Wang, X. Luo, H. Luo, Y. Cai, and C. Zeng. 2015a. Efficiency and safety of proprotein convertase subtilisin/kexin 9 monoclonal antibody on hypercholesterolemia: a meta-analysis of 20

randomized controlled trials. Journal of the American Heart Association. 4:e001937.

Li, H., B. Dong, S. W. Park, H. S. Lee, W. Chen, & J. Liu. 2009. HNF1α plays a critical role in PCSK9 gene transcription and regulation by a natural hypocholesterolemic compound berberine. Journal of Biological Chemistry. jbc-M109.

Li, J., C. Tumanut, J.-A. Gavigan, W.-J. Huang, E.N. Hampton, R. Tumanut, K.F. Suen, J.W. Trauger, G. Spraggon, and S.A. Lesley. 2007. Secreted PCSK9 promotes LDL receptor degradation independently of proteolytic activity. Biochemical Journal. 406:203-207.

Li, S., R. Xu, Y. Zhang, Y. Guo, C. Zhu, G. Liu, Q. Dong, and J. Li. 2015b. Relation of resistin to proprotein convertase subtilisin–kexin type 9 levels in coronary artery disease patients with different nutritional status. Journal of endocrinological investigation. 38:1291-1299.

Liang, J.-s., X. Wu, H. Jiang, M. Zhou, H. Yang, P. Angkeow, L.-S. Huang, S.L. Sturley, and H. Ginsberg. 1998. Translocation efficiency, susceptibility to proteasomal degradation, and lipid responsiveness of apolipoprotein B are determined by the presence of β sheet domains. Journal of Biological Chemistry. 273:35216-35221.

Liao, W., B.H.J. Chang, M. Mancini, and L. Chan. 2003. Ubiquitin-dependent and-independent proteasomal degradation of apoB associated with endoplasmic reticulum and golgi apparatus, respectively, in HepG2 cells. Journal of cellular biochemistry. 89:1019-1029.

Lindholm, M.W., J. Elmén, N. Fisker, H.F. Hansen, R. Persson, M.R. Møller, C. Rosenbohm, H. Ørum, E.M. Straarup, and T. Koch. 2012. PCSK9 LNA antisense oligonucleotides induce sustained reduction of LDL cholesterol in nonhuman primates. Molecular Therapy. 20:376-381.

Lintner, N.G., K.F. McClure, D. Petersen, A.T. Londregan, D.W. Piotrowski, L. Wei, J. Xiao, …and K.F. Geoghegan. 2017. Selective stalling of human translation through small-molecule engagement of the ribosome nascent chain. PLoS biology. 15:e2001882.

Liu, M., G. Wu, J. Baysarowich, M. Kavana, G.H. Addona, K.K. Bierilo, J.S. Mudgett, G. Pavlovic, A. Sitlani, and J.J. Renger. 2010. PCSK9 is not involved in the degradation of LDL receptors and BACE1 in the adult mouse brain. Journal of lipid research. 51:2611-2618.

Liu, Z., K.J. Lavine, I.H. Hung, and D.M. Ornitz. 2007. FGF18 is required for early chondrocyte proliferation, hypertrophy and vascular invasion of the growth plate. Developmental biology. 302:80-91.

Luhr M, F. Sætre F, N. Engedal N. 2018. The Long-lived Protein Degradation Assay: an Efficient Method for Quantitative Determination of the Autophagic Flux of Endogenous Proteins in Adherent Cell Lines. Bio-Protocol. 5;8(9).

Luo, L., J. Li, H. Liu, X. Jian, Q. Zou, Q. Zhao, Q. Le, H. Chen, X. Gao, and C. He. 2017. Adiponectin Is Involved in Connective Tissue Growth Factor-Induced Proliferation, Migration and Overproduction of the Extracellular Matrix in Keloid Fibroblasts. International journal of molecular sciences. 18:1044.

Luo, W., H. Wang, C. Guo, J. Wang, J. Kwak, K.L. Bahrou, and D.T. Eitzman. 2012. Haploinsufficiency of E-selectin ligand-1 is associated with reduced atherosclerotic plaque macrophage content while complete deficiency leads to early embryonic lethality in mice. Atherosclerosis. 224:363-367.

Lusis, A. Atherosclerosis Nature, 2000, 407 (6801), 233-241. DOI. 10:35025203.

Lutgens, E., M. Daemen, M. Kockx, P. Doevendans, M. Hofker, L. Havekes, H. Wellens, and E.D. de Muinck. 1999. Atherosclerosis in APOE* 3-Leiden transgenic mice: from proliferative to atheromatous stage. Circulation. 99:276-283.

Ly, K., R. Essalmani, R. Desjardins, N.G. Seidah, and R. Day. 2016. An unbiased mass spectrometry approach identifies Glypican-3 as an interactor of proprotein convertase subtilisin/Kexin type 9 (PCSK9) and low density lipoprotein receptor (LDLR) in hepatocellular carcinoma cells. Journal of Biological Chemistry. 291:24676-24687.

Ma, A., D.J. Bell, A.A. Mittal, and H.H. Harrison. 1994. Immunocytochemical detection of extracellular annexin II in cultured human skin keratinocytes and isolation of annexin II isoforms enriched in the extracellular pool. J Cell Sci. 107:1973-1984.

Ma, Y., W. Wang, J. Zhang, Y. Lu, W. Wu, H. Yan, and Y. Wang. 2012. Hyperlipidemia and atherosclerotic lesion development in Ldlr-deficient mice on a long-term high-fat diet. PloS one. 7:e35835.

Macchiaiolo, M., M.G. Gagliardi, A. Toscano, P. Guccione, and A. Bartuli. 2012. Homozygous familial hypercholesterolaemia. The Lancet. 379:1330.

Mahley, R.W. 1988. Apolipoprotein E: cholesterol transport protein with expanding role in cell biology. Science. 240:622-630.

Mahmood S.S, D. Levy, R.S. Vasan, T.J. Wang. 2014. The Framingham Heart Study and the epidemiology of cardiovascular disease: a historical perspective. The lancet. 383:999-1008.

Marques-Pinheiro, A., M. Marduel, J.-P. Rabès, M. Devillers, L. Villéger, D. Allard, J. Weissenbach, M. Guerin, Y. Zair, and D. Erlich. 2010. A fourth locus for autosomal dominant hypercholesterolemia maps at 16q22. 1. European Journal of Human Genetics. 18:1236.

Massagué, J., and Y.-G. Chen. 2000. Controlling TGF-β signaling. Genes & development. 14:627-644.

Mathers, C. D., A. Lopez, C. Stein, D. Ma Fat, C. Rao, M. Inoue, K. Shibuya, N. Tomijima, C. Bernard, and H. Xu. 2005. Deaths and disease burden by cause:

global burden of disease estimates for 2001 by World Bank Country Groups. Disease Control Priorities Project Working Paper. 18.

Mathers, C. D., R. Sadana, J.A. Salomon, C. J. Murray, and A.D. Lopez. 2001. Healthy life expectancy in 191 countries, 1999. The Lancet. 357: 1685-1691.

Mathers, CD., D. Loncar. Projections of global mortality and burden of disease from 2002 to 2030. 2006. PLoS medicine. 3(11): e442.

Mayer, G., S. Poirier, and N.G. Seidah. 2008. Annexin A2 is a C-terminal PCSK9-binding protein that regulates endogenous low density lipoprotein receptor levels. Journal of Biological Chemistry. 283:31791-31801.

Maxwell, K. N., R. E. Soccio, E. M. Duncan, E. Sehayek, & J. L Breslow. 2003. Novel putative SREBP and LXR target genes identified by microarray analysis in liver of cholesterol-fed mice. Journal of lipid research, 44: 2109-2119.

Maxwell, K.N. and J.L. Breslow. 2004. Adenoviral-mediated expression of Pcsk9 in mice results in a low-density lipoprotein receptor knockout phenotype. Proceedings of the National Academy of Sciences, 101:7100-7105.

Mendel, D. B., & Crabtree, G. R. (1991). HNF-1, a member of a novel class of dimerizing homeodomain proteins. J Biol Chem, 266(2), 677-680.

McGill, H.C., C.A. McMahan, A.W. Zieske, G.D. Sloop, J.V. Walcott, D.A. Troxclair, G.T. Malcom, R.E. Tracy, M.C. Oalmann, and J.P. Strong. 2000. Associations of coronary heart disease risk factors with the intermediate lesion of atherosclerosis in youth. Arteriosclerosis, thrombosis, and vascular biology. 20:1998-2004.

McKenney, J.M., M.J. Koren, D.J. Kereiakes, C. Hanotin, A.-C. Ferrand, and E.A. Stein. 2012. Safety and efficacy of a monoclonal antibody to proprotein convertase subtilisin/kexin type 9 serine protease, SAR236553/REGN727, in patients with primary hypercholesterolemia receiving ongoing stable atorvastatin therapy. Journal of the American College of Cardiology. 59:2344-2353.

McMahon, H.T., and I.G. Mills. 2004. COP and clathrin-coated vesicle budding: different pathways, common approaches. Current opinion in cell biology. 16:379-391.

McNutt, M.C., H.J. Kwon, C. Chen, J.R. Chen, J.D. Horton, and T.A. Lagace. 2009. Antagonism of secreted PCSK9 increases low density lipoprotein receptor expression in HepG2 cells. Journal of Biological Chemistry. 284:10561-10570.

McNutt, M.C., T.A. Lagace, and J.D. Horton. 2007. Catalytic activity is not required for secreted PCSK9 to reduce low density lipoprotein receptors in HepG2 cells. Journal of Biological Chemistry. 282:20799-20803.

Melone, M., L. Wilsie, O. Palyha, A. Strack, and S. Rashid. 2012. Discovery of a new role of human resistin in hepatocyte low-density lipoprotein receptor

suppression mediated in part by proprotein convertase subtilisin/kexin type 9. Journal of the American College of Cardiology. 59:1697-1705.

Mendel, DB., GR. Crabtree. 1991. HNF-1, a member of a novel class of dimerizing homeodomain proteins. Journal of Biological Chemistry. 266(2):677-80.

Mensenkamp, AR., B. Teusink, JF. Baller, H. Wolters, R. Havinga, KW. van Dijk, LM. Havekes, F. Kuipers. 2001. Mice expressing only the mutant APOE3Leiden gene show impaired VLDL secretion. Arteriosclerosis, thrombosis, and vascular biology. 21(8):1366-72.

Merat, S., F. Casanada, M. Sutphin, W. Palinski, and P.D. Reaven. 1999. Western-type diets induce insulin resistance and hyperinsulinemia in LDL receptor-deficient mice but do not increase aortic atherosclerosis compared with normoinsulinemic mice in which similar plasma cholesterol levels are achieved by a fructose-rich diet. Arteriosclerosis, thrombosis, and vascular biology. 19:1223-1230.

Miller, E.A., and R. Schekman. 2013. COPII—a flexible vesicle formation system. Current opinion in cell biology. 25:420-427.

Mitchell, T., G. Chao, D. Sitkoff, F. Lo, H. Monshizadegan, D. Meyers, S. Low, K. Russo, R. DiBella, and F. Denhez. 2014. Pharmacologic profile of the Adnectin BMS-962476, a small protein biologic alternative to PCSK9 antibodies for low-density lipoprotein lowering. Journal of Pharmacology and Experimental Therapeutics. 350:412-424.

Miyaoka, Y., H. Kato, K. Ebato, S. Saito, N. Miyata, T. Imamura, and A. Miyajima. 2011. Retention in the Golgi apparatus and expression on the cell surface of Cfr/Esl-1/Glg-1/MG-160 are regulated by two distinct mechanisms. Biochemical Journal. 440:33-41.

Miyaoka, Y., M. Tanaka, T. Imamura, S. Takada, and A. Miyajima. 2010. A novel regulatory mechanism for Fgf18 signaling involving cysteine-rich FGF receptor (Cfr) and delta-like protein (Dlk). Development. 137:159-167.

Miyazono, K., U. Hellman, C. Wernstedt, and C. Heldin. 1988. Latent high molecular weight complex of transforming growth factor beta 1. Purification from human platelets and structural characterization. Journal of Biological Chemistry. 263:6407-6415.

Miyazono, K., H. Ichijo, and C.-H. Heldin. 1993. Transforming growth factor-β: latent forms, binding proteins, and receptors. Growth Factors. 8:11-22.

Miyazono, K., A. Olofsson, P. Colosetti, and C.-H. Heldin. 1991. A role of the latent TGF-beta 1-binding protein in the assembly and secretion of TGF-beta 1. The EMBO journal. 10:1091-1101.

Miyazono, K., J. Thyberg, and C. Heldin. 1992. Retention of the transforming growth factor-beta 1 precursor in the Golgi complex in a latent endoglycosidase H-sensitive form. Journal of Biological Chemistry. 267:5668-5675.

Mizushima, N., and T. Yoshimori. 2007. How to interpret LC3 immunoblotting. Autophagy. 3:542-545.

Mizushima, N., T. Yoshimori, and B. Levine. 2010. Methods in mammalian autophagy research. Cell. 140:313-326.

Mombelli, G., S. Castelnuovo, and C. Pavanello. 2015. Potential of PCSK9 as a new target for the management of LDL cholesterol. Res Rep Clin Cardiol. 6:73-86.

Moon, Y.S., C.M. Smas, K. Lee, J.A. Villena, K.-H. Kim, E.J. Yun, and H.S. Sul. 2002. Mice lacking paternally expressed Pref-1/Dlk1 display growth retardation and accelerated adiposity. Molecular and cellular biology. 22:5585-5592.

Moore, K. J., F. J. Sheedy & E. A. Fisher. 2013. Macrophages in atherosclerosis: a dynamic balance. Nature Reviews Immunology. 13: 709.

Moore, K.J., and I.J. Goldberg. 2016. Emerging roles of PCSK9: more than a one-trick pony. Am Heart Assoc.

Morris, S.M., and J.A. Cooper. 2001. Disabled-2 colocalizes with the LDLR in clathrin-coated pits and interacts with AP-2. Traffic. 2:111-123.

Mourão, P.A., and C.A. Bracamonte. 1984. The binding of human aortic glycosaminoglycans and proteoglycans to plasma low density lipoproteins. Atherosclerosis. 50:133-146.

Mourelatos, Z., J.O. Gonatas, L.M. Nycum, N.K. Gonatas, and J.A. Biegel. 1995. Assignment of the GLG1 gene for MGF-160, a fibroblast growth factor and E-selectin binding membrane sialoglycoprotein of the Golgi apparatus, to chromosome 16q22-q23 by fluorescence in situ hybridization. Genomics. 28:354.

Müller, C. 1938. Xanthomata, hypercholesterolemia, angina pectoris. Journal of Internal Medicine. 95:75-84.

Mullard, Asher. 2017. Nine paths to PCSK9 inhibition. Nature Reviews Drug Discovery. 16:299-301.

Naureckiene, S., L. Ma, K. Sreekumar, U. Purandare, C.F. Lo, Y. Huang, L.W. Chiang, J.M. Grenier, B.A. Ozenberger, and J.S. Jacobsen. 2003. Functional characterization of Narc 1, a novel proteinase related to proteinase K. Archives of Biochemistry and Biophysics. 420:55-67.

Neurath, H. 1989. The diversity of proteolytic enzymes in Proteolytic Enzymes: A Practical Approach (Beynon, RJ, and Bond, JS, eds.) pp. 1-13. IRL Press, Oxford.

Ni, M., and A.S. Lee. 2007. ER chaperones in mammalian development and human diseases. FEBS letters. 581:3641-3651.

Nielsen, M.S., C. Jacobsen, G. Olivecrona, J. Gliemann, and C.M. Petersen. 1999. Sortilin/neurotensin receptor-3 binds and mediates degradation of lipoprotein lipase. Journal of Biological Chemistry. 274:8832-8836.

Nilsson, S.K., S. Christensen, M.K. Raarup, R.O. Ryan, M.S. Nielsen, and G. Olivecrona. 2008. Endocytosis of apolipoprotein AV by members of the low density lipoprotein receptor and the VPS10p domain receptor families. Journal of Biological Chemistry. 283:25920-25927.

Nordestgaard, B.G., M.J. Chapman, S.E. Humphries, H.N. Ginsberg, L. Masana, O.S. Descamps, O. Wiklund, R.A. Hegele, F.J. Raal, and J.C. Defesche. 2013. Familial hypercholesterolaemia is underdiagnosed and undertreated in the general population: guidance for clinicians to prevent coronary heart disease: consensus statement of the European Atherosclerosis Society. European heart journal. 34:3478-3490.

Nordestgaard, B.G., S.J. Nicholls, A. Langsted, K.K. Ray, and A. Tybjærg-Hansen. 2018. Advances in lipid-lowering therapy through gene-silencing technologies. Nature Reviews Cardiology.

Odom, D. T., N. Zizlsperger, D. B. Gordon., G. W. Bell, N. Rinaldi, H. L. Murray, H. L., ... & E. Fraenkel. 2004. Control of pancreas and liver gene expression by HNF transcription factors. Science. 303:1378-1381.

Ohbayashi, N., M. Shibayama, Y. Kurotaki, M. Imanishi, T. Fujimori, N. Itoh, and S. Takada. 2002. FGF18 is required for normal cell proliferation and differentiation during osteogenesis and chondrogenesis. Genes & development. 16:870-879.

Ohsaki Y., J. Cheng, A. Fujita, T. Tokumoto, T. Fujimoto T. 2006. Cytoplasmic lipid droplets are sites of convergence of proteasomal and autophagic degradation of apolipoprotein B. Molecular biology of the cell. 17:2674-83.

Okada, F., K. Yamaguchi, A. Ichihara, and T. Nakamura. 1989. Purification and structural analysis of a latent form of transforming growth factor-β from rat platelets. The Journal of Biochemistry. 106:304-310.

O'Keefe, JH., L. Cordain, WH. Harris, RM. Moe, R. Vogel. 2004. Optimal low-density lipoprotein is 50 to 70 mg/dl: lower is better and physiologically normal. Journal of the American College of Cardiology. 43(11):2142-6.

Olivecrona, G. 2016. Role of lipoprotein lipase in lipid metabolism. Current opinion in lipidology, *27*: 233-241.

Olofsson, A., U. Hellman, P. Ten Dijke, S. Grimsby, H. Ichijo, A. Morén, K. Miyazono, and C.-H. Heldin. 1997. Latent transforming growth factor-beta complex in Chinese hamster ovary cells contains the multifunctional cysteine-rich fibroblast growth factor receptor, also termed E-selectin-ligand or MG-160. Biochemical Journal. 324:427.

Olofsson, A., K. Miyazono, T. Kanzaki, P. Colosetti, U. Engström, and C. Heldin. 1992. Transforming growth factor-beta 1,-beta 2, and-beta 3 secreted by a human glioblastoma cell line. Identification of small and different forms of large latent complexes. Journal of Biological Chemistry. 267:19482-19488.

Olofsson, S.-O., and J. Borén. 2012. Apolipoprotein B secretory regulation by degradation. Arteriosclerosis, thrombosis, and vascular biology. 32:1334-1338.

Ouguerram, K., M. Chetiveaux, Y. Zair, P. Costet, M. Abifadel, M. Varret, C. Boileau, T. Magot, and M. Krempf. 2004. Apolipoprotein B100 metabolism in autosomal-dominant hypercholesterolemia related to mutations in PCSK9. Arteriosclerosis, thrombosis, and vascular biology. 24:1448-1453.

Ouimet, M., V. Franklin, E. Mak, X. Liao, I. Tabas, and Y.L. Marcel. 2011. Autophagy regulates cholesterol efflux from macrophage foam cells via lysosomal acid lipase. Cell metabolism. 13:655-667.

Palmer-Smith, H., and A. Basak. 2010. Regulatory effects of peptides from the pro and catalytic domains of proprotein convertase subtilisin/kexin 9 (PCSK9) on low-density lipoprotein receptor (LDL-R). Current medicinal chemistry. 17:2168-2182.

Pan, M., A.I. Cederbaum, Y.-L. Zhang, H.N. Ginsberg, K.J. Williams, and E.A. Fisher. 2004. Lipid peroxidation and oxidant stress regulate hepatic apolipoprotein B degradation and VLDL production. The Journal of clinical investigation. 113:1277-1287.

Pan, M., V. Maitin, S. Parathath, U. Andreo, S.X. Lin, C.S. Germain, Z. Yao, F.R. Maxfield, K.J. Williams, and E.A. Fisher. 2008. Presecretory oxidation, aggregation, and autophagic destruction of apoprotein-B: a pathway for late-stage quality control. Proceedings of the National Academy of Sciences. 105:5862-5867.

Pariyarath, R., H. Wang, J.D. Aitchison, H.N. Ginsberg, W.J. Welch, A.E. Johnson, and E.A. Fisher. 2001. Co-translational interactions of apoprotein B with the ribosome and translocon during lipoprotein assembly or targeting to the proteasome. Journal of Biological Chemistry. 276:541-550.

Park, S.W., Y.-A. Moon, and J.D. Horton. 2004. Post-transcriptional regulation of low density lipoprotein receptor protein by proprotein convertase subtilisin/kexin type 9a in mouse liver. Journal of Biological Chemistry. 279:50630-50638.

Parks W.C., C.L. Wilson, Y.S. Lopez-Boado. 2004. Matrix metalloproteinases as modulators of inflammation and innate immunity. Nature Review Immunology 4:617-629

Parthasarathy, S., M.T. Quinn, and D. Steinberg. 1988. Is oxidized low density lipoprotein involved in the recruitment and retention of monocyte/macrophages in the artery wall during the initiation of atherosclerosis? In Oxygen Radicals in Biology and Medicine. Springer. 375-380.

Patchell, B.J., K.R. Wojcik, T.-L. Yang, S.R. White, and D.R. Dorscheid. 2007. Glycosylation and annexin II cell surface translocation mediate airway epithelial wound repair. American Journal of Physiology-Lung Cellular and Molecular Physiology. 293:L354-L363.

Patterson, G.I., and R.W. Padgett. 2000. TGFβ-related pathways: roles in Caenorhabditis elegans development. Trends in genetics. 16:27-33.

Piedrahita, J.A., S.H. Zhang, J.R. Hagaman, P.M. Oliver, and N. Maeda. 1992. Generation of mice carrying a mutant apolipoprotein E gene inactivated by gene targeting in embryonic stem cells. Proceedings of the National Academy of Sciences. 89:4471-4475.

Piper, D.E., S. Jackson, Q. Liu, W.G. Romanow, S. Shetterly, S.T. Thibault, B. Shan, and N.P. Walker. 2007. The crystal structure of PCSK9: a regulator of plasma LDL-cholesterol. Structure. 15:545-552.

Plump, A.S., and J.L. Breslow. 1995. Apolipoprotein E and the apolipoprotein E-deficient mouse. Annual review of nutrition. 15:495-518.

Plump, A.S., J.D. Smith, T. Hayek, K. Aalto-Setälä, A. Walsh, J.G. Verstuyft, E.M. Rubin, and J.L. Breslow. 1992. Severe hypercholesterolemia and atherosclerosis in apolipoprotein E-deficient mice created by homologous recombination in ES cells. Cell. 71:343-353.

Poirier, S., G. Mayer. 2013. The biology of PCSK9 from the endoplasmic reticulum to lysosomes: new and emerging therapeutics to control low-density lipoprotein cholesterol. Drug design, development and therapy. 7:1135.

Poirier, S., G. Mayer, S. Benjannet, E. Bergeron, J. Marcinkiewicz, N. Nassoury, H. Mayer, J. Nimpf, A. Prat, and N.G. Seidah. 2008. The proprotein convertase PCSK9 induces the degradation of low density lipoprotein receptor (LDLR) and its closest family members VLDLR and apoER2. Journal of Biological Chemistry. 283:2363-2372.

Poirier, S., G. Mayer, V. Poupon, P.S. McPherson, R. Desjardins, K. Ly, M.-C. Asselin, R. Day, F.J. Duclos, and M. Witmer. 2009. Dissection of the endogenous cellular pathways of PCSK9-induced low density lipoprotein receptor degradation evidence for an intracellular route. Journal of Biological Chemistry. 284:28856-28864.

Poirier, S., H. Hamouda, A. Villeneuve, L. Demers, A. & G. Mayer. 2016. Trafficking dynamics of PCSK9-induced LDLR degradation: focus on human PCSK9 mutations and C-terminal domain. PloS one. 11(6): e0157230.

Poirier, S., M. Mamarbachi, W.-T. Chen, A.S. Lee, and G. Mayer. 2015. GRP94 regulates circulating cholesterol levels through blockade of PCSK9-induced LDLR degradation. Cell reports. 13:2064-2071.

Polonovski, J., I. Beucler. 1983. Structure and metabolism of plasma lipoproteins. Pathologie-biologie. 31(4):225-34.

Ponugoti, B., D. H Kim, Z. Xiao, Z. Smith, J. Miao, M. Zang, … & J. K. Kemper. 2010. SIRT1 deacetylates and inhibits SREBP-1C activity in regulation of hepatic lipid metabolism. Journal of Biological Chemistry. jbc-M110.

Proudlock, J., A. Day, and R. Tum. 1973. Cholesterol-esterifying enzymes of foam cells isolated from atherosclerotic rabbit intima. Atherosclerosis. 18:451-457.

Raabe, M., M.M. Véniant, M.A. Sullivan, C.H. Zlot, J. Björkegren, L.B. Nielsen, J.S. Wong, R.L. Hamilton, and S.G. Young. 1999. Analysis of the role of microsomal triglyceride transfer protein in the liver of tissue-specific knockout mice. The Journal of clinical investigation. 103:1287-1298.

Rader, D.J., J. Cohen, and H.H. Hobbs. 2003. Monogenic hypercholesterolemia: new insights in pathogenesis and treatment. The Journal of clinical investigation. 111:1795-1803.

Rashid, S., D.E. Curtis, R. Garuti, N.N. Anderson, Y. Bashmakov, Y. Ho, R.E. Hammer, Y.-A. Moon, and J.D. Horton. 2005. Decreased plasma cholesterol and hypersensitivity to statins in mice lacking Pcsk9. Proceedings of the National Academy of Sciences of the United States of America. 102:5374-5379.

Rashid, S., and J.J. Kastelein. 2013. PCSK9 and resistin at the crossroads of the atherogenic dyslipidemia. Expert review of cardiovascular therapy. 11:1567-1577.

Ray, K.K., U. Landmesser, L.A. Leiter, D. Kallend, R. Dufour, M. Karakas, T. Hall, R.P. Troquay, T. Turner, and F.L. Visseren. 2017. Inclisiran in patients at high cardiovascular risk with elevated LDL cholesterol. New England Journal of Medicine. 376:1430-1440.

Razani, B., C. Feng, T. Coleman, R. Emanuel, H. Wen, S. Hwang, J.P. Ting, H.W. Virgin, M.B. Kastan, and C.F. Semenkovich. 2012. Autophagy links inflammasomes to atherosclerotic progression. Cell metabolism. 15:534-544.

Reddick, R.L., S.H. Zhang, and N. Maeda. 1994. Atherosclerosis in mice lacking apo E. Evaluation of lesional development and progression. Arteriosclerosis, Thrombosis, and Vascular Biology. 14:141-147.

Rescher, U., and V. Gerke. 2004. Annexins–unique membrane binding proteins with diverse functions. Journal of cell science. 117:2631-2639.

Ricci, C., A. Corsini, M. Accomazzo, G. Rovati, M. Camera, L. Rossetti, and N. Ferri. 2017. PCSK9 and resistin: Not only a structural sharing. Nutrition, Metabolism and Cardiovascular Diseases. 27:e34.

Roche-Molina, M., D. Sanz-Rosa, F.M. Cruz, J. García-Prieto, S. López, R. Abia, F.J. Muriana, V. Fuster, B. Ibáñez, and J.A. Bernal. 2015. Induction of Sustained Hypercholesterolemia by Single Adeno-Associated Virus–Mediated Gene Transfer of Mutant hPCSK9Significance. Arteriosclerosis, thrombosis, and vascular biology. 35:50-59.

Roncaglioni, M.C., L. Santoro, B. D'avanzo, E. Negri, A. Nobili, A. Ledda, F. Pietropaolo, M.G. Franzosi, C. La Vecchia, and G.A. Feruglio. 1992. Role of family history in patients with myocardial infarction. An Italian case-control study. GISSI-EFRIM Investigators. Circulation. 85:2065-2072.

Ross, R. 1999. Atherosclerosis—an inflammatory disease. New England journal of medicine. 340:115-126.

Roth, G.A., C. Johnson, A. Abajobir, F. Abd-Allah, S.F. Abera, G. Abyu, M. Ahmed, B. Aksut, T. Alam, and K. Alam. 2017. Global, regional, and national burden of cardiovascular diseases for 10 causes, 1990 to 2015. Journal of the American College of Cardiology. 70:1-25.

Roy C.C., E. Levy, P.H. Green, A. Sniderman, J. Letarte, J.P. Buts, J. Orquin, P. Brochu, A.M. Weber, C.L. Morin, Y. Marcel, and R.J. Deckelbaum. 1987. Malabsorption, hypocholesterolemia, and fat-filled enterocytes with increased intestinal apoprotein B. Chylomicron retention disease. Gastroenterology 92:390–399

Roubtsova, A., M.N. Munkonda, Z. Awan, J. Marcinkiewicz, A. Chamberland, C. Lazure, K. Cianflone, N.G. Seidah, and A. Prat. 2011. Circulating proprotein convertase subtilisin/kexin 9 (PCSK9) regulates VLDLR protein and triglyceride accumulation in visceral adipose tissue. Arteriosclerosis, thrombosis, and vascular biology. 31:785-791.

Rubinsztein, D.C., G. Mariño, and G. Kroemer. 2011. Autophagy and aging. Cell. 146:682-695.

Ruff, C.T., and E. Braunwald. 2011. The evolving epidemiology of acute coronary syndromes. Nature Reviews Cardiology. 8:140.

Russell, J., C.J. Epstein, M.B. Grisham, J.S. Alexander, K.-Y. Yeh, and D.N. Granger. 2000. Regulation of E-selectin expression in postischemic intestinal microvasculature. American Journal of Physiology-Gastrointestinal and Liver Physiology. 278:G878-G885.

Russell D.W., M. Brown, and J. Goldstein. 1989. Different combinations of cysteine-rich repeats mediate binding of low density lipoprotein receptor to two different proteins. J Biol Chem. 264:21682–21688

Rustaeus, S., K. Lindberg, J. Borén, and S.-O. Olofsson. 1995. Brefeldin A reversibly inhibits the assembly of apoB containing lipoproteins in McA-RH7777 cells. Journal of Biological Chemistry. 270:28879-28886.

Safarova, MS and Kullo J. 2016. Family, cholesterol and the genes from the ground up or why screening matters. https://atlasofscience.org

Sanan, DA., DL. Newland, R. Tao, S. Marcovina, J. Wang, V. Mooser, Hammer RE, Hobbs HH. 1998. Low density lipoprotein receptor-negative mice expressing human apolipoprotein B-100 develop complex atherosclerotic lesions on a chow diet: no accentuation by apolipoprotein (a). Proceedings of the National Academy of Sciences. 95(8):4544-9.

Sander, J.D., and J.K. Joung. 2014. CRISPR-Cas systems for editing, regulating and targeting genomes. Nature biotechnology. 32:347.

Sané, A., E. Seidman, S. Spahis, V. Lamantia, C. Garofalo, A. Montoudis, V. Marcil and E. Levy. 2015. New insights in intestinal Sar1B GTPase regulation and role in cholesterol homeostasis. Journal of cellular biochemistry. 116:2270-2282.

Sarzi-Puttini, P., F. Atzeni, and M. Carrabba. 2003. Cardiovascular risk factors in systemic lupus erythematosus and in antiphospholipid syndrome. Minerva medica. 94:63-70.

Schiffelers, R.M., A. Ansari, J. Xu, Q. Zhou, Q. Tang, G. Storm, G. Molema, P.Y. Lu, P.V. Scaria, and M.C. Woodle. 2004. Cancer siRNA therapy by tumor selective delivery with ligand-targeted sterically stabilized nanoparticle. Nucleic acids research. 32:e149-e149.

Schmidt, A.F., L.S. Pearce, J.T. Wilkins, J.P. Casas, and A.D. Hingorani. 2018. Cochrane corner: PCSK9 monoclonal antibodies for the primary and secondary prevention of cardiovascular disease. BMJ Publishing Group Ltd and British Cardiovascular Society.

Schneeberger, A., M. Mandler, W. Zauner, P. Dal-Bianco, M. Schmitz, A. Kutzelnigg, S. Kasper, M. Brunner, M. Mueller, and F. Mattner. 2010. Development of AFFITOPE vaccines for Alzheimer's disease. Alzheimer's & Dementia: The Journal of the Alzheimer's Association. 6:S584-S585.

Schroeder, C.I., J.E. Swedberg, J.M. Withka, K.J. Rosengren, M. Akcan, D.J. Clayton, N.L. Daly, O. Cheneval, K.A. Borzilleri, and M. Griffor. 2014. Design and synthesis of truncated EGF-A peptides that restore LDL-R recycling in the presence of PCSK9 in vitro. Chemistry & biology. 21:284-294.

Schrott, H.G., J.L. Goldstein, W.R. Hazzard, M.M. Mcgoodwin, and A.G. Motulsky. 1972. Familial hypercholesterolemia in a large kindred: Evidence for a monogenic mechanism. Annals of internal medicine. 76:711-720.

Scott, J. 1989. The molecular and cell biology of apolipoprotein-B. Molecular biology & medicine, 6: 65-80.

Seidah, N. G., Poirier, S., Denis, M., Parker, R., Miao, B., Mapelli, C., ... & Mayer, G. (2012). Annexin A2 is a natural extrahepatic inhibitor of the PCSK9-induced LDL receptor degradation. PloS one, 7(7), e41865.

Seidah, N.G., Z. Awan, M. Chrétien, and M. Mbikay. 2014. PCSK9: a key modulator of cardiovascular health. Circulation research. 114:1022-1036.

Seidah, N.G., S. Benjannet, L. Wickham, J. Marcinkiewicz, S.B. Jasmin, S. Stifani, A. Basak, A. Prat, and M. Chrétien. 2003. The secretory proprotein convertase neural apoptosis-regulated convertase 1 (NARC-1): liver regeneration and neuronal differentiation. Proceedings of the National Academy of Sciences. 100:928-933.

Seo, Y.K., T. Jeon, H. Chong, J. Biesinger, X. Xie, and T. Osborne. 2011. Genome-wide localization of SREBP-2 in hepatic chromatin predicts a role in autophagy. Cell metabolism. 13:367-375.

Shan, L., L. Pang, R. Zhang, N.J. Murgolo, H. Lan, and J.A. Hedrick. 2008. PCSK9 binds to multiple receptors and can be functionally inhibited by an EGF-A peptide. Biochemical and biophysical research communications. 375:69-73.

Shapiro, M.D., and S. Fazio. 2017. PCSK9 and atherosclerosis-lipids and beyond. Journal of atherosclerosis and thrombosis. 24:462-472.

Shi, Y., and J. Massagué. 2003. Mechanisms of TGF-β signaling from cell membrane to the nucleus. Cell. 113:685-700.

Slater, M., A.V. Perruccio, and E.M. Badley. 2011. Musculoskeletal comorbidities in cardiovascular disease, diabetes and respiratory disease: the impact on activity limitations; a representative population-based study. BMC public health. 11:77.

Smith, J.D., and J. Breslow. 1997. The emergence of mouse models of atherosclerosis and their relevance to clinical research. Journal of internal medicine. 242:99-109.

Smith, M.J., and G.L. Koch. 1987. Isolation and identification of partial cDNA clones for endoplasmin, the major glycoprotein of mammalian endoplasmic reticulum. Journal of molecular biology. 194:345-347.

Sniderman, A., P. Couture, and J. De Graaf. 2010. Diagnosis and treatment of apolipoprotein B dyslipoproteinemias. Nature Reviews Endocrinology. 6:335.

Soutar, A.K., and R.P. Naoumova. 2007. Mechanisms of disease: genetic causes of familial hypercholesterolemia. Nature Reviews Cardiology. 4:214.

Soutar, A.K., R.P. Naoumova, and L.M. Traub. 2003. Genetics, clinical phenotype, and molecular cell biology of autosomal recessive hypercholesterolemia. Arteriosclerosis, thrombosis, and vascular biology. 23:1963-1970.

Sparks, J.D., T.L. Phung, M. Bolognino, and C.E. Sparks. 1996. Insulin-mediated inhibition of apolipoprotein B secretion requires an intracellular trafficking event and phosphatidylinositol 3-kinase activation: studies with brefeldin A and wortmannin in primary cultures of rat hepatocytes. Biochemical Journal. 313:567.

Sporn, M.B., and A.B. Roberts. 1990. The multifunctional nature of peptide growth factors. In Peptide growth factors and their receptors I. Springer. 3-15.

Sreeramkumar, V., M. Leiva, A. Stadtmann, C. Pitaval, I. Ortega-Rodríguez, M.K. Wild, B. Lee, A. Zarbock, and A. Hidalgo. 2013. Coordinated and unique functions of the E-selectin ligand ESL-1 during inflammatory and hematopoietic recruitment in mice. Blood. 122:3993-4001.

Steegmaier, M., E. Borges, J. Berger, H. Schwarz, and D. Vestweber. 1997. The E-selectin-ligand ESL-1 is located in the Golgi as well as on microvilli on the cell surface. Journal of cell science. 110:687-694.

Steegmaler, M., A. Levinovitz, S. Isenmann, E. Borges, M. Lenter, H.P. Kocher, B. Kleuser, and D. Vestweber. 1995. The E-selectin-ligand ESL-1 is a variant of a receptor for fibroblast growth factor. Nature. 373:615.

Stein, E.A., S. Kasichayanula, T. Turner, T. Kranz, U. Arumugam, L. Biernat, and J. Lee. 2014. LDL cholesterol reduction with BMS-962476, an adnectin inhibitor

of PCSK9: results of a single ascending dose study. J Am Coll Cardiol. 63:A172.

Stein, E.A., and G.D. Swergold. 2013. Potential of proprotein convertase subtilisin/kexin type 9 based therapeutics. Current atherosclerosis reports. 15:310.

Steppan, C.M., S.T. Bailey, S. Bhat, E.J. Brown, R.R. Banerjee, C.M. Wright, H.R. Patel, R.S. Ahima, and M.A. Lazar. 2001. The hormone resistin links obesity to diabetes. Nature. 409:307.

Steppan, C.M., and M.A. Lazar. 2004. The current biology of resistin. Journal of internal medicine. 255:439-447.

Stieber, A., Z. Mourelatos, Y. Chen, N. Le Douarin, and N. Gonatas. 1995. MG160, a membrane protein of the Golgi apparatus which is homologous to a fibroblast growth factor receptor and to a ligand for E-selectin, is found only in the Golgi apparatus and appears early in chicken embryo development. Experimental cell research. 219:562-570.

Stone, N.J., J.G. Robinson, A.H. Lichtenstein, C.N.B. Merz, C.B. Blum, R.H. Eckel, A.C. Goldberg, D. Gordon, D. Levy, and D.M. Lloyd-Jones. 2014. 2013 ACC/AHA guideline on the treatment of blood cholesterol to reduce atherosclerotic cardiovascular risk in adults: a report of the American College of Cardiology/American Heart Association Task Force on Practice Guidelines. Journal of the American College of Cardiology. 63:2889-2934.

Strom, S.C., J. Davila, and M. Grompe. 2010. Chimeric mice with humanized liver: tools for the study of drug metabolism, excretion, and toxicity. In Hepatocytes. Springer. 491-509.

Suhy, D.A., S.-C. Kao, T. Mao, L. Whiteley, H. Denise, B. Souberbielle, A.D. Burdick, K. Hayes, J.F. Wright, and H. Lavender. 2012. Safe, long-term hepatic expression of anti-HCV shRNA in a nonhuman primate model. Molecular Therapy. 20:1737-1749.

Sun, H., R.M. Krauss, J.T. Chang, and B.-B. Teng. 2017. PCSK9 deficiency reduces atherosclerosis, apolipoprotein B secretion and endothelial dysfunction. Journal of lipid research:jlr. M078360.

Sun, H., A. Samarghandi, N. Zhang, Z. Yao, M. Xiong, and B.-B. Teng. 2012. Proprotein convertase subtilisin/kexin type 9 interacts with apolipoprotein B and prevents its intracellular degradation, irrespective of the low-density lipoprotein receptor. Arteriosclerosis, thrombosis, and vascular biology. 32:1585-1595.

Surdo, P.L., M.J. Bottomley, A. Calzetta, E.C. Settembre, A. Cirillo, S. Pandit, Y.G. Ni, B. Hubbard, A. Sitlani, and A. Carfí. 2011. Mechanistic implications for LDL receptor degradation from the PCSK9/LDLR structure at neutral pH. EMBO reports. 12:1300-1305.

Takahashi, Y., M. Nishikawa, and Y. Takakura. 2009. Nonviral vector-mediated RNA interference: its gene silencing characteristics and important factors to

achieve RNAi-based gene therapy. Advanced drug delivery reviews. 61:760-766.

Tavori, H., D. Fan, J.L. Blakemore, P.G. Yancey, L. Ding, M.F. Linton, and S. Fazio. 2013. Serum Proprotein Convertase Subtilisin/Kexin Type 9 and Cell Surface Low-Density Lipoprotein ReceptorClinical Perspective: Evidence for a Reciprocal Regulation. Circulation. 127:2403-2413.

Ten Dijke, P., M.J. Goumans, F. Itoh, and S. Itoh. 2002. Regulation of cell proliferation by Smad proteins. Journal of cellular physiology. 191:1-16.

Tennyson, G.E., C.A. Sabatos, K. Higuchi, N. Meglin, and H.B. Brewer. 1989. Expression of apolipoprotein B mRNAs encoding higher-and lower-molecular weight isoproteins in rat liver and intestine. Proceedings of the National Academy of Sciences. 86:500-504.

Tian, J., H. Pei, J.M. Sanders, J.F. Angle, I.J. Sarembock, A.H. Matsumoto, G.A. Helm, and W. Shi. 2006. Hyperlipidemia is a major determinant of neointimal formation in LDL receptor-deficient mice. Biochemical and biophysical research communications. 345:1004-1009.

Tseng, Y.-C., S. Mozumdar, and L. Huang. 2009. Lipid-based systemic delivery of siRNA. Advanced drug delivery reviews. 61:721-731.

Tsukamoto, K., M. Kinoshita, K. Kojima, Y. Mikuni, M. Kudo, M. Mori, M. Fujita, E. Horie, N. Shimazu, T. Teramoto. Synergically increased expression of CD36, CLA-1 and CD68, but not of SR-A and LOX-1, with the progression to foam cells from macrophages. Journal of atherosclerosis and thrombosis. 9(1):57-64.

Twisk, J., D.L. Gillian-Daniel, A. Tebon, L. Wang, P.H.R. Barrett, and A.D. Attie. 2000. The role of the LDL receptor in apolipoprotein B secretion. The Journal of clinical investigation. 105:521-532.

Ukkola, O., and M. Santaniemi. 2002. Adiponectin: a link between excess adiposity and associated comorbidities? Journal of molecular medicine. 80:696-702.

Ummarino, D. 2017. Dyslipidaemia: Anti-PCSK9 vaccines to halt atherosclerosis. Nature Reviews Cardiology. 14:442.

Van der Westhuyzen, D., M. Stein, H. Henderson, A. Marais, A. Fourie, and G. Coetzee. 1991. Deletion of two growth-factor repeats from the low-density-lipoprotein receptor accelerates its degradation. Biochemical Journal. 277:677-682.

Van Poelgeest, EP., MR. Hodges, M. Moerland, Y. Tessier, AA. Levin, R. Persson, MW. Lindholm, K. Dumong Erichsen, H. Ørum, AF. 2015. Cohen, J. Burggraaf. Antisense-mediated reduction of proprotein convertase subtilisin/kexin type 9 (PCSK9): a first-in-human randomized, placebo-controlled trial. British journal of clinical pharmacology. 80(6):1350-61.

Van Vlijmen, B., A. Van den Maagdenberg, M. Gijbels, H. Van Der Boom, H. HogenEsch, R.R. Frants, M.H. Hofker, and L.M. Havekes. 1994. Diet-induced hyperlipoproteinemia and atherosclerosis in apolipoprotein E3-Leiden transgenic mice. The Journal of clinical investigation. 93:1403-1410.

VanderLaan, P.A., C.A. Reardon, and G.S. Getz. 2004. Site specificity of atherosclerosis: site-selective responses to atherosclerotic modulators. Arteriosclerosis, thrombosis, and vascular biology. 24:12-22.

VanderLaan, P.A., C.A. Reardon, R.A. Thisted, and G.S. Getz. 2009. VLDL best predicts aortic root atherosclerosis in LDL receptor deficient mice. Journal of lipid research. 50:376-385.

Varret, M., J.-P. Rabes, B. Saint-Jore, A. Cenarro, J.-C. Marinoni, F. Civeira, M. Devillers, M. Krempf, M. Coulon, and R. Thiart. 1999. A third major locus for autosomal dominant hypercholesterolemia maps to 1p34. 1-p32. The American Journal of Human Genetics. 64:1378-1387.

Vassar, R., B.D. Bennett, S. Babu-Khan, S. Kahn, E.A. Mendiaz, P. Denis, D.B. Teplow, S. Ross, P. Amarante, and R. Loeloff. 1999. β-Secretase cleavage of Alzheimer's amyloid precursor protein by the transmembrane aspartic protease BACE. science. 286:735-741.

Véniant, M.M., C.H. Zlot, R.L. Walzem, V. Pierotti, R. Driscoll, D. Dichek, J. Herz, and S.G. Young. 1998. Lipoprotein clearance mechanisms in LDL receptor-deficient. The Journal of clinical investigation. 102:1559-1568.

Véniant, M.M., S. Withycombe, and S.G. Young. 2001. Lipoprotein size and atherosclerosis susceptibility in apoe−/− and Ldlr−/− mice. Arteriosclerosis, thrombosis, and vascular biology. 21:1567-1570.

Vergeer, M., A.G. Holleboom, J.J. Kastelein, and J.A. Kuivenhoven. 2010. The HDL hypothesis: does high-density lipoprotein protect from atherosclerosis? Journal of lipid research. 51:2058-2073.

Veseli, B.E., P. Perrotta, G. De Meyer, L. Roth, C. Van der Donckt, W. Martinet, and G. De Meyer. 2017. Animal models of atherosclerosis. European journal of pharmacology, 816, pp.3-13.

Villéger, L., M. Abifadel, D. Allard, J.P. Rabès, R. Thiart, M.J. Kotze, C. Béroud, C. Junien, C. Boileau, and M. Varret. 2002. The UMD-LDLR database: additions to the software and 490 new entries to the database. Human mutation. 20:81-87.

Vickers, T. A., & S. T. Crooke. 2014. Antisense oligonucleotides capable of promoting specific target mRNA reduction via competing RNase H1-dependent and independent mechanisms. PloS one, 9: e108625.

Vielma, S. A., M. Mironova, J. R. Ku & M. F. Lopes-Virella, (2004). Oxidized LDL further enhances expression of adhesion molecules in Chlamydophila pneumoniae-infected endothelial cells. Journal of lipid research, 45(5): 873-880.

Wakefield, L., D. Smith, K. Flanders, and M. Sporn. 1988. Latent transforming growth factor-beta from human platelets. A high molecular weight complex containing precursor sequences. Journal of Biological Chemistry. 263:7646-7654.

Wang, W.Y., B.J. Barratt, D.G. Clayton, and J.A. Todd. 2005. Genome-wide association studies: theoretical and practical concerns. Nature Reviews Genetics. 6:109.

Wang, X., E. Berry, S. Hernandez-Anzaldo, D. Sun, A. Adijiang, L. Li, D. Zhang, and C. Fernandez-Patron. 2015. MMP-2 inhibits PCSK9-induced degradation of the LDL receptor in Hepa1-c1c7 cells. FEBS letters. 589:490-496.

Ward, N.C., and G.F. Watts. 2018. PCSK9 monoclonal antibody on a knife-edge: an article of faith in FH? Elsevier.

Wasan, K.M., D.R. Brocks, S.D. Lee, K. Sachs-Barrable, and S.J. Thornton. 2008. Impact of lipoproteins on the biological activity and disposition of hydrophobic drugs: implications for drug discovery. Nature Reviews Drug Discovery. 7:84.

Wasco, W., S. Gurubhagavatula, M. d Paradis, D.M. Romano, S.S. Sisodia, B.T. Hyman, R.L. Neve, and R.E. Tanzi. 1993. Isolation and characterization of APLP2 encoding a homologue of the Alzheimer's associated amyloid β protein precursor. Nature genetics. 5:95.

Watanabe, R., and H. Riezman. 2004. Differential ER exit in yeast and mammalian cells. Current opinion in cell biology. 16:350-355.

Weber, C., H. Noels. 2011. Atherosclerosis: current pathogenesis and therapeutic options. Nature medicine. 17(11):1410.

Werneburg, S., F.F. Buettner, L. Erben, M. Mathews, H. Neumann, M. Mühlenhoff, and H. Hildebrandt. 2016. Polysialylation and lipopolysaccharide-induced shedding of E-selectin ligand-1 and neuropilin-2 by microglia and THP-1 macrophages. Glia. 64:1314-1330.

Whitehead, K.A., R. Langer, and D.G. Anderson. 2009. Knocking down barriers: advances in siRNA delivery. Nature reviews Drug discovery. 8:129.

Wild, M.K., M.-C. Huang, U. Schulze-Horsel, P.A. van der Merwe, and D. Vestweber. 2001. Affinity, kinetics, and thermodynamics of E-selectin binding to E-selectin ligand-1. Journal of Biological Chemistry. 276:31602-31612.

Wilkinson, I.B., C.M. McEniery, and J.R. Cockcroft. 2009. Arteriosclerosis and atherosclerosis: guilty by association. Hypertension. 54:1213-1215.

Williams, H.D., N.L. Trevaskis, S.A. Charman, R.M. Shanker, W.N. Charman, C.W. Pouton, and C.J. Porter. 2013. Strategies to address low drug solubility in discovery and development. Pharmacological reviews. 65:315-499.

Williams, K. J., & I. Tabas. 1995. The response-to-retention hypothesis of early atherogenesis. Arteriosclerosis, thrombosis, and vascular biology, 15: 551-561.

Willnow, T.E., J. Horton, H. Otani, J. Braun, R. Hammer and J. Herz. 1996. RAP, a specialized chaperone, prevents ligand-induced ER retention and degradation of LDL receptor-related endocytic receptors. The EMBO journal, 15: 2632-2639.

Witting, P.K., K. PETTERSSON, A.-M. ÖSTLUND-LINDQVIST, C. Westerlund, A.W. Eriksson, and R. Stocker. 1999. Inhibition by a coantioxidant of aortic lipoprotein lipid peroxidation and atherosclerosis in apolipoprotein E and low density lipoprotein receptor gene double knockout mice. The FASEB journal. 13:667-675.

Wojcik, J., O. Hantschel, F. Grebien, I. Kaupe, K.L. Bennett, J. Barkinge, R.B. Jones, A. Koide, G. Superti-Furga, and S. Koide. 2010. A potent and highly specific FN3 monobody inhibitor of the Abl SH2 domain. Nature Structural and Molecular Biology. 17:519.

Wright, A.V., and J.A. Doudna. 2016. Protecting genome integrity during CRISPR immune adaptation. Nature Structural and Molecular Biology. 23:876.

Wu, Q., Z.H. Tang, J. Peng, L. Liao, L.H. Pan, C.Y. Wu, Z.S. Jiang, G.X. Wang, and L.S. Liu. 2014. The dual behavior of PCSK9 in the regulation of apoptosis is crucial in Alzheimer's disease progression. Biomedical reports. 2:167-171.

Xia, L., M. Sperandio, T. Yago, J.M. McDaniel, R.D. Cummings, S. Pearson-White, K. Ley, and R.P. McEver. 2002. P-selectin glycoprotein ligand-1–deficient mice have impaired leukocyte tethering to E-selectin under flow. The Journal of clinical investigation. 109:939-950.

Xu, S., M. Luo, Z. Zhu, J. Xu. 2018. Small molecules as inhibitors of PCSK9: Current status and future challenges. European journal of medicinal chemistry.

Yamamoto, H., N. Kuroda, H. Uekita, I. Kochi, A. Matsumoto, R. Niinaga, T. Funahashi, I. Shimomura, and S. Kihara. 2016. E-selectin ligand-1 (ESL-1) is a novel adiponectin binding protein on cell adhesion. Biochemical and biophysical research communications. 470:425-430.

Yang, T., I. Grafe, Y. Bae, S. Chen, Y. Chen, T.K. Bertin, M.-M. Jiang, C.G. Ambrose, and B. Lee. 2013. E-selectin ligand 1 regulates bone remodeling by limiting bioactive TGF-β in the bone microenvironment. Proceedings of the National Academy of Sciences. 110:7336-7341.

Yang, T., R. Mendoza-Londono, H. Lu, J. Tao, K. Li, B. Keller, M.M. Jiang, R. Shah, Y. Chen, and T.K. Bertin. 2010. E-selectin ligand–1 regulates growth plate homeostasis in mice by inhibiting the intracellular processing and secretion of mature TGF-β. The Journal of clinical investigation. 120:2474-2485.

Yasmin-Karim, S., M.R. King, E.M. Messing, and Y.-F. Lee. 2014. E-selectin ligand-1 controls circulating prostate cancer cell rolling/adhesion and metastasis. Oncotarget. 5:12097.

Yeatman, T., T. Updyke, M. Kaetzel, J. Dedman, and G. Nicolson. 1993. Expression of annexins on the surfaces of non-metastatic and metastatic human and rodent tumor cells. Clinical & experimental metastasis. 11:37-44.

Yin W, Carballo-Jane E, E. Carballo-Jane, D. G. McLaren, V. H. Mendoza, K. Gagen, N. S. Geoghagen, L. Ann McNamara. 2012. Plasma lipid profiling across species for the identification of optimal animal models of human dyslipidemia. Journal of lipid research. 53(1):51-65.

Yokoyama, C., X. Wang, M.R. Briggs, A. Admon, J. Wu, X. Hua, and M.S. Brown. 1993. SREBP-1, a basic-helix-loop-helix-leucine zipper protein that controls transcription of the low density lipoprotein receptor gene. Cell. 75: 187-197.

Yusuf, S., S. Hawken, S. Ôunpuu, T. Dans, A. Avezum, F. Lanas, M. McQueen, A. Budaj, P. Pais, and J. Varigos. 2004. Effect of potentially modifiable risk factors associated with myocardial infarction in 52 countries (the INTERHEART study): case-control study. The lancet. 364:937-952.

Zaid, A., A. Roubtsova, R. Essalmani, J. Marcinkiewicz, A. Chamberland, J. Hamelin, M. Tremblay, H. Jacques, W. Jin, and J. Davignon. 2008. Proprotein convertase subtilisin/kexin type 9 (PCSK9): hepatocyte-specific low-density lipoprotein receptor degradation and critical role in mouse liver regeneration. Hepatology. 48:646-654.

Zhang SH, R. Reddick, J. Piedrahita, N. Maeda. 1992. Spontaneous hypercholesterolemia and arterial lesions in mice lacking apolipoprotein E. Science. 258:468-71.

Zhang, D.-W., R. Garuti, W.-J. Tang, J.C. Cohen, and H.H. Hobbs. 2008. Structural requirements for PCSK9-mediated degradation of the low-density lipoprotein receptor. Proceedings of the National Academy of Sciences. 105:13045-13050.

Zhang, D.-W., T.A. Lagace, R. Garuti, Z. Zhao, M. McDonald, J.D. Horton, J.C. Cohen, and H.H. Hobbs. 2007. Binding of proprotein convertase subtilisin/kexin type 9 to epidermal growth factor-like repeat A of low density lipoprotein receptor decreases receptor recycling and increases degradation. Journal of Biological Chemistry. 282:18602-18612.

Zhang, J., and H. Herscovitz. 2003. Nascent lipidated apolipoprotein B is transported to the Golgi as an incompletely folded intermediate as probed by its association with network of endoplasmic reticulum molecular chaperones, GRP94, ERp72, BiP, calreticulin, and cyclophilin B. Journal of Biological Chemistry. 278:7459-7468.

Zhang, Y., C. Eigenbrot, L. Zhou, S. Shia, W. Li, C. Quan, J. Tom, P. Moran, P. Di Lello, and N.J. Skelton. 2014. Identification of a small peptide that inhibits PCSK9 protein binding to the low density lipoprotein receptor. Journal of Biological Chemistry. 289:942-955.

Zhao, Z., Y. Tuakli-Wosornu, T.A. Lagace, L. Kinch, N.V. Grishin, J.D. Horton, J.C. Cohen, and H.H. Hobbs. 2006. Molecular characterization of loss-of-function mutations in PCSK9 and identification of a compound heterozygote. The American Journal of Human Genetics. 79:514-523.

Zhao, Z., S. Pompey, H. Dong, J. Weng, R. Garuti, & P. Michaely. 2013. S-nitrosylation of ARH is required for LDL uptake by the LDL receptor. Journal of lipid research. 54: 1550-1559.

Zhou, Z., M.E. Zuber, L.W. Burrus, and B.B. Olwin. 1997. Identification and characterization of a fibroblast growth factor (FGF) binding domain in the cysteine-rich FGF receptor. Journal of Biological Chemistry. 272:5167-5174.

Zöllner, O., and D. Vestweber. 1996. The E-selectin ligand-1 is selectively activated in Chinese hamster ovary cells by the α (1, 3)-fucosyltransferases IV and VII. Journal of Biological Chemistry. 271:33002-33008.

Zsebo, K.M., A. Yaroshinsky, J.J. Rudy, K. Wagner, B. Greenberg, M. Jessup, and R.J. Hajjar. 2013. Long term effects of AAV1/SERCA2a gene transfer in patients with severe heart failure: analysis of recurrent cardiovascular events and mortality. Circulation research:CIRCRESAHA. 113.302421.

Zuber, M.E., Z. Zhou, L.W. Burrus, and B.B. Olwin. 1997. Cysteine-rich FGF receptor regulates intracellular FGF-1 and FGF-2 levels. Journal of cellular physiology. 170:217-227.